International Ocean Colour Science Meeting 2013

Advancing Global Ocean Colour Observations

SUBMITTED ABSTRACTS (alphabetic order)

In Situ Observation Strategies Supporting Future Ocean Color Science

S. G. Ackleson

SA Ocean Services, LLC, 6508 33rd Street, Falls Church, VA, 22043
Email: steve@saoceans.com

Summary

The global ocean ecosystem is displaying unprecedented rates of change, forced by a warming climate, higher levels of carbon dioxide, and altered precipitation and land use patterns, all fueled by increasing human population. Ecological stresses resulting from acidification, water column stratification, coastal pollution, and sedimentation are expected to intensify for the remainder of the century, endangering marine services related to food and recreation. Addressing these problems will require science-based decisions supported by accurate and complete knowledge of the Earth ecosystem. Ocean color science, based on a foundation of accurate, in situ observations employing emerging ocean observatory infrastructures and evolving profiling float technology, is poised to play a key role in building that knowledge base. However, deploying and maintaining in situ optical and biogeochemical sensors within a sustained, autonomous observatory presents quality control and assurance challenges that the international ocean color science community must solve to fully realize the capability of future ocean color satellites.

Introduction

Ocean color remote sensing using well-calibrated sensors aboard satellites has emerged as a key contributor to basic knowledge of oceanic and coastal ecology. Continuous and consistent observations stretching back over three decades have revealed optical signals related to seasonal, annual, and decadal scale variability in phytoplankton and suspended sediments and bio-optical responses to extreme events. The satellite data records define historical conditions on a global scale that serve as benchmarks with which to compare future changes. However, emerging oceanic problems related to climate change, e.g., oceanic uptake of atmospheric CO_2 and resulting impacts of ocean acidification, requires that we develop the capability to monitor ocean biogeochemical processes in greater detail and fidelity. To meet these challenges, future ocean color satellite systems, such as the NASA Pre-Aerosol, Clouds, and ocean Ecosystem (PACE) and Geostationary Coastal and Air Pollution Events (GEO-CAPE) missions, will include sensors capable of imaging the ocean throughout the visible and near-infrared spectrum with greater spatial and spectral resolution and radiometric sensitivity. These enhanced capabilities are expected to result in better understanding of phytoplankton populations and primary production rate, relationships between ocean biological and physical processes, carbon transport between terrestrial, atmospheric, and oceanic environments, and impacts of climate variability and trends on present and future ocean services.

Providing accurate information derived from ocean color imagery requires a well coordinated and executed program of in situ observations designed to aid in the calibration of satellite sensors and validate operational and emerging product algorithms; a process collectively referred to as CAL/VAL. Historically, this has been accomplished through field operations involving research vessels, moorings (e.g. MOBY and BOUSSOLE), and stationary offshore platforms (e.g., the Aqua Alta Oceanographic Tower) and dedicated to CAL/VAL objectives. While these approaches serves well the development and production of heritage standard products and should be continued to support future satellite systems, future in situ operations must also be more integrated with physical and biogeochemical observation

activities if we are to maximize the value of future ocean color remote sensing systems and achieve the stated ocean color science goals related to climate change.

Over the last quarter century, autonomous ocean observing systems have emerged to yield continuous data streams of increasingly interdisciplinary scope. These ocean observatories, using both moored and mobile platforms, have resulted in new insights regarding biogeochemical processes, often in response to ocean physical, atmospheric, and terrestrial forcing. Optical (spectral a, b_b, c, E_s, E_d, and PAR) and biogeochemical (DO, pH, CO_2, and nutrient) sensors, of utility in ocean color research, have evolved to form the core of many modern ocean observatories, such as the Australian Integrated Marine Observing System (IMOS) and the United States Integrated Ocean Observing System (IOOS). In the case of IOOS, the Ocean Observatories Initiative (OOI) component currently under construction will come on line in 2015 and will field a variety of optical and biogeochemical sensors within moored arrays and on ocean gliders at two coastal sites (the Pioneer array off the northeast coast of the US and the Endurance Array off the northwest coast) and four high latitude sites (the Irminger Sea in the North Atlantic, Ocean Station PAPA in the North Pacific, the Argentine Basin in the South Atlantic, and the South Pacific off the southwest coast of Chile). Observatories such as these can potentially fill critical ocean color science data needs in the future.

In addition to fixed observatories, the international Argo program offers opportunities to develop profiling floats with optical and biogeochemical sensors and to deploy them in consort with the 3000+ existing Argo floats collecting temperature and conductivity data. The Argo program plans to start deploying floats equipped with dissolved oxygen sensors, in addition to temperature and salinity.

In order to continue the production of heritage products and achieve future ocean color science goals, in situ observations must exceed the accuracy requirements of the remote sensing algorithm. While this can largely be achieved using ship-based operations, biofouling often corrupts moored optical and biogeochemical sensors within a few days to weeks of deployment unless anti-biofouling measures are incorporated into the sensor and/or deployment design and combined with appropriate operations and maintenance plans. While protocols have been established for ship-based operations in support of ocean color science, such protocols have yet to be established for sustained deployments characteristic of modern ocean observatories and profiling drifters. Given the international scope of problems that ocean color science will address and the need for in situ data representing the global ocean, it is proposed that a working group composed of observatory and float operators be established with international support and participation to develop protocols and standards for sustained, in situ optical an biogeochemical observations.

Conclusions

Ocean color science, based on a foundation of accurate, in situ observations employing emerging ocean observatory infrastructures and evolving profiling float technology, is poised to play a key role in understanding climate-related changes in global ocean ecology. However, deploying and maintaining the necessary in situ optical and biogeochemical sensors within a sustained, autonomous observatory presents quality control and assurance challenges that must be met before the data can be used for CAL/VAL activities or employed in ocean biogeochemical process studies.

Assessments of VIIRS Ocean Color data retrieval performance in coastal regions

S. Ahmed[1], A. Gilerson[1], S. Hlaing[1], A. Weidemann[2], R. Arnone[3], and M. Wang[4]

[1] Optical Remote Sensing Laboratory, City College, New York, NY 10031, United States
[2]Naval Research Laboratory, Stennis Space Center, MS 39529, United States
[3]University of Southern Mississippi, MS 39529, United States
[4]NOAA/NESDIS Center for Satellite Applications and Research, College Park, MD 20740.
Email: ahmed@ccny.cuny.edu

Summary

The quality of the VIIRS Ocean Color (OC) products, namely the normalized water-leaving radiances (nLw) and atmospheric products (i.e., aerosol optical thickness and Angstrom exponent), are analyzed for coastal waters conditions encountered at the LISCO and WaveCIS AERONET-OC sites. Through statistical analysis carried out between the VIIRS, MODIS and AERONET-OC data, the impacts of the different processing schemes on the VIIRS's OC data retrievals are assessed in order to aid the scientific community to better interpret the physical or biogeochemical meaning of the VIIRS data in coastal areas.

Introduction

The Suomi National Polar-orbiting Partnership (NPP) spacecraft was successfully launched on October 27, 2011 bearing several Earth observing instruments, including the Visible-Infrared Imager Radiometer Suite (VIIRS). In processing of OC data from VIIRS, the NASA Ocean Biology Processing Group (OBPG) is deriving a continuous temporal calibration based on the on-board calibration measurements for the visible bands, and then reprocessing the full mission to produce a continuously calibrated sensor data record (SDR) product. In addition, an additional vicarious calibration during SDR to OC Level-2 processing is applied [1, 2]. In this latest processing (version 2012.2), the vicarious calibration is derived from the Marine Optical Buoy (MOBY) data [3] whereas previously it was derived from a sea surface reflectance model and a climatology of chlorophyll-a concentration in the initial processing [2]. More recently, in fulfillment of the mission of the U.S. National Oceanic and Atmospheric Administration (NOAA), the Interface Data Processing Segment (IDPS) developed by Raytheon Intelligence and Information Systems, for the processing of the environmental data products from sensor data records, has gained beta status for evaluation. Consequently , assessments of the VIIRS ocean color products are necessary, especially for coastal, waters to evaluate the consistency of these processing and calibration schemes.

Discussion and results

The ocean color component of the Aerosol Robotic Network (AERONET-OC) has been designed to support long-term satellite ocean color investigations through cross-site measurements collected by autonomous multispectral radiometer systems deployed above water. As part of this network, the Long Island Sound Coastal Observatory (LISCO) near New York City and WaveCIS in the Gulf of Mexico expand those observational capabilities with continuous monitoring, and for the LISCO site, with additional assessment of the hyper-spectral properties of these coastal waters [4]. From investigations carried out over a period of almost one year, there is now a VIIRS dataset based on the data from two coastal AERONET-OC sites, where it has been observed that the VIIRS sensor can capture well the seasonal and

temporal variations in the *nLw* data, while exhibiting significant correlation with in-situ data (*R* equal to 0.968 and 0.977 for LISCO and WaveCIS respectively). For the WaveCIS site, VIIRS *nLw* data retrieval is improved with version 2012.2 processing schemes, reducing the retrieval biases at every wavelength. However, that is not the case for the LISCO site, which shows more frequent occurrences of negative water-leaving radiances, and where underestimation in VIIRS *nLw* data is further exacerbated. This points out that the impacts of vicarious calibration procedures are not the same for the coastal areas with different water/atmosphere conditions and probably suggests the need to take into account comparisons between AERONET-OC and satellite data for coastal sites before making decisions on changes of sensor gains.

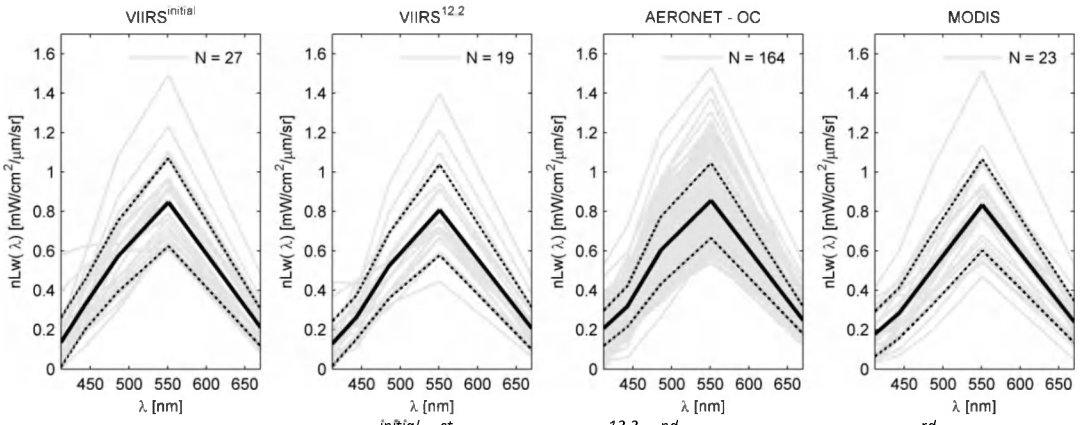

Figure 1. nLw(λ)match-up spectra of VIIRS^{initial}(1stcolumn), VIIRS$^{12.2}$(2nd column), SeaPRISM (3rd column) and MODIS (4th column) for the LISCO site. N is the total number of spectra for each sensor. Grey lines represent the individual spectra. Thick black solid lines indicate average and thick dashed lines indicate ± one standard deviation).

Strong consistency between the time-series *nLw* data retrieved from the VIIRS and MODIS sensors was also observed. Evaluations of the aerosol optical thickness, τ_a, data exhibits significant correlation but with substantial overestimations in the case of VIIRS data. Impacts of the aerosol model selection over the atmospheric correction procedure will be also discussed.

REFERENCES

[1] B. A. Franz, S. W. Bailey, P. J. Werdell, and C. R. McClain, "Sensor-independent approach to the vicarious calibration of satellite ocean color radiometry," Applied optics 46, 5068-5082 (2007).

[2] P. J. Werdell, S. W. Bailey, B. A. Franz, A. Morel, and C. R. McClain, "On-orbit vicarious calibration of ocean color sensors using an ocean surface reflectance model," Applied optics 46, 5649-5666 (2007).

[3] D. K. Clark, M. A. Yarbrough, M. Feinholz, S. Flora, W. Broenkow, Y. S. Kim, B. C. Johnson, S. W. Brown, M. Yuen, and J. L. Mueller, "MOBY, a radiometric buoy for performance monitoring and vicarious calibration of satellite ocean color sensors: measurement and data analysis protocols," Ocean Optics Protocols for Satellite Ocean Color Sensor Validation, Revision 4, 3-34 (2003).

[4] T. Harmel, A. Gilerson, S. Hlaing, A. Tonizzo, T. Legbandt, A. Weidemann, R. Arnone, and S. Ahmed, "Long Island Sound Coastal Observatory: assessment of above-water radiometric measurement uncertainties using collocated multi and hyperspectral systems," Applied optics 50, 5842-5860 (2011).

Towards phytoplankton community structure detection thanks to the synergy between theoretical approach and in situ observations.

ALVAIN, Severine[1]; Loisel, Hubert[1]; Dessailly, David[1] ; Thyssen Melilotus[3] ;Morin Pascal[2] ;Guiselin Natacha[1] ; Macé Eric[2].

[1]LOG - CNRS 32 avenue Foch, Wimereux, 62930, France

[2]Station Biologique de Roscoff, CNRS-UPMC, Roscoff France

[3]Mediterranean Institute of Oceanology, 13288 Marseille

Despite observations in good agreement with *in situ* measurements, the underlying theoretical explanation of methods based on radiances anomalies to detect phytoplankton groups (like the PHYSAT one) is missing. This prevents improvements of the methods and limits characterization of uncertainties on the inversed products. In a recent study, radiative transfer simulations have been used in addition to in-situ measurements to understand the organization of the radiances anomalies used in the PHYSAT method. Sensitivity analyses have been performed to assess the impact of the variability of the following three parameters on the reflectance anomalies: specific phytoplankton absorption, colored dissolved organic matter absorption, and particles backscattering. While the later parameter explains the largest part of the anomalies variability, results show that each group is generally associated with a specific bio-optical environment which should be considered in future studies. We will show that the magnitude of the theoretically defined anomalies for the three main PHYSAT groups is in good agreement with specific anomalies empirically highlighted before. Complementary studies, based on large *in situ* database of IOPs measurements, will be necessary in the future to obtain a better agreement between the theoretical and PHYSAT spectral anomalies for the different groups. A project based on automatic in situ measurements approaches on board ferry-box is proposed. We will show also how our recent work opens doors for improving phytoplankton groups' detection when coupled with in situ expertise. For example, the definition of the validity ranges for each group based on their optical properties in order to avoid misclassification. This also opens new potential development by considering phytoplankton groups and composition and their environmental conditions together.

Satellite-derived ocean primary production inferred by an optimality-based phytoplankton model

Lionel Arteaga, Markus Pahlow and Andreas Oschlies

GEOMAR | Helmholtz Centre for Ocean Research Kiel
Email: larteaga@geomar.de

Summary

Optimality-based models of phytoplankton growth offer the potential to help understand the interrelations between phytoplankton stoichiometry and primary production in the ocean. Here we apply an optimality-based model to analyze remote-sensing and in-situ data in order to infer seasonally varying patterns of growth colimitation by light, nitrogen, and phosphorus in the global ocean. Based on these results, we seek to estimate global marine primary production, derived from satellite estimations of nutrient (nitrogen) and light, using a model that accounts for acclimation of the chlorophyll to carbon ratio (Chl:C). One of the aims of this study is to investigate to what extent having a flexible Chl:C ratio alters primary production estimations with respect to more traditional ocean color derived algorithms.

Introduction

Our current understanding of the physical and biogeochemical controls on marine biological production does not allow to accurately describe its future evolution under changing climate and environmental conditions. To better assess how primary production and phytoplankton growth may change in the future, it is essential to know what limits production under present circumstances. While limitation by a single resource is possible, different flavors of colimitation can occur as well [1]. Which combination of factors limits growth may control both magnitude and sign of the response of the ecosystem to CO_2-driven global changes such as warming-induced stratification.

Here we use the optimality-based chain model [3] as a mechanistic foundation for the physiological regulation of nutrient acquisition and light harvesting to diagnose N, P, and light limitation, based on field and satellite data of nutrients, light, and temperature in the surface ocean. Based on these results, we also use the model to estimate global marine primary productivity.

Results and Discussion

Our model-based results indicate nitrogen and light as the main two factors controlling phytoplankton growth in the global ocean. There is essentially no ocean region with dominant phosphorus limitation. While our current version of the model does not include iron, we believe that acounting for this nutrient will accentuate light limitation

in well known iron limited areas such as the Southern Ocean.

As nitrogen is identified as the major limiting nutrient, we use a multiple linear model to estimate nitrate concentrations in the surface ocean, from satellite data of sea surface temperature, mixed layer depth, and chlorophyll. Photosynthetically active radiation is represented by the "Median Mixed Layer Light Level" [I_g, 4]. I_g approximates the average light intensity experienced by phytoplankton in the surface mixed layer.

So far our carbon-based primary production estimates are higher than those obtained by more traditional ocean color models [e.g. 5]. Our next step is to analyze differences in marine productivity resulting from the physiological acclimation of phytoplankton to different seasonal nutrient and light limitation regimes.

This work is a contribution of the Seventh Framework Programme (FP7) - project "Ocean Strategic Services beyond 2015" (www.oss2015.eu).

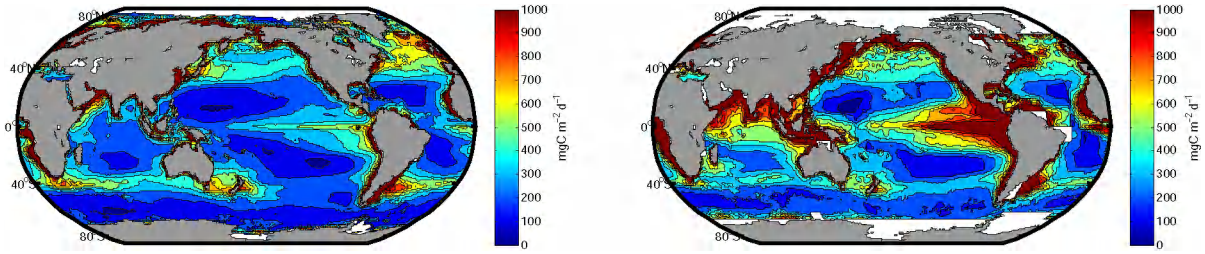

Figure 1: Global marine primary production derived from satellites. Left: Vertical Generalized Production Model (VPGM) [5]. Right: Combined satellite and optimality-based model.

References

[1] Saito, M. A., Goepfert, T. J. & Ritt, J. J. Some thoughts on the concept of colimitation: Three definitions and the importance of bioavailability. *Limnol. Oceanogr.* **53**, 276–290 (2008).

[2] Riebesell, U., Kötzinger, A. & Oschlies, A. Sensitivities of marine carbon fluxes to ocean change. *Proc. Nat. Acad. Sci. USA.* **106**, 20602–20609 (2009).

[3] Pahlow, M. & Oschlies, A. Chain model of phytoplankton P, N and light colimitation. *Mar. Ecol. Prog. Ser.* **376**, 69–83 (2009).

[4] Behrenfeld, M. J., Boss, E., Siegel, D. A. & Shea, D. M. Carbon-based ocean productivity and phytoplankton physiology from space. *Global Biogeochem. Cycles* **19**, GB1006 (2005). Doi:10.1029/2004GB002299.

[5] Behrenfeld, M. J. & Falkowski, P. G. Photosynthetic rates derived from satellite-based chlorophyll concentration. *Limnol. Oceanogr.* **42**, 1–20 (1997).

DIMITRI: the Database for Imaging Multi-Spectral Instruments and Tools for Radiometric Intercomparison

M. Bouvet[1], K. Barker[2], A. Tichit[2], D. Marrable[2]

[1]ESA / Estec, Noordwijk, postbus 299, 2200 AG Noordwijk, Netherlands
[2]ARGANS Ltd, 19 Research Way, Tamar Science Park, Plymouth, Devon, PL6 8BT, UK
Email: mbouvet@esa.int

Summary

There is a growing use of satellite remote sensing data in the visible and near infrared spectral band range in short and long term environmental monitoring studies; therefore, there is a need to ensure satellite instruments are accurately calibrated. One approach is to compare measurements between two space sensors, at the TOA measurement level, over the same target at the same time, under the same viewing geometries and in identical spectral bands. Such direct comparison also removes the need for in-situ measurements and radiative transfer forward or inverse modeling. The Database for Imaging Multi-Spectral Instruments and Tools for Radiometric Intercomparison (DIMITRI) was developed with this approach and aims towards the goals of the Global Earth Observation System of Systems for an operational radiometric calibration system. DIMITRI is open-source and gives users the capability of long term monitoring of instruments for systematic biases and calibration drift. It was included in the CEOS/IVOS intercomparison of methodologies making use of pseudo-invariant sites for vicarious calibration or for radiometric intercomparisons. A full report is available on the CalVal Portal at: http://calvalportal.ceos.org/cvp/web/guest/ivos/wg4.

DIMITRI functionalities

DIMITRI (Fig 1) comes with a suite of tools for comparison of the L1b radiance and reflectance values originating from various medium resolution sensors over a number of radiometrically homogenous and stable sites (Table 1) at TOA level, within the 400nm – 4µm wavelength range. The date range currently available is 2002 to 2012. DIMITRI has been developed with a user-friendly interface enabling radiometric intercomparisons based on user-selection of a reference sensor, against which other sensors are compared. DIMITRI contains site reflectance averages and standard deviation (and number of valid pixels in the defined region of interest, or ROI), viewing and solar geometries and auxiliary information. Each observation is automatically cloud screened; manual cloud screening is also visually performed using product quicklooks. DIMITRI also provides a platform for radiometric intercalibration from User defined matching parameters: geometric, temporal, cloud

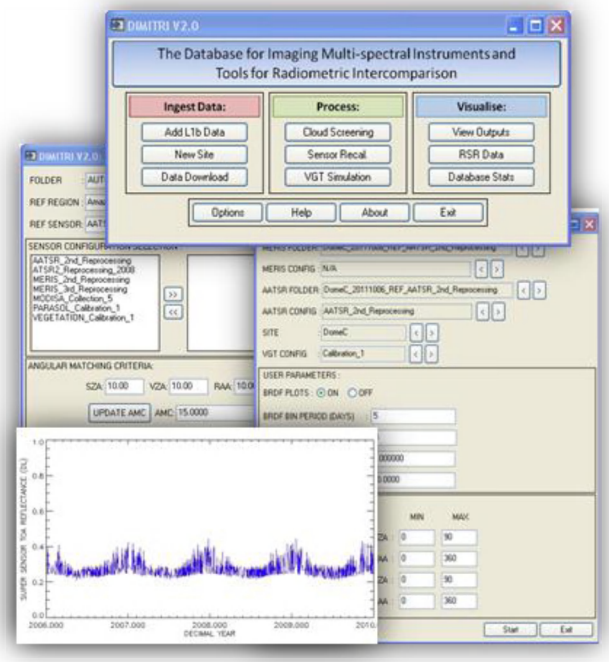

Fig. 1 The DIMITRI graphical user interface

and ROI coverage. Other capabilities and functions include: product reader and data extraction routines, radiometric recalibration & bidirectional reflectance distribution function (BRDF) modelling, quicklook generation with ROI overlays, instrument spectral response comparison tool, VEGETATION simulation.

Table 1: Sensors and sites included in the DIMITRI V2.0 database

SENSOR	Supplier
AATSR (Envisat)	ESA
MERIS, 2nd & 3rd reprocessing (Envisat)	ESA
ATSR-2 (ERS-2)	ESA
MODIS-A (Aqua)	NASA
POLDER-3 (Parasol)	CNES
VEGETATION-2 (SPOT5)	CNES

Site	Site type
Salar de Uyuni, Bolivia	Salt lake
Libya-4, Libyan Desert	Desert
Dome-Concordia, Antarctica	Snow
Tuz Golu, Turkey	Salt Lake
Amazon Forest	Vegetation
BOUSSOLE, Mediterranean Sea	Marine
South Pacific Gyre (SPG)	Marine
Southern Indian Ocean (SIO)	Marine

DIMITRI methodologies

Two methodologies are presently implemented in DIMITRI:

1. **Radiometric intercomparison based on angular and temporal matching:** Concomittant observations ("doublets") made under similar geometry and within a defined temporal window are intercompared at similar spectral bands. This assumes the TOA reflectance angular distribution obeys the principle of reciprocity and is symmetrical with respect to the principal plane [1]. The day offset and strictness of angular matching between observations of two sensors, as well as the allowable cloud cover percentage values can be user defined, and the closest geometric match is selected and stored in the time series. It is estimated that the systematic uncertainty of this methodology is approximately 3%, and its random uncertainty component approximately 2%. For intercalibration, doublets are intercompared, and a least squares regression used to apply a polynomial fit to the temporal differences between the calibration and reference sensor doublets for each intercomparable band, from which the entire calibration sensor time series can be recalibrated over a validation site to the same radiometric scale as the reference sensor. The two complete time series over the validation site are then stored as a "super sensor" time series.
2. **Radiometric intercomparison of VEGETATION simulated and actual observations:** DIMITRI makes use of the super sensor time series from methodology 1 to fit a 3-parameter BRDF model to all observations falling within a defined binning period, for each spectral band corresponding to a reference sensor, MERIS (with the 1.6 µm band coming from ATSR-2). These spectral BRDF models are used to simulate TOA spectra (corrected for the atmospheric gaseous absorption transmission) at the date and in the geometry of VEGETATION-2 acquisitions, then ultimately convolved with VEGETATION-2 spectral responses, and compared to the observed VEGETATION-2 reflectances [2].

How to get DIMITRI:

DIMITRI is maintained by ESA and ARGANS, and is freely available at http://www.argans.co.uk/dimitri/.

References

[1] Bouvet, M. (2006). Intercomparisons of imaging spectrometers over the Salar de Uyuni (Bolivia). *Proc. 2nd MERIS and AATSR Calibration and Geophysical Validation Meeting (MAVT-2006)*, 20-24 March 2006, ESRIN.

[2] Bouvet M., Goryl P., Chander G. Santer R., and Saunier S. 2007. Preliminary radiometric calibration assessment of ALOS AVNIR-2. Proc. Geoscience and Remote Sensing Symposium, IGARSS 2007

The MERis MAtchup In-situ Database (MERMAID) and Validation Facility

Kathryn Barker[1], Constant Mazeran[2], Christophe Lerebourg[2], Jean-Paul Huot[3],

[1]ACRI-ST, 260 route du Pin Montard, Sophia Antipolis, 06600, France
[2]ARGANS Ltd, 19 Research Way, Tamar Science Park, Plymouth, Devon, PL6 8BT, UK
[3]ESA / Estec, Noordwijk, postbus 299, 2200 AG Noordwijk, Netherlands

Summary

MERMAID is a freely available facility for validation and development of marine bio-optical algorithms, consisting of a database of bio-optical match-ups, i.e. concurrent in-situ and Earth-Observation data, developed in collaboration with Principal Investigators, including a detailed documentation of the protocols, sanity and quality checks of the datasets and further processings to best match the satellite data. MERMAID complements the Optical Data processor of ESA (ODESA, see dedicated presentation), providing validation against data of known quality in a perfectly controlled configuration.

1. Introduction

An integral requirement for optical satellite sensor cal/val activities is the gathering of reliable match-ups between in-situ data of known quality, and concurrent satellite data extraction. In 2007 the European Space Agency (ESA) initiated together with ACRI-ST and ARGANS the MERMAID facility (http://hermes.acri.fr/mermaid; [1], [2]) to meet this goal for the MERIS sensor, involving closely a community of Principle Investigators (PIs). Since 2011 MERMAID has become a facility open to any ocean colour researcher, aimed at solving two major difficulties: i) bringing together communities of PIs and algorithm developers with traceable protocols, clear data proprietary rights, and easy-to-use data extractions; ii) merging different sources of data, for providing statistically and physically relevant number of match-ups.

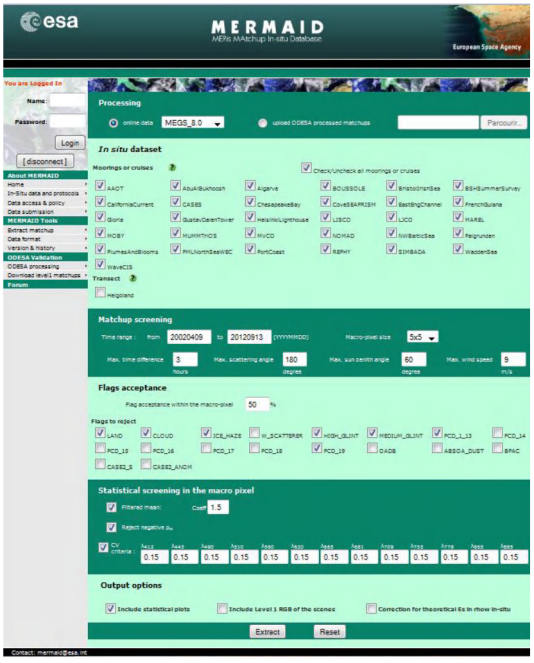

MERMAID interactive interface

MERMAID is an ever-developing database; new scientists are welcome (contact mermaid@esa.int). Use of MERMAID follows adherence to a data policy ensuring PIs' data ownership and MERMAID service acknowledgment.

2. Data Catalogue

MERMAID comprises more than 30 in-situ sites worldwide with associated MERIS data extractions (1km resolution). Datasets derive from permanent stations, cruises or transect profiles, and are classified as i) Long-term permanent stations for sensor calibration and validation; ii) Occasional national or international oceanographic cruises; iii) Regular regional measurements by research laboratories; iv) Regular measurements for national water monitoring.

Available in-situ quantities include (not exhaustively):

- **Apparent Optical Properties (AOPs):** e.g. normalised water reflectance (ρ_{wN}) at measurement wavelengths and satellite wavelengths when possible, solar illumination (*Es*);
- **Inherent optical properties (IOPs):** Total absorption coefficient (*a*, including pure seawater absorption a_w), and component absorption coefficients; total scattering (*b*, including pure seawater scattering b_w), and component scattering coefficients; particulate backscattering (b_{bp});
- **Bio-optical constituents concentration:** Total Chl-a and chl_a only derived from HPLC, spectrophotometric chlorophyll-a, fluorometric chlorophyll-a, total suspended matter (TSM);
- **Atmospheric measurements:** aerosol optical thickness (τ) and the angstrom exponent (α) for AERONET-OC sites, both provided at two times bracketing the sensor overpass.

3. Features, facilities and quality control

- **In-situ measurement protocols and QC documentation:** Accompanying all in-situ measurements on the website: i) *AOPs* and *ii) IOPs and in-water constituents.*
- **Interactive matchups building:** MERMAID's interactive interface builds match-ups according to a number of user-selected criteria, with default options following [3]. Criteria include: macro-pixel size, time difference between in-situ and satellite, geometry and flagging to remove unreliable pixels. Statistical screening removes outliers in the macro-pixel.
- **Text data files (merged in-situ and satellite), statistics and graphics:** Statistics of the satellite versus in-situ data; scatter plots and stacked histograms; True colour images of 10°x10°.
- **QC indicators:** to indicate adherence to a clearly defined measurement and processing protocols by the PI, and post-submission quality control performed on the in-situ data;
- **Marine reflectance normalisation:** A bidirectional effects correction on ρ_w; same approach as that used in the MERIS processor and AERONET-OC data.
- **Optical bandshifting:** To minimise potential error caused by mismatched wavebands between in-situ and satellite, the bandshift correction scheme described in [4] is applied in the MERMAID processing of AAOT, Gustav-Dahlen Tower and Helsinki Lighthouse.
- **Correction for in-situ solar irradiance in ρ_w:** To negate potential effects of tilt on buoys in the measured Es values, and to bring consistency in the solar illumination used in the computation of the in-situ reflectance, with the MERIS formulation of Es estimated at ground level.
- **Correction for the skydome on in-situ ρ_w:** AERONET-OC SeaPRISM and MUMMTrios datasets [5].

References

[1] Barker, K., Mazeran, C., Lerebourg, C., Bouvet, M., Antoine, D., Ondrusek, M. E., Zibordi, G. & Lavender, S. J. (2008). MERMAID: The MERis MAtchup In-situ Database. In Proc. 2nd MERIS (A)ATSR Users Workshop, Frascati, Italy. September 2008.

[2] Mazeran, C., Lerebourg, L., Barker. K., Kent, C. and Huot, J.-P. MERMAID and ODESA: Complementary Marine Bio-optical Processing and Validation Facilities. Proc. Ocean Optics XXI, Glasgow October 2012.

[3] Bailey, S.W. &Werdell, P.J. (2006). A multi-sensor approach for the on-orbit validation of ocean color Satellite data products. Remote Sensing of the Environment 102: 12-23.

[4] Zibordi, G., Berthon, J.-F., Mélin, F., D'Alimonte, D. & Kaitala, S. (2009b). Validation of satellite ocean color primary products at optically complex coastal sites: Northern Adriatic Sea, Northern Baltic Proper and Gulf of Finland. Remote Sensing of the Environment doi:10.1016/j.rse.2009.07.013: 18.

[5] Santer, R. and F. Zagolski (2012). ATBD: Correction of the water-leaving radiance for the Fresnel reflection of the sky dome accounting for the polarization, ADRINORD, for ESA; 9 January, 2012.

Absorption and pigment characteristics of phytoplankton size classes in the Mozambique Channel

R. Barlow[1,2], T. Lamont[2,3]

[1]Bayworld Centre for Research & Education, Oceanography Unit, Cape Town 8012, South Africa
[2]Marine Research Institute, University of Cape Town, Rondebosch 7701, South Africa
[3]Department of Environmental Affairs, Oceans & Coasts Research, Cape Town 8012, South Africa
Email: rgb.barlow@gmail.com

Summary

An in situ study of the absorption and pigment properties of phytoplankton size classes in the Mozambique Channel was undertaken with a view towards application of satellite data to monitor seasonal and interannual change in community structure in the Channel. The relationship between a_{ph} (443) and TChla displayed the usual power function but there was a distinct separation between the size classes in their absorption and TChla characteristics. There were very few data points dominated by microplankton but these were associated with absorption coefficients >0.06 m^{-1} and TChla >0.8 mg m^{-3}. Picoplankton had absorption coefficients of <0.026 m^{-1} and TChla of <0.25 mg m^{-3}. The absorption coefficients for nanoplankton were within the range 0.026-0.06 m^{-1} and the TChla associated with nanoplankton was 0.25-0.8 mg m^{-3}.

Introduction

Satellite ocean colour sensors have provided the means to acquire remotely sensed data on phytoplankton for the world ocean [1], and further developments have allowed more detailed observations on the composition of communities from space [2]. Water-leaving radiances that are detected by the satellite sensors are related to the absorption and backscattering of light in the ocean, and size structure of particles influences both absorption and scattering properties [3]. There are established links between phytoplankton classes and biomarker pigments [4] and oceanographic observations have shown links between absorption properties and phytoplankton pigments [5]. This has enabled the development of bio-optical models relating absorption at 443 nm to phytoplankton size classes derived from diagnostic pigments, which can be applied to satellite data to investigate community structure on large scales [6]. In this study, an in situ absorption and pigment data set acquired for the Mozambique Channel was used to examine the absorption characteristics of phytoplankton size classes with a view towards a regional application of satellite data to monitor seasonal and interannual change in community structure in the Channel. The Mozambique Channel is unique in that the physical oceanography is dominated by the flow of anticyclonic and cyclonic eddies through the Channel that has a strong influence on the distribution pattern of phytoplankton.

Discussion

Discrete samples were drawn from the surface and the deep chlorophyll maximum on 3 research cruises in the Channel during 2008-2010 and analysed for spectral absorption by the filter pad technique [7] and pigments using liquid chromatography [8]. Seven diagnostic pigments and weighted coefficients were used to proportion the contribution of the taxonomic groups to the total chlorophyll *a* concentration (TChla) [9]. The taxonomic groups were then allocated to either the micro-, nano- or picoplankton classes. Relationships between absorption at 443 nm (a_{ph} (443)) and TChla associated with each size were examined to determine the absorption characteristics for each class.

Plots of the weighted biomarker pigment/total diagnostic pigment ratio versus TChla confirmed that Fuc and Per could be allocated to the microplankton and Zea to the picoplankton. Similarly, Hex, But and Allo were allocated to the nanoplankton. In the Uitz et al method [9], Chlb plus divinyl Chlb were allocated to the picoplankton but in this study Chlb and divinyl Chlb were partially separated by the HPLC method and Chlb could be quantified as an independent biomarker. The Chlb ratios were very low at TChla levels <0.25 mg m^{-3} and were highest in the 0.25-0.8 mg m^{-3} TChla range. Chlb was therefore allocated to the nanoplankton.

The relationship between a_{ph} (443) and TChla displayed the usual power function but there was a distinct separation between the size classes in their absorption and TChla characteristics. There were very few data points dominated by microplankton but these were associated with absorption coefficients >0.06 m^{-1} and TChla >0.8 mg m^{-3}. Picoplankton had absorption coefficients of <0.026 m^{-1} and TChla of <0.25 mg m^{-3}. The absorption coefficients for nanoplankton were therefore within the range 0.026-0.06 m^{-1} and the TChla for nanoplankton was 0.25-0.8 mg m^{-3}.

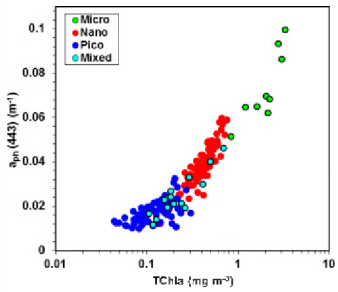

a_{ph} (443) versus TChla

Conclusions

In situ observations in the Mozambique Channel indicated that picoplankton generally dominated the surface waters in anticyclonic and cyclonic eddies [10]. But microplankton and nanoplankton could be significant in frontal zones between eddies, and near the Mozambique shelf due to eddy interaction with the continental slope [10]. It is the intention to apply the in situ size class absorption characteristics derived in this study to satellite absorption data to map the surface distribution of micro- nano- and picoplankton in more detail across the Mozambique Channel. A mesoscale investigation of the seasonal and interannual variation in community structure in relation to environmental and climate change can then be undertaken.

References

[1] Antoine D, Morel A, Gordon H, Banzon V, Evans R. 2005. Bridging ocean colour observations of the 1980s and 2000s in search of long-term trends. J. Geophys. Res., 110: C06009.
[2] Alvain S, Moulin C, Dandonneau Y, Breon F. 2005. Remote sensing of phytoplankton groups in case 1 waters from global SeaWiFS imagery. Deep-Sea Res. I, 52: 1989-2004.
[3] Mouw C, Yoder J. 2010. Optical determination of phytoplankton size composition from global SeaWiFS imagery. J. Geophys. Res., 115: C12018.
[4] Barlow R, Aiken, J, Holligan P, Cummings, D, Maritorena S, Hooker S. 2002. Phytoplankton pigment and absorption characteristics along meridional transects in the Atlantic Ocean. Deep-Sea Res. I, 47: 637-660.
[5] Fishwick J, Aiken, J, Barlow R, Sessions H, Bernard, S, Ras J. 2006. Functional relationships and bio-optical properties derived from phytoplankton pigments, optical and photosynthetic parameters: a case study in the Benguela ecosystem. J. Mar Biol. Assn. UK, 86: 1267-1280.
[6] Hirata T, Aiken J, Hardman-Mountford N, Smyth T, Barlow R. 2008. An absorption model to determine phytoplankton size classes from satellite ocean colour. Remote Sensing Environ., 112: 3153-3159.
[7] Bricaud A, Stramski D. 1990. Spectral absorption coefficients of living phytoplankton and nonalgal biogenous matter: A comparison between the Peru upwelling area and the Sargasso Sea. Limnol. Oceanogr., 35: 562-582.
[8] Barlow R, Lamont T, Kyewalyanga M, Sessions H, Morris T. 2010. Phytoplankton production and physiological adaptation on the southeastern shelf of the Agulhas ecosystem. Cont. Shelf Res., 30: 1472-1486.
[9] Uitz J, Claustre H, Morel A, Hooker S, 2006. Vertical distribution of phytoplankton communities in open ocean: an assessment based on surface chlorophyll. J. GeophYS. Res., 111: C08005.
[10] Barlow R, Lamont T, Morris T, Sessions H, van den Berg M. 2013. Adaptation of phytoplankton communities to mesoscale eddies in the Mozambique Channel. Deep-Sea Res. II, (submitted).

Issues related to ocean colour in coastal zones and inland waters

Stewart Bernard[1,4], Tim Moore[2], Kevin Ruddick[3], Lisl Robertson[4], Mark Matthews[4], Mark Dowell[5] and Stefan Simis[6]

1. NRE Earth Observation, Council for Scientific and Industrial Research, Cape Town, South Africa
2. Tim Moore, Ocean Process Analysis Laboratory, Univ. New Hampshire, Durham NH, USA
3. MUMM, Royal Belgian Institute of Natural Sciences, Brussels, Belgium
4. Oceanography Department, University of Cape Town, Cape Town, South Africa
5. Joint Research Centre, European Commission, Ispra, Italy
6. Finnish Environment Institute (SYKE), Marine Research Centre, Helsinki, Finland

Email: Stewart Bernard <sbernard@csir.co.za>

A review is presented of the principal challenges facing application of ocean colour radiometry to coastal and inland waters, focusing on the ecological, bio-optical and algorithmic aspects. Several example ecosystems are used as illustration: systems that encompass much of the ecological and optical complexity from global coastal and inland water bodies currently suitable for ocean colour application. These are the highly productive Benguela upwelling system, the tidally-dominated North Sea with variable sediment influence, the highly-stratified Baltic showing gelbstoff-rich waters and periodic cyanobacterial blooms, the large meso- to hyper-trophic Lake Erie, and the very small hypertrophic Hartbeespoort Dam in South Africa. A preliminary ecological review is conducted to determine the main temporal scales of variability concerning physical/biogeochemical drivers and biological response and impact. The range in optical complexity of the systems in time and space is also reviewed. The two analyses are used to provide a brief summary of the ocean colour user requirements needed to resolve ecological variability of the systems from the event scale upwards. Useful conceptual frameworks for harmful algal bloom observations, as a major application across coastal and inland water types, are discussed.

More detailed analyses are then used to spectrally characterise the range of water types seen across this diversity of systems - waters dominated by different eukaryotic and prokaryotic phytoplankton functional types at oligo-mesotrophic to hypertrophic biomass; and waters strongly influenced by both suspended sediment and gelbstoff at similar ranges of phytoplankton biomass. Spectral clustering and principal component analyses on hyper-spectral reflectance and associated inherent optical properties from recent publications and work in progress are used. These spectral signal analyses show how the main signal-carrying wavelengths shift to the green – NIR range at high biomass, the resultant importance of the fluorescence and 709 nm bands, and the need to consider the combined effects of reflectance shape and magnitude changes in waters with considerable scattering from both phytoplankton and non-algal particles.

Coupled inherent optical property/radiative transfer models, using optical models of equivalent algal populations and the Ecolight radiative transfer model, are then assessed and used to extend this study more systematically. Causal effects of IOPs on reflectance are considered across trophic ranges; phytoplankton functional types determined by assemblage size, pigment type and vacuole content; and effects of non-algal particles and gelbstoff. Model output is used to more systematically identify key spectral shifts in reflectance, isolate effects of IOP variability, and summarize the diversity in optical properties of coastal and inland waters. A brief summary is then made of the atmospheric

correction issues facing ocean colour use in coastal and inland waters: highly turbid waters, optically complex atmospheres and the need for alternative atmospheric corrections algorithms; and the problems of adjacency and geo-registration, particularly for small water bodies.

Focus is then shifted to community needs for more effective use of ocean colour radiometry in coastal and inland water types. There is a compelling need for more validation data, and standardized methods of data acquisition. Some of the major challenges confronting the acquisition of radiometric and other bio-optical data in turbid and hypertrophic waters are examined, such as significant sub-pixel variability, and instrument/ data processing issues in highly attenuating waters. The need for new bio-optical protocols for such water types, and perhaps new conceptual models for resolving spatial and temporal mismatch, is highlighted. The major advantages and potential disadvantages of synthetic data sets are also assessed, with particular regard to the need for adequate simulation of the natural covariance amongst primary constituents, and appropriate numerical simulation of phytoplankton biodiversity, succession and bio-volume related abundance.

Examples of algorithm options for coastal and inland waters are considered. Several algorithms that bypass the need for aerosol correction in hypertrophic waters are presented, and are used to discuss the advantages of phenological approaches to ocean colour based ecological analyses. Examples of other algorithm types are discussed: empirical, semi-analytical and coupled neural network approaches. The opportunities for system-transferable algorithms and algorithm structures are presented through spectral classification algorithms, with examples from both the global ocean and coastal/inland waters to demonstrate the scalable nature of this approach. The benefits of class- vs regionally-based approaches to algorithm selection and application are briefly discussed.

Finally, the sensor and programmatic outlook for ocean colour application in coastal and inland waters is summarised, with a focus on the user systems needed to maximize the value of forthcoming ocean colour constellations.

Hidden secrets of absolute radiometric calibration

A. Bialek[1], C. L. Greenwell[1], E. R. Woolliams[1], N. Fox[1], G. Zibordi[2]

[1]NPL, Optical Measurement Group, Teddington, TW11 0LW, UK
[2]JRC, Institute for Environment and Sustainability, Ispra, Italy
Email: agnieszka.bialek@npl.co.uk

Summary

This work aimed to reduce absolute radiometric uncertainties for Ocean Colour (OC) radiometers used for *in-situ* measurements (currently typically >2 % for both irradiance and radiance mode [1]) using NMI (National Measurement Institute) traceable irradiance standards. In order to achieve this objective we characterised the radiometers and the calibration approach using a primary NPL traceable irradiance source and provide a comprehensive uncertainty budget for these measurements. This paper provides recommendations for the OC community on absolute radiometric calibration techniques that could reduce uncertainties, and robust uncertainty budget evaluation.

Introduction

In order to determine the reliability of *in-situ* measurements, an uncertainty budget must be established. The components of the budget will vary depending on the measurement method; i.e. for in-water or above-water systems. Additionally, the specific features of a particular measurement platform or system must be accounted for in the uncertainty budget. Radiometric calibration uncertainties are always present in the uncertainty budgets for OC *in-situ* measurements and they make a significant contribution to the overall uncertainty budget. Currently the uncertainty associated with OC *in-situ* measurements are typically around 5 % for blue and green and rapidly increase over the red part of the spectrum [2], and the absolute radiometric calibration is ~2 % of this.

In this paper we describe an absolute irradiance-mode calibration of OC radiometers, using an FEL lamp as a spectral irradiance reference standard and then we present possible areas of improvement. This paper concentrates on irradiance calibration, as the irradiance of the lamp is both used directly, for irradiance calibration, and as a part with a reflectance tile for radiance calibration.

Discussion

The research was performed on multispectral radiometers manufactured by Satlantic. Each radiometer has seven separate spectral bands each in a physically different position on the instrument head.

The uncertainty associated with the spectral irradiance of a typical primary lamp from an NMI is around 1 % - 0.6 %, k=2 across the visible spectral range. That associated with secondary lamp irradiances is ~1.4 % - 1.2 %, k=2 in the same spectral range. When used to calibrate OC radiometers, additional uncertainties due to alignment, repeatability and current will affect the measurements and must be included in the uncertainty budget. The resultant uncertainty associated with the OC radiometer calibration, including lamp irradiance, alignment, repeatability and current setting will be >2 %.

The uncertainty associated with alignment and repeatability can be easily evaluated from the standard deviation of repeat measurements taken (with and without realignment, respectively). The uncertainty associated with alignment could be reduced through a careful alignment procedure, accurate distance settings, efficient stray light shielding, etc. and this would improve repeatability. The tests at NPL considered aspects of the measurement that are not routinely checked. The general recommendation

for a radiance calibration is to increase the lamp tile distance to increase radiance uniformity. However, irradiance responsivity is still measured with a 500 mm lamp-radiometer distance. Figure 1 presents the results of an example FEL lamp irradiance uniformity scan at this distance; the seven blue circles represent the positions of the multispectral radiometer channels. The exact map will vary from lamp to lamp, but generally [1, 3] the maximum irradiance from an FEL is around 2 cm above the optical axis; less frequently a horizontal shift is observed. We found the difference in calibration coefficient between typical calibrations (i.e. with the central channel aligned with the optical axis) and centring each of the channels in turn with the optical axis is up to 1.4 %. This component will influence the results of a standard calibration but is usually not reported.

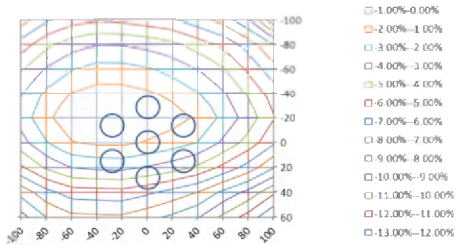

Figure 1 FEL lamp uniformity at 500 mm distance and OCI-200 radiometers channels positions

Another often unreported aspect of calibration is lamp current accuracy. The standard irradiance values from the calibration certificate are only valid for the lamp current setting used in the lamp's calibration and a small offset of 10 mA can lead to a lamp irradiance change of 0.46 % at 515 nm, with increased effect at short wavelengths.

Conclusions

Absolute radiometric calibration is essential for SI-traceable measurements. Uncertainties can be reduced by using a primary irradiance lamp (rather than a secondary standard), through careful alignment procedures and by placing each channel in turn in the centre of the optical axis. Using these approaches we reduced the uncertainty associated with OC-radiometer irradiance responsivity to around 1 % (k = 2). It is important to understand the uniformity of an irradiance source and to provide a correction, either by measuring each channel centrally, or by obtaining a lamp-uniformity scan. The lamp current should be monitored, and ideally controlled, during the calibration and, if any offset noticed, the current offset correction should be applied to the lamp irradiance values.

We expect to achieve further improvements using a monochromatic source, which will allow full spectral responsivity information for each channel. Such sources can also provide higher irradiance, especially in the blue part of the spectrum. NPL has developed a monochromatic source [4] that is portable and suitable for the calibration of both multispectral instruments, such as the ones studied here, and the newer hyperspectral instruments.

This research was performed as a part of the MetEOC Metrology for Earth Observation and Climate Joint Research Project funded by the European Metrology Research Programme EMRP.

References

[1] Hooker, S.B., et al., (1999). The Seventh Sea WiFS Intercalibration Round-Robin Experiment (SIRREX), in NASA Technical Memorandum 2002–206892.
[2] Zibordi, G. and Voss K.J., (2010). Field Radiometry and Ocean Color Remote Sensing. p. 307-334.
[3] Harrison, N.J., Woolliams E.R., and Fox N.P., (2000). Evaluation of spectral irradiance transfer standards. Metrologia, 37(5): p. 453-456.
[4] Levick, A., et al., (2013). A spectral radiance source based on a supercontinuum laser and wavelength tunable bandpass filter: the Spectrally Tuneable Absolute Irradiance and Radiance Source (STAIRS). awaiting publication.

Using in situ fluorescence from animal-borne sensors in the Southern Ocean

L Biermann[1], L Boehme[1], A Brierley[2]

[1] University of St. Andrews, Sea Mammal Research Unit, Scottish Oceans Institute, St. Andrews, KY16 8LB, UK
[2]University of St. Andrews, Pelagic Ecology Research group, Scottish Oceans Institute, St. Andrews, KY16 8LB, UK

Email: lb66@st-andrews.ac.uk

Summary

In the open ocean, phytoplankton are not often masked by dissolved organic matter (CDOM/Gelbstoff), and estimating concentrations of surface Chl-a should be comparatively simple. However, direct measurements are often not possible and limitations of remote sensing tend to be amplified in the high latitudes. Furthermore, satellites can give little resolution of vertical structure of the water column. Fluorescence data returned by animal-borne instruments may provide the means to 'fill in the gaps', provided that information is processed in a way that is useful to the ocean colour community.

Introduction

Phytoplankton respond to light and in summer the euphotic zone often extends as much as 4 times deeper than what satellites can 'see' to. Deep chlorophyll maxima (DCM) are predominantly found over deep ocean basins at depths between 40m - 90m, representing a layer of high biomass that cannot be quantified remotely [1]. In the high latitudes, these phenomena appear to be patchy, yet persistent.

In situ validation is clearly vital. In the Southern Ocean, ship time is especially expensive and limited to a narrow transect in space and time, and autonomous instruments are vulnerable to damage from ice. Fortunately, advances in sampling technologies have made it possible to instrument southern elephant seals (*Mirounga leonina*) with tags capable of measuring and transmitting a range of behavioral and oceanographic data (Sea Mammal Research Unit, University of St. Andrews). Tags are glued to the fur on a seal's head to allow for an Argos-linked aerial to emerge and provide at-sea location during surfacing events [3], and they fall off for retrieval during the annual molt. Salinity, temperature and depth satellite relay data loggers (CTD-SRDL's) are capable of transmitting vertical profiles of salinity (conductivity resolution: 0.003 mS/cm; accuracy: 0.04 mS/cm), temperature (resolution: 0.001°C; accuracy: 0.02°C) and pressure to depths of approximately 2000m [4]. More recently, tags are also capable of measuring fluorescence [5].

Discussion

In order to collect fluorometry data, a Turner Cyclops 7 has been added to the body of a 'conventional' CTD tag. The instrument is programmed to record fluorescence every 2 seconds from 175m to 5m during an ascent, but data is compressed onboard into 10m bins before being relayed to the ARGOS satellite network [4]. Despite this sacrifice in fine-scale resolution, in areas of the Southern Ocean where physical information is difficult to collect using conventional oceanographic methods, animal-borne technologies are invaluable.

For the first time, an adult female southern elephant seal from Marion Island was tagged with a FCTD-SRDL and tracked during the summer of 2012. With insight into deep chlorophyll discovered in other regions of the Southern Ocean, it was hypothesized that a DCM signal would be present over the broad ocean basin to the west of Marion Island. Fluorescence data retrieved through the ARGOS network has shown this to be true, with a strong signal found between 60m – 80m.

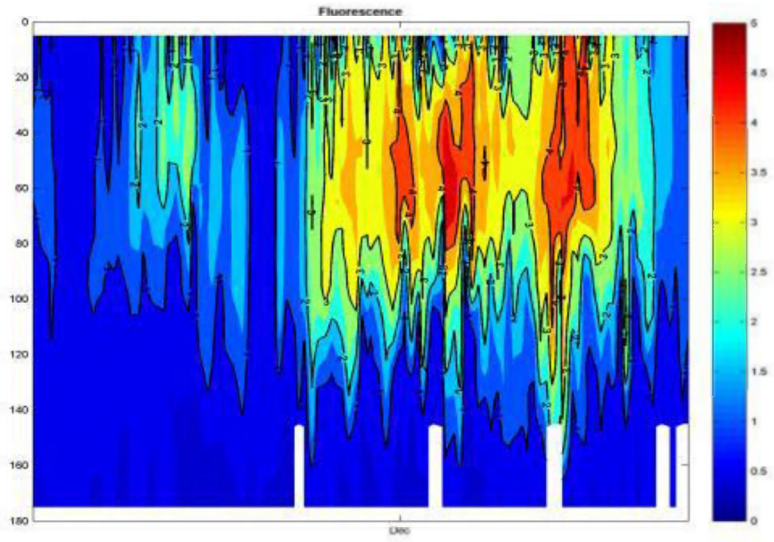

Figure 1. Vertical profiles of fluorescence from the surface to 180m, as collected by an instrumented southern elephant seal from mid-November to late December 2012.

Data were divided into quenched and non-quenched based on the time of day the fluorescence signal was collected, and each dataset was then reviewed separately. Quenched data shows good agreement with MODIS Fluorescence Line Height (L3 8-day composites), whereas non-quenched data shows a relatively good correlation with MODIS Chlorophyll-a (L3 8-day composites).

Conclusion

Currently, animal-borne instruments which measure fluorescence are a useful but possibly underutilized tool for *in situ* validation of ocean colour products. Furthermore, on a vertical scale, this resource may provide the means of elucidating DCM on regional scales.

References

1. O. Holm-Hansen and C.D. Hewes (2004). Deep chlorophyll-a maxima (DCMs) in Antarctic waters. Polar Biology, 27(11):699-710.
2. M.A. Fedak, S.S. Anderson, and M.G. Curry (1983). Attachment of a radio tag to the fur of seals. Journal of Zoology, 200(2):298-300.
3. L. Boehme, P. Lovell, M. Biuw, F. Roquet, J. Nicholson, S.E. Thorpe, M.P. Meredith and M. Fedak (2009). Technical note: Animal-borne ctd-satellite relay data loggers for realtime oceanographic data collection. Ocean Science.
4. X. Xing, H. Claustre, S. Blain, F. D'Ortenzio, D. Antoine, J. Ras, C. Guinet (2012). Quenching correction for in vivo chlorophyll fluorescence acquired by autonomous platforms: a case study with instrumented elephant seals in the Kerguelen region (Southern Ocean). Limnology and Oceanography*: Method*. 10, 483-495.
5. J. Charrassin *et al* (2010). New insights into Southern Ocean physical and biological processes revealed by instrumented southern elephant seals. Proceedings of Ocean Observations 21-25 September 2009: Vol.2

Spatio-temporal variability of water quality parameters in the Van Diemen Gulf coastal waters from 10 years of MERIS Reduced Resolution Satellite Data.

David Blondeau-Patissier[1], Thomas Schroeder[2], Stefan Maier[1], Vittorio Brando[3], Arnold Dekker[3]

[1]Charles Darwin University, The Research Institute for the Environment and Livelihoods, Darwin, NT0909, Australia

[2]CSIRO Land and Water, Brisbane, QLD 4102, Australia

[3] CSIRO Land and Water, Canberra, ACT 2601, Australia

Email: David.Blondeau-Patissier@cdu.edu.au

Summary

The Van Diemen Gulf is a poorly flushed, semi-enclosed embayment of Northern Australia characterised by shallow but optically deep coastal waters (<30m) and a large tidal range (3-8m). High energy local tide currents and seasonal winds provide the main mixing mechanism. The adjacent land is scarcely populated but increasing pressure is placed on the marine environment through expanding fishing and shipping activities, as well as industrial development for oil and gas production and climate change. Despite its environmental and cultural richness, very few studies have reported on the spatio-temporal ecological changes of Van Diemen Gulf's coastal waters over the past decade. This study will present, for the first time, the results of a climatology and time-series analysis to assess change in three main water quality parameters, namely chlorophyll-a, suspended sediment and coloured dissolved organic matter (CDOM), over a period of 10 years (2002-2012).

Introduction

The marine environment of the Northern Territory (Australia) is one of the least human-impacted coastal regions on the planet [1]. Part of this unique coastline is the Van Diemen Gulf, which stretches over an area of ~14,000 km^2 and connects to the Arafura Sea by the Clarence and Dundas straits (*Figure 1*). The oceanographic complexity of the region has long been recognized [2], and enhanced mixing and seasonal upwelling contribute to the sustaining of a persistently turbid surface layer at the edge of the continental shelf throughout the year [3]. While heavy tropical rainfall during the wet season (November-March) produces significant freshwater discharges of sediments, CDOM and nutrients into the Gulf, south-easterly winds transport dry, warm air over the region during the dry season (May-September) and generate the upwelling of cooler, nutrient-rich water. The months of April and October are transition months [4]. The scientific knowledge of material fluxes over space and time in the Van Diemen Gulf is currently very limited and a detailed understanding of these processes is required for future monitoring. This is of particular importance if the frequency and intensity of rainfall continue to increase in this region in the future [5]. With the recent end of the MEdium Resolution Imaging Spectrometer (MERIS) mission, water quality change detection with moderate resolution (1 km) satellite data now relies on Moderate Resolution Imaging Spectroradiometer (MODIS). However the potential of the full mission of MERIS reduced resolution imagery can provide a wealth of information for coastal waters. For this study, Chlorophyll-a, CDOM and total suspended matter derived from 10 years of MERIS Case-2 algorithm FUB [6] will be used to quantify trends.

Discussion and conclusion

Land to coast freshwater discharges during the wet season months result in an increase of the suspended sediment concentrations in the surface waters, which is likely to limit light penetration and in turn, phytoplankton growth. During the dry season however, the waters are likely dominated by coloured dissolved organic matter and a generally higher phytoplankton biomass is observed [7] due to upwelling of nutrients.

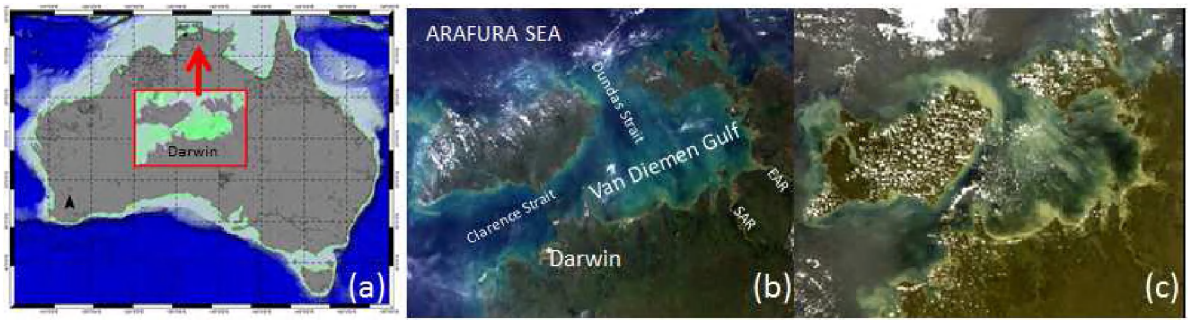

Figure 1 From left to right: (a) Location of the study region with a colour shaded bathymetry and MERIS images showing typical (b) dry and (c) wet season conditions. The two major rivers are shown (SAR: South Alligator River and EAR: East Alligator River)

The absorption properties sampled during the first bio-optical campaign in April 2012 (transition month) helped characterise this system as optically complex. MERIS FUB Case-2 algorithm has been proven to perform generally well in CDOM-dominated temperate waters [8] but its performance remains yet to be tested in the tropical waters of the Van Diemen Gulf. There is an evident lack of in situ measurements for the validation of satellite ocean colour algorithms for those waters however, mainly due to the remoteness of the region. Thus to optically characterise this marine environment and for the validation (and parameterisation) of the satellite algorithms, more bio-optical campaigns are needed.

References

1. Halpern, B.S., et al. (2008). A Global Map of Human Impact on Marine Ecosystems. Science, 319: p. 948-952.
2. Wyrtki, K., *Physical Oceanography of the Southeast Asian waters*. Naga Report. Vol. 2. 1961, La Jolla, California: The University of California, Scripps Institution of Oceanography, UC San Diego.
3. Condie, S.A. (2011). Modeling seasonal circulation, upwelling and tidal mixing in the Arafura and Timor Seas. Continental Shelf Research, 31: p. 1427-1436.
4. Susanto, R.D., T.S. Moore, and J. Marra (2006). Ocean color variability in the Indonesian Seas during the SeaWiFS era. Geochemistry, Geophysics, Geosystems, 7: p. Q05021.
5. Pittock, B. *Droughts and flooding rains: climate change models predict increases in both*. The Conversation, 2012.
6. Schroeder, T., M. Schaale, and J. Fisher (2007). Retrieval of atmospheric and oceanic properties from MERIS measurements: A new Case-2 water processor for BEAM. International Journal of Remote Sensing, 28: p. 5627–5632.
7. Ilahude, A.G. and K. Mardanis (1990). On the hydrology and productivity of the northern Arafura Sea. Netherland Journal of Sea Research, 25: p. 573-583.
8. Kratzer, S., C. Brockmann, and G. Moore (2008). Using MERIS full resolution data to monitor coastal waters -- A case study from Himmerfjärden, a fjord-like bay in the northwestern Baltic Sea. Remote Sensing of Environment, 112: p. 2284-2300.

GMES-PURE:

SHAPING THE MARINE GMES/COPERNICUS USER REQUIREMENTS

P. Gorringe[1], E. Kwiatkowska[2], H. Bonekamp[2], G. Dybkjær[3], K. Nittis[1], P. Albert[2]

[1] EUROGOOS, Brussels, Belgium
[2] EUMETSAT, Darmstadt, Germany
[3] DMI, Copenhagen Denmark
Email: hans.bonekamp@eumetsat.int

Summary

The Copernicus/GMES Marine Core Service (MCS) as currently implemented by MyOcean-2 will become operational in 2014. Recently, the European Commission (EC) has started the two-year project called GMES-PURE (Partnership for User Requirements Evaluation), to define and apply a structured process (see Figure 1) for the elaboration of the future MCS user requirements and their translation into service specifications, service data and technical requirements. While the focus for service data requirements is on space observations, high-level data requirements for in-situ observations will be captured and delivered as well. GMES-PURE constitutes a unique opportunity for MCS users to ensure that their current and emerging requirements are captured in time and to influence the future evolution of the MCS. The establishment and maintenance of long-term user driven operational services requirements and related coherent service specifications include a weighing of evolving user needs, scientific and technological capabilities, cost-effectiveness and affordability. This presentation will explain GMES-PURE approach and roadmap and how users can get and will be involved in the project.

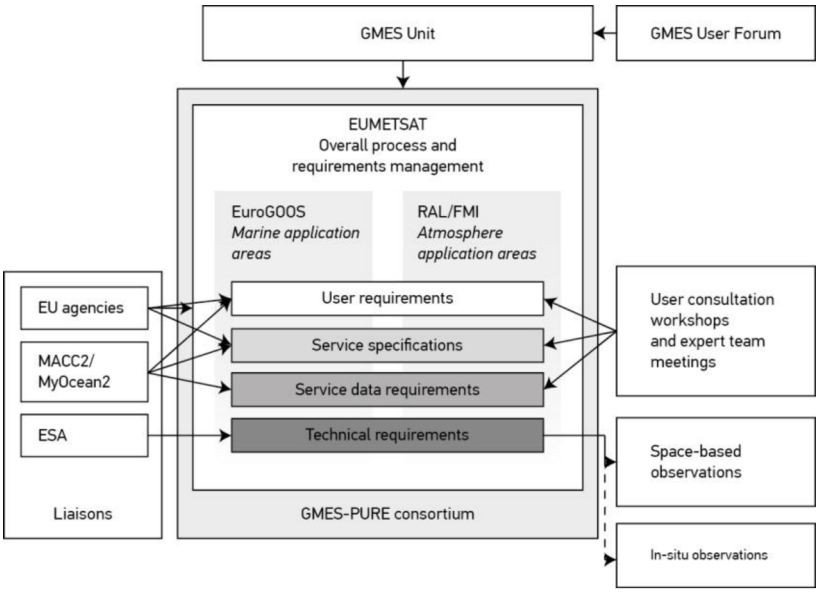

Figure 1 Overview of the GMES PURE project structure.

Using in-line systems for calibration/validation of Ocean Color; The Tara Oceans example.

E. Boss, J. Werdell, A. Chase, C. Proctor and T. Leeuw.

The 2.5yr long around-the-world Tara Expedition has provided a unique and extensive data set of particulate absorption and attenuation (>300,000 minute averaged spectra). Such data provides the possibility to obtain a significant increase in match-up opportunities as well as to assess sub-pixel variability of IOPs and hence of associated modulation in reflectance. We present preliminary analysis of matching OC products with Tara data (e.g. Chlorophyll, PFTs) and the distribution of sub-pixel variability. We also introduce the upcoming Tara Arctic Circle expedition (5-11/2013) where additional in-line sensors which include the Mote Marine Labs's CDOM Mapper, the WETLabs ALFA and an in-line WETLabs backscattering sensor. This expanded suite of variable could be used validate additional OC products (CDOM, bbp, and additional PFTs).

Ocean colour products from hyper-spectral satellite data of SCIAMACHY using the PhytoDOAS method and the radiative transfer model SCIARAN

Astrid Bracher[1], T. Dinter[1], A. Sadeghi[1], M. Altenburg Soppa[1], B. Taylor[1], J.P. Burrows[2], V. Rozanov[2]
[1]PHYTOOPTICS Group at the Institute of Environmental Physics, University of Bremen and the Alfred Wegener Institute for Polar and Marine Research, Bussestraße 24, 27570 Bremerhaven, Germany
[2]Physics and Chemistry of the Atmosphere, Institute of Environmental Physics, University of Bremen, Otto Hahn Allee 1, 28359 Bremen, Germany
Email: Astrid.Bracher@awi.de

Summary

Quantitative distributions of major functional PFTs of the world ocean improve the understanding of the role of marine phytoplankton in the global marine ecosystem and biogeochemical cycles. Information on the attenuation and light penetration depth tells us the extend of phytoplankton primary production and until which depth satellite obtain information on ocean colour.

In this study, global ocean color satellite products of different dominant phytoplankton functional types' (PFTs') biomass and the vibrational Raman scattering (VRS, i.e. the inelastic light scattering at water molecules, for different wavelength ranges retrieved from hyperspectral satellite data of the satellite sensor SCIAMACHY (SCanning Imaging absorption spectrometer for Atmospheric ChartographY on board ENVISAT, operating 2002-2012) using Differential Optical Absorption Spectroscopy applied to phytoplankton (PhytoDOAS) are presented (see also Vountas et al. 2007, Bracher et al. 2009, Sadeghi et al. 2012a).

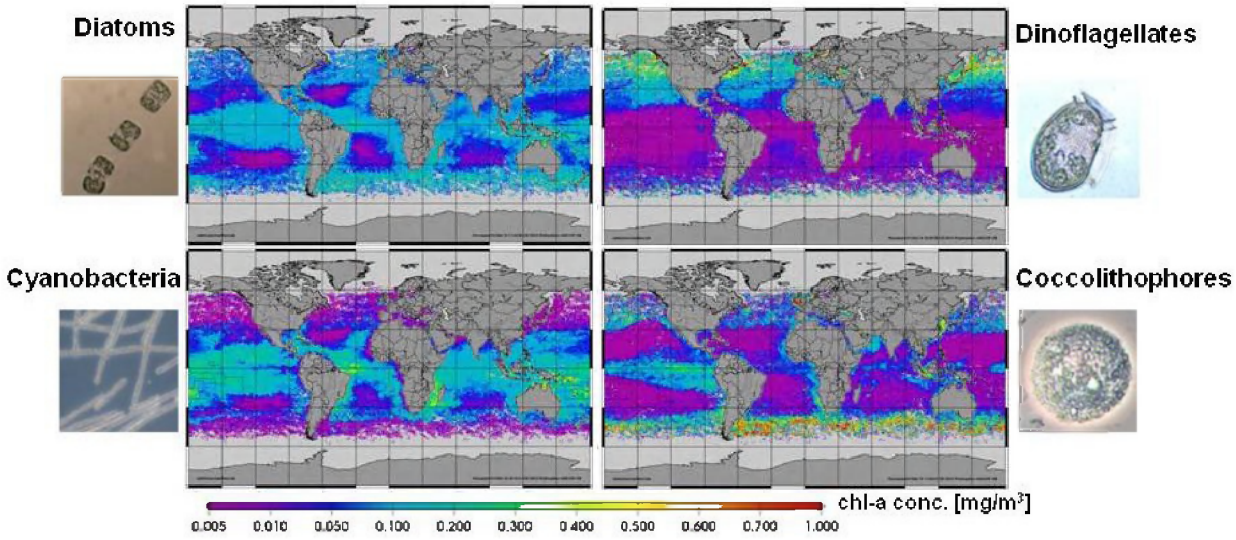

Figure 1 Mean chl-a conc. in March 2007 of different phytoplankton groups derived with PhytoDOAS from SCIAMACHY data. Representative photographs for each group from S. Kranz and S. Wiegmann (AWI).

PhytoDOAS allows the determination of biomass of the four different phytoplankton groups (Sadeghi et al. 2012a, Fig. 1) analytically and independent from a priori information using high spectrally resolved satellite data from SCIAMACHY. The method is an extension of the Differential Optical Absorption Spectroscopy (DOAS by Platt 1974), used for satellite retrievals of trace gas columns (Burrows et al. 1999). In addition to atmospheric compounds, PhytoDOAS also accounts for the differential absorption of water and its constituents.

VRS has been retrieved following the approach of Vountas et al. (2007) but now the radiative transfer model SCIATRAN (Rozanov et al. 2005) now fully coupled for atmospheric and oceanic transfer (Blum et al. 2012) was used to model the pseudo-absorption spectra to be used in PhytoDOAS which account for the differential spectral effect of filling-in of Fraunhofer lines. The radiative transfer calculation were used to calculate inelastic scattering at the whole UV-VIS wavelength range and different wavelength ranges (UV-a, blue) were identified where due to strong differential VRS structures the inelastic scattering effect could be used to retrieve its signature in satellite data. In addition radiative transfer calculations were used to calculate the dependence of VRS at different wavelength ranges to the light penetration depth and attenuation coefficient. By this a UV and blue attenuation coefficient data product is developed with a retrieval which is not influenced by interfering effects of phytoplankton, other particle or CDOM absorption and scattering. As for the PhytoDOAS PFT products, this hyperspectral ocean color products are retrieved analytically, simultaneously with atmospheric components from level-1 (top of atmosphere) SCIAMACHY radiances. The retrieval is less dependent on a-priori assumptions and empirical relationships than multispectral ocean color products. Comparisons of these hyperspectral data to ocean color products from multispectral sensors and application of the hyperspectral data set in studying phytoplankton dynamics are shown (Sadeghi et al. 2012b). Although current hyperspectral sensors have poor spatial resolution (>30 km x 30 km), they are useful for the verification and improvement of the high spatially resolved multi-spectral ocean color products. Future applications of PhytoDOAS retrieval to other hyperspectral sensors and its synergistic use with information gained from multispectral ocean color sensors are proposed.

References

1. Blum M., Rozanov V., Burrows, J. P., Bracher A. (2012) Coupled ocean-atmosphere radiative transfer model in framework of software package SCIATRAN: Selected comparisons to model and satellite data. Advances in Space Research 49(12): 1728-1742

2. Bracher A., Vountas M., Dinter T., Burrows J.P., Röttgers R., Peeken I. (2009) Quantitative observation of cyanobacteria and diatoms from space using PhytoDOAS on SCIAMACHY data. Biogeosciences 6: 751-764

3. Rozanov V.V. Buchwitz M., Eichmann K.-U., de Beek R., Burrows J.P. (2002) SCIATRAN – a new radiative transfer model for geophysical application in the 240-2400 nm region: the pseudo-spherical version. Advances in Space Research 29(12): 1831-1835

4. Sadeghi A., Dinter T., Vountas M., Taylor B., Altenburg Soppa M., Bracher A. (2012) Remote sensing of coccolithophore blooms in selected oceanic regions using the PhytoDOAS method applied to hyper-spectral satellite data. Biogeosciences 9: 2127-2143

5. Sadeghi A., Dinter T., Vountas M., Taylor B., Peeken I., Altenburg Soppa M., Bracher A. (in press) Improvements to the PhytoDOAS method for identification of coccolithophores using hyper-spectral satellite data. Ocean Sciences 8: 1055-1070

6. Vountas M., Dinter T., Bracher A., Burrows J.P., Sierk B. (2007) Spectral Studies of Ocean Water with Space-borne Sensor SCIAMACHY using Differential Optical Absorption Spectroscopy (DOAS). Ocean Science 3: 429-440

Overview on algorithms to derive phytoplankton community structure from satellite ocean colour

Astrid Bracher[1], Nick Hardman-Mountford[2]

[1]PHYTOOPTICS Group at the University of Bremen and Alfred Wegener Institute for Polar and Marine Research (AWI), Bussestraße 24, 27570 Bremerhaven, Germany
[2]CSIRO Centre for Environment and Life Sciences, Underwood Avenue, Floreat, Perth, WA 6014, Australia
Email: Astrid.Bracher@awi.de

Summary

Different bio-optical and ecological methods have been established that use ocean color data to identify and differentiate between phytoplankton functional types (PFTs) or phytoplankton size classes (PSCs) in the surface ocean. These can be summarized into four main types: spectral-response methods which are based on differences in the shape of the light reflectance/absorption spectrum for different PFTs/PSCs, methods which use information on the magnitude of chlorophyll biomass or light absorption to distinguish between PFTs or PSCs, methods that retrieve the particle size distribution from satellite-derived backscattering signal and derive PSCs, and ecological-based approaches which use information on environmental factors. Within this presentation we will give an overview over the presently available algorithms. Based on the input we get from the algorithm developers we will try within the short time to present for each product its spatial and temporal coverage, (potential) applications, uncertainties, benefits and short comings.

Using the near pixels of ocean colour images to perform the atmospheric correction over turbid waters.

J. Brajard[1], C. Jamet[2]
[1]UPMC, LOCEAN/IPSL, Paris, France
[2]ULCO, LOG, Wimereux, France
Email: julien.brajard@locean-ipsl.upmc.fr

Summary

A new approach is proposed to perform atmospheric correction over turbid water. This approach makes no assumption on the water-leaving reflectance spectrum in the near-infrared and uses the spatial context of the pixel. It was applied to MERIS image in the Adriatic Sea.

Introduction

Ocean colour sensors measure the solar flux reflected by the ocean and the atmosphere. In order to estimate the oceanic component, a critical step in the processing of the top-of-atmosphere (TOA) measurements is the so-called atmospheric correction. This involves the removal of the atmospheric signal in order to deduce the contribution of the ocean only.

Following Gordon (1997), we consider (out of the glitter region and neglecting the whitecaps influence):

$$\rho_{toa}(\lambda) = \rho_{path}(\lambda) + t(\lambda)\cdot \rho_w(\lambda) \quad (1)$$

where ρ_{toa} is the total reflectance derived from the satellite measurement ρ_{path} is the atmospheric reflectance (accounting for the scattering and absorption of aerosol and molecules) , t is the diffuse transmittance, ρ_w is the water-leaving reflectance and λ is the wavelength of the measurement.

For most of the non-turbid waters, the atmospheric correction is named "clear water process" hereinafter. We can assume that ρ_w is negligible in the near-infrared part of the signal (λ>700nm). Making this assumption, it is possible to derive the aerosol model from the near-infrared part of the signal. Then the atmospheric contribution ρ_{path} and t can be estimated for the whole spectrum. It is then easy to deduce the water leaving reflectance in visible part of the spectrum applying Eq.1 for which the only unknown term is ρ_w.

Over turbid waters, though, the variability of ocean content (presence of substances other than phytoplankton) induces a signal in the near-infrared part of the signal that can cause errors during the atmospheric correction process. Several solutions were applied to solve this problem (Moore et al. IJRS 1999, Chomko and Gordon AO 2001, Stumpf et al. NASA tech 2003, Stamnes et al. AO 2003, Bailey et al. IJRS 2010, Schroeder et al. IJRS 2007, Brajard et al. RSE 2012). In any case, it is necessary to make a-priori hypothesis on the water-leaving reflectance spectrum in the near-infrared which reduce the generality of the approach. Another family of algorithms proposes to use spatial information of the ocean colour image (Ruddick et al. 2000[1]). The assumption here is that aerosol properties are spatially homogenous on a region of 10km to 100km (Hu et al. 2000[2]). This last approach reduces the number of assumptions to be made on the near-infrared part of the water-leaving reflectance spectrum. The present work addresses this method and proposes to generalize the algorithm making no hypotheses on the turbid water-leaving reflectance spectrum.

Method

The algorithm proposed here can be considered as a generalization of the approach proposed by Hu et al. 2000. In this work, the spatial neighbourhood is used to determine both the aerosol type and optical thickness. An objective spatial interpolation was performed to take into account the spatial correlations. Here are the steps of the algorithm:

1) Classification of the image pixels: turbid or clear water

2) Application of the clear-water process and estimation ,for each clear-water pixel, of the aerosol optical thickness τ and the Angtröm exponent α linked to the aerosol model.
3) For each turbid pixel, τ and α are estimated with the following equation:

$$x_0 = \sum_{i \in V} \lambda_i \cdot x_i \qquad (2)$$

where x stands for τ or α, the index 0 designs the turbid pixel, V is the ensemble of the 10 clear-water pixels that are the nearest (in the sense of the geographic distance) from the pixel x_0, λ_i are weighted coefficient that decreases with the distance (the furthest a pixel is , the less it is correlated to the turbid pixel).
4) Using τ_0, α_0 determined previously, assuming a Junge size distribution and non-absorbing aerosols, ρ_{path} and t are computed at all wavelengths using artificial neural networks (Brajard et al. NN, 2006).
5) The water-leaving reflectance is deduced using Eq. 1.

First result

The algorithm is applied on MERIS image, June 2, 2009 in the north of the Adriatic Sea. The figure 1 presents a comparison between the standard MERIS processing and the modified product using the algorithm described here for the Angström exponent and the water-leaving reflectance at 490nm. The MERIS flags CASE2_S, CASE2_ANOM and CASE2_Y were used to determine turbid waters. For each turbid pixel, the 10 nearest pixels were considered. It can be noticed that the standard Angström exponent is strongly related to the turbidity of the water, which is likely an artefact of the atmospheric correction process. It can be seen, that it is not the case for the new algorithm proposed here (it is particularly visible off the north coast). Even if the new algorithm seems to presents some bias for strong aerosol optical thickness (not shown here), the water-leaving reflectance presents some realistic values and pattern that are to be validated using in-situ data (e.g. Helgoland site P.I. R. Doerffer). It validates the assumption that it is possible to use spatial information to perform atmospheric correction over turbid waters.

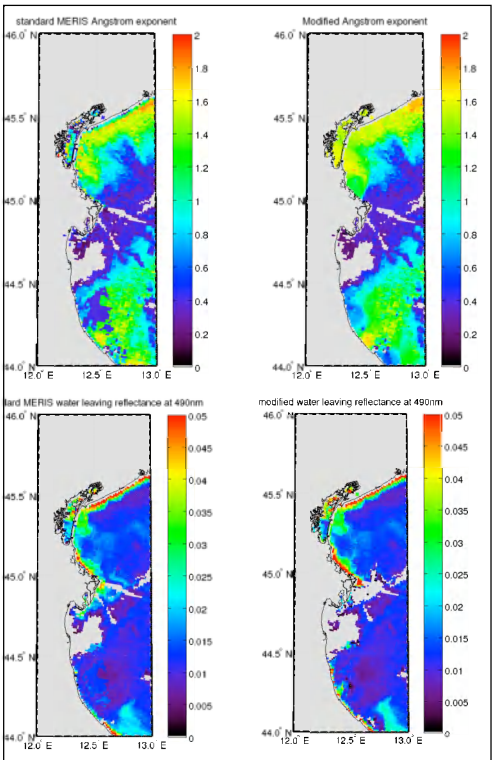

Figure 1. Standard MERIS products (left) compared to the new algorithm products (right) for α (up) and ρ_w(490nm) (bottom).

Conclusion

The method proposes here is a first step to explore the possibilities of using image information to solve inverse problems for ocean colour data. The use of interpolations techniques could give objective criteria to quantify uncertainty of the result. The approach proposed here makes the maximal assumption that the signal over turbid waters cannot be used at all to estimate the aerosol contribution. This simplification was made in order to evaluate the effects of this algorithm only. In the future, it is likely that accurate results can be obtained using a mixed approach using both the neighbouring pixels and the signal over turbid waters.

Principal references

[1] Ruddick, K., Ovidio, F., Rijkeboer, M. (2000). Atmospheric correction of SeaWiFS imagery for trbid coastal and inland waters, App. Opt., 39 (6), 897-912.
[2] Hu C.M., Carder K.L., Muller-Karger F.E. (2000), Atmospheric correction of SeaWiFS imagery over turbid coastal waters: A practical method. Remote Sens. Environ. 74: (2) 195-206.

Autonomous Ship Based Ocean Color Observations on Australian Research Vessels

V. E. Brando[1], J. Lovell[2], E. King[2], R. Keen[1], P. Daniel[1], D. Mckenzie[2],L. Woodward[2], R. Palmer[2], D. Mills[2], L. Besnard[3], M. Slivkoff[4], W. Klonowski[4]
[1] *CSIRO Land and Water, Canberra, 2601, Australia*
[2] *CSIRO Marine & Atmospheric Research, Hobart, 7001, Australia*
[3] *IMOS, Hobart, 7001, Australia*
[4] In-situ Marine Optics Pty. Ltd, Bibra Lake, 6163 Australia
Email vittorio.brando@csiro.au

Summary

As part of Australia's Integrated Marine Observing System, a "Dynamic above water radiance and irradiance collector" (DALEC) was commissioned in August 2011 on the RV Southern Surveyor to provide an automated stream of hyperspectral information from Australian waters. The DALEC is a radiometrically calibrated spectroradiometer which measures above water-leaving radiance, sky radiance and downwelling irradiance. Designed for autonomous ship deployment, the DALEC incorporates a passive 2 axis gimbal, solar azimuth tracking, embedded GPS, compass and accelerometers for recording sensor geometry. Radiometric data streams from the DALEC are collected in real-time and recorded over the ship's local area network. Preliminary results will be presented from the 9 DALEC deployments carried out in 2011 and 2012 around the Australian Continent.

Introduction

Ships provide an ideal platform to collect spatially diverse ocean color calibration data. As part of Australia's Integrated Marine Observing System, an autonomous ship based system was commissioned in 2011 to provide an above water hyperspectral radiometry data-stream from Australian waters.

The DALEC

The "Dynamic above water radiance and irradiance collector" (DALEC) is a radiometrically calibrated hyperspectral radiometer specifically developed by "In situ Marine Optics" for autonomous ship based deployment [1]. The DALEC contains three Zeiss UV-Vis enhanced spectroradiometers which are designed to measure spectral upwelling radiance (L_u), downwelling radiance (L_{sky}) and downwelling irradiance (E_d) in a near-simultaneous fashion, above water. Each spectroradiometer records 200 channels with spectral resolution of 10 nm, spaced at 3.3 nm intervals. The DALEC sensor head houses the instruments and is designed to be mounted on a boom positioned over the water, typically off the ship's bow. Radiance channel viewing angles (θ_v, θ_s) are fixed to 40◦ off nadir (L_u) and zenith (L_{sky}) when the sensor is held level.

A passive gimbal mount with adjustable damping stabilises the instrument during transit. This allows spectroradiometric measurements to be collected with consistent geometry whilst the ship is in motion. Pitch and roll sensors record data for quality control purposes. An embedded compass, GPS and motor control adjust the sun-relative azimuth angle (ϕ) during data collection. To avoid viewing the ship, the DALEC automatically seeks the 'ideal' sun-relative azimuth within user-defined boom-relative limits. UTC time and GPS coordinates of spectroradiometric measurements are logged allowing quick data comparisons with other transecting measurements and satellite pixels.

A DALEC instrument has been deployed since July 2011 on Australia's Marine National Facility, the RV Southern Surveyor (RV SS). RV SS operates across all of Australia's territorial waters, providing an ideal deployment platform (Fig 1).

The instrument is deployed approximately three meters clear of the RV SS's foredeck protruding one meter forward of the bow to provide an uninterrupted sea viewing angle of ~270° and to reduce the effects of spray from the ship's bow.
The measurement cycle is started at the beginning of each day at sea and stopped at sunset, with data collection at approximately 10 sec intervals. Under normal operating conditions the instrument is left in place on the deployment boom and retrieved only for routine maintenance. Under rough conditions or extended port periods the sensor head is retrieved and the boom is stowed against the forestay.

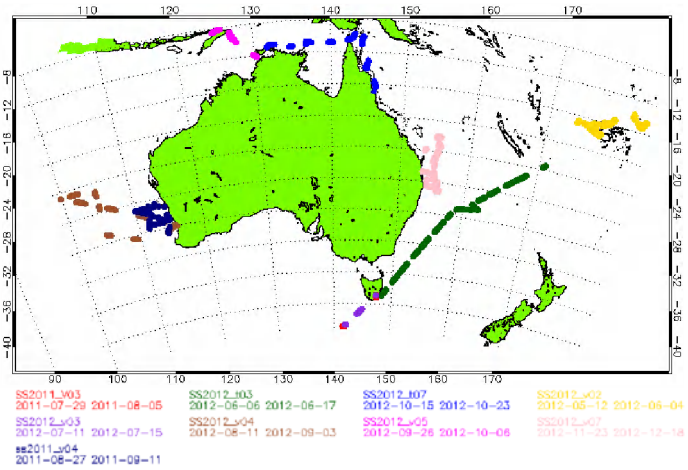

Figure 1. Location of the 119 daily DALEC L1B data files acquired on board RV Southern Surveyor in 2011 and 2012.

Radiometric data stream from the DALEC is collected in real time via a PC installed in the RV SS bridge. The data is tagged with location and orientation metadata recorded over the ship's LAN, allowing for future integration into the onboard data management system.

Results and Discussion

In 2011 and 2012, ~1.4 million spectral triplets (near-simultaneous measurements of L_u, L_{sky} and E_d) were collected during 9 research voyages (Fig 1). Consistent with the IMOS data policy, all DALEC Level 1B data collected to date (119 daily files, ~6.65GB) are freely available to the Australian and international oceanographic community via the IMOS Ocean Portal [http://imos.aodn.org.au/webportal].
For further analysis, the measured DALEC spectra are filtered by applying thresholds on ancillary QC parameters including pitch and roll, sun zenith angle and ship geometry [1]. Data is then processed to L2 reflectances using automated quality control approaches specifically developed for shipborne measurements [e.g. 1, 2]. We will present preliminary results of matchup analysis of L2 DALEC reflectances collected in 2011 and 2012 around the Australian Continent with MODIS data

Conclusions

The commissioning of an automated above water hyperspectral radiometry data-stream from Australian waters significantly augmented Australia's ability to contribute to global and regional Ocean Colour validation and algorithm design activities.

Acknowledgment

IMOS is supported by the Australian Government through the National Collaborative Research Infrastructure Strategy and the Super Science Initiative.

References

[1] Slivkoff, M. (2013). Ocean Colour Remote Sensing of the Great Barrier Reef Waters. PhD thesis, Department of Imaging & Applied Physics, School of Science, Curtin University
[2] Simis, S.G.H., J. Olsson (2013). Unattended quality control of shipborne hyperspectral reflectance measurements. Remote Sensing of Environment (minor revision)

Use of Ocean Color Derived Products to Constrain and Optimize a Global Ocean Biogeochemistry Model as Part of NASA's Carbon Monitoring System Flux Project

H. Brix[1], D. Menemenlis[2], C. Hill[3], S. Dutkiewicz[3], K. Bowman[2]

[1]University of California, Los Angeles, CA 90095, USA
[2]California Institute of Technology, Jet Propulsion Laboratory, Pasadena, CA 91109, USA
[3]Massachusetts Institute of Technology, Cambridge, MA 02139, USA

Summary

NASA's Carbon Monitoring System (CMS) Flux Project is characterizing the evolution of global carbon sources and sinks based on satellite and in situ observations and on numerical models. As part of the CMS Flux Project, the ECCO2-Darwin ocean carbon cycle model aims to estimate the spatiotemporal evolution of air-sea carbon fluxes. ECCO2-Darwin is based on a global, eddying, data-constrained estimate of the time-evolving physical ocean state provided by the Estimating the Circulation and Climate of the Ocean, Phase II (ECCO2) project and on the Massachusetts Institute of Technology (MIT) Darwin ecosystem model. Together, ECCO2 and Darwin provide a time-evolving physical and biological environment for carbon biogeochemistry, which is used to compute surface fluxes of carbon at high spatial and temporal resolution. We describe the ECCO2-Darwin ocean carbon cycle model and present preliminary results on the adjustment of initial biogeochemistry conditions and gas exchange coefficients using a Green's function approach. We carried out 11 model sensitivity experiments modifying initial fields of dissolved inorganic carbon, alkalinity, and oxygen, as well as gas exchange coefficients and other biogeochemical model parameters. Data constraints include primary production estimates derived from ocean color remote sensing data, in situ observations of carbon dioxide partial pressure (pCO_2), the Takahashi air-sea CO_2 flux atlas, and an estimate of the global mean air-sea CO_2 exchange. An optimized linear combination of the different initial conditions and exchange coefficients was obtained using a least-squares minimization. Integrating the model with this new set of initial conditions and exchange coefficients yields more realistic estimates of air-sea carbon fluxes. There remain, however, regions that require further improvement, for example, in the Southern Ocean.

Introduction / Model Description and the Initialization Problem

The components of the global carbon cycle interact through fluxes between the carbon reservoirs on our planet: atmosphere, land, oceans, and the geosphere. Understanding the exchange processes between these reservoirs requires knowledge about these fluxes. As there is no global scale observation network in place that could provide these flux estimates, we need to combine existing observations with models to compute them indirectly. To achieve the most realistic results, models can be constrained by observational data, especially global space-based observations that provide information about the physical and biological state of the land, atmosphere, or ocean. The goal of the NASA CMS Flux Project is to utilize the full suite of NASA data, models, and assimilation capabilities in order to attribute changes in the atmospheric accumulation of carbon dioxide to spatially resolved fluxes. The oceanic component of these fluxes is of critical importance as it is estimated that the oceans have absorbed 48±9% of the anthropogenic CO_2 emitted during 1880–1994 [1]. The current oceanic CO_2 uptake is estimated to be about a quarter of the anthropogenic emissions [2]. The ECCO2-Darwin model provides spatially resolved oceanic CO_2 fluxes constrained by observations of the physical ocean and ship-based CO_2 measurements for the CMS project. The ocean fluxes serve as a priori surface forcing for the ``top-down'' atmospheric flux estimates in the CMS project.

Model initialization is a difficult challenge when setting up high-resolution Ocean Biogeochemistry General Circulation Models like ECCO2-Darwin. Long integrations that reduce model drift are not practical because of computational cost. In the ocean, where circulation is slow compared to the atmosphere, it can take thousands of (model) years to reach an equilibrium state. Another problem associated with long spin-ups is model drift, that is, the increasing biases between the model simulation and nature. For short model integrations that circumvent these drift issues and allow high resolution and model complexity, choosing initial conditions therefore becomes a critical issue. The availability of oceanic data at any given point in time chosen to be the model's starting point is extremely limited. To solve this initialization problem for all biogeochemical quantities simultaneously and to avoid producing unrealistic air-sea carbon flux estimates, we use a simple, physically-consistent data assimilation approach based on model Green's functions, that is, on forward model sensitivity experiments [3].

Implementation and Results

Out of a large number of possible combinations of parameters and model sensitivity runs we choose seven runs that differed in their initial conditions, the piston velocity formulation used, and the ratio of particulate inorganic to particulate organic carbon. The data constraints we used for an initial optimization of our results included in situ surface pCO_2 data [4], the Takahashi air-sea CO_2 flux atlas, and an estimate of the global mean air-sea CO_2 exchange. The optimized model simulation yielded substantial cost (that is, data-model mismatch) reductions. In a second step we expanded our data constraints to observed full-depth profiles of dissolved inorganic carbon and alkalinity (see Fig.1) as well as ocean color derived primary production (Vertically Generalized Production Model, VGPM) [5]. Initial results indicate that these constraints improve our air-sea fluxes further. Still, some critical regions for improvement persist, for instance, regions of overly strong carbon uptake in the Southern Ocean and weak outgassing the Equatorial Pacific.

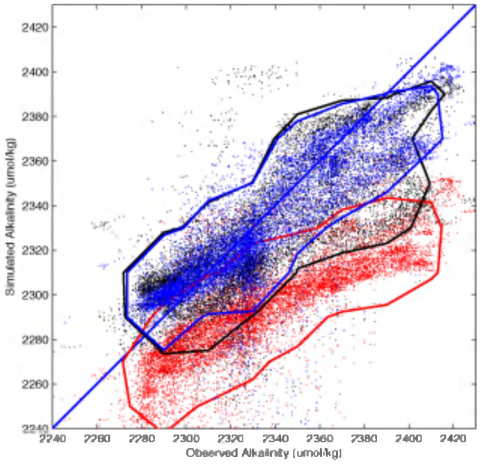

Fig. 1: Data-model comparison, initial run (red), using only pCO_2 (black), and pCO_2, DIC, and alkalinity (blue) as constraints. The contour lines denote regions where scatter plot density is greater than 0.5 points per ppm^2.

References

[1] Sabine, C.L., Feely, R.A., Gruber, N., Key, R.M., Lee, K., Bullister, J.L., Wanninkhof, R., Wong, C.S., Wallace, D.W.R., Tilbrook, B., Millero, F.J., Peng, T.H., Kozyr, A., Ono, T., Rios, A.F., 2004. The oceanic sink for anthropogenic CO2. Science 305, 367–371.

[2] Le Quéré, C., Takahashi, T., Buitenhuis, E.T., Rödenbeck, C., Sutherland, S.C., 2010. Impact of climate change and variability on the global oceanic sink of CO_2. Global Biogeochemical Cycles 24, GB4007, 10pp.

[3] Menemenlis, D., Fukumori, I., Lee, T., 2005a. Using green's functions to calibrate an ocean general circulation model. Monthly Weather Review 133, 1224–1240.

[4] Takahashi, T., Sutherland, S., Kozyr, A., 2011. Global Ocean Surface Water Partial Pressure of CO2 Database: Measurements Performed During 1957-2010 (Version 2010). Technical Report ORNL/CDIAC-159, NDP-088(V2010). Carbon Dioxide Information Analysis Center, Oak Ridge National Laboratory, U.S. Department of Energy. Oak Ridge, Tennessee.

[5] Behrenfeld, M.J. and Falkowski, P.G., 1997. Photosynthetic rates derived from satellite-based chlorophyll concentration. Limnology and Oceanography 42, 1-20.

Phytoplankton size classes in the Eastern Atlantic Ocean: using Earth Observation to understand the structure of Marine Ecosystems

Vanda Brotas[1,2], Robert Brewin[2], Carolina Sá[1], Ana Brito[1], Alexandra Silva[1], Rafael Mendes[1], Glen Tarran[2], Shubha Sathyendranath[2], Steve Groom[2]

[1] Centro de Oceanografia, Faculdade de Ciências, Universidade de Lisboa, Campo Grande, 1749-016 Lisboa, Portugal

[2] Plymouth Marine Laboratory, Prospect Place, PL1 3DH Plymouth, UK

In recent years, the global distribution of Phytoplankton Functional Types (PFT) and Phytoplankton Size Classes (PSC) has been determined by remote sensing. Many of these methods rely on interpretation of phytoplankton size or type from pigment data, but independent validation of the methods has been difficult because of lack of appropriate in situ data on cell size.

This work presents in situ data along a trophic gradient in the Eastern North Atlantic and has the following objective:

- To produce a map cell abundance from remotely-sensed chlorophyll a, using photosynthetic pigments concentration and cell abundances to test a previously developed conceptual model, which calculates the fractional contributions of pico-, nano- and micro-plankton to total phytoplankton chlorophyll biomass (Brewin et al., 2010)

Chlorophyll-a for each size class was estimated from the three component model, and divided by the mean chlorophyll-a per unit cell obtained from combining information from the model, microscope cell counts and flow cytometry.

A previously developed global scale model, which calculates the fractional contributions of pico-, nano- and micro-plankton to total phytoplankton abundances was applied to the database. Intracellular chlorophyll a (Chla) per cell, for each size class, was computed from the cell enumeration results (microscope counts and flow cytometry) and the chlorophyll-a concentration for that size class given by the model. The median intracellular chlorophyll-a values computed were 0.004, 0.224 and 26.78 pg Chla $cell^{-1}$ for pico-, nano-, and microplankton respectively. This is generally consistent with intracellular chlorophyll-a concentrations of different size classes from the literature, thereby providing an indirect validation of the method.

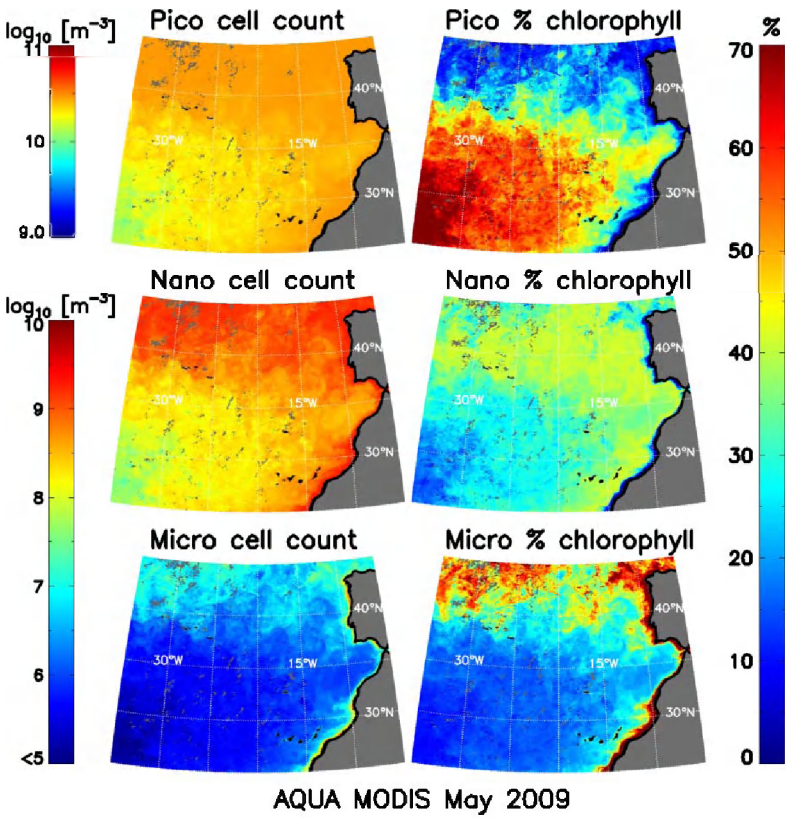

Figure 1 - *Cell abundance estimation and chlorophyll-a relative contribution for the three size classes from remote sensing chlorophyll-a. A Aqua MODIS May 2009 monthly L3 composite was used.*

Using a satellite-derived composite image of chlorophyll-a for the study area, a map of cell abundance was generated based on the computed intracellular chlorophyll-a for each size-class, thus extending the remote-sensing method for mapping size classes of phytoplankton from chlorophyll-a concentration to mapping cell numbers in each class. The map reveals the ubiquitous presence of picoplankton, and shows that all size classes are more abundant in more productive areas.

Our results support the assumption that there is an overall dominance of picoplankton, in terms of cell numbers from oligotrophic to eutrophic regions. More productive areas present higher cell numbers in all cell size classes, but the increase in chlorophyll-a is given by the increment in chlorophyll-a fraction due to larger cells (more details can be seen in Brotas et al, 2013).

The approach presented in this work, whereby the abundance of cell-size classes of phytoplankton can be derived from satellite imagery is a novel and promising contribution to the understanding of the biogeochemical role of phytoplankton in our planet.

References

Brewin, R. J. W., Sathyendranath, S., Hirata, T., Lavender, S., Barciela, R. M., Hardman-Mountford, N. J. (2010). A three-component model of phytoplankton size class for the Atlantic Ocean. Ecological Modelling, 1472-1483.

Brotas, V. Brewin, B., Sá, C., Brito, A., , Silva, A., Mendes, R., Diniz, T., Kaufmann, M., 3, Tarran, G., Groom, S., Platt, T., Sathyendranath, S. 2013. Deriving phytoplankton size classes from satellite data: validation along a trophic gradient in the Eastern Atlantic. Remote Sensing of Environment 134:66-77. DOI: 1016/j.rse.2013.02.013.

ABSOLUTE CALIBRATION OF SEAWIFS USING RAYLEIGH SCATTERING

Véronique Bruniquel[1], Guillaume Fontanilles[1], Ludovic Bourg[2], Bertrand Fougnie[3], Patrice Henry[3]

[(1)]ACRI-ST, 8 esplanade Compans-Caffarelli, Toulouse, France
[(2)]ACRI-ST, 260 route du Pin Montard, BP 234, Sophia-Antipolis, France
[(3)]CNES, 18 avenue Edouard Belin, Toulouse, France
Email: veronique.bruniquel@acri-st.fr

Summary

This paper presents the assessment of the SeaWiFS absolute calibration using the Rayleigh signal above oceanic surfaces. Results obtained in the frame of this study show a high stability of the absolute calibration and a slight temporal calibration drift from 2005.

Introduction

The "Rayleigh calibration method" developed by the French Space Agency (CNES) and used in the frame of this study to assess the absolute calibration of the SeaWiFS instrument, is based on the exploitation of Top Of Atmosphere (TOA) signal measured above oceanic surfaces in the short wavelengths, i.e. from blue to red regions (<700 nm). This signal mainly corresponds to the molecular scattering signal (Rayleigh signal) which can reach 90% of the total signal. The other contributions to the TOA signal are linked to the aerosol amount and type, the marine surface reflectance which is driven by several parameters such as chlorophyll concentration, water sediments and foam presence. Consequently, considering conditions minimizing the influence of the non-Rayleigh contributions, it is possible to assess the variation of the absolute calibration coefficients comparing measured and simulated observations. In this context, CNES has developed an operational multi-sensors calibration software environment (MUSCLE) [1] allowing to assess the absolute calibration of several instruments. The "Rayleigh method" is one of the techniques implemented in MUSCLE. This environment is coupled to the SADE database [2] which includes appropriate observations for applying the selected calibration method.

Discussion

Our study of which the results are details in [3], is split into several steps:

1. Collection and pre-processing of SeaWiFS products: SeaWiFS data acquired over the six operational oceanic areas defined in Fougnie et al. [4] are exploited in the frame of this study. These areas correspond to oligotrophic areas chosen for their spatial homogeneity and their low and stable seasonal variation in chlorophyll concentration. SeaWIFS L1A GAC products have been pre-processed to generate TOA reflectances.

2. Development of a filtering tool to select appropriate SeaWiFS observations for Rayleigh calibration and insertion into the SADE database: This selection is based on the minimization of the non-Rayleigh contributions applying several successive criteria: observations located sufficiently far from coastal areas, non-cloudy observations or sufficiently far from clouds to avoid adjacency effects, observations with low wind speed in order to limit the foam influence, observations sufficiently far from sunglint conditions, observations with low aerosols concentration at 865 nm, non-degraded quality observations.

3. Assessment of the SeaWiFS absolute calibration for the visible bands (< 700 nm) using the Rayleigh method available through the MUSCLE environment. The Rayleigh absolute calibration method [5] consists in comparing, for each observation, the SeaWiFS TOA reflectance assuming a reference calibration to evaluate with the corresponding TOA reflectance simulated using a Radiative Transfer model. The ratio defined as measured

signal / simulated signal (called $\Delta A_k = A_k / A_{k\_ref}$), allows to estimate the absolute calibration difference from the reference one. The following general formula is used to calculate the TOA reflectance:

$$\rho_{TOA}(\theta_s, \theta_v, \Delta\varphi) = T_g(\theta_s, \theta_v).\left[\rho_{atm}(\theta_s, \theta_v, \Delta\varphi) + \rho_w(\theta_s, \theta_v, \Delta\varphi).\frac{T(\theta_s).T(\theta_v)}{(1 - s.\rho_w)}\right]$$

Absolute calibration results obtained for SeaWiFS have shown:

- A very high stability of the reference calibration: Quarterly absolute coefficients ratios ΔA_k are close to 1 for all spectral bands and throughout the SeaWiFS life;
- A very low scattering of the ΔA_k with a standard deviation always lower than 0.018;
- A decrease of the ΔA_k scattering with the increase of the spectral bands: standard deviation is lower in the red band than in the blue band;
- No correlation of ΔA_k vs. several analysed parameters: date, sun and viewing geometry, measured radiance, aerosol optical thickness, wave angle, wind speed, atmospheric pressure, ozone content, geographic location, et.

Concerning the ΔA_k temporal evolution we observe an averaged increase of 1 to 1.5% throughout the mission life and for all spectral bands. ΔA_k are particularly stable until 2004 and increase from 2005. This trend is all the more obvious that the spectral band increases.

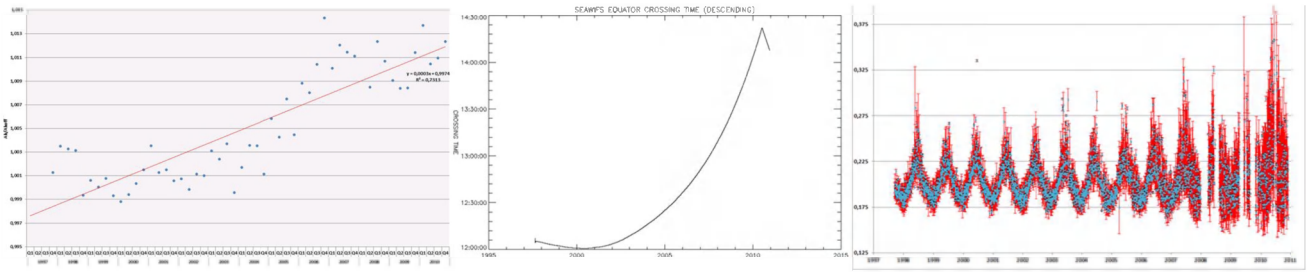

(Left) Temporal evolution of ΔA_k from top to bottom: 670 nm; (Centre) SeaWiFS equator crossing time drift; (Right) Temporal evolution of mean daily TOA reflectances at 412 nm over the PacSE area (selected observations)

The ΔA_k temporal increase is very close to the accuracy of the Rayleigh method and different contributors could explain such a small effect (aerosol, etc.). However, the impact of the orbit node drift is a potential lead to investigate. Indeed, the node-crossing time is stable and close to noon until 2004 and changes rapidly to reach ~14:30 in 2010. The viewing geometry change resulting from this orbit node drift leading to a larger scattering angle range, could impact absolute calibration results. Figure 8 shows the temporal evolution of mean daily TOA reflectances at 412 nm for SADE observations selected over South-East Pacific area. We note the regularity of the reflectances on the first half of the mission life time and the larger and larger scattering of the measurements from 2005, explained by the viewing geometry change. An accurate error budget study needs now to be carried out in order to identify the main impacting sources of errors.

References

[1] Manuel utilisateur de l'atelier d'étalonnage MUSCLE/SADE

[2] Manuel utilisateur et description des utilitaires SADE

[3] Bruniquel V. et al., 2012, Etalonnage absolu SeaWiFS en utilisant le signal Rayleigh, réf. A948-NT-003-ACR.

[4] B. Fougnie, B., P. Henry, et al., "Identification and Characterization of Stable Homogeneous Oceanic Zones: Climatology and Impact on In-flight Calibration of Space Sensor over Rayleigh Scattering", Ocean Optics XVI, 18-22 November 2002.

[5] Hagolle, O. et al., Results of POLDER In-Flight Calibration, IEEE Trans. on Geosci. Remote Sensing, Vol.37, 1999.

Diatoms blooms detected by remote sensing

N.M. Bucair[1], P.B. Oliveira[2], J. Dubert[1], A. Silva[2], B. Domingues[2], M.T. Moita[2], R. Nolasco[1]

[1] University of Aveiro, Department of Physics, Aveiro, 3810-193, Portugal
[2] IPMA, Av. Brasilia, Lisboa, 1449-006, Portugal
Email: nayarabucair@ua.pt

Summary

Diatom blooms are recurrent along the Portuguese coast during summer in response to the prevailing upwelling conditions. Preexistent algorithms to differentiate this group from other phytoplankton communities were used and adapted for the study area. Normalized water-leaving radiance (nLw) was analyzed to distinguish the specific diatoms group for the particular conditions of the region. The satellite data were compared with in situ data, obtained from an oceanographic cruise carried out in summer 2011. An empiric approach demonstrates that diatoms correspond to high reflectance on the wavelength of 412nm.

Introduction

Early satellite ocean color missions were designed to provide synoptic chlorophyll a (Chl.a) concentration fields. Currently, the foremost application is to monitor the response of the marine ecosystem to climate change. This has been mainly accomplished by the ability to trace changes in the spatial and temporal distribution of the phytoplankton concentration. In addition to its contribution to the ocean's primary production, marine phytoplankton takes part of important biogeochemical cycles. Some species incorporate nitrogen as feedstock, as the cyanobacteria's group, while others as coccolithophores are responsible to capture calcium carbonate from the system to build their calcite plates. Another representative group are the diatoms, that contribute to about 40% of the total marine primary production. This group is usually found in nutrient-rich waters, dominating the phytoplankton assemblages during the spring blooms in temperate and Polar regions [1]. Both diatoms and coccolithophores have high sinking rates contributing to the carbon export into the deep ocean [2].

Previous studies show that summer oceanographic conditions along the west Portuguese coast are influenced by coastal upwelling driven by persistent equatorward winds [3], providing the necessary conditions for phytoplankton growth [4]. Studies on coastal upwelling ecosystems revealed that diatoms are also the dominating group during the intensification phase of upwelling events [5].

Aiming to detect the occurrence of diatom blooms in the central Portuguese coast, the concept of Plankton Functional Type (PFT) has been adopted. The specific absorption coefficients of phytoplankton cells can vary because of differences in the pigment composition and size structure of phytoplankton populations [6]. As chl.a are present in almost all marine phytoplankton, the discrimination of PFT must be performed analyzing accessories pigments (biomarkers)[7].

Discussion

Diatom populations are known to be related to high chl.a concentration [7]. Their signature is readily observed on the images obtained during the 2011 summer cruise off the NW Portuguese coast, using a

range of Chl.a between 0.04 and 3.0 mg m^{-3}. The use of this range allows to focus the analysis on areas out of both the influence of oceanic oligotrophic and continental sediment dominated waters (figure 1).

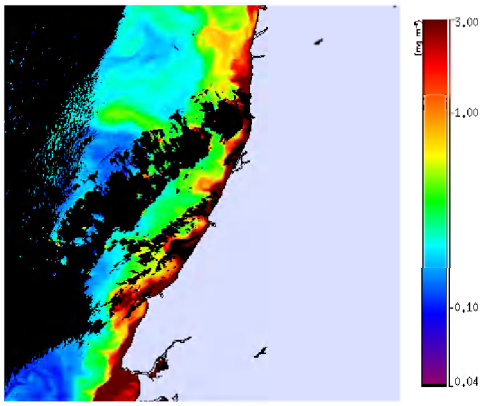

Figure 1: Chlorophyll a concentration

The higher Chl.a concentrations detected on the satellite data are comparable with in situ diatom distribution.

Water dominated by diatoms is associated with the highest backscattering, and exhibit much lower absorption coefficient than other phytoplankton populations [6]. Being in some cases, detectable at short wavelength (412 and 443 nm) however, the absorption by the yellow substance is a potential error source because it may influence nLw values on this spectral range.

Conclusions

Using adequate algorithms, it is possible to associate same parameters to distinguish diatoms from the other marine phytoplankton groups, mainly due to the high nLw at short wavelengths, such as Rrs 412. The results suggest that an empirical approach may be used to discriminate diatoms blooms using remote sensing off the Portuguese coast.

References

[1] Sarthou, G., Timmermans, K.R., Blain, S., Tréguer, P. (2005). Growth physiology and fate of diatoms in the ocean: a review. J Sea Res, 53: 25–42.

[2] Nair, A., Sathyendranath, S., Platt, T., Morales, J., Stuart, V., Forget, M-H., Devred, E., Bouman, H.(2009). Remote sensing of phytoplankton functional types. Remote Sens Environ, 112: 3366–75.

[3] Oliveira, P.B., Nolasco, R., Dubert, J., Moita, T., Peliz, Á. (2009). Surface temperature, chlorophyll and advection patterns during a summer upwelling event off central Portugal. Cont Shelf Res, 29: 759–74.

[4] Largier, J.L., Lawrence, C.A., Roughan, M., Kaplan, D.M., Dever, E.P., Dorman, C.E., et al. (2006). WEST: A northern California study of the role of wind-driven transport in the productivity of coastal plankton communities. Deep-Sea Res II, 53: 2833–49.

[5] Oliveira, P.B., Moita, T., Silva, A., Monteiro, I.T., Sofia, P. A. (2009). Summer diatom and dinoflagellate blooms in Lisbon Bay from 2002 to 2005: Pre-conditions inferred from wind and satellite data. Prog Oceanogr, 83: 270–7.

[6] Sathyendranath, S., Watts, L., Devred, E., Platt, T., Caverhill, C., Maass, H. (2004). Discrimination of diatoms from other phytoplankton using ocean-colour data. Mar Eco Prog Ser, 272: 59–68.

[7] Alvain, S., Moulin, C., Dandonneau, Y., Bréon, F.M. (2004). Remote sensing of phytoplankton groups in case 1 waters from global SeaWiFS imagery. Deep-Sea Res I, 52: 1989–2004.

Strategies for autonomous sensors

I. Cetinić[1], N. Briggs[1], E. Rehm[2], C. Lee[2], E. D'Asaro[2], M.J. Perry[1]

[1]University of Maine, School of Marine Sciences and Ira C. Darling Marine Center, Walpole ME 04573-3307, USA
[2]University of Washington, Applied Physics Laboratory, Washington, WA 98105, USA
Email: icetinic@gmail.com

Summary

The growing application of autonomous platforms and optical instruments to the study of biogeochemical processes offers a new source for validation of ocean color satellite data and derived biogeochemical products. However, this exciting development also demands new approaches for rigorous calibration of *in-situ* optical measurements and development of optical proxies for biogeochemical variables. Here we present a set of protocols developed during 2008 North Atlantic Experiment that were used to cross-calibrate optical sensors on multiple autonomous platforms, with the final goal of extrapolating biogeochemical parameters to larger spatial and longer temporal scales.

Introduction

The use of optical sensors on autonomous platforms has the potential to expand data sets for validation of ocean color satellite. However, such applications require that *in-situ* sensors are rigorously calibrated. For many optical sensors, pre- and post-deployment laboratory calibration is insufficient, and should be augmented with other approaches, including direct *in-situ* calibration, cross-calibration against well-characterized references, and the use of redundant and/or related sensors. This is particularly critical for arrays of sensors. A mechanistic understanding of the variability in the biogeochemical optical proxies is also necessarily for reducing uncertainty in the derived biogeochemical parameters.

Discussion

The 2008 North Atlantic Bloom (NAB 2008) experiment characterized the patch-scale evolution of the spring phytoplankton bloom using four gliders, a Lagrangian float and intensive ship-based sampling, underpinned by an aggressive sensor calibration effort. Proxy sensors were used for carbon cycle components, with ship-based efforts providing direct calibration and data for constructing proxy relationships. Direct calibrations were propagated to other autonomous sensors through deliberate cross-calibration profiles. NAB 2008 illustrates an effective approach for implementing process-scale calibration of autonomous sensors and provides guidance for the design of larger-scale efforts.

The development of the backscattering-based particulate organic carbon proxy provides a good example of the NAB08 proxy calibration process. All backscattering sensors used during the experiment (n=6) underwent bulk laboratory (factory) pre- and post-calibration [1]. The ship-based backscattering sensor was used as a reference ("gold standard"). Dark counts for the ship-based sensor were measured *in-situ,* and cross checked with manufacturer's dark counts. Factory dark voltage counts (gliders and float) were subtracted from the data, and additional offsets were applied to bring all pre-bloom deep-water values into agreement. Outputs with dark counts subtracted were first converted to volume scattering function, then to particulate backscattering using the factory calibration and current protocols. Near-simultaneous ship-glider and ship-float casts were obtained and used as a base for cross-calibration of

autonomous based measurements against the ship-based "gold standard". Ultimately, ship-based particulate organic carbon and backscattering relationship was used to obtain the high-resolution biogeochemical dataset [2], increasing the sample number from n=321 to n=1.5 x 10^6.

Conclusion

The growing number of autonomous, based optical measurements has the potential to become a primary source of validation data in the future, but the community has to be mindful of the challenges associated with this approach. These, and many similar approaches developed during NAB 2008 [3, 4], demonstrated that attention to details, rigorous cross-calibration may remove some of the uncertainties associated with this large pool of optical and biogeochemical measurements, and facilitate its use ocean color validation.

References

[1] N. Briggs. (2011). Backscatter_Calibration-NAB08, http://osprey.bcodmo.org/dataset.cfm?id=13820&flag=view. Biol. and Chem. Oceanogr. Data Manage. Office, Woods Hole, MA, USA.
[2]. I. Cetinić, M. J. Perry, N. T. Briggs, E. Kallin, E. A. D'Asaro, and Lee, C. M. (2012). Particulate organic carbon and inherent optical properties during 2008 North Atlantic Bloom Experiment. J. Geophys. Res. 117, C06028.
[3].E. D'Asaro. (2011). Chlorophyll_Calibration-NAB08, http://osprey.bcodmo.org/dataset.cfm?id=13820&flag=view. Biol. and Chem. Oceanogr. Data Manage. Office, Woods Hole, MA, USA.
[4] E. Rehm. (2011). C-Star Calibration-NAB08, http://osprey.bcodmo.org/dataset.cfm?id=13820&flag=view. Biol. and Chem. Oceanogr. Data Manage. Office, Woods Hole, MA, USA.

Multi-sensor, ecosystem-based approaches for estimation of Particulate Organic Carbon

I. Cetinić[1], M.J. Perry[1], N. Poulton[2], W.H. Slade[3]

[1]University of Maine, School of Marine Sciences and
Ira C. Darling Marine Center, Walpole ME 04573-3307, USA
[2]Bigelow Laboratory for Ocean Sciences, East Boothbay, ME 04544, USA
[3]Sequoia Scientific, Inc., Bellevue, WA 98005, USA
Email: icetinic@gmail.com

Summary

Uncertainties in remote-sensing retrieval of the particulate organic carbon concentration in the ocean can be attributed in part to differences in methodology among researchers and in part to inherent variability in the nature of oceanic particles themselves and the relationships between these particles and their optical properties. Here we present a novel approach that could lead to a better understanding of the underlying mechanisms that govern the variability of particulate organic carbon optical relationships. By using new and improved *in-situ* optical methodologies, we aim to develop a new multi-sensor, ecosystem-based remote sensing algorithm for assessing particulate organic carbon.

Introduction

Particulate organic carbon (POC) in the surface ocean is a major, dynamic carbon reservoir, and through the biological pump, provides a means for the transfer and potential storage of atmospheric CO_2 into the deep ocean. Total POC, as well as the phytoplankton fraction, is of great interest in biogeochemical studies, in part because of the potential changes in the biological pump due to climatic impacts. However, the variability of POC both regionally and globally is poorly understood due to a lack of direct measurements at sufficient spatial and temporal scales. The availability of high-resolution optical measurements from ocean color remote sensing and *in-situ* optical instrumentation has stimulated interest in the development of optical POC proxies that allow quantification of POC on temporal and spatial scales that surpass traditional, discrete water sampling methods. Current POC algorithms are based on both particulate beam attenuation and particulate backscattering coefficients (e.g., Fig. 1), but both display great variability as a function of geographical regime and/or investigator, leading us to ask the following questions:

1. What are the mechanisms responsible for the observed variability in optical proxy algorithms? Is the variability natural (inherent to the specific ecosystem or regime) or due to methodology (both chemically-measured and optical proxy POC)?

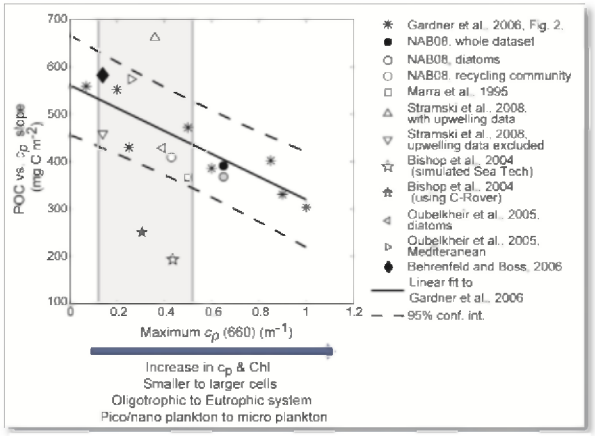

Figure 1. *POC vs. c_p slope as a function of maximum c_p observed for each data set from [1]. The regression includes eight data sets summarized by [2] (r^2=0.82). Most of the literature values fall within the 95% confidence interval (dashed line). Gray shaded area depicts the oceanic c_p threshold range (from the ACE/PACE white paper appendix).*

2. If the variability is natural, what are the drivers of the observed variability? We hypothesize that part of the variability in the optical proxy algorithms is related to differences in phytoplankton taxa and community composition, composition of non-phytoplankton particles, and ecosystem function (i.e., recycling community or not).
3. Can we build better proxies by taking these differences, as well as other environmental parameters that can be remotely sensed, into consideration?

Discussion

We are entering an era (*or we are already there?*) when most estimates of POC are derived using optical proxies (both *in-situ* and remotely sensed). These estimates of POC have been - and will continue to be used - to derive carbon budgets and ecosystem predictions, with potential impacts on environmental public policy and decision-making. Hence, it is an imperative to improve the understanding of POC optical proxy algorithms by evaluating all aspects of variability for POC and optical measurements, and by assessing uncertainties in the proxy-derived POC concentrations.

In order to address these issues, the "Multi-sensor, ecosystem-based approaches for estimation of particulate organic carbon" project goals are to:

- Conduct an intensive field program (taking advantage of ship time and space provided by collaborators) that will allow us to collect data on hydrography, inherent optical properties (including polarized angular scattering), POC, suspended particulate matter (SPM), particle size distribution (PSD), HPLC pigments, and plankton size and carbon biomass from a dynamic range of ecosystem types.
- Use best-practice POC and other biogeochemical parameter sampling and analysis protocols and use carefully calibrated (and inter-calibrated) optical instruments to constrain methodological sources of variability in both optical and POC measurements.
- Use this extensive dataset to develop a multi-sensor, ecosystem-based remote sensing algorithm that will improve estimation of the oceanic POC pool, thereby allowing new insights into the dynamics of POC, as well as SPM and phytoplankton carbon biomass, in the surface ocean.
- Evaluate the applicability of newly available remote sensing products such as Sea Surface Salinity (Aquarius/NASA) and polarized scattering measurements (PARASOL/CNES, future PACE and ACE/NASA) to improve retrieval of POC, and reduce uncertainty in its estimation.

References

[1] I. Cetinić, M. J. Perry, N. T. Briggs, E. Kallin, E. A. D'Asaro, and Lee, C. M. (2012). Particulate organic carbon and inherent optical properties during 2008 North Atlantic Bloom Experiment. J. Geophys. Res. 117, C06028.
[2] W. D. Gardner, A. Mishonov, and Richardson, M. J. (2006). Global POC concentrations from in-situ and satellite data. Deep-Sea Res. (Part II: Top. Stud. Oceanogr.) 53, 718-740.

Observed dominance of submesoscale features to subtropical chlorophyll

Haidi Chen[1]*, Galen A. McKinley[1], Colleen Mouw[2]

[1]University of Wisconsin-Madison, Department of Atmospheric and Oceanic Science, Madison, WI 53706, United States
[2]Michigan Technological University, Department of Geological and Mining Engineering and Sciences, Houghton, MI 49931, United States
Email: hchen224@wisc.edu

Summary

We apply the surface quasi-geostrophic (SQG) to newly-available cloud-free high-resolution satellite sea surface temperature data and modeled interior state to show that sub-mesoscale physics have a strong impact on surface chlorophyll. In the oligotrophic North Atlantic Subtropical Gyre (NASG), as the resolution increasing from 25km to 10 to 1km leads to a factor of three of increase in the chlorophyll found in coherent vorticies, but a factor of five increase in the chlorophyll found in oceanic fronts. This enhancement is due to the revelation of small-scale frontal dynamics at high resolution. These dynamics are associated with density and vorticity gradients around and between vorticies. This is the first direct observational evidence that pervasive sub-mesoscale frontal structures that are associated with the bulk of chlorophyll in the oligotrophic subtropical oceans; and strong evidence that submesoscale frontal upwelling is the missing link that can close the nutrient budget of the NASG.

Introduction

Mesoscale eddies at O(10-100)km have received considerable attention in plankton patchiness studies after Jenkins [1] brought the relative importance of vertical flux of nutrients due to mesoscale eddies to the forefront. The strong influence of the currents is apparent in the eddy and filamental structures traced out by satellite ocean color. However, there is no agreement on mesoscale eddies' contribution to nutrient injection and many studies point to the issue of spatial resolution of numerical models [2-4]. Mahadevan and Archer[5] performed high-resolution modeling experiments. They reported up to a factor of three increase in primary productivity when model resolution was increased from 40km to 10km in an oligotrophic region. Increasing numerical resolution from 6 km to 2 km led to a doubling of the primary production in the model of Levy et al.[6]. This increase is due to the resolution of intense vertical velocities (typically 10-100 m/d compared to mesoscale eddies of 1-10 m/d), captured within filaments of strong vorticity gradients which surround eddies or which are ejected by the eddies.

Satellite altimeters do not resolve the sub-mesoscale of O(1-10) km and our knowledge of mesoscale and sub-mesoscale influence on phytoplankton ecology is almost exclusively derived from numerical simulations, which it is clearly not yet possible to provide effective eddy parameterizations. This study, different from previous approach using eddy-permitting numerical models, takes advantage of newly-available high-resolution satellite SST data and MODIS chlorophyll data, to directly estimate how much chlorophyll is found in mesoscale eddies as opposed to submesoscale fronts.

Results

In the North Atlantic study region (28°N~38°N, -75° W~ -45°W), 20-30% of the chlorophyll that is associated with mesoscale eddies when including the contribution from eddy edges (~20%). If surface chlorophyll is linearly related to primary production, this is an upper bound of mesoscale eddies' contribution to nutrient flux that ultimately drives that productivity and much less than the estimated

contribution of eddies core from previous numerical modeling. As resolution increases from 25km to 1km, numerous fronts with a high temperature gradient (>0.6 C°/km) and vorticity gradient emerge at the center of subtropical gyre, mainly between the edges of submesoscale eddies, indicating that eddy-eddy interaction can generate intense fronts [7-8].

Frontal filaments are further parsed into warm and cold fronts based on resolved flow fields, as relative vorticity is negative on the warm side of the front and positive on the cold side. In the whole region, chlorophyll within positive-vorticity filaments are ~2.3 times higher than within negative-vorticity filaments at mesoscale, while comparable (~1.1) at submesoscale. This result suggests that regions of high phytoplankton are principally concentrated along the thin negative vorticity filaments as resolution increasing. This finding is largely consistent with results from the numerical simulations of Levy et al [6]. In their submesoscale experiment with no wind forcing, they found that strong injections of nutrients and high chlorophyll concentrations are concentrated on the negative vorticity side when density gradients along the front are growing. However, they also found high chlorophyll on the positive side when density gradients are decaying, a phenomena that we do not find in our analysis.

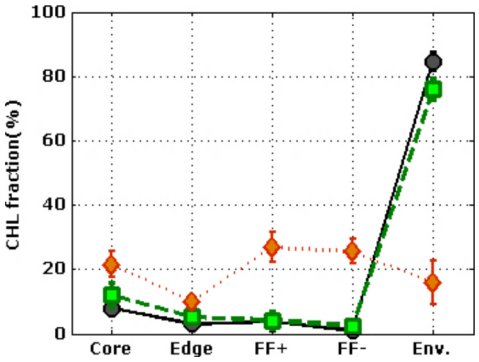

Figure 1. Additional contribution of eddies core, eddies edge, fronts of positive vorticity (FF+), fronts of negative vorticity (FF-) and the remaining environment to total chlorophyll field by increasing the flow resolution from 25km to 10km to 1km within the entire region. Mean and standard deviations are plotted, by repeating the experiments at four different random days with good satellite chlorophyll coverage: Jun 23,2010, Sep 1, 2010, Oct 12, 2010 and Mar 17, 2011.

Conclusion

This study has focused on the impact of meso and sub-mesoscale physics on surface phytoplankton patchiness, which is related with new production and an indications of nutrient fluxes in the oligotrophic oceans. Results from high-resolution satellite observations reveal that the sub-mesoscale physical features are associated with more than 1/2 of chlorophyll concentrations across the North Atlantic subtropical gyre. Consistent with the results of previous numerical studies, this is the first direct observational evidence of the significant impact of mesoscale physics on surface ocean productivity.

References

[1] Jenkins, W. J. and Goldman, J. C. (1985). Seasonal oxygen cycling and primary production in the Sargasso Sea. *J. Mar. Res.* **43,** 465

[2] Oschlies A. (2002a). Can eddies make ocean desert blooms? *Glob. Geochem. Cycles* **16,1830**

[3] Oschlies A. (2002b). Nutrient supply to the surface waters of the north atlantic: a model study. *J. Geophys.* Res.107:275

[4] McGillicuddy, D. J., Anderson, L. A., Doney, S. C. and Maltrud, M.E. (2003). Eddy-driven sources and sinks of nutrients in the upper ocean: Results from a 0.1 degree resolution model of the North Atlantic, *Global Biogeochem. Cycles,* **17(2),** 1035.

[5] Mahadevan, A. and Archer, D. (2000). Modeling the impact of fronts and mesoscale circulation on the nutrient supply and biogeochemistry of the upper ocean. *J. Geophys. Res.* **105,** 1209–1225

[6] Levy, M., Klein, P. and Treguier, A.M. (2001). Impact of submesoscale physics on production and subduction of phytoplankton in an oligotrophic regime, *J. Mar. Res.,* **59,** 535–565

[7] Levy, M., Ferrari, R., Franks, P.J.P, Martin, A.P. and Rivière, P. (2012). Bringing physics to life at the submesoscale, *GRL frontier article,* **39,**L14602

[8] Lima, I. D., Olson, D. B., and Doney, S. C. (2002). Biological response to frontal dynamics and mesoscale variability in oligotrophic environments: Biological production and community structure, *J. Geophys. Res.,* **107(C8),** 3111.

Development of the Next Geostationary Ocean Color Imager (GOCI-II) in Korea

Seongick CHO[1,2], Ki-Beom Ahn[1], Eunsong Oh[1], Young-Je Park[1], Yu-Hwan Ahn[1], Joo-Hyung Ryu[1]

[1]Korea Ocean Satellite Center, Korea Institute of Ocean Science & Technology, Seoul, 425-600, Korea
[2]Space Optics Laboratory, Dept. of Astronomy, Yonsei University, Seoul, 120-749, Korea
Email : sicho@kioat.ac

Summary

The development of GOCI-II, the successive mission of GOCI, was started in the late 2012. Major Enhanced performance requirements of GOCI-II are around 250m GSD(Ground Sampling Distance) with 13 spectral bands, and newly implemented Full Disk observation coverage. GOCI-II is expected to increase the applicability of ocean remote sensing products with increased data accuracy and addition of new products such as PFT.

Introduction

After the successful launch and operation of Geostationary Ocean Color Imager(GOCI) [1], necessity of succession of GOCI mission, ocean environment monitoring with ocean color, is highly increasing into ocean color remote sensing users in Korea as well as international users.
As a successor of GOCI mission, development of GOCI-II was started in 2012 and is planned to be launched in 2018.

Discussion

The mission and user requirements of GOCI-II are defined by Korea Institute of Ocean Science & Technology (KIOST) and domestic and international GOCI PI(Principal Investigator)s. GOCI-II has two nominal observation modes; FD (Full Disk) which can observe nearly full Earth disk area (East-West direction: inside 60 degrees at latitude, North-South direction: inside 60 degrees at longitude) on 128.2˚E longitude in Geostationary Earth Orbit (GEO), with 1km GSD (Ground Sampling Distance) at Nadir, and LA (Local Area) of which observation region can be freely definable by the user with 250m GSD at Nadir with 30 minutes imaging time and 1 hour interval. The scheduled LA observations are 10 times per day with 1 hour interval. The number of daily LA acquisition time is increased from 8 to 10 comparing with GOCI. The major enhancements of GOCI-II are around two time better GSD than GOCI's GSD and implementation of FD observation with 13 spectral bands. The comparison of performance requirements between GOCI and GOCI-II is summarized in Table 1. Additional 4 spectral bands and a dedicated wideband (presumably panchromatic band) for INR processing will be added to improve the accuracy of data products such as chlorophyll concentration, total suspended sediments, and dissolved organic matters, and to have a novel capability such as PFT(Phytoplankton Functional Type). GOCI-II has a plan to implement the user-definable local area observation mode to satisfy the user requests such as ocean observation over clear sky without clouds and special ocean event area. We are expecting this new capability will produce more applicable data products about special event area such as typhoon, oil spill, green algae bloom, and etc. These enhanced features will enable the monitoring and research of long-term ocean environment change with better image quality. For the research of long-term climate change in ocean, FD observation with one time per day is planned for nominal operation plan of GOCI-II.

Requirements	GOCI	GOCI-II

Mission life time	7.7 years	≥ 10 years
Reliability	≥ 0.85 @ EOL	≥ 0.85 @ EOL (7 years)
Duty Cycle (LA)	8 times / 1day	10 times / 1day
Duty Cycle (FD)	-	1 time / 1day
Observation Time	LA : ≤ 30 min	LA : ≤ 30 min FD : ≤ 240 min
Spatial Resolution	500m (LA)	effective GSD (LA) ≤ 250m (@ 130E, 0N) effective GSD (FD) ≤ 1,000m (@ 130E, 0N)
Spectral Range	400nm – 900nm	370nm – 900nm
# of Spectral Bands	8 (VIS/NIR)	13 (VIS/NIR, Wideband for INR)
SNR	> ~1,000 @ nominal radiance	≥ ~1,000 @ nominal radiance
MTF	> 0.3 (NS/EW) @ Nyquist frequency	> 0.25 (NS/EW) @ Nyquist frequency (Payload) > 0.10 (NS/EW) @ Nyquist frequency (System)
Inter-Slot Radiometric Discrepancy	-	≤ 0.2%
Band Center Wavelength Accuracy	± 0.5 nm	≤ ± 2.0 nm (≤ ± 0.5nm for band center at 680nm)
Radiometric Accuracy	≤ 4 % (over Saturation Radiance) ≤ 5 % (over Max. Cloud Radiance)	≤ 3 % (on ground before launch) ≤ 4 % (in orbit)
Out of band Response	≤ 1.0 %	≤ 1.0 %
Polarization	< 2 %	≤ 1.5 % (≤ 3.0 % for B1 (380nm))
Straylight	-	≤ 1.0 % (LA, ground processing)

Table 1 The summary of comparison of performance requirements between GOCI and GOCI-II

Conclusions

The international co-development of GOCI-II payload is planned to be started from June, 2013. Joint Development Team which consists of KARI (Korea Areospace Research Institute), KIOST and satellite development company outside Korea takes in charge of GOCI-II development. Dedicated ground station and data processing S/W for the operation of GOCI-II will be established or developed by 2018

Reference

[1] Joo-Hyung Ryu, Hee-Jeong Han, Seongick Cho, Young-Je Park, and Yu-Hwan Ahn (2012). Overview of Geostationary Ocean Color Imager(GOCI) and GOCI Data Processing System(GDPS). Ocean Sci. J. 47(3):223-233.

Application of Geostationary Satellite Images to the monitoring of dynamic variations

Jong-Kuk Choi, Young-Je Park, Joo-Hyung Ryu

Korea Ocean Satellite Centre, Korea Ocean Research & Development Institute, 787 Haean-no, Ansan, 426-744, Korea
Email : jkchoi@kiost.ac

Summary

The primary advantage of the Geostationary Ocean Color Imager (GOCI), the world's first geostationary ocean color observation satellite, over other ocean color satellite imagers is that it can obtain data every hour during the daytime, allowing ocean monitoring in near real time. Here, we introduce and investigate various applications using GOCI to monitor the dynamic variations that are observed in the coverage of GOCI, in particular in the west coast of Korean peninsula along with land part applications.

Introduction

The Geostationary Ocean Color Imager (GOCI) is the world's first ocean color observation satellite placed in a geostationary orbit. GOCI was launched in June 2010 for near real-time monitoring of marine environments in northeast Asia with a 500-m spatial resolution. GOCI covers the 2,500 x 2,500 km square around Korean peninsula centered at 36°N and 130°E and is comprised of sixteen (4x4) slot images. GOCI has six visible bands with band center 412 nm, 443 nm, 490 nm, 555 nm, 660 nm and 680 nm, and two near-infrared bands with band center 745 nm and 865 nm [1]. Unlike the existing polar-orbit satellites, GOCI can gather data every hour from 10 a.m. to 5 p.m. local time (eight times per day) around the Korean Sea [2]. This temporal resolution of GOCI is very efficient for ocean environmental analysis. A more detailed time-series monitoring is possible for the spread and movement of a red tide, SS, DOM and other polluting materials. GOCI also has higher radiometric, spectral resolution and temporal resolution, so that more precise processing of the atmosphere for aerosol type analysis, yellow dust and cloud detection is feasible [3]. Moreover, some land applications including vegetation management, forest fire, heavy snowfall and inland flood detection and monitoring are also possible.

Band	*Central wavelengths*	*Band Width*	*Primary Application*
B1	412 nm	20 nm	Yellow substance and turbidity
B2	443 nm	20 nm	Chlorophyll absorption maximum
B3	490 nm	20 nm	Chlorophyll and other pigments
B4	555 nm	20 nm	Turbidity, suspended sediment
B5	660 nm	20 nm	Baseline of fluorescence signal, Chlorophyll, suspended sediment
B6	680 nm	10 nm	Atmospheric correction and fluorescence signal
B7	745 nm	20 nm	Atmospheric correction and baseline of fluorescence signal
B8	865 nm	40 nm	Aerosol optical thickness, vegetation, water vapor reference over the ocean

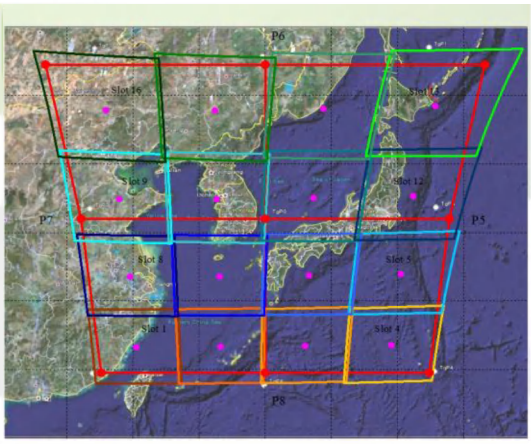

Spectral Bands Characteristics and primary applications of each band along with the target area of GOCI

Applications of GOCI

GOCI can be employed to investigate dynamic variations in the coastal water properties, in particular, in an environment affected by semi-diurnal tides such as the west coast of the Korean Peninsula. GOCI was effectively employed to the monitoring of coastal water turbidity variations based on the tidal cycle [1]. These hourly variations in coastal water properties can be basic dataset to develop an algorithm for catching the ocean current movement, i.e. velocity and direction which are crucial information for seawater circulations, fisheries, shipping control, military purpose, etc. in coastal area [4]. Another excellent application of GOCI in terms of the short-term variability is surveillance of waste disposal activity at sea. GOCI could even clearly trace the disposal activity of a sewage sludge disposal ship near-real time for several hours due to its great temporal resolution. Through that hourly-based traceable variability, the ship's cruising speed could also be estimated [5]. Although it is not the oceanic phenomena, sea fog movement can be clearly seen from 1-h interval GOCI images. GOCI-based near real-time monitoring of the sea fog can be greatly helpful for preventing safety accident and supporting fishery activities

Conclusions

The dynamics of ocean properties, especially near the coastal region can be successfully estimated using geostationary satellite images with high frequency like GOCI. To this end, algorithms for atmospheric correction, SSC, Chl and other parameters both in the open ocean and in high turbid water suited for GOCI with high accuracies are inevitable, which is still challenging. These accurate estimates of ocean parameters also make it possible to identify other various dynamic variability which have been impossible with polar-orbit satellite systems; differences in chlorophyll-a distribution before- and after-typhoon, which can be a clue to understand the transformation of ecological environment relating to the natural hazards, sea ice velocities along with its distribution, etc.

Reference

[1] Choi, J.-K., Park, Y.J., Ahn, J.H., Lim, H.-S., Eom, J., & Ryu, J.-H. (2012). GOCI, the world's first geostationary ocean color observation satellite, for the monitoring of temporal variability in coastal water turbidity, J. Geophys. Res., 117, C09004

[2] Cho, S.I., Ahn, Y.H., Ryu, J.H., Kang, G.S. and Youn, H.S. (2010). Development of Geostationary Ocean Color Iamger (GOCI) (Korean ed.). Korean Journal of Remote Sensing, 26(2), 157-165.

[3] Ryu, J. H., J. K. Choi, J. Eom, and J. H. Ahn (2011). Temporal and daily variation in the Korean coastal waters by using Geostationary Ocean Color Imager. Journal of Coastal Research, J Coastal Res, SI 64 (Proceedings of the 11th International Coastal Symposium), 1731-1735.

[4] Choi, J. K., Hyun Yang, H. J. Han, Ryu, J. H. and Park, Y.J. (2013). Quantitative estimation of the suspended sediment movements in the coastal region using GOCI, Proceedings 12th International Coastal Symposium (Plymouth, England), Journal of Coastal Research, Special Issue No. 65, ISSN 0749-0208.

[5] Hong, G. H., D. B. Yang, Hyun-Mi Lee, Sung Ryull Yang, Hee Woon Chung, Chang Joon Kim, Young-Il Kim, Chang Soo Chung, Yu-Hwan Ahn, Young-Je Park, and Jeong-Eon Moon (2012). Surveillance of Waste Disposal Activity at Sea using Satellite Ocean Color Imagers: GOCI and MODIS, Ocean Sci. J., 47(3), 387-394.

Australian waters Earth Observation Phytoplankton-type products (AEsOP).

Clementson, L.A.[1], Hardman-Mountford, N.[2], Mueller, H.[3], Brando, V[4], King, E.[1],

Terhorst, A.[3], Kelly, P.[1]

[1] CSIRO Marine and Atmospheric Research, Hobart, Tasmania, Australia

[2] CSIRO Marine and Atmospheric Research, Perth, Western Australia,

[3] ICT Centre, CSIRO Marine and Atmospheric Research, Hobart, Tasmania, Australia

[4] CSIRO Land and Water, Canberra, ACT, Australia

Email: lesley.clementson@csiro.au

Summary

The The Australian waters Earth Observation Phytoplankton-type products (AEsOP) project aims to establish an in situ database specifically for the calibration and validation of regional algorithms. The dataset will include multiple coincident parameters such as HPLC pigments (including size fractionated pigments where available), pigment concentration and composition, full spectral absorption (a_{ph}, a_d, a_g), total suspended mater (TSM), Secchi depth and processed data from radiometers, hydroscat, ac-9, ac-s and other instruments from 1997 to the present day. It is envisaged that the first version of this database will available by mid 2013.

Introduction

Since the launch of SeaWiFS, in 1997, satellite-retrieved estimates of chlorophyll-a (chl-a) have been used as a proxy for phytoplankton biomass. The unprecedented spatial and temporal coverage of satellite-generated products, such as chl-a, has enhanced our knowledge of trends in productivity and extended our understanding of biogeochemical processes, on both regional and global scales. Currently standard global algorithms developed for use with the SeaWiFS, MODIS, MERIS or other sensors have been primarily based on atmospheric corrections and *in situ* bio-optical data collected in the northern hemisphere. These conditions are not always applicable to regions within the southern hemisphere. The Australian waters Earth Observation Phytoplankton-type products (AEsOP) project aims to address this situation by establishing an interrogative database of in situ bio-optical measurements which will aid in the development of robust regional algorithms and, when added to the global datasets, enhance the applicability of the standard global algorithms to both hemispheres.

The AEsOP database will build on the bio-optical data archive established by Australia's Integrated Marine Observing System (IMOS) which was established in 2007 and will provide data to the Phytoplankton Functional Types (PFTs) database, currently being established by the International Working Group for PFT Algorithm Development.

Discussion

The NASA bio-optical Marine Algorithm Dataset (NOMAD) is a dataset of *in situ* bio-optical data for use in ocean colour algorithm development and satellite data product validation. NOMAD was compiled using data archived in the SeaWiFS Bio-optical Archive and Storage System (SeaBASS) and comprises data from over 3400 samples, although not all samples have data for all parameters. Comparison of the the values of the chl-a concentration and the absorption coefficients due to phytoplankton, non-algal matter and CDOM between NOMAD and a datset of 1200 values from Australian waters show all the parameters to be significantly lower in Australian waters than they are in waters of the northern hemisphere. Figure 1 illustrates difference, showing an image processed with SeaDAS compared to one processed with a regional algorithm.

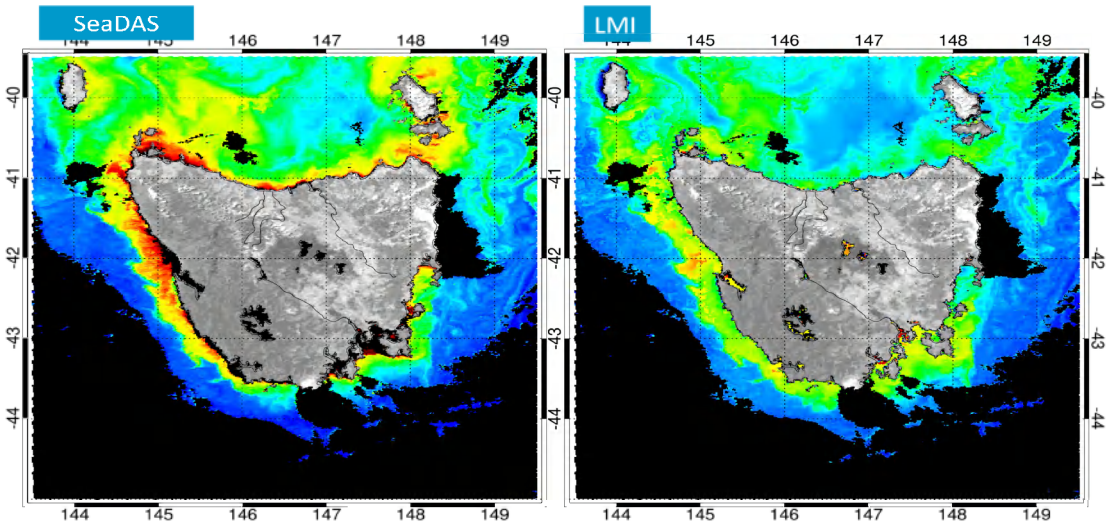

Figure 1 Ocean colour images of the chl-a distribution in Tasmanian coastal waters (13 October 2003) processed by SeaDAS and a regional algorithm

This clearly indicates why the standard global algorithms based on an average bio-optical model for satellite retrieval of parameters such as chl-a, TSM or CDOM often fail in Australian waters.

Conclusions

An interrogative database of bio-optical parameters for Australian waters is being established by the AEsOP project. This database will provide in situ data for the development of robust regional algorithms and, the enhancement standard global algorithms in the future

Acknowledgements

The authors acknowledge funding for the AEsOP project from the CSIRO Earth Observation Informatics-TCP.

A dataset of global in situ observations for the development and comparison of Phytoplankton Functional Type (PFT) algorithms.

Clementson, L.A.[1], Hardman-Mountford, N.[2], Hirata, T.[3], Barlow, R.[4], Hirawake, T.[3], Brewin, R.[5], Bracher, A.[6]

[1] CSIRO Marine and Atmospheric Research, Hobart, Tasmania, Australia

[2] CSIRO Marine and Atmospheric Research, Floreat, WA, Australia

[3] Hokkaido University, Sapporo, Japan

[4] Bayworld Centre Research and Education, Cape Town, South Africa

[5] Plymouth Marine Laboratory, Plymouth, UK

[6] PHYTOOPTICS Group, Alfred-Wegener Institute Helmholtz Center for Polar and Marine Research and Institute of Environmental Physics at University of Bremen, Germany

Email: lesley.clementson@csiro.au

Summary

The International Working Group for PFT Algorithm Development aims to establish an in situ dataset specifically for the calibration and validation of PFT algorithms. The dataset will include multiple coincident parameters such as HPLC pigments (including size fractionated pigments where available), flow cytometry, microscopic cell counts, particle size and in-water optical measurements from both the northern and southern hemispheres. It is envisaged that the first version of this dataset will be publically available in 2014.

Introduction

Since the launch of SeaWiFS, in 1997, satellite-retrieved estimates of chlorophyll-a (chl-a) have been used as a proxy for phytoplankton biomass. The unprecedented spatial and temporal coverage of satellite-generated products, such as chl-a, has enhanced our knowledge of trends in productivity and extended our understanding of biogeochemical processes, on both regional and global scales. However in recent years researchers have required greater detail about the phytoplankton community composition responsible for the productivity and whether the phytoplankton community consisted of taxonomic groups with specific functions, such as silicification, calcification and nitrogen fixation. Phytoplankton with these functions have been termed Phytoplankton Functional Types (PFTs) and in response to the requirement for greater detail about the phytoplankton community composition, PFT algorithms have been developed. Some of the algorithms generate estimates of phytoplankton composition by determining size structure while others estimate taxonomic groupings. At present it is difficult to compare the outputs of PFT algorithms as each algorithm has used an individual input dataset.

It is the intention of the International Working Group for PFT Algorithm Development to establish an in situ dataset specifically for the calibration and validation of PFT algorithms. The dataset will include

multiple coincident parameters such as HPLC pigments (including size fractionated pigments where available), flow cytometry, microscopic cell counts, particle size and in-water optical measurements from both the northern and southern hemispheres. The availability of the dataset will allow better comparison of the outputs from different PFT algorithms and also allow validation of the algorithms over different regions. The Working Group acknowledge that databases and datasets such as SeaBASS and NOMAD (NASA) already exist, but believe that the PFT dataset with the added phytoplankton-specific parameters will only enhance the information available to researchers.

Discussion

Collection of in situ data from various investigators is underway, building on existing datasets (e.g. Hirata et al. 2011) and it is envisaged that by May 2013 the PFT dataset will contain substantial data from the southern hemisphere. This data will come from the Australian, South African, New Zealand and Southern Ocean regions. By mid-year, data from the northern hemisphere will be added to the dataset.

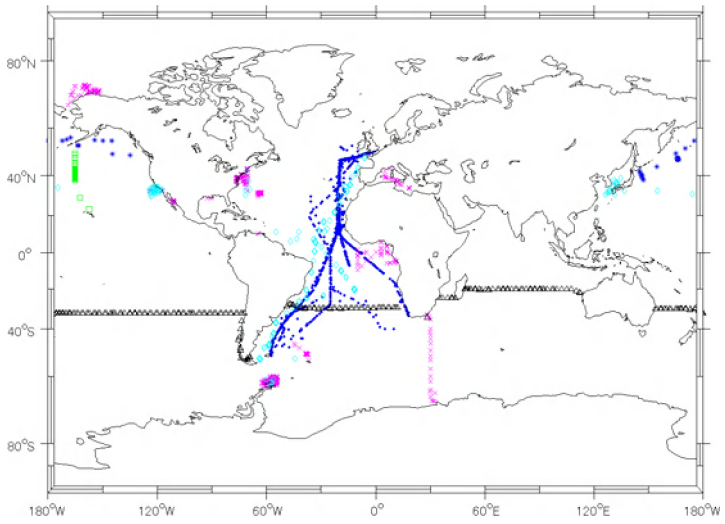

Fig. 1. In situ data used for the development of a global PFT algorithm by Hirata et al. (2011).

Acknowledgements

The authors Clementson and Hardman-Mountford acknowledge funding to assist this work from the EOI-TCP for the AEsOP project.

References

Hirata, T., Hardman-Mountford, N.J., Brewin, R.J.W., Aiken, J., Barlow, R. (2011). Synoptic relationships quantified between surface Chlorophyll-a and diagnostic pigments specific to phytoplankton functional types. *Biogeosciences* **8**: 311-327

MODIS atmospheric correction and chlorophyll products in the Strait of Georgia, British Columbia, Canada.

M. Costa[1], T. Carswell[1], E. Young[1], N. Komick[2], L. Zhai[3]
[1]University of Victoria, Department of Geography, Victoria, BC, Canada
[2]Department of Fisheries and Ocean, Pacific Biologic Station, Nanaimo, BC, Canada
[3]Bedford Institute of Oceanography, Halifax, NS, Canada
Email:maycira@uvic.ca

Summary

MODIS derived aerosol optical depth (AOD) and chlorophyll (Chl) and were compared with in situ AERONET and extracted chlorophyll, respectively, and weekly binned for deriding bloom metrics for the Strait of Georgia (SOG), an optically complex estuarine environment on the West Coast of Canada. A total of 101 images were considered in the evaluation of the atmospheric strategies: (1) the management unit of the North Sea mathematical models (MUMM) with SWIR band, (2) the fixed Angstrom coefficient derived from AERONET, and (3) the standard NIR approach. In the next step, the sensor derived chlorophyll estimates were determined using the OC3M model and compared with extracted chlorophyll acquired within 24 hrs, 6hrs, and 2 hrs on imagery acquisition. The results showed indicated that the MUMM+SWIR (r^2= 0.6-0.7; average slope ~1.1; $RMSE_{443nm}$= 0.7% and $RMSE_{869nm}$= 0.9% compared with in situ AERONET AOD) and the MUMM+SWIR and OC3M chlorophyll (24hrs: n=42, r^2=0.4, and slope=0.6; 6hrs: n=21, r^2=0.6, and slope=0.9; and 2hrs: n=11, r^2=0.7, and slope=1.1 compared with in situ chlorophyll) resulted in the best estimates of chlorophyll. These products were further weekly binned and bloom metrics derived.

Introduction

Fraser River salmon, specifically sockeye, are one of the most important fisheries for the British Columbia commercial and recreational fishing sectors. However, the stocks have experienced variations of return rates in the past 50 years, and a general decline in the past decade, thus adding several uncertainties in the management of this valuable resource [1]. Return rate variability of Fraser sockeye have been attributed to several factors, including oceanographic variability in the Strait of Georgia (SoG) [2] such as zooplankton availability, which is to a certain extent groups related to the phytoplankton bloom conditions in the SoG [3]. As such, the important role of the spring bloom on the survival of juvenile salmon has been hypothesized [1]. The objective of this work is to define the appropriate method to determine phytoplankton bloom metrics (initiation, amplitude, and duration) in the SoG based on MODIS imagery. The first step is the validation of the atmospheric correction strategy; second step the validation of the estimated chlorophyll model; and third, the binning of imagery and generation of temporal bloom metrics.

Results and Discussion

Image data (level 1a) were accessed from NASA's OceanColor web portal, and processed in SeaDAS (Seawifs Data Analysis System) environment. All available MODIS-Aqua images (n=465, 2007, 2008, and 2012) were processed. In the first step, a total of 101 images were considered in the evaluation of three different atmospheric strategies: (1) the management unit of the North Sea mathematical models (MUMM) with SWIR band, (2) the fixed Angstrom coefficient derived from AERONET, and (3) the standard NIR approach. The results showed significant agreement between in situ AERONET AOD at visible and near-infra red wavelengths and MODIS derived AOD for the different atmospheric

approaches: MUMM+SWIR (r^2= 0.6-0.7; average slope ~1.1; $RMSE_{443nm}$= 0.7% and $RMSE_{869nm}$= 0.9%); fixed Angstrom (r^2= 0.7-0.8; average slope ~1.3; $RMSE_{443nm}$= 1.3% and $RMSE_{869nm}$= 0.8%); and standard NIR (r^2= 0.7-0.8; average slope ~1.1; $RMSE_{443nm}$= 1.2% and $RMSE_{869nm}$= 0.6%).

In the second step, the sensor derived Chl estimates were determined using the OC3M model [4] and compared with extracted chlorophyll acquired within 24 hrs, 6hrs, and 2 hrs on imagery acquisition. The results indicated that the MUMM+SWIR and OC3M Chl resulted in the best estimates when compared with in situ data acquired within 2 hrs of imagery acquisition (24hrs: n=42, r^2=0.4, and slope=0.6; 6hrs: n=21, r^2=0.6, and slope=0.9; and 2hrs: n=11, r^2=0.7, and slope=1.1) compared with the NIR and OC3M approach (24hrs: n=48, r^2=0.12, slope=0.8; 6hrs: n=23; r^2=0.4, and slope=0.9; 2hrs: n=12, r^2=0.6, slope=0.6). There were no images corrected with the fixed Angstrom coefficient coincident with in situ data acquisition, thus highlighting the issue of needing AERONET data to guide the atmospheric correction step.

After the previous evaluation, the MUMN+SWIR and OC3M Chl derived images were spatially binned and finally temporally binned to derive mean 'weekly' Chl concentrations. Mean weekly Chl values were collected for a central region the south SoG. The number of available binned (weekly) images were 20 (2007); 19 (2008); 21 (2012). In order to derive bloom dynamics that help describe underlying physical and biological forcing, a set of objective metrics were derived based on a shifted Gaussian function of time fitted to the time-series of binned weekly imagery mean *chl* concentrations [5]. The earliest timing of initiation (week 6.6 – mid February) was defined in 2008. This is much earlier than 2007 and 2012 years, 12.0 (~end March) and 12.9 (~beginning of April) week, respectively. Further, 2007 and 2012 are also similar in regard to week of maxima observed Chl (~week 15) and maximum observed concentrations (~16.0 mg m^-3). Much lower maximum Chl were determined in 2008 (3.4 mg m^{-3}) but for a long duration (~ 10 weeks). The determined week of initiation of bloom conditions in 2012 was beginning of April. Our methods further defined that the 2012 maximum Chl was approximately 16.0 mg m^{-3} and the bloom last for about 4 weeks. Determining inter-annual relationships between the timing/magnitude/duration of the spring bloom and the residence/condition of juvenile salmon entering from lotic systems may be paramount for ecological based fisheries management. Our approach applied to a 10 years time series of data will help to understand these relationships.

References

[1]Marmorek, D., D. Pickard, A. Hall, K. Bryan, L. Martell, C. Alexander, K. Wieckowski, L. Greig and C. Schwarz. 2011. Fraser River sockeye salmon: data synthesis and cumulative impacts. ESSA Technologies Ltd. Cohen CommissionTech. Rep. 6. 273p. Vancouver, B.C. www.cohencommission.ca.

[2]Thomson, R.E.; Beamish R. R.; Beacham, T.D.; Trudel, M.; Whitfield, P.H.; Hourston, R.A.S. (2012). Anomalous ocean conditions may explain the recent extreme variability in Fraser River sockeye salmon production. *Marine and costal Fisheries: Dynamics, Management, and Ecosystem Sciences*, 4:415-437.

[3]Kleppel,G. (1993). On the diets of calanoid copepods. *Marine Ecology Progress Series*, 99, 183-195.

[4]Komick, N., Costa, M., Gower, J. (2009). Bio-optical algorithm evaluation for MODIS for western Canada coastal waters: an exploratory approach using *in-situ* reflectance. *Remote Sensing of Environment,* 113(4), 794-804.

[5]Zhai, L., Platt, T., Tang, C., Sathyendranath, S., Hernandez Walls, R. (2011). Phytoplankton phenology on the Scotian Shelf. *ICES Journal of Marine Science*, 68(4),781-791.

Statistical Derivation of Inherent Optical Properties and Chlorophyll *a* From an Optically Complex Coastal Site

Susanne E. Craig[1], Jennifer Cannizzaro[2], Chuanmin Hu[2], Chris T. Jones[1], Paul Carlson[3]
[1]Dalhousie University, Dept. of Oceanography, B3H 4R2, Canada; [2]University of South Florida, College of Marine Sciences, FL 33701, USA; [3]Florida Fish & Wildlife Research Institute, FL 33701, USA
Email: susanne.craig@dal.ca

Summary

A statistically based model, trained using regional data, accurately derives chlorophyll *a* concentration and various inherent optical properties (IOPs) from *in situ* measurements of remote sensing reflectance in the waters of Big Bend, FL, USA – an area where conventional approaches often yield poor results due to optical complexity (high CDOM absorption, bottom reflectance) and challenges in achieving atmospheric correction. The approach is also successfully applied to MODIS data, and, despite imperfect atmospheric correction, successfully derives accurate estimates of chlorophyll *a* and IOPs. Results indicate the potential of the approach to derive important biogeochemical parameters from ocean colour under very challenging conditions in this ecologically and commercially important coastal region.

Introduction

Big Bend, Florida, USA is an area of both commercial and ecological importance and is home to several large fisheries, seagrass habitat and popular tourist destinations. Measurement of ocean colour offers a powerful means to achieve such monitoring and can capture synoptic patterns in biological and physical processes at various temporal and spatial scales. However, accurate retrieval of proxies for these processes (e.g. chlorophyll a concentration or backscattering coefficient) from ocean colour is often challenging in this region due to the non co-varying nature of the optically active water constituents and to the difficulty in achieving accurate atmospheric correction. Here we present a region specific, statistical approach[1] for deriving inherent optical properties (IOPs) and chlorophyll *a* concentration from measurements of ocean colour around the Big Bend region of FL, USA. We first show results for an extensive *in situ* dataset, then use the same approach for MODIS measurements of the study area.

The algorithm of Craig *et al.*[1] was used to derive chlorophyll *a* concentration (*Chl a*; mg m^{-3}) and IOPs from *in situ* measurements of remote sensing reflectance ($R_{rs}(\lambda)$; sr^{-1}). This is a statistical approach that uses empirical orthogonal function (EOF) analysis to identify the dominant modes of variance in the shape of $R_{rs}(\lambda)$ spectra and then builds a model based on the relationship of the EOF modes with either *Chl a* or IOPs. The model was trained using a subset (70%) of an extensive *in situ* radiometric and water sample dataset that covered various water types including those dominated by coloured dissolved organic material (CDOM) absorption and those influenced by bottom reflection. The model was then tested on the remaining 30% of the dataset. Following

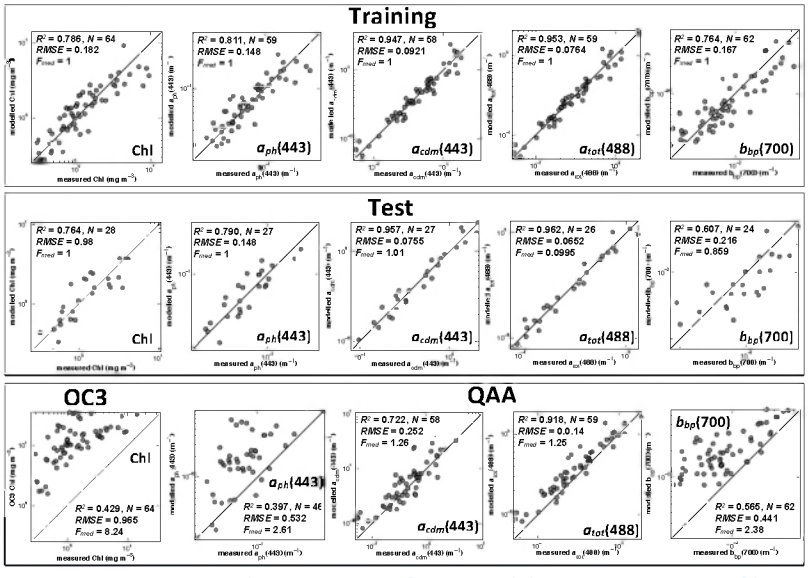

Fig. 1. Training, test and comparison of EOF models. F_{med} is a metric of bias: 1 = no bias, 2 = model overestimates x2, 0.5 = model underestimates x2

implementation of the model on the *in situ* data, the approach was also tested on MODIS imagery of the same region.

Discussion

Training and test results for the model for *Chl a*, phytoplankton absorption at 443 nm ($a_{ph}(443)$; m^{-1}), detrital and CDOM absorption at 443 nm ($a_{cdm}(443)$; m^{-1}), total absorption at 488 nm ($a_{tot}(488)$; m^{-1}) and particulate backscattering at 700 nm ($b_{bp}(700)$; m^{-1}) are shown in Fig. 1, rows 1-2. The models performed very well, especially in deriving absorption coefficients. Many of the spectra were obtained from sites where CDOM absorption comprised up to 80% of total absorption or where $R_{rs}(\lambda)$ spectral shape was significantly modified by bottom reflectance, showing the ability of the EOF approach to accurately detect very small variations in spectral shape that may otherwise be 'swamped' by more dominant signals. Test results showed only a modest decrease in modest skill, suggesting that the model had been adequately trained. For comparison, *Chl a* derived using the OC3 algorithm[2] and IOPs using the quasi-analytical algorithm (QAA)[3] are shown in Fig. 1, row 3. It should be pointed out that the EOF algorithm is trained using regional data, whereas both the OC3 and QAA algorithms are global models. It is not unexpected, therefore, that our model performed better. However, what we present here is the application of a *generic approach* that is computationally inexpensive, straightforward to apply and that can be applied in any instance in which a modestly sized[1] radiometric and corresponding validation dataset is available.

The models derived from the *in situ* data were then applied to MODIS $R_{rs}(\lambda)$ from the same region, but *Chl a* and IOP estimates were poor. Upon comparison of MODIS $R_{rs}(\lambda)$ with match up *in situ* $R_{rs}(\lambda)$, it was evident that inadequate atmospheric correction was likely deforming the spectral shape, meaning that the model coefficients derived from the *in situ* data were not appropriate. It was decided, therefore, to train a new set of models using only MODIS $R_{rs}(\lambda)$ in order to account for the deformation of the spectral shape, especially in the blue. The MODIS dataset was split into 60:40 training:test subsets and the results are shown in Fig. 2. $a_{tot}(488)$ and $a_{cdm}(443)$ are estimated most accurately, and in general, model skill is comparable to the *in situ* models (Fig. 1). Only 33 data points were available for the training and testing procedures, but these initial results are very encouraging and suggest that accurate estimates of biogeochemical parameters in this optically complex site can be derived even under conditions of imperfect atmospheric correction. This is a significant finding, indeed, and underscores the ability of the EOF approach to 'tease out' spectral signatures of optically active water constituents from imperfectly atmospherically corrected satellite data.

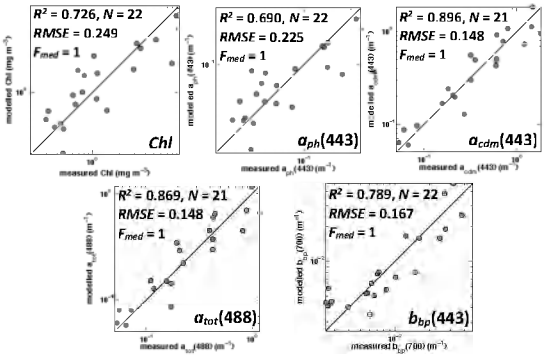

Fig. 2. EOF model results for MODIS data

Conclusions

A statistically based, computationally inexpensive, regional model accurately estimates *Chl a* and various IOPs from both *in situ* and satellite measurements of $R_{rs}(\lambda)$ from very optically complex waters. The model performs very well despite modification of $R_{rs}(\lambda)$ spectral shapes from high CDOM concentration, bottom reflectance and imperfect atmospheric correction, pointing strongly to its potential as a valuable tool in coastal ocean colour applications.

References

1 Craig, S. E. *et al.* Deriving optical metrics of coastal phytoplankton biomass from ocean colour. *Remote Sensing of Environment* **119**, 72-83, doi:10.1016/j.rse.2011.12.007 (2012).

2 O'Reilly, J. E. *et al.* SeaWiFS postlaunch calibration and validation anlayses, part 3. 58 (NASA, Greenbelt, Maryland, 2000).

3 Lee, Z. P., Carder, K. L. & Arnone, R. A. Deriving inherent optical properties from water colour: a multiband quasi-analytical algorithm for optically deep waters. *Applied Optics* **41**, 5755-5772 (2002).

Comparison between MERIS and Regional High-Level Products in European Seas

Davide D'Alimonte[1], Giuseppe Zibordi[2], Tamito Kajiyama[3], Jean-François Berthon[2]

[1]Centro de Inteligência Artificial, Departamento de Informática, Faculdade de Ciências e Tecnologia, Universidade Nova de Lisboa, Quinta da Torre, Caparica, Portugal
[2]European Commission, Joint Research Centre, Institute for Environment and Sustainability, Ispra, Italy
[3]Centro de Investigação Informática e Tecnologias da Informação, Faculdade de Ciências e Tecnologia, Universidade Nova de Lisboa, Quinta da Torre, Caparica, Portugal
Email: davide.dalimonte@gmail.com

Summary

Standard ocean color data products from the Medium Resolution Imaging Spectrometer (MERIS) are compared with equivalent regional products determined for European seas exhibiting different bio-optical properties: the northern Adriatic Sea, the Baltic Sea and the Western Black Sea. Comparison results are consistent across the investigated European seas. Findings indicate the relevance of using regional bio-optical algorithms to evaluate standard products as a complement to match-up analysis relying on pairs of in situ and satellite data.

Introduction

In this poster, standard ocean color data products from the Medium Resolution Imaging Spectrometer (MERIS) are compared with equivalent regional products determined for European seas exhibiting different bio-optical properties: the northern Adriatic Sea, the Baltic Sea and the Western Black Sea (ADRS, BLTS and BLKS, respectively). Investigated quantities are those relevant to optically complex waters: 1) the algal-2 pigment index, alg2; 2) the composite absorption coefficient of yellow substance and non-pigmented particles at 442nm, a_{dg}; and 3) the concentration of Total Suspended Matter, TSM. Regional data products are created using Multi Layer Perceptron (MLP) neural nets [1] trained with field measurements from the Coastal Atmosphere and Sea Time Series (CoASTS) [2, 3] and Bio-Optical mapping of Marine Properties (BiOMaP) programs [4].

Discussion

Case-2 water data products addressed in this study are MERIS alg2, a_{dg} and TSM values generated with MEGS 8.0. These quantities have been compared with equivalent regional products computed with MLPs trained using BiOMaP and CoASTS field measurements (e.g., Figure 1). Applied methods include the revision and integration of former schemes for the identification of the applicability of regional algorithms [5], the retrieval of pigment index values [6] and the assessment of data products [7]. Data product comparisons based on selected ROIs have shown consistent results in all investigated regions. Specifically, MERIS alg2 values overestimate the output of regional algorithms. An underestimate is instead observed for a_{dg}. MERIS TSM values are lower than MLP products in ADRS and BLKS, while a slight overestimate is reported for BLKS. The convergence between MERIS and regional products is hence significantly better for TSM than for alg2 and a_{dg}. These assessments are in agreement with independent findings exclusively based on match-ups of satellite and in situ data [8].

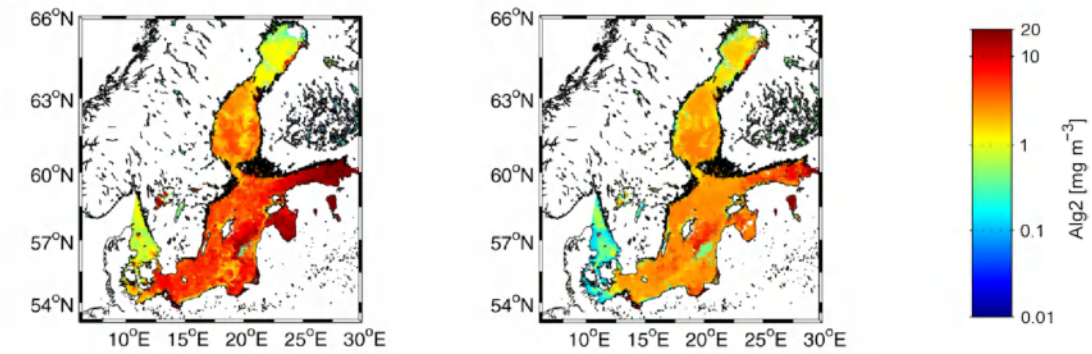

Figure 1 Example of alg2 product maps for the Baltic Sea. MERIS standard product and corresponding result from the application of the regional MLP are in the left and right column panel, respectively.

Conclusion

By presenting a comprehensive framework for the development, performance assessment, verification of applicability and products comparison, this poster intends to emphasize the feasibility and strategic importance of using regional algorithms to timely evaluate operational space mission results as a cost-effective complement to match-up analyses. Underpinning elements are the maintenance of programs to collect high-quality field measurements and the development of regional ocean color inversion schemes with defined ranges of applicability. The relevance of these recommendations is fully in line with accuracy requirements in optically complex waters of recent and forthcoming space sensors (e.g., VIIRS and OCLI).

References

[1] D. D'Alimonte, G. Zibordi, J.-F. Berthon, E. Canuti, and T. Kajiyama, "Performance and Applicability of Bio-optical Algorithms in Different European Seas," *Remote Sensing of Environment*, vol. 124, no. 0, pp. 402–412, 2012.

[2] G. Zibordi, J.-F. Berthon, J. P. Doyle, S. Grossi, D. van der Linde, C. Targa, and L. Alberotanza, *Coastal Atmosphere and Sea Time SERIES (CoASTS): A Long-term Measurement Program*, ser. SeaWiFS postlaunch Technical Report SERIES. Greenbelt, MD: NASA Goddard Space Flight Center, TM-2001-206892, 2002, vol. 19, pp. 1–29.

[3] J.-F. Berthon, G. Zibordi, J. P. Doyle, S. Grossi, D. van der Linde, and C. Targa, *Coastal Atmosphere and Sea Time Series (CoASTS): Data Analysis*, ser. SeaWiFS postlaunch Technical Report. Greenbelt, MD: NASA Goddard Space Flight Center, TM-2002-206892, 2002, vol. 20, pp. 1–25.

[4] G. Zibordi, J.-F. Berthon, F. Mélin, and D. D'Alimonte, "Cross-site consistent in situ measurements for satellite ocean color applications: the biomap radiometric dataset," *Remote Sens. Environ.*, vol. 115, no. 8, pp. 2104–2115, August 2011.

[5] D. D'Alimonte, F. Mélin, G. Zibordi, and J.-F. Berthon, "Use of the Novelty Detection Technique to Identify the Range of Applicability of Empirical Ocean Colour Algorithms," *IEEE Trans. Geosc. Rem. Sens.*, vol. 41, pp. 2833–2843, 2003.

[6] T. Kajiyama, D. D'Alimonte, and G. Zibordi, "Regional algorithms for European seas: a case study based on MERIS data," *IEEE Geosci. Remote Sens. Lett.*, vol. 10, no. 2, pp. 283–287, March 2013.

[7] ——, "Match-up Analysis of MERIS Radiometric Data in the Northern Adriatic Sea," *IEEE Geosci. Remote Sens. Lett.*, 2013, accepted for publication.

[8] G. Zibordi, F. Mélin, J.-F. Berthon, and E. Canuti, "Assessment of meris ocean color data products for european seas," *Ocean Science Discussions*, vol. 10, no. 1, pp. 219–259, 2013. [Online]. Available: http://www.ocean-sci-discuss.net/10/219/2013/

A satellite-based operational system for remote sensing of the Baltic ecosystem

M. Darecki[1], B. Woźniak[1], M. Ostrowska[1], A. Krężel[2], D. Ficek[3], K. Furmańczyk[4]

[1] Institute of Oceanology of the Polish Academy of Science, Sopot, Poland
[2] Institute of Oceanography, University of Gdańsk, Gdańsk, Poland
[3] Institute of Physics, Pomeranian University, Słupsk, Poland
[4] Institute of Marine and Coastal Sciences, University of Szczecin, Szczecin,Poland
Email: darecki@iopan.gda.pl

Introduction

The Baltic Sea is of great importance to the countries surrounding it and its ecosystem is evolving as a result of human activities. This requires a regular monitoring of environmental processes in the Baltic Sea which, together with in situ analysis at selected sites and times, can only be effective with the implementation of remote sensing technology.
To meet these needs, a consortium of four Polish research institutions execute in years 2010 - 2014 the SatBałtyk project [1]. The project is aiming to prepare a technical infrastructure and set in motion operational procedures for the satellite monitoring of the Baltic ecosystem. The system will deliver on a routine basis the variety of structural and functional properties of this sea, based on data provided by relevant satellites and supported by hydro-biological models. Among them: the solar radiation influx to the sea's waters in various spectral intervals, energy balances of the short- and long-wave radiation at the Baltic Sea surface and in the upper layers of the atmosphere over the Baltic, sea surface temperature distribution, dynamic states of the water surface, concentrations of chlorophyll a and other phytoplankton pigments in the Baltic water, distributions of algal blooms, the occurrence of upwelling events, and the characteristics of primary organic matter production and photosynthetically released oxygen in the water and many others. It is also intended to develop and, where feasible, to implement satellite techniques for detecting slicks of petroleum derivatives and other compounds, evaluating the state of the sea's ice cover, and forecasting the hazards from current and future storms and providing evidence of their effects in the Baltic coastal zone.

Discussion

The satellite component of the SatBaltic operational system is based on the most efficient of the available modern algorithms applicable to the Baltic Sea, most of them developed within DESAMBEM project carried out in Poland in years 2001- 2005 [2,3]. Due to high cloudiness typical over the Baltic, which partially or wholly precludes the use of satellite sensors for remote sensing of the water properties based on DESAMBEM algorithms, the system has to be supplemented by the component, which provides reliable data in these situations. The most rational means of providing such a data is to use data generated by prognostic ecohydrodynamic models. The development and implementation of a packet of prognostic models together with procedures for assimilating satellite data are the second component of the system (see Figure).
To secure the highest quality of data delivered by SatBaltic system, also the development and implementation of methods for the continuous calibration of the system (systematic measurements from research vessels, platforms and sea buoys) is also carried out within the Project.
Only when all above described system components are developed and synchronized, the SatBaltic operational system will be launched. The system, designed and equipped with appropriate procedures for the continuous spatial and temporal monitoring of the main structural and functional characteristics

of the entire Baltic Sea, and not just of instantaneous and local situations from the very restricted study areas accessible from ships and buoys or from often limited by clouds the satellite data.

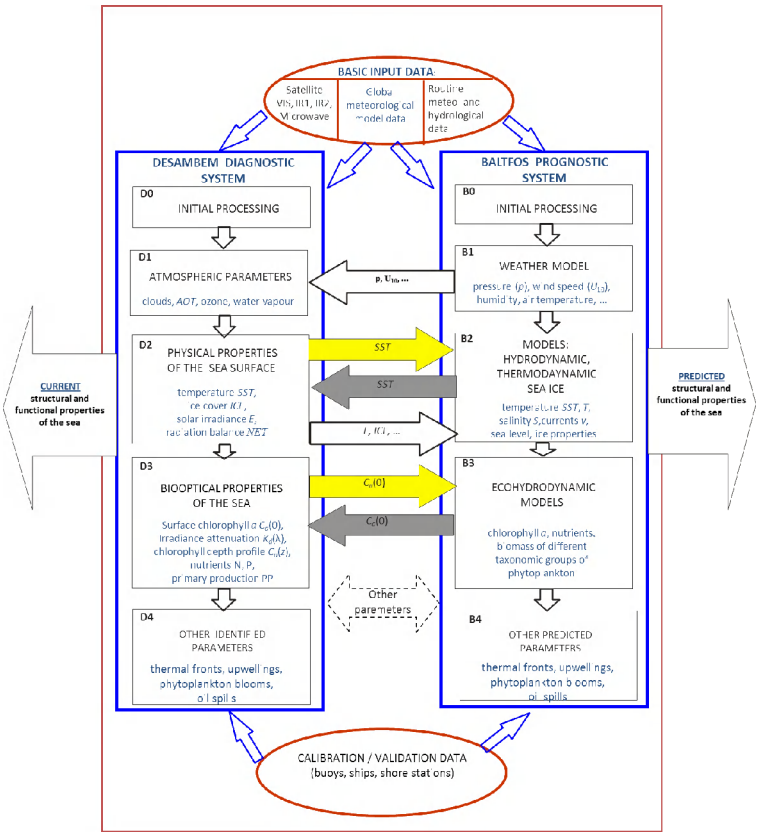

Figure illustrates the main components of the SatBaltic operational system. The system consists of two independent but coordinating subsystems: the DESAMBEM Diagnostic System and the Baltic Forecasting System (BALTFOS).

References

[1] Woźniak B., Bradtke K., Darecki M., Dera J., Dudzińska-Nowak J., Dzierzbicka-Głowacka L., Ficek D., Furmańczyk K., Kowalewski M., Krężel A., Majchrowski R., Ostrowska M., Paszkuta M., Stoń-Egiert J., Stramska M., Zapadka T., 2011a, SatBaltic – a Baltic environmental satellite remote sensing system-an ongoing project in Poland. Part 1: Assumptions, scope and operating range, Oceanologia 53(4) 897-924.

[2] Woźniak B., Krężel A., Darecki M., Woźniak S.B., Majchrowski R., Ostrowska M., Kozłowski Ł., Ficek D., Olszewski J., Dera J., 2008, Algorithm for the remote sensing of the Baltic ecosystem (DESAMBEM). Part 1: Mathematical apparatus, Oceanologia, 50 (4), 451–508.

[3] Darecki M., Ficek D., Krężel A., Ostrowska M., Majchrowski R., Woźniak S.B., Bradtke K., Dera J., Woźniak B., 2008, Algorithms for the remote sensing of the Baltic ecosystem (DESAMBEM). *Part 2:* Empirical validation, Oceanologia, 50(4), 509-538.

The Pre-Aerosol Clouds and ocean Ecosystems Mission – PACE

Carlos E. Del Castillo
for the PACE Science Definition Team
http://decadal.gsfc.nasa.gov/pace.html

The PACE mission relies on a combination of satellite remote sensing, field measurements (e.g. ship, mooring, and drifter), Earth system modeling, and synthesis efforts designed to address specific science questions. At the core of the PACE mission is a satellite-based optical sensors designed to provide the most advanced hyperspectral visible (VIS) and short-wave infrared (SWIR) observations ever collected of the world's pelagic and coastal ecosystems. This advanced Ocean Color Imager will provide scientific and societal benefits that cannot be achieved by any other satellite ocean sensor.

The PACE mission has been designed to address the following Ocean Ecology and Biogeochemistry questions. Table 1 shows measurements and mission requirements needed to address the science question.

SQ1: What are the standing stocks, compositions, and productivity of ocean ecosystems? How and why are they changing?

SQ2: How and why are ocean biogeochemical cycles changing? How do they influence the Earth system?

SQ3: What are the material exchanges between land and ocean? How do they influence coastal ecosystems and biogeochemistry? How are they changing?

SQ4: How do aerosols influence ocean ecosystems & biogeochemical cycles? How do ocean biological & photochemical processes affect the atmosphere?

SQ5: How do physical ocean processes affect ocean ecosystems & biogeochemistry? How do ocean biological processes influence ocean physics?

SQ6: What is the distribution of both harmful and beneficial algal blooms and how is their appearance and demise related to environmental forcing? How are these events changing?

SQ7: How do changes in critical ocean ecosystem services affect human health and welfare? How do human activities affect ocean ecosystems and the services they provide? What science-based management strategies need to be implemented to sustain our health and well-being?

Conclusions: The PACE mission will provide significant advancements in Ocean Ecology and Bigeochemistry research. In essence, the hyperspectral capabilities of PACE permits an unprecedented global spectroscopy from space that will open many opportunities for Earth Systems Science research that yield new discoveries and unique applications.

DRAFT

Table 1. List of threshold measurement requirements as specified by the PACE Science Definition Team Report[1]

Threshold Requirements

Orbit	• sun-synchronous polar orbit • equatorial crossing time between 11:00 and 1:00 • orbit maintenance to ±10 minutes over mission lifetime
Global Coverage	• 2-day global coverage to solar zenith angle of 75° • mitigation of sun glint • multiple daily observations at high latitudes • view zenith angles not exceeding ±60° • mission lifetime of 5 years
Navigation and Registration	• pointing accuracy of 2 IFOV and knowledge equivalent to 0.1 IFOV over the full range of viewing geometries (e.g., scan and tilt angles) • pointing jitter of 0.01 IFOV between adjacent scans or image rows • spatial band-to-band registration of 80% of one IFOV between any two bands, without resampling • simultaneity of 0.02 second
Instrument Performance Tracking	• characterization of all detectors and optical components through monthly lunar observations through Earth-viewing port • characterization of instrument performance changes to ±0.2% within the first 3 years and maintenance of this accuracy thereafter for the duration of the mission • monthly characterization of instrument spectral drift to an accuracy of 0.3 nm • daily measurement of dark current and observations of a calibration target/source, with knowledge of daily calibration source degradation to ~0.2%
Instrument Artifacts	• Prelaunch characterization of linearity, RVVA, polarization sensitivity, radiometric and spectral temperature sensitivity, high contrast resolution, saturation, saturation recovery, crosstalk, radiometric and band-to-band stability, bidirectional reflectance distribution, and relative spectral response • overall instrument artifact contribution to TOA radiance of <0.5% • initial image striping of < 0.5% & correction for image striping to noise levels or below • crosstalk contribution to radiance uncertainties 0.1% at L_{typ} • polarization sensitivity of ≤1% and knowledge of polarization sensitivity to ≤ 0.2% • no detector saturation for any science measurement bands at L_{max} • RVVA of <5% for the entire view angle range and by <0.5% for view angles that differ by less than 1° •Stray light contamination < 0.2% of L_{typ} 3 pixels away from a cloud • out-of-band contamination of <0.01 for all multispectral channels • radiance-to-counts relationship characterized to 0.1% over full dynamic range (from L_{typ} to L_{max})
Spatial Resolution	• Global spatial coverage of 1 km x 1 km (±0.1 km) along-track
Atmospheric Corrections	• retrieval of $[\rho_w(\lambda)]_N$ for open-ocean, clear-water conditions and standard marine atmospheres with an accuracy of the maximum of either 5% or 0.001 over the wavelength range 400 – 710 nm • two NIR atmospheric correction bands comparable to heritage, one of which is centered at 865 nm • NUV band centered near 350 • SWIR bands centered at 1240, 1640, and 2130 nm
Science Spectral Bands	• 5 nm spectral resolution from 355 to 800 nm • complete ground station downlink and archival of 5 nm data.
Signal-to-noise	• SNR at L_{typ} of 1000 from 360 to 710 nm; 300 @ 350 nm; 600 @ NIR bands; 250, 180, and 15 @ 1240, 1640, & 2130 nm
Data Reprocessing,	• full reprocessing capability of all PACE data at a minimum frequency of 1 – 2 times annually.

References

1-NASA-PACE Science Definition Team Report - 2012
http://decadal.gsfc.nasa.gov/pace_documentation/PACE_SDT_Report_final.pdf

Atmospheric scattering and ocean color: errors due to the spherical atmosphere

D. Jolivet, D. Ramon, P. Y. Deschamps
HYGEOS, Lille, 59000, France
Email: pyd@hotmail.com

Summary

The atmospheric correction for ocean color requires very accurate computations of the scattering by aerosols and molecules. This is usually done assuming an infinite plane parallel atmosphere. In order to evaluate the errors due to this approximation, we have developed a radiative transfer code for a spherical atmosphere. The results of the computations by the two codes, plane parallel and spherical, both of them using a Monte Carlo method, have been compared. The relative error between the two computations remains below 1 % up to an incidence angle of about xxx° above which it is necessary to use the spherical atmosphere for atmospheric correction. Nevertheless, even at nadir, the error is significant enough to suggest to systematically computing the atmospheric scattering of a spherical atmosphere for atmospheric correction of ocean color.

Atmospheric scattering for a spherical atmosphere – Monte Carlo Code

Calculations are performed with a Monte Carlo radiative transfer code used in backward mode. It includes polarization, a rough sea surface, Rayleigh scattering, aerosols and gaseous absorption. The atmosphere is vertically extended up to 100 km altitude to take into account high-level molecules.

Comparison of the spherical and plane parallel results

Figure 1 shows a comparison between results for plane parallel and spherical atmosphere. It is actually the ration of the two computations so that a one value means no error. The relative error increases with the wavelength, but remains critical at the shorter wavelengths where the molecular scattering is important. Most of the effect comes from the scatterers at the highest altitude Adding aerosol with a lower altitude profile does not change much these results. The errors increases rapidly at viewing and solar zenith angles above 60 °, so that spherical calculations are strictly necessary for ocean color observations at high latitudes or with a large swath. For nadir observations, the error may still be within 1 % and using the computations for a spherical atmosphere is recommended.

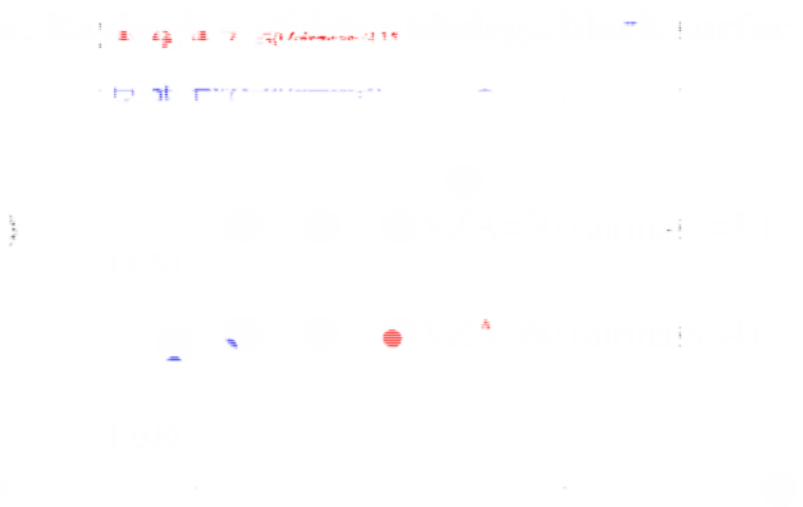

Figure 1: Wavelength dependence of the ration of plane parallel (PPA) to spherical (SSA) atmospheric scatterings.

Discussion

Our results show a larger effect of the sphericity of the atmosphere, contrary to a previous study [1] that misses part of the effect by using a molecular layer limited to a 8 km altitude. We recommend that advanced atmospheric corrections make a systematic use of computations of atmospheric scattering with a realistic spherical atmosphere, in particular when having a wide swath and large incidence angles (VIIRS, geostationary)

References

[1] Ding, K. and Gordon, H. R. (1994). Atmospheric correction of ocean color sensors: effects of the Earth's curvature. Appl. Opt., 33, 30, 7096-7106

The Information content of reflectance spectra and the uncertainties of derived IOPs of coastal waters

Roland Doerffer[1,2], Carsten Brockmann[1], Rüdiger Röttgers[2], Marc Bouvet[3]

[1] Brockmann Consult Geesthacht, Geesthacht, 21502, Germany,
[2] Helmholtz Zentrum Geesthacht, Geesthacht, 21502, Germany,
[3] ESA-ESTEC, Nordwijk, Netherlands
Email: roland.doerffer@hzg.de

Summary

Optical properties of coastal waters are characterized in many cases by a large number of different water constituents, including different phytoplankton species, mineralic and organic particles and dissolved matter such as humic substances. This large variety together with the impact of the atmosphere makes it difficult to determine inherent optical properties (IOPs) and the concentration of water constituents from reflectance spectra with an uniform quality. Sensitivity analysis of different constellations of water constituents, demonstrate that the uncertainties can be so large that the data become useless. To take these problems into account, we have developed a system of algorithms, which allows us to estimate the uncertainty and also to identify reflectance spectra, which are out of scope of the retrieval algorithm.

Introduction

Top of atmosphere radiance or reflectance spectra of coastal waters are determined by a large number of factors. Even in case 1 water, which is defined as water, the optical properties of which can be described by only one component, i.e. phytoplankton, uncertainties occur already due to the variability of the optical properties of phytoplankton [1, 2]. On the other hand, the information content of spectra in most cases is limited to a few (2-3) components, which can be derived with sufficient accuracy. The nature of these components may vary with the optical water type and depends on the dominating water constituents, aerosols, thin clouds etc., s. figure 1. Furthermore, the importance of spectral bands changes with optical water types. Different algorithms or systems of algorithms exist, to decompose reflectance spectra [3, 4], which partly include also the determination of uncertainties [5].

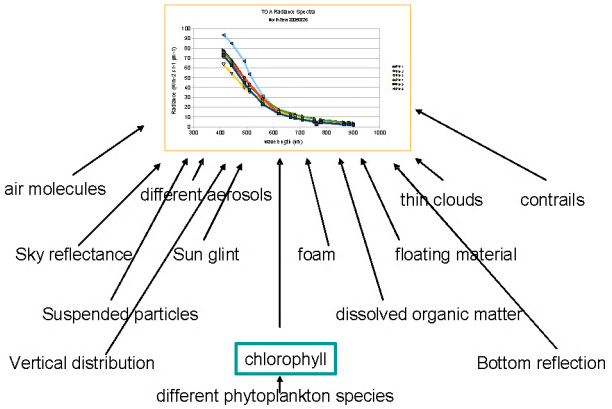

A large number of factors determine TOA radiance spectra, here of the North Sea. On the other side, these spectra are rather similar and the information content is much smaller, than the number of factors, which determine the spectra.

Discussion

The large number of factors, which determine top of atmosphere (TOA) and water reflectances of some

types of coastal waters imply issues and uncertainties when we derive water reflectances from TOA reflectances and, in turn, IOPs from water reflectances. Uncertainties can be large for components, which are sub-dominant and thus above the acceptance level. In particular high concentrations of suspended matter may totally mask the effect of other substances on reflectance spectra, such as phytoplankton. In these cases the uncertainty can easily surmount a factor of 2 or even 10. User of such data without any warning can easily be misleaded. In extreme cases also the atmospheric correction may lead to large uncertainties in water reflectances or may even fail. Sensitivity studies within the ESA Water Radiance project have demonstrated that the determination of the uncertainty range is crucial for the use of remote sensing data of coastal waters. Thus, it is necessary to determine these uncertainties on a pixel by pixel bases. For this purpose a system of algorithms has been developed (1) to check if a reflectance spectrum is within the scope of the algorithm, and (2) to determine the uncertainty range. This system is based on neural networks [6], which have been trained using a case 2 water bio-optical model and radiative transfer simulations [7] for water and atmosphere.

Conclusions

Uncertainties of IOPs and concentrations of coastal water constituents, when derived from reflectance spectra, can be variable and large so that products such as concentration maps of coastal waters provided from data of earth observing satellites, should be complemented by co-registered maps of uncertainties and flags, which indicates out of scope conditions.

References

[1] Bricaud, A., M. Babin, A. Morel and H. Claustre. 1995. Variability in the chlorophyll-specific absorption coefficients of natural phytoplankton: analysis and parameterization, J. Geophys. Res., 100, 13321–13332.

[2] Röttgers, R., C. Häse, and R. Doerffer. 2007. Determination of the particulate absorption of microalgae using a point-source integrating-cavity absorption meter: verification with a photometric technique, improvements for pigment bleaching, and correction for chlorophyll fluorescence. Limnol. Oceanogr. Methods 5: 1-12.

[3] IOCCG. 2006. IOCCG Report 5: Remote Sensing of Inherent Optical Properties: Fundamentals, Tests of Algorithms, and Applications. Edited by ZhongPing Lee, pp. 126.

[4] Franz, B.A. and P.J. Werdell. 2010. A Generalized Framework for Modeling of Inherent Optical Properties in Remote Sensing Applications. White Paper, Proc. Ocean Optics 2010, Anchorage, Alaska, USA.

[5] Maritorena S., D.A. Siegel and A. Peterson. 2002. Optimization of a Semi-Analytical Ocean Color Model for Global Scale Applications. Applied Optics, 41(15), 2705-2714.

[6] Doerffer R. and H. Schiller (2007). The MERIS Case 2 water algorithm, , International Journal of Remote Sensing, 28, (3-4): 517-535.

[7] Mobley, C. D. 1994. Light and water. Radiative transfer in natural waters. San Diego. Academic Press.

Can a single turbidity algorithm be used in all turbid waters?

A.I. Dogliotti[3], K.G. Ruddick[2], B. Nechad[2], D. Doxaran[1], E., E. Knaeps[4]

[1] Instituto de Astronomía y Física del Espacio (IAFE), CONICET/UBA. Buenos Aires, Argentina
[2] Royal Belgian Institute for Natural Sciences (RBINS), 100 Gulledelle, 1200 Brussels, Belgium
[3] Laboratoire d'Océanographie de Villefranche (LOV), CNRS/UPMC, B.P. 8, Villefranche-sur-Mer, 06230, France
[4] Flemish Institute for Technological Research (VITO), Boeretang 200, B-2400 Mol, Belgium
Email: adogliotti@iafe.uba.ar

Summary

Ocean color remote sensing has shown to be a useful tool to map turbidity (T) and total suspended sediment (TSM) concentration in turbid coastal waters. Different algorithms to retrieve T and TSM from water reflectance already exist. However there are important questions as to whether these algorithms need to be calibrated specifically for different regions. In the present work we use a set of 180 simultaneous measurements of water reflectance and turbidity in five different highly turbid regions to validate a single band algorithm using the near infrared (NIR) band at 859 nm. The good performance of the algorithm for all these regions, despite different sediment characteristics, suggests the global applicability of the algorithm to map turbidity within a certain range.

Introduction

Suspended particles modify the transmission of light under water affecting the biological productivity and underwater visibility as well as pollutant and nutrient transport. Turbidity (T), defined from the measurement of 90° scattered light at 860nm, is a relevant optical parameter for certain water quality applications, like water transparency. It is relatively cheap and easy to measure, and is highly correlated to the total suspended sediment (TSM) concentration (which is more expensive and time consuming to measure), making it an interesting parameter to retrieve from optical remote sensing. Even though many regional algorithms to estimate T and TSM have been already developed [e.g. 1, 2], the generality of these algorithms for remotely estimating sediment concentrations and/or turbidity is currently not established because of possible regional variation of specific optical properties.
In a previous work, a single band turbidity algorithm [1] using reflectance at 859 nm was re-calibrated using *in situ* T and reflectance measurements performed in the Southern North Sea (SNS) and the Scheldt River (SR) with T values higher than 10 FNU [3]. The algorithm was applied to MODIS satellite-retrieved Rayleigh-corrected reflectance data in the Samborombón Bay region (located to the south of Río de la Plata River, Argentina) and validated with in situ T measurements. A good agreement between modelled and *in situ* measurements was found, but no *in situ* water reflectance measurements were available to directly validate the algorithm. The objective of the present study is to validate the single band algorithm and test its generality using water reflectance and turbidity measurements performed in five different turbid regions of the world: the Southern North Sea (SNS), French Guyana (FG), and the Scheldt (SC, in Belgium), Gironde (GIR, in France), Río de la Plata (RP in Argentina) rivers; these regions have quite different sediment composition (refractive index, density) and range of concentrations.

Discussion

Turbidity measured in the five regions covered a wide range of values, from 10 to 900 FNU (Formazin Nephelometric Units). Good performance of the algorithm was found with correlations > 0.75 for each site and a higher correlation ($r=0.96$, $p<0.00001$) for all sites together (Figure 1).

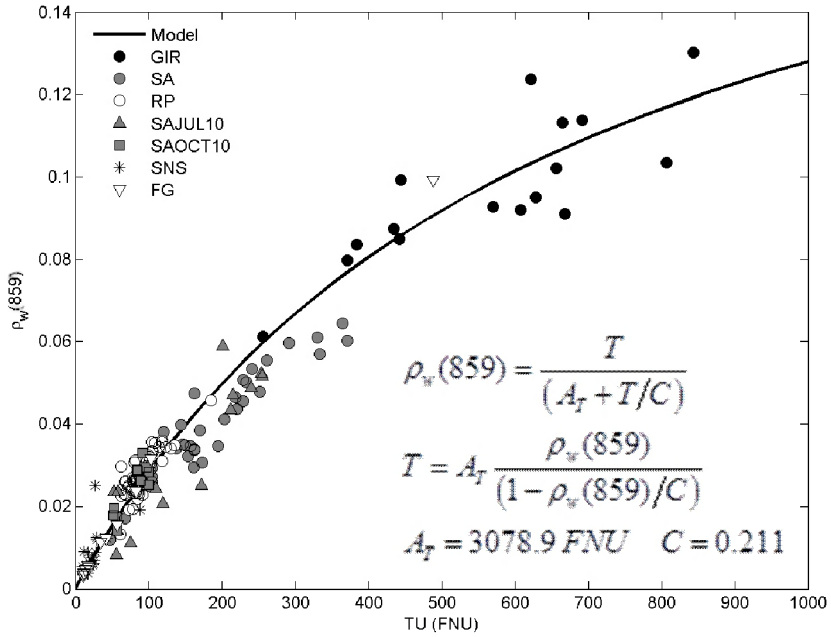

Fig. 1: In situ water reflectance and T values measured for various regions (see text for abbreviations) and the single band model validated in the present study (solid line)

Even though the algorithm was calibrated with a dataset from two specific regions (SNS and SC), it showed good performance in all five regions analyzed here, suggesting the general applicability of the algorithm for coastal/estuarine waters with this turbidity range.

Conclusions

A single band algorithm [1, 2] using 859nm was validated using *in situ* turbidity and reflectance measurements from five different turbid water regions. A good agreement between modelled and *in situ* measurements was found. These results suggest that a general algorithm can be used for mapping turbidity using NIR bands present in different ocean colour satellites such as MODIS, MERIS, SeaWIFS, GOCI, OLCI, HIOC, etc provided atmospheric correction is possible. The impact of the regional variability of the relationship between T and ρ_w859 is expected to be low because: a) unlike TSM, T is an optical property closely related to the side/backscattering processes affecting ρ_w859, b) ρ_w859 is hardly affected by particulate absorption which may vary significantly between regions. The main limitation of this algorithm will be related to the range of T rather than geographic region or particle type. TSM concentration, the parameter of main interest in sediment transport studies, could subsequently be retrieved by ocean colour remote sensing if a region-specific relation between T and TSM is known.

References

[1] Nechad B., K. G. Ruddick & Neukermans, G. (2009). Calibration and validation of a generic multisensor algorithm for mapping of turbidity in coastal waters. In: SPIE, Rem Sens of the Ocean, Sea Ice, and Large Water Regions. Vol. 7473, 74730H.

[2] Doxaran, D., J.M. Froidefond, S. Lavender and Castaing, P. (2002) Spectral signature of highly turbid waters Application with SPOT data to quantify suspended particulate matter concentrations. *Rem Sens Env 81 (2002);* pp. 149-161.

[3] Dogliotti A. I., K. G. Ruddick, B. Nechad, C. Lasta, A. Mercado, C. Hozbor, R. Guerrero, G. Riviello López, and Abelando, M. (2011). Calibration and validation of an algorithm for remote sensing of turbidity over La Plata River estuary, Argentina. *EARSeL eProceedings*, 10(2): 119-130.

An improved correction method for field measurements of particulate light backscattering in turbid waters

D. Doxaran[1], E. Leymarie[1], B. Nechad[2], K.G. Ruddick[2], A.I. Dogliotti[3], E. Knaeps[4]

[1] Laboratoire d'Océanographie de Villefranche (LOV), CNRS/UPMC, B.P. 8, Villefranche-sur-Mer, 06230, France
[2] Royal Belgian Institute for Natural Sciences (RBINS), 100 Gulledelle, 1200 Brussels, Belgium
[3] Instituto de Astronomía y Física del Espacio (IAFE), CONICET/UBA, Buenos Aires, Argentina
[4] Flemish Institute for Technological Research (VITO), Boeretang 200, B-2400 Mol, Belgium
Email: doxaran@obs-vlfr.fr

Summary

Light backscattering by suspended particles in natural waters is a key parameter in marine optics and for ocean colour remote sensing purposes. The particulate backscattering coefficient is highly correlated to the concentration of suspended solids [1] and its spectral variations are representative of the particle size distribution [2], especially in sediment-dominated coastal and estuarine waters. However field measurements of the particulate backscattering coefficient in turbid waters is problematic mainly due to (i) saturation effects of most sensors developed for the open ocean and (ii) the strong light attenuation along the sensor pathlength which is difficult to accurately account for in highly-reflective waters. Based on results obtained using Monte Carlo simulations, we present an improved correction method for such measurements. The method takes into account the absorption, scattering and particulate volume scattering function of the sampled waters. It is applied to field measurements from the Río de la Plata estuary (Argentina) and a factor 2 difference is observed with the standard correction method. Based on optical closure with the water reflectance signal also measured in the field, we quantify the improvement of the new correction method.

Introduction

Ocean colour remote sensing is a well-established method for retrieving the absorption (a) and backscattering (b_b) coefficients of natural waters. The b_b coefficient is highly correlated to the concentration of suspended solids and is used for mapping of concentrations of suspended particulate matter (SPM) (e.g., [1]) and for retrieving information on the particle size distribution [2]. The development of SPM retrieval algorithms at regional scales therefore requires field measurements of spectral b_b values together with SPM concentration, composition and size distribution. Backscattering sensors initially developed for the open ocean are not adapted to turbid sediment-dominated waters due to saturation problems (e.g., Wetlabs ECO-BB sensors). The Hobilabs Hydroscat sensor is more adapted as it selects the appropriate gain automatically, based on the amount of backscattering detected as well as the amount of background light [3]. This sensor allows the light backscattered at the fixed angle of 140° to be measured at various wavelengths covering the visible, near-infrared and shortwave infrared spectral ranges. However the standard method which corrects for light attenuation from the light source to the detector, due to light absorption and scattering, does not take into account the wide variations of the particulate backscattering ratio encountered in coastal and estuarine waters [4]. This correction simply assumes that that light attenuation is equal to the light absorption coefficient plus 40% of the scattering coefficient, without evidence from radiative transfer calculations or measurements. This certainly leads to great errors in the measured b_b coefficient.

Discussion

Taking into account the exact design of the Hydroscat (HS) sensor, a Monte Carlo code [4] is used to compare the true (imposed) backscattering coefficient to the one obtained applying the standard

correction method to the measured signal. Results are used to (i) quantify and explain the errors associated to the standard processing then (ii) propose an improved correction method associated to mininm errors. This new method requires simultaneous measurements of the absorption and scattering coefficients to correct HS data. Several iterations are necessary to determine the true particulate scattering ratio, then quantify the exact light attenuation to be corrected for. The results obtained are valid for a wide spectral range and a wide range of inherent optical waters representative of coastal and estuarine waters.

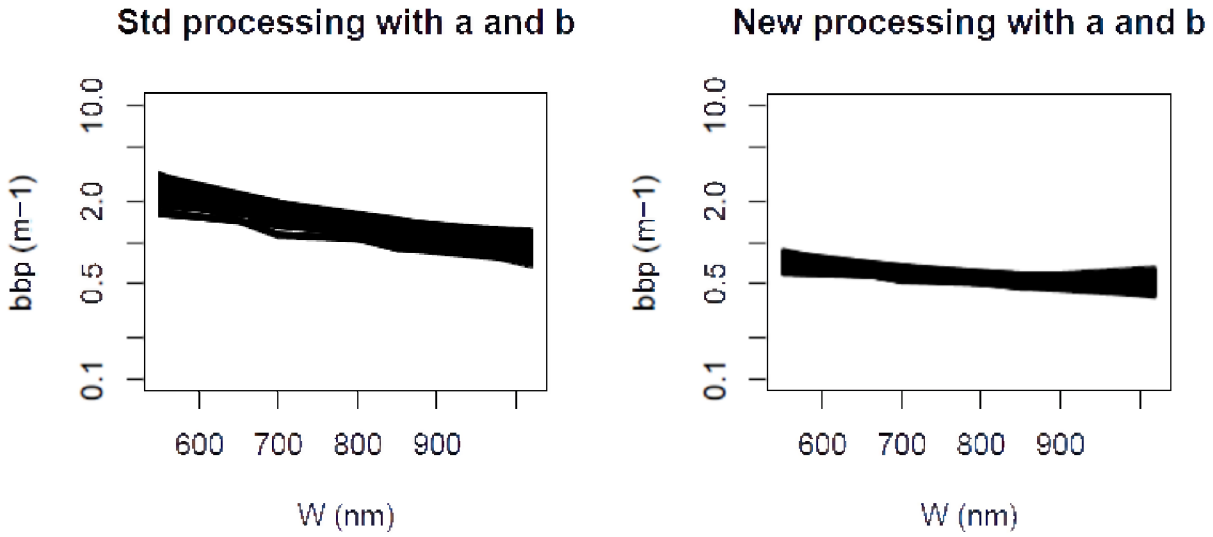

Fig. 1: Particulate backscattering coefficient spectra (b_{bp} in m^{-1}, 550 – 1020 nm) measured in the Río de la Plata estuary using a Hydroscat-4 sensor (HOBI Labs). Comparisons between results (spectral b_{bp} values) obtained using the standard (left) and new processing (right).

The method is applied to a field dataset (light absorption, scattering, backscattering and water reflectance measurements) from the Río de la Plata estuary (for SPM concentrations ranging from 20 to 120 $g.m^{-3}$).

Conclusions

Depending on the correction method applied (standard or Monte Carlo based), a fctor-2 difference is typically observed between the b_b coefficients obtained from HS measurements. The standard correction method actually greatly overestimates light attenuation due to particulate scattering, which results in a large overestimation of the b_b signal. Radiative transfer simulations are finally used to compute the water reflectance signal using as inputs the measured absorption and (back)scattering coefficients. Optical closure with the measured reflectance signal allows assessment of the accuracy of the retrieved b_b signal.

References

[1] Nechad, B., Ruddick, K.G. and Park, Y. (2010). Calibration and validation of a generic multisensor algorithm for mapping of Total Suspended Matter in turbid waters. Rem Sens Env 114: p. 854-866.
[2] Morel, A. (1973). Diffusion de la lumière par les eaux de mer; résultats expérimentaux et approche théorique, in AGARD Lect. Ser., pp. 3.1.1.-3.1.76.
[3] HydroScat-4 Spectral Backscattering Sensor User's Manual (2008). HOBI Labs, Revision E.
[4] Leymarie, E., D. Doxaran, and M. Babin (2010). Uncertainties associated to measurements of inherent optical properties in natural waters, Applied Optics, 49, 5415-5436.

Summer bio-optical properties in the southeastern Bering Sea

Eurico J. D'Sa[1], Joaquim I. Goés[2], Puneeta Naik[1], Colleen B. Mouw[3], Helga do R. Gomes[2]
[1]Louisiana State University, LA, ejdsa@lsu.edu
[2]Lamont-Doherty Earth Observatory, NY
[3]Michigan Technological University, MI

Spatial patterns of bio-optical properties were studied in the southeastern Bering Sea during cruises in July/August of 2008 and 2009. Phytoplankton and CDOM absorption were highly variable with phytoplankton absorption dominating offshore waters and CDOM absorption dominating in the coastal domain. At most locations elevated sub-surface values of CDOM absorption were associated with chlorophyll-a (chl-a) maxima suggesting the biological source of CDOM in these waters. Water-column spectral optical properties of absorption, scattering and backscattering reflected the vertical variability in phytoplankton and CDOM concentrations. Using an extensive IOP and AOP dataset collected during 2008, good optical closure in spectral remote sensing reflectance was observed between radiometric derived and those modeled using IOPs. CDOM was found to significantly influence both the spectral remote sensing reflectance and diffuse attenuation coefficient. The standard NASA chlorophyll-a algorithm (OC4.v6) was found to overestimate chl-a at low values and underestimate chl-a at high values. We present a regional 3-band MODIS empirical algorithm that addresses this issue in the standard algorithm in the offshore waters of the Bering Sea.

Optically black water in Lake Taihu

Hongtao Duan

State Key Laboratory of Lake Science and Environment, Nanjing Institute of Geography and Limnology, Chinese Academy of Sciences, Nanjing 210008, China

Email: htduan@niglas.ac.cn

Summary

In the summer of 2007, water quality problems associated with masses of "black" water in Lake Taihu, left more than 1 million people in the city of Wuxi without drinking water. Due to its intermittent nature and limited spatial extent, it has not been possible to identify the origin of these water masses. In May 2012, two black water masses were observed in the same area of the lake, allowing us to characterize their optical and biochemical properties and explore possible causes.

Introduction

Lake Taihu, the third largest freshwater lake in China, provides fundamental services to a large surrounding population. Yet it is one of the most severely polluted freshwater reservoirs in China. In the summer of 2007, water quality problems, initially associated with algal blooms, left more than 1 million people in the city of Wuxi without drinking water [1]. Further studies indicated that algal blooms were not the direct cause of problems for Wuxi. The apparent cause was the intrusion of a black water "agglomerate" of unknown origin into the main water intake of the city [2]. No successive black water masses were observed, either in *in-situ* surveys or in the daily satellite based monitoring program that is used to monitor lake water quality. In May 2012, black water masses were observed in the same area of the lake during regular *in-situ* bloom monitoring activities. Field measurements were made immediately to determine the optical and biochemical properties of two of these black water masses. These data provided an opportunity to gain a further understanding of: 1) their optical characteristics; 2) the possible causes of their intermittent occurrence; and 3) the possibilities for optical detection by remote sensors. To the best of our knowledge, this is the first study to address the occurrence of black water masses using optical methods.

Discussion

The color perceived by the human visual system depends largely on the total radiance incident

upon each type of cone and the comparative response (i.e., contrast) between the three cone classes (red, green, and blue) [3]. In the visible spectrum, a highly reflective surface will reflect the spectrum of the incident light, while a highly absorbing medium will appear dark. The water surface color, transposed using the CIE color matching functions from *in situ* measured water-leaving radiance, indicates that the color of the upwelling radiance observed in the black water zones was not black. The color of the lake water from Zone 1 should appear dark olive drab green and the Zone 2 should appear olive-green, while Zone 3 would appear sea-green color. Although black is generally defined as the visual impression experienced when no visible light reaches the eye, water masses look "black" when there is a significant reduction in the light reflected back to the observer with respect to the surrounding surfaces. Zones 1 and 2 appeared "black" due to the high contrast with the surrounding lake waters with a relatively higher R_{rs}. This contrast allows for the determination of an edge, basic for the recognition of shapes.

Conclusions

The presence of black water zones in Lake Taihu has been associated with a general degradation of the water quality in this important lake and has led to the loss of its use as a potable water source. The observation of these water masses in areas dominated by macrophytes indicates that the latter may play a direct or indirect role in their generation. The present analysis indicates that the black water areas are optically characterized by elevated CDOM and phytoplankton absorption and reduced SPIM backscattering. The present analysis indicates that an indirect effect might also be the generation of "black" water masses. Future monitoring of these occurrences with the present availability of remote optical sensors is limited, largely due to their intermittent spatial and temporal nature.

References

[1] L. Guo, "Doing battle with the green monster of Taihu Lake," Science, vol. 317, no. 5842, pp. 1166, Aug 31, 2007.

[2] M. Yang, J. W. Yu, Z. L. Li et al., "Taihu Lake not to blame for Wuxi's woes," Science, vol. 319, no. 5860, pp. 158-158, Jan 11, 2008.

[3] H. M. Dierssen, R. M. Kudela, J. P. Ryan et al., "Red and black tides: Quantitative analysis of water-leaving radiance and perceived color for phytoplankton, colored dissolved organic matter, and suspended sediments," Limnology and Oceanography, vol. 51, no. 6, pp. 2646-2659, Nov, 2006.

Role of optical constituents in setting in water and water leaving optical properties

S. Dutkiewicz*[1], A. E. Hickman*[2], O. Jahn[1], W. W. Gregg[3], M. J. Follows[1]

1. Massachusetts Institute of Technology, Earth Atmosphere and Planetary Sciences, Cambridge, MA 02139, USA
2. University of Southampton, National Oceanography Centre, Southampton, SO14 3ZH, U.K.
3. NASA Goddard Space Flight center, Greenbelt, MD, 20771, USA
* These authors contributed equally to this work
Email: stephd@mit.edu

Summary

We present results from a global three-dimensional numerical model coupled to new irradiance module that captures the spectral absorption and scattering properties of water, phytoplankton, detritus and coloured dissolved organic matter (CDOM). We use the model as a tool to explore the sensitivity of the light field, and the feedbacks on the ecosystem and primary production, when we remove or modify the spectral properties of the optical constituents. For example, we show that higher absorption of CDOM strongly favouring some species, significantly altering community structure.

Introduction

Though crucial to understanding autotroph productivity, traditionally, marine ecosystem models have employed extremely simple models of downwelling, integrated photosynthetically available radiation (PAR). The resolution of radiative transfer in the water column and inherent optical properties of the particles (including phytoplankton) and dissolved matter will provide a more mechanistic representation of the light field and enables a closer connection between modeled and remotely measured properties. As a result, spectrally-resolving radiative transfer schemes have recently been implemented in some global ocean models [1,2]. Here we couple an irradiance model to our existing global biogeochemical/ecosystem model [3,4] and use the model to explore the consequences of different assumptions about the spectral properties of the optical water constituents for primary production, community structure and surface reflectance.

Model Description and Evaluation

The water-column radiative transfer model is based on the code of Ocean-Atmosphere Spectral Irradiance Model (OASIM [1]), but with an exact solver. PAR is represented as three streams (downward direct and diffuse, and upwelling irradiance) and in the default simulations is resolved in 25nm bands from 400nm to 700nm. Light is absorbed by water molecules, CDOM, phytoplankton (with pigment specific absorption spectra assigned to several different phytoplankton "functional" types), and non-algal particles. The model also includes forward and back-scattering by water molecules, phytoplankton (type specific spectra), and non algal particles. The specification of absorption spectra, and its ecological impact, is documented in [4]. The model qualitatively captures the distribution of chlorophyll-a, phytoplankton light absorption and spectral light penetration observed during the Atlantic Meridional

Transect Programme AMT15 cruise. Surface, spectrally-resolved, upwelling irradiance and reflectance are prognostic in the model, and capture the gradients observed in satellite derived reflectance data.

Atlantic Merdional Transect (AMT) observation and model comparison. (a,c,e) from AMT15 transect (Sep 2004); (b,d,f) current version of MIT ecosystem, biogeochemical, and optical model. (a,b) Chlorophyll a; (c,d) colored dissolved organic matter (CDOM) absorption at 450nm [5], in the model we represent an explicit CDOM-like tracer; (e,f) phytoplankton absorption at 450nm, in the model we resolve 8 phytoplankton types with different absorption spectra. Magenta line indicates 1% light level - in (a,b) for photosynthetically available radiation between 400-700nm; in (c,d,e,f) for 450nm wavelength. By capturing appropriate absorption (and scattering, not shown) in the model we obtain vertical distribution of light and chlorophyll seen in the observations.

Sensitivity Studies

We use the model as a tool to explore the sensitivity of the light field, and the feedbacks on the ecosystem and primary production. We perform a series of sensitivity experiments where we remove or modify the absorption and scattering spectral properties of the optical constituents (water, CDOM, detritus, phytoplankton). First we consider how each component affects PAR penetration and surface reflectance given the same distribution of the various constituents. We then explore how these different experiments evolve in time and feedback on the system. For example, very strong absorption by CDOM favours cyanobacteria over other phytoplankton. Additionally, we assess the difference in ecosystem, productivity, and light penetration with different resolutions of the spectral light field (e.g. broadband versus 25nm bandwidths). These sensitivities are considered both with depth along the AMT-like transect in the model and on the model derived surface reflectance.

References

[1] Gregg, W.W. and N.W. Casey (2007), Modeling Coccolithophores in the Global Oceans. *Deep- Sea Res. II,* 54, 447-477.

[2] Fujii, M., E. Boss, and F. Chai (2007). The value of adding optics to ecosystem models: a case study. *Biogeosciences*, 4, 817-835.

[3] Dutkiewicz, S., B. A. Ward, F. Monteiro, and M. J. Follows (2012). Interconnection of nitrogen fixers and iron in the Pacific Ocean: Theory and numerical simulations, *Global Biogeochem. Cycles,* 26, GB1012, doi:10.1029/2011GB004039.

[4] Hickman, A.E., S. Dutkiewicz, R.G. Williams, and M.J. Follows (2010), Modelling the effects of chromatic adaptation on phytoplankton community structure in the oligotrophic ocean. *Mar. Ecol. Prog. Ser.,* 406, 1-17, doi:10.3354/meps08588

[5] Stubbins, A., G. Uher, C.S. Law, K. Mopper, C. Robinson, R.C. Upstill-Goddard (2006), Open-ocean carbon monoxide photoproduction. *Deep- Sea Res. II,* 53, 1695-1705.

UNCERTAINTY ANALYSIS AND APPLICATION OF IN SITU MEASUREMENTS OF SEA SURFACE TEMPERATURE MEASUREMENT ALONG COASLINE OF LAGOS, NIGERIA: OCEAN COLOUR CONCEPT AND FINDING SOLUTION TO A PERSITENT PROBLEM OF MARINE DEBRIS.

O A Ediang[1**1] *Marine Division, Nigerian Meteorological Agency, PMB1215 OSHODI Lagos, Nigeria*
Email: ediang2000@yahoo.com
AA Ediang[2 2] *The Nigerian Maritime Administration and Safety Agency, 6 Burmal Road, Apapa, Lagos, Nigeria.*
Email: ediang2005@yahoo.com

ABSTRACT

Increased SST may alter coastal ocean currents that have influence on the residence time of water in near shore environments which may have negative consequences on the growth and survival of many aquatic animals and also the ocean colour in that region. We discuss in this paper environmental changes along the coastal line of Nigeria, especially in the region around Lagos, basing on provisional multi-disciplinary analyses of meteorological and maritime observations. The study has revealed that the environmental change in the Nigerian coastal region has been much more apparent than before(i.e. some few years back 1989-2007 and this has an affect on the ocean colour around). Various kinds of ocean debris, transported mainly by coastal wind, are affecting marine and coastal environment severely. Since the current ocean monitoring system is found to be troubled by ocean debris, it is urgent to establish a new system to obtain reliable observational data to monitor and basic knowledge of the definitions of preserving the environment of the coastal region and improving the ocean colour of the environment.

The role of sea surface processes in anchovy larvae distribution in the Strait of Sicily (Central Mediterranean).

F. Falcini[1], L. Palatella[2], A. Cuttitta[3], F. Bignami[1], B. Patti[3], R. Santoleri[1], F. Fiorentino[4]

[1]CNR, ISAC, Rome, 00133, Italy
[2]CNR, ISAC, Lecce, 73100, Italy
[3]CNR, IAMC, Capo Granitola, 91021, Italy.
[4]CNR, IAMC, Mazara del Vallo, 91026, Italy.
E-mail: f.falcini@isac.cnr.it

Summary

We present a comparison between anchovy larval survey data and remote sensing data in the Strait of Sicily. We analyze larvae distribution in the Strait with respect to sea surface currents and hydrographic/biogeochemical patterns. We find a strong correlation between the satellite date set, which in turn marks ocean and wind dynamics in the Strait, and the larvae distribution. Our analysis allows for the investigation of cross-shore transport processes of anchovy larvae.

Introduction

The European Anchovy (Engraulis encrasicolus, Linnaeus, 1758) is one of the most important resources of the Mediterranean Sea. The anchovy population off the Mediterranean coasts exhibits a patchy distribution which is not well understood. Moreover, the influence of the environment on such a distribution, and its variability, is poorly known. [1]

The Strait of Sicily, where a robust ichthyoplankton data set is available, represents a particularly appropriate region for investigating the relation among ocean dynamics and anchovy distribution. The Strait is characterized by upwelling regions, fronts, vortices, and filaments. The mean surface circulation is given by the Atlantic Ionian Stream (AIS), a meandering current of Atlantic origin [2]. The AIS climatologically encircles two cyclonic vortices: the Adventure Bank Vortex (ABV) and the Ionian Shelf Break Vortex (IBV), and describes a pronounced anticyclonic meander in between (Maltese Channel Crest, MCC) [2]. The AIS path and variability have consequences for anchovy spawning and larvae distribution [3].

To analyze such a distribution we use ichthyoplankton measurements collected in the Strait during the peak spawning season. These measurements are then paired to remote sensing data such as sea surface temperature (SST), chlorophyll (Chl), primary production, surface wind speed as well as light attenuation, absorption, and particle backscattering coefficients (e.g., K490).

Discussions

All oceanographic patterns that characterize the Strait of Sicily are identified by the cruise averaged SST map: the cyclonic vortices by their cold surface signature and the MCC by the intrusion of warm water to the shore in between ABV and IBV. Both the ABV and the IBV well mark a high presence of larvae, while the higher distribution of samples in the IBV confirms the retention of larvae in the frontal structure originated from the AIS and Ionian Sea water masses interface [3]. In the southern part of the

Channel, we also observe that anchovy larvae laid along a cold belt, a feature that may indicate the important role of mesoscale activity, such as filaments, in delivering larvae cross-shore. Samples were approximately collected in areas characterized by medium values of both Chl and K490. The spawning habitat was generally confined to shelf edges of the Channel. Larvae whose age is greater than 8 days are mostly collected around the south-east end of the coast, confirming that larvae are mainly transported along the Sicilian shelf. However, the presence of 6-8 days old larvae offshore, in the central portion of the Strait, also shows that cross-shore transport processes plays an important role.

Conclusions

The development of environmental indicators that give support to fishery sustainability are becoming an important goal in the marine science community. Our investigation seek to recognize those multidisciplinary data that play a physical based role in building such indicators. Our analysis on the European Anchovy shows and quantifies how the AIS path and variability, as well as the upwelling-induced south Sicilian coastal current, have consequences for anchovy spawning and larvae distribution. Surface currents transport anchovy larvae towards the Sicilian coast's south-eastern tip. However, significant cross-shore transport events due to mesoscale and/or wind-induced activity were also observed. All these dynamics are fairly well recognized by the remote sensing data we used.

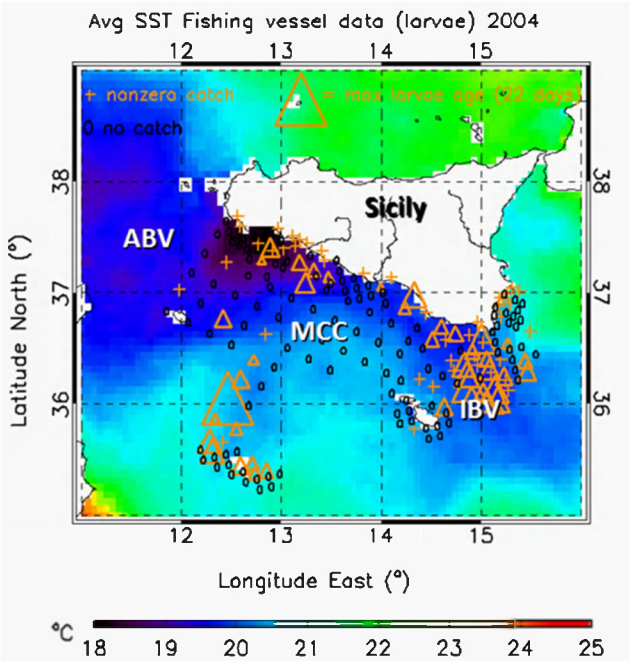

Cruise-averaged SST (°C) map, superimposed to ichthyoplankton survey data of anchovy larvae (18 June to 7 July, 2004); triangles are proportional to larvae age; o = no catch, + = catch with no larvae size/age measurement

References

[1] Cuttitta, A., Carini, V., Patti, B., Bonanno, A., Basilone, G., Mazzola, S., Garcia Lafuente, J., Garcia, A. Buscaino, G., Aguzzi, L., Rollandi, L., Morizzo, G. and Cavalcante, C. (2003). Anchovy egg and larval distribution in relation to biological and physical oceanography in the Strait of Sicily. Hydrobiologia 503: 117–120.

[2] Lermusiaux, P.F.J. and Robinson, A.R. (2001). Features of dominant mesoscale variability, circulation patterns and dynamics in the Strait of Sicily. Deep-Sea Res I 48: 1953–1997.

[3] García-Lafuente, J., García, A., Mazzola, S., Quintanilla, L., Delgado, A., Cuttita, A. and Patti, B. (2002). Hydrographic phenomena influencing early life stages of the Sicilian Channel anchovy. Fish. Oceanogr. 11: 31–44.

A remote sensing approach for linking the historic 2011 Mississippi River flood to wetland sedimentation on the Delta

F. Falcini[1], S. Colella[1], G. Volpe[1], R. Santoleri[1], N.S. Khan[2], L. Macelloni[3], D.J. Jerolmack[2]

[1] Consiglio Nazionale delle Ricerche, 2Istituto di Scienze dell' Atmosfera e del Clima, Rome, 00133, Italy
[2] University of Pennsylvania, Department of Earth and Environmental Science, Philadelphia, 19104, USA
[3] University of Mississippi, Mississippi Mineral Resources Institute, University, 38677, USA.
E-mail: f.falcini@isac.cnr.it

Summary

We use field calibrated satellite data to quantify differences in sediment-plume patterns between the Mississippi and Atchafalaya River, and to assess the impact of these extreme outflows on wetland sedimentation. We show that a focused, high-momentum jet emerged from the leveed Mississippi, and delivered sediment far offshore. In contrast, the plume from the Atchafalaya was more diffuse; diverted water inundated a large area, and sediment was trapped within the coastal current.

Introduction

Wetlands in the Mississippi River deltaic plain are deteriorating in part because levees and control structures starve them of sediment [1]. In spring 2011 a record-breaking flood brought discharge on the lower Mississippi River to dangerous levels. To relieve pressure on levees along the downstream portion of the Mississippi River in New Orleans, the Morganza Spillway was opened for the first time in almost 40 years. 3500m^3 s^{-1} of water was being diverted into the Atchafalaya Basin, flooding the swamps and marshes along the entire length of the Atchafalaya River. Although both the Mississippi River and Atchafalaya River channels had obvious sediment-laden plumes emanating from their mouths, the differences in plume patterns and extent of inundation were striking.

We performed time-series analysis of suspended sediment concentration (SSC) from MODIS satellite data, calibrated using field measurements. Satellite SSC data were obtained using processed Level-1A products by following a procedure for estimating suspended load from remote-sensing reflectance high-resolution band 1 at 645 nm [2]. To investigate the Mississippi River plume dynamics during this extraordinary event, and to calibrate satellite data, we also carried out oceanographic transects off the Mississippi Delta during the peak of the flood. Moreover, we conducted a sedimentation survey of 45 sites by helicopter across the Mississippi Birdsfoot, Barataria, Terrebonne and Atchafalaya basin wetlands.

Discussions

The Mississippi River, whose floodwaters upstream were completely contained within artificial levees, exhibited narrow and focused jets of sediment-laden water, especially from Southwest Pass, which penetrated the coastal current with limited mixing for the duration of the flood. The intentionally flooded Atchafalaya Basin inundated a ~100-km-wide coastal zone, and sediment from its broad plume seemed to be trapped in the nearshore zone for four weeks, where it thoroughly mixed with marine waters. The sedimentation survey confirmed a greater wetland sedimentation over a broad area in the Atchafalaya Basin, from both direct deposition by floodwaters and indirect deposition through coastal

reworking of the plume. Our analysis suggests that river-mouth hydrodynamics influenced sediment deposition patterns during the spring 2011 flood.

Conclusions

The historic Morganza Spillway opening simulated a more natural flooding scenario in the Atchafalaya River: this diffuse plume-influenced by coastal currents and winds-delivered substantial sediment over a broad area, both directly to wetlands through inundation and to the nearshore zone where tides and currents could potentially carry it onshore. Although the Mississippi River carried a larger sediment load than the Atchafalaya River, it produced less sedimentation. Flow confinement promotes delivery of vast quantities of sediment far offshore, where it cannot build a land platform to support wetlands. If the Mississippi River plume was diffuse, its sediments would probably have been carried shoreward with the coastal current to produce substantial deposition at Barataria and Terrebonne. Our work shows how fine sediments carried in a flood and diverted to shallow marine settings could contribute substantially to marsh sedimentation.

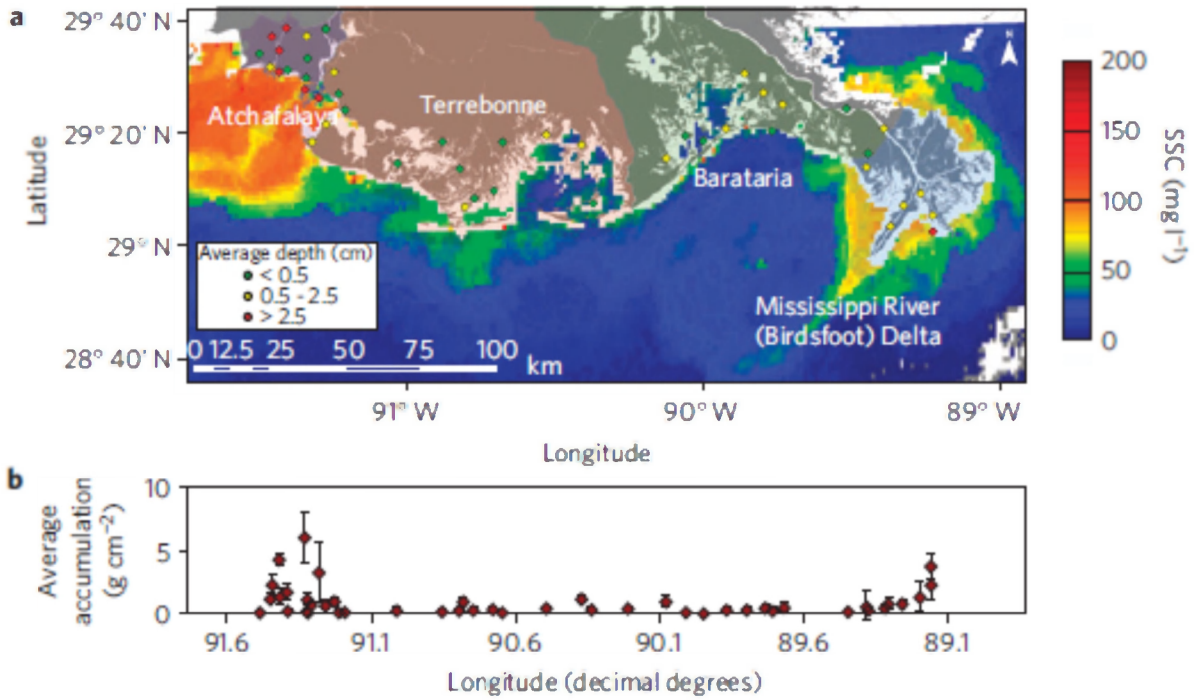

*Spatial distribution of sediment during the 2011 flood. **a**, Locations, and measured recent sediment accumulation, from shallow cores along the delta shoreline (circles), merged with a map of remote sensing SSC on 1 June 2011. **b**, Recent sediment accumulation at each sampling site.*

References

[1] Paola, C. et al. (2001). Natural processes in delta restoration: Application to the Mississippi Delta. Annu. Rev. Mar. Sci., 3: 67-91.

[2] Rodríguez-Guzmán, V. and Gilbes-Santaella, F. (2009). Using MODIS 250 m imagery to estimate total suspended solids in a Tropical Open Bay. Int. J. of Systems Applications, Engineering & Development, 3: 36–44.

Assessment of MODIS-Aqua Ocean Color and Aerosol Products in the US Northeastern Coastal Region using AERONET-Ocean Color Measurements,

Hui Feng[1], Heidi Sosik[2], and Tim Moore[1]

1: Ocean Process Analysis Laboratory (OPAL),University of New Hampshire
39 College Rd., Morse Hall, Rm. 142, Durham, NH 03824, USA. Hui.Feng@unh.edu

2 : Biology Department, MS 32,Woods Hole Oceanographic Institution
Woods Hole, MA 02543, USA. hsosik@whoi.edu

Abstract

Optical complexity of both waters and atmospheres in coastal environments likely leads to significant issues in the quality of satellite-retrieved ocean color and aerosol products. Routine validation for satellite data product quality is desired and requires high-quality in-situ measurements and matchup analysis. One aspect of a NASA-Ocean Biology and Biogeochemistry program funded project focuses on the coastal satellite ocean color validation near the Martha's Vineyard Coastal Observatory (MVCO) in Massachusetts. The key field component monitors the multi-spectral water-leaving radiances and aerosol optical properties using an above-water automatic sun-photometer, the AERONET-Ocean Color (AERONET-OC, i.e. SeaPRISM) deployed at the MVCO tower since 2004.

Our earlier studies have shown that MODIS-Aqua ocean color products produced by SeaDAS version 6 with a new atmospheric correction scheme (Ahmad et al., 2010; Bailey et al., 2010) improves MODIS-Aqua ocean color products. Recently, a major reprocessing for the MODIS-Aqua ocean color data was released to address issues with instrument degradation, particularly from 2010 to the present.

This study presents an inter-comparison of MODIS-Aqua ocean color and aerosols products by reprocessing 2012 (R2012.0) and by reprocessing (R2010) using AERONET-OC measurements as a reference. It has been found that the MODIS-Aqua water leaving radiance at 412nm in R2012 is significantly lower than that in R2010 starting at the late year 2009 to 2010. At a selected open ocean site (35°N, 64°W), a similar feature in nLw 412nm is shown. Between reprocessing R2012 and R2010 there are slight differences in water leaving radiance at 443nm and little differences at longer wavelengths. There are no apparent differences in MODIS-retrieved aerosol properties (i.e. Angstrum exponent (531,869) and AOT at 869nm). Once the latest MODIS-Aqua reprocessing R2013 that is a partial mission reprocessing (2011–2013) becomes available updated validation will be presented in this work.

SENTINEL-3 Optical Sensors Products and Algorithms

Carla Santella [(1)], Roberto Sciarra[(1)], Philippe Goryl[(2)], Alessandra Buongiorno[(2)], Vincent Fournier-Sicre [(3)], Vincenzo Santacesaria[(3),] Hilary Wilson[(3)]

(1) SERCO SpA (c/o ESA-ESRIN), Italy (2) ESA-ESRIN, Italy (3) EUMETSAT, Germany

The Sentinel-3 mission objectives encompass the commitment to consistent, long-term collection and operational provision of remotely sensed marine and land data, to measure sea surface topography, sea/land surface temperature and ocean/land surface colour in support of ocean forecasting systems and for environmental and climate monitoring.

The objective of this poster is to introduce the Sentinel-3 Level 2 geophysical products generated from data acquired by the OLCI and SLSTR optical sensors, with a special focus on ocean color products and the algorithms used for products retrieval.

An overview of the complete set of Sentinel-3 optical sensors products and their characteristics will be also provided to offer a complete view of the “Sentinel-3 Optical Products” that will be generated within the Sentinel-3 Payload Data Ground Segment by the Sentinel-3 Instrument Processing Facilities (IPFs) and disseminated to the users.

The SENTINEL-3 Payload Data Ground Segment

Carla Santella[(1)], Carolina Nogueira Loddo[(2)], Vincent Fournier-Sicre[(2)], Vincenzo Santacesaria[(2)], Jan Løvstad[(2)], Hilary Wilson[(2)], Alessandra Buongiorno[(3)], Roberto Sciarra[(1)], Eric Monjoux[(3)], Philippe Goryl[(3)], Pierre Féménias[(3)], Michela Sunda(4), Marc Niezette[(4)]

(1) SERCO SpA (c/o ESA-ESRIN), (2) EUMETSAT, Germany (3) ESA-ESRIN, Italy (4) TELESPAZIO-VEGA, Germany

The Sentinel-3 PDGS is part of the GMES Space Component which is responsible for providing EO data capable of supporting the GMES Services, to the GMES Service Component. In this context the Sentinel-3 PDGS will be in charge of executing all functions allowing the exploitation of the Sentinel-3 data, i.e. acquisition, processing, archiving and dissemination of data from the OLCI (Ocean and Land Colour instrument), the SLSTR (Sea and Land Surface Temperature Radiometer), the SRAL (Synthetic Aperture Radar Altimeter), the MWR (Microwave Radiometer) instruments, and the GNSS and DORIS assembly embarked on the Sentinel-3 satellite.

The Sentinel-3 Payload Data Ground Segment will consist of different centres with specific functionalities:

- **Core Ground Station** providing acquisition and Near-Real-Time LAND Processing functionality;
- **Land Centre*(s)*** providing Offline (Short-Time-Critical & Non-Time-Critical) L1 & LAND L2 Processing, User Interface and Long Term archiving for LAND products functionalities;
- **Marine Centre** providing Near-Real-Time and Offline L0/L1 & Marine L2 Processing, Mission Planning, Auxiliary Data Coordination, User Interface, Mission Performance Monitoring and Long Term archiving for MARINE products functionalities;
- **Mission Performance Centre** performing activities related to the performance of the Sentinel-3 mission products.

Circulation, Short Term Archiving, Online Archiving and Monitoring functionality are common to all Centres.

This poster provides an overview of the Sentinel-3 Payload Data Ground Segment, with its different centres and functionalities.

Bayesian Methodology for Ocean Color Remote Sensing

Robert Frouin, Scripps Institution of Oceanography, La Jolla, USA
Bruno Pelletier, University of Rennes 2, Rennes, France

The inverse ocean color problem, i.e., the retrieval of marine reflectance from top-of-atmosphere (TOA) reflectance, is examined in a Bayesian context. The solution is expressed as a probability distribution that measures the likelihood of encountering specific values of the marine reflectance given the observed TOA reflectance. This conditional distribution, the posterior distribution, allows the construction of reliable multi-dimensional confidence domains of the retrieved marine reflectance. The expectation and covariance of the posterior distribution are computed, which gives for each pixel an estimate of the marine reflectance and a measure of its uncertainty. The p-value is also computed to identify situations for which forward model and observation are incompatible. Prior distributions of the forward model parameters that are suitable for use at the global scale, as well as a noise model, are determined. Numerical approximations of the expectation and covariance are defined and implemented. Performance is evaluated on simulated data, and the ill posed nature of the inverse problem is illustrated and discussed. The theoretical concepts and inverse models are applied to SeaWiFS imagery, and comparisons are made with estimates from the standard atmospheric correction algorithm and in situ measurements. Conclusions are given in terms of performance, robustness, and generalization. Regionalization of the inverse models is a natural development to improve retrieval accuracy, for example by including explicit knowledge of the space and time variability of atmospheric variables.

A case study on bio-optical and radiometric quantities in northwest European shelf seas

S. Garaba and O. Zielinski
Institute for Chemistry and Biology of the Marine Environment - Terramare, Carl von Ossietzky University of Oldenburg, Schleusenstraße 1, 26382 Wilhelmshaven, Germany;
shungu.garaba@uni-oldenburg.de; oliver.zielinski@uni-oldenburg.de

Summary

Colour of seawater has become an integral tool in understanding surface marine ecosystems and processes. Additionally, operational oceanographic observatories are becoming more prominent these days while at the same time hyperspectral radiometric sensors are becoming increasingly affordable. This has driven a wide spread use of these hyperspectral sensors to measure reflectance above the water surface from stationary and mobile platforms alike. As enormous amounts of data are produced and favourably processed in real-time, effective quality control procedures become more than just supporting tools, but a crucial prerequisite for trustworthy and manageable information.

Introduction

We use bio-geophysical and hyperspectral radiometric measurements from German Bight (GB), North Sea (NS), Inner Seas (ISS), Irish Sea (IS) and Celtic Sea (CS) to identify and establish relationships between colour producing agents (CPAs) and perceived colour of seawater. In order to obtain valid optical measurements, meteorological and sunglint contamination were mitigated using state-of-the-art quality control protocols (Garaba et al., 2012). The remote sensing reflectance measured is transformed into discrete Forel-Ule numerical indices (FUI), 1 - indigo-blue, oligotrophic to 21 - cola brown, hyper-eutrophic (Wernand, 2011). The typical classification of water bodies is based on the concentration of dissolved and particulate material and water transparency. Taking advantage of the long record of Forel-Ule ocean colour observations, we implement a new colorimetric calculation system (Wernand, 2011) to transform hyperspectral radiometric reflectance into discrete Forel-Ule Indices. The aim of this study is to identify and establish relationships between CPAs and perceived colour of seawater in northwest European shelf seas. We present measurements of environmental properties like CDOM, Chl-a, SPM, Secchi disk depth, remote sensing reflectance, and salinity. Hyperspectral radiometric quantities were collected underway on 15 minute intervals from start to end of field campaign. To complement these underway radiometric measurements biogeophysical properties were measured at selected stations. These measurements are used to interpret how perceived colour changes are influenced by environmental properties observed.

Discussion

We present a novel approach of estimating which of the three main CPAs of seawater control perceived colour of seawater. Our bio-optical models for estimating FUI for measured CPAs; chlorophyll (Chl-a), coloured dissolved organic material (CDOM) and suspended particulate material (SPM) had correlation coefficients, R^2 (GB = 0.98, NS = 0.23, ISS=0.99, IS=0.63, CS = 0.16). It was also observed that salinity can be estimated from coloured dissolved organic matter with good accuracy, R^2 (GB = 0.94, NS = 0.44, ISS=0.90, IS=0.85, CS = 0.51). We show that ocean colour products i.e. reflectance and perceived colour of seawater can be used to infer, with good accuracy, environmental parameters e.g. Chl-a, CDOM, SPM, salinity and Secchi depth of the investigated waters providing an effective and affordable tool for operational marine observations

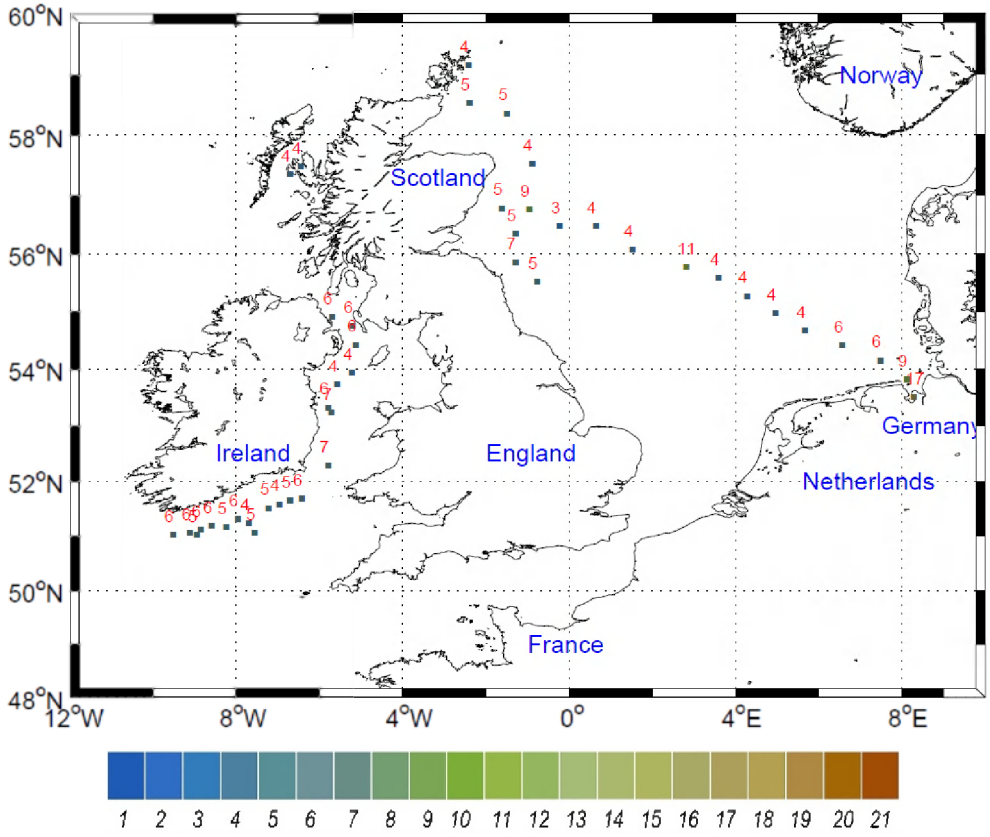

Figure 1 Map showing approximated colour of seawater from the sampled stations during the field campaign aboard R/V Heincke cruise HE302 between 21 April and 14 May 2009. The Forel-Ule information was computed using the derived R_{RS}. The numbers represent the Forel-Ule Index matching the colour on the scale reproduced after Wernand (2011).

Conclusion

The use of Forel-Ule Index determined from hyperspectral radiometry has recently been revived. In this study we develop regional bio-optical models based on shipborne observations to determine perceived colour of seawater using CDOM, Chl-a and SPM as input parameters. We also show that salinity and Secchi-disk depth can be inferred from remote sensing and related CPAs. The sensitivity of these bio-optical models still needs to be advanced, and more extensive accurate biogeochemical measurements will be vital. In this study we also show that the colorimetric transformation of spectral information into numerical values as proposed by Wernand (2011), avoids the ambiguity of marine environment classification into case I or case II waters (Mobley et al., 2004). Improved and extensive field investigations are required to further enhance the sensitivity/accuracy of such region specific bio-optical models.

References

Garaba, S.P., Schulz, J., Wernand, M.R., and Zielinski, O., 2012, Sunglint detection for unmanned and automated platforms: Sensors, v. 12 (9), doi:10.3390/s120912545, p. 12545-12561.

Mobley, C.D., Stramski, D., Bissett, W.P., and Boss, E., 2004, Optical modeling of ocean waters: Is the Case 1 - Case 2 classification still useful?: Oceanography, v. 17 (2), p. 60-67.

Wernand, M.R., 2011, Poseidons paintbox : historical archives of ocean colour in global-change perspective [PhD Thesis], Utrecht University.

Routine monitoring of bathymetry and habitat maps derived from HICO imagery: Case study of Shark Bay, Western Australia.

R.A. Garcia [1], P.R.C.S. Fearns [1], L.I.W. McKinna [1]
[1] Curtin University, Department of Imaging and Applied Physics, Bentley, WA 6102, Australia
Email: Rodrigo.Garcia@postgrad.curtin.edu.au

Summary
The purpose of this study was to investigate and develop approaches to atmospheric correction, level-2 (L2) processing, and geo-location of HICO imagery for routine monitoring of shallow coastal water ecosystems. A total of nine HICO images, spanning November 2011 - August 2012, over the Shark Bay World Heritage Area, Western Australia, were examined. We have implemented a semi-analytical shallow water inversion model to retrieve bathymetry and a two class benthic habitat map. Within this research, challenges regarding atmospheric correction of HICO imagery, tide correction of bathymetry products, and geo-location accuracy are discussed.

Introduction

The Hyperspectral Imager for the Coastal Ocean (HICO) is a prototype sensor, onboard the International Space Station, designed with the necessary specifications for the remote sensing of coastal marine environments [1]. HICO has a spatial resolution of 100 × 100 m with 87 contiguous spectral bands between 400-900 nm, which has the potential for the generation of improved shallow water remote sensing products such as bathymetry and benthic habitat maps.

Bathymetry and benthic habitat maps are important not only for coastal resource managers, but also for research utilizing hydrodynamic models in which depth and benthic habitat type influence tide, currents, wave energy and consequently sediment/nutrient transportation mechanisms [2]. Furthermore, coastal resource managers and researchers often require 'environmental baselines' to assess the natural/seasonal variability in benthic habitat type(s) and bathymetry prior to industrial/commercial development or anthropogenic disturbances. This, however, requires routine monitoring of such products within coastal regions of interest. To date, there has been limited work reported on the routine monitoring of bathymetry and benthic habitats using standardized processing of satellite hyperspectral imagery.

A case study showing the routine monitoring of HICO-derived bathymetry and benthic habitat maps is presented for the World Heritage Area of Shark Bay, Western Australia. In this study, the semi-analytical shallow water inversion algorithm, BRUCE [3], was implemented to retrieve imagery of water column depth (bathymetry), inherent optical properties (IOPs) of the water column and the benthic albedos of sand and seagrass.

Discussion and conclusion

Several processing steps have been implemented that convert HICO L1B, calibrated radiances, to the desired bathymetry and benthic habitat map L2 products. Briefly, these steps include: (1) Tafkaa 6S [4] atmospheric correction to generate the above water remote sensing reflectances; (2) a per-pixel quality control that masks land, cloud and pixels that were over-corrected in step 1; (3) sunglint removal; (4) derivation of L2 products using the BRUCE model (Figure 1); (5) uncertainty propagation through the inversion model using the method proposed by Hedley et al. [5]; (6) Image smoothing and tide correction of the bathymetry product and; (7) Geo-referencing and manual geo-rectification using ground control points.

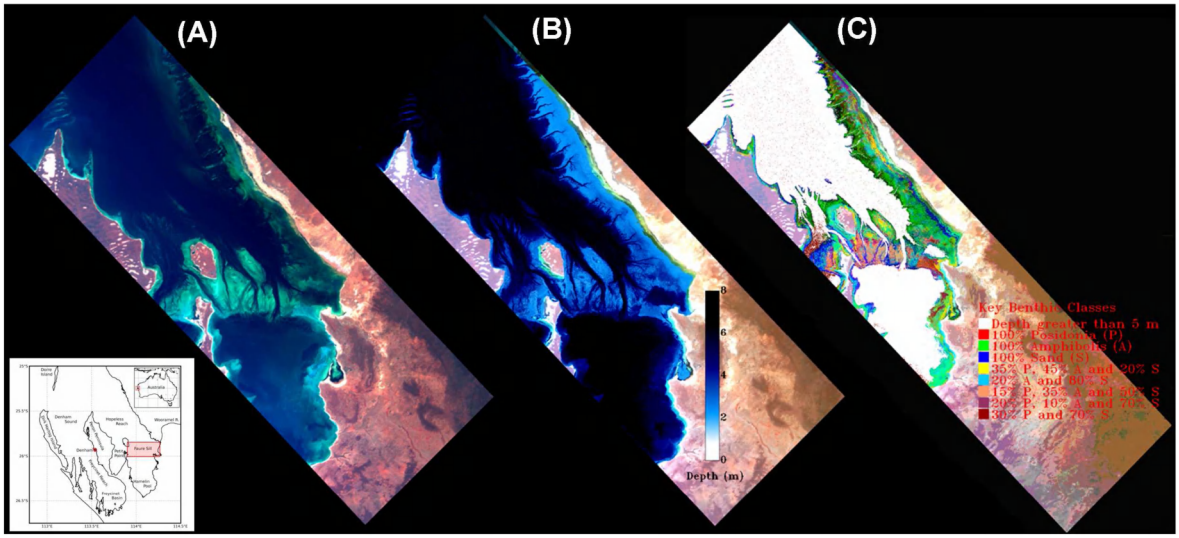

Figure 1: HICO imagery of Shark Bay, Western Australia (central latitude/longitude 25.62°S/ 113.89 °E) on 01 June 2012; (a) quasi-true color image; (b) derived bathymetry, and; (c) derived substrate classification of sand and seagrass and various proportions of these two classes.

Preliminary results show relative changes through time between the two substrate classes (sand and seagrass). This may be attributed to seasonal variability in the proportion of seagrass present. However, further work is needed to assess if this variation is statistically significant above the uncertainty propagated through the BRUCE model.

The routine monitoring of bathymetry of Shark Bay has also raised the following key issues: (1) Tafkaa 6S often overcorrects the atmospheric radiance signal, resulting in non-physical reflectance signatures in the blue and red portions of the spectrum. This overcorrection is particularly evident in HICO swaths captured during high solar zenith angles. Further work is needed to improve atmospheric correction; (2) Geo-referencing using the distributed geographic lookup tables does not generate the desired geospatial consistency through time. Analysis showed that clearly identifiable land features varied by approximately 1° in latitude and longitude across the HICO images. Additional geo-registration using distinct land features as ground control points improved the geo-location. Based on analysis of image features, we estimate the geo-location accuracy has improved to within 100-300 m, and; (3) Tide correction proved challenging over shallow regions of Shark Bay where shallow water tidal harmonics are prevalent. The lack of water level height data prevented direct correction of these tidal influences, and thus an empirical image based tide correction technique was employed to correct all bathymetry images to a relative datum.

References

[1] Lucke, R.L., Corson, M., McGlotlin, et al. (2011), Hyperspectral imager for the coastal ocean: instrument description and first images, *Appl Optics*, 50: 1501-1516.

[2] Burling, M.C., Pattiaratchi, C. B., Ivey, G.N. (2003), The tidal regime of Shark Bay, Western Australia, Estuar Coast Shelf Sci. 57: 725-735

[3] Klonowski, W.M., Fearns, P.R.C.S., Lynch, M.J. (2007), Retrieving key benthic cover types and bathymetry from hyperspectral imagery, J Appl Rem Sens, 1: 011505

[4] Gao, B-C., Montes, M.J., Ahmad, Z., Davis, C.O. (2000), Atmospheric correction algorithm for hyperspectral remote sensing of ocean color from space. Appl Optics, 39: 887-896.

[5] Hedley, J., Roelfsema, C., Phinn, S.R. (2010), Propagating uncertainty through shallow water mapping algorithm based on radiative transfer model inversion, In: *Proceedings of Ocean Optics XX*, Anchorage Alaska.

Biological response to the 1997-98 and 2009-10 El Niño events in the equatorial Pacific Ocean

Michelle M. Gierach[1], Tong Lee[1], Daniela Turk[2,3], and Michael McPhaden[4]
[1]Jet Propulsion Laboratory / California Institute of Technology
[2]Dalhousie University
[3]Lamont-Doherty Earth Observatory, Earth Institute at Columbia University
[4]NOAA Pacific Marine Environmental Laboratory

Gierach, M.M., T. Lee, D. Turk, and M.J. McPhaden (2012), Biological response to the 1997-98 and 2009-10 El Niño events in the equatorial Pacific Ocean, *Geophys. Res. Lett.*, 39, L10602, doi:10.1029/2012GL051103.

El Niño-Southern Oscillation (ENSO) significantly influences atmospheric and ocean circulations in the Pacific Ocean, which in turn affect biological production and ecosystem characteristics. Much of our existing knowledge about the relationship between ENSO and biology is with respect to the classic El Niño (i.e., EP-El Niño), which has maximum warming in the eastern equatorial Pacific (EEP) (Fig. 1e). However, since the 1990s, there have been frequent occurrences of a new flavor of El Niño (i.e., CP-El Niño) that has maximum warming in the central equatorial Pacific (CEP) (Fig. 1f). The impact of the latter on biology is not well understood. Biophysical responses in the equatorial Pacific Ocean to the 1997-98 and 2009-10 El Niño (i.e., the strongest EP- and CP-El Niño event in the last three decades) are analyzed using satellite observations and reanalysis products. Significant differences in chlorophyll-a (chl-a) are found between the two events associated with different patterns of anomalies for the physical variables (Fig. 1). An adjoint tracer analysis is used to examine the difference in the origin and pathway of water masses in the upper equatorial Pacific Ocean that control the difference in nutrient supply and thus chl-a.

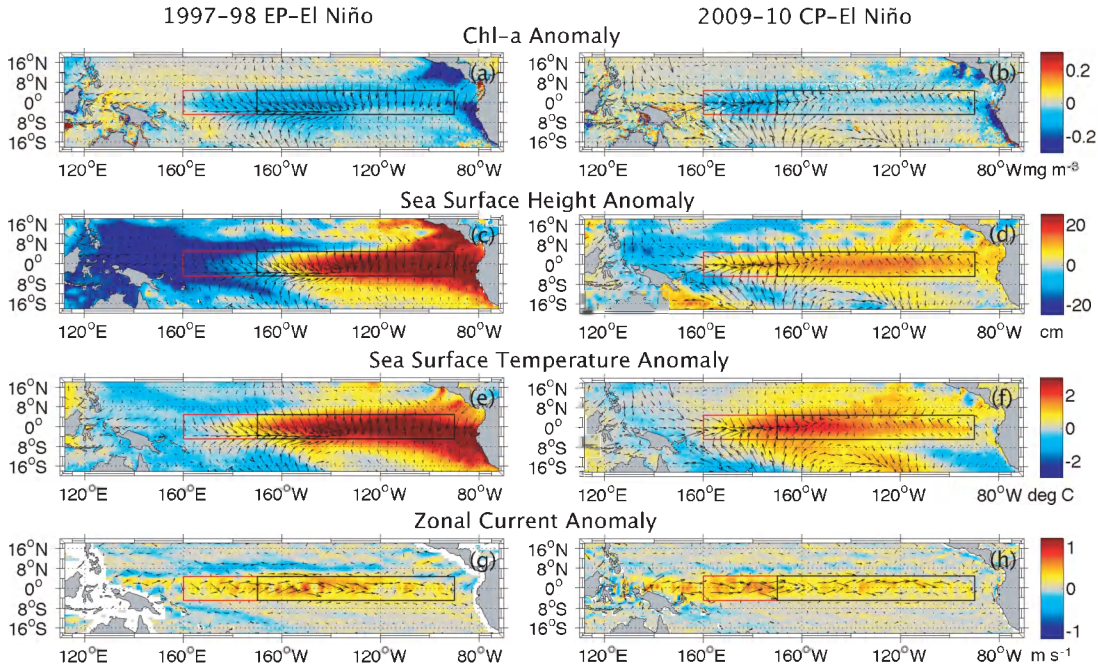

Fig. 1. November-December-January averaged anomalies of (a-b) chl-a, (c-d) sea surface height, (e-f) sea surface temperature, and (g-h) zonal ocean surface currents for the 1997-98 EP-El Niño and 2009-10 CP-El Niño. Wind vector anomalies are overlaid on (a-f) and ocean surface current vector anomalies on (g-h). The black and red boxes denote the EEP (5°S-5°N, 170°W-90°W) and CEP (5°S-5°N, 160°E-170°W) regions.

The retrieval of attenuation and scattering coefficients of marine particles from polarimetric observations

A. Gilerson, A. Ibrahim, J. Stepinski, A. El-Habashi, S. Ahmed

Optical Remote Sensing Laboratory, the City College of the City University of NY,
New York, NY, 10031, United States
Email: gilerson@ccny.cuny.edu

Summary

Polarized light in the oceans carries intrinsic information that can be utilized to estimate the optical and microphysical properties of the oceanic hydrosols. It is especially sensitive to the scattering coefficient, which cannot be retrieved from the unpolarized light used in current ocean color remote sensing algorithms. Based on extensive simulations using the vector radiative transfer program RayXP, the attenuation-to-absorption ratio (c/a), from which b is readily computed, is shown to be closely related to the DoLP. The relationship is investigated for the upwelling polarized light for several wavelengths in the visible part of the spectrum, for a complete set of viewing geometries, and for varying water compositions including open ocean and coastal waters. A large dataset of Stokes components is collected for various water compositions, measured in the field with a hyper-spectral and multi-angular polarimeter for validation purposes.

Introduction

Light-scattering properties of particles in the ocean and atmosphere have been extensively studied [1]. Taking note that solar radiation is initially completely unpolarized, once it reaches the Earth's atmosphere, scattering events, such as Rayleigh (molecular) and particulate scattering, cause it to become partially polarized. Light exhibits, as a result of scattering, some degree of polarization (DoP) in different directions and this polarization is directly related to the source of the radiation and to the properties of the scatterers. Thus, the polarization state of light carries information about the atmosphere-ocean system (AOS) that can be utilized for remote sensing of microphysical and optical properties of particulates including the oceanic hydrosols and it is sensitive to the scattering coefficient. Through the unpolarized remote sensing reflectance (R_{rs}), the classical algorithms can only estimate *back*scattering coefficients b_b, but the *total* scattering coefficient b could be retrieved based on the characteristics of polarized light.

Discussion

Based on extensive simulations using the vector radiative transfer program RayXP, the attenuation-to-absorption ratio (c/a), from which b is readily computed, is shown to be closely related to the degree of linear polarization (DoLP). The relationship is investigated for the upwelling polarized light for several wavelengths in the visible part of the spectrum, for a complete set of viewing geometries, and for varying concentrations of phytoplankton, non-algal particles, and color dissolved organic matter (CDOM) in the aquatic environment that resembles coastal waters (Case II waters) [2]. Another dataset of bio-optical properties for open ocean (Case I waters) that includes only phytoplankton particles and its bi-products has been ingested into the RayXP program to simulate the polarized radiance. It is shown, for Case I and Case II waters, that there is an excellent correlation between the DoLP and c/a for a wide range of viewing geometries. That correlation is investigated theoretically using fitting techniques, which show that it depends not only on the general composition of water but also on the particle size

distribution (PSD) of the (mainly non-algal) particles for Case II waters according to the power law in Equation (1).

$$\left\{\left(\frac{c}{a}\right)_{\text{fit}}\right\}_{\xi_{\text{nap}}=3.5,4.0,4.5} = \left\{\chi(DoLP)^{\gamma}\right\}_{\xi_{\text{nap}}=3.5,4.0,4.5}, \quad (1)$$

where a and c are the absorption and attenuation coefficients, respectively; χ and γ are the fitting coefficients and ξ_{NAP} is a PSD slope. The relationship between the IOPs (c/a ratio) and the DoLP is parameterized as a power law as in Equation (1) with a good coefficient of determination R^2 opening the possibility for an accurate retrieval technique of the c/a ratio and further attenuation and scattering coefficients.

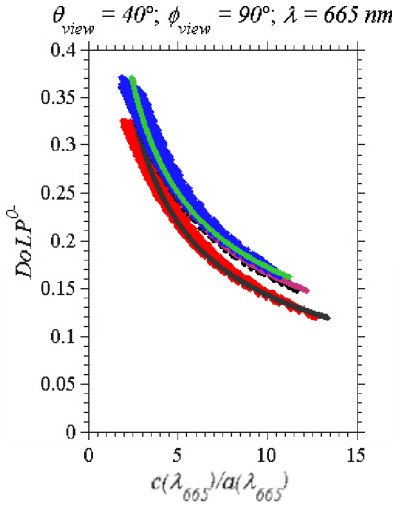

Fitted relationship between DoLP and c/a at 665 nm

An interesting result is that the fits for both ξ_{nap} of 4.0 and 4.5 are similar for the all three wavelengths 440, 550 and 665nm (only results for 665nm are shown in the figure). In coastal waters, the slope ξ_{nap} of PSD of NAP largely falls in the range of 4.0-4.5, where these particles are small in size. Since the relationship weakly depends on the PSD of chlorophyllic particles, a rough estimate of ξ_{nap} to be in its typical range may not induce large errors in, for example, retrieval analysis. On the other hand, the relationship between the DoLP and c/a for Case I waters is more linear especially at the 550 nm where maximum dependency in relationship falls onto the optical properties of the phytoplankton particles. At the blue and red wavelengths, the relationship becomes more dependent on the optical properties of the water molecules (Rayleigh scattering at the blue and high water absorption at the red spectral region).

Conclusions

While attenuation and scattering coefficients are not retrievable from the scalar reflectance measurements, a relationship between the degree of linear polarization (DoLP) and the attenuation to absorption coefficients ratio (c/a) has been investigated using vector radiative transfer simulations for open ocean and coastal waters for conditions just below and above the air-water interface. The parameterized relationship allows the direct retrieval of the scattering coefficient b of the hydrosols using polarimetric observations of the ocean. A large dataset of Stokes components for various water compositions, measured in the field with a hyper-spectral and multi-angular polarimeter, then provides the opportunity to validate the parameterized relationship between DOLP and c/a. This study opens the possibility for the retrieval of additional inherent optical properties (IOPs) from air- or space-borne DoLP measurements of the ocean.

References

[1] Timofeyeva, V. A. (1970) “Degree of polarization of light in turbid media,” Izvestiya Akademii Nauk SSSR Fizika Atmosfery. I. Okeana. **6**, 513.

[2] Ibrahim, A., Gilerson, A., Harmel, T., Tonizzo, A., Chowdhary, J., and Ahmed, S. (2012) "The relationship between upwelling underwater polarization and attenuation/absorption ratio," Opt. Express **20**, 25662-25680.

Ecosystem disruption in the Arabian Sea linked to climate change and the spread of hypoxia

Joaquim I. Goes[1], Helga do R. Gomes[1], S. G. Prabhu Matondkar[2], S. Basu[2], S. G. Parab[2], and R.M. Dwivedi[3]

[1]Lamont Doherty Earth Observatory at Columbia University, Palisades, New York, USA,10964,
[2]National Institute of Oceanography, Dona Paula, Goa, India, 403004,
[5]Space Applications Centre, Indian Space Research Organization, Ahmedabad, India, 380015
E-mail: jig@ldeo.columbia.edu

Summary

The northern Arabian Sea has been witnessing unprecedented blooms of a green mixotrophic dinoflagellate *Noctiluca scintillans* during the winter monsoon. First seen in smaller numbers off Oman, *Noctiluca* blooms have now become more pervasive and widespread throughout the northern Arabian Sea replacing diatoms as the dominant winter-time bloom forming phytoplankton. Here we have used shipboard and ocean color satellite observations to show that the unprecedented appearance of *Noctiluca* blooms may be tied to the influx of oxygen deficient waters into the upper euphotic column and the extraordinary ability of its endosymbiont *Pedinomonas noctilucae* to photosynthesize more efficiently over other phytoplankton under reduced oxygen conditions. We also present examples that demonstrate the promise and potential of ocean color imagery for identifying the origin and dynamics of this unusual bloom, and the long-term implications of these recurrent blooms for carbon cycling in the Arabian Sea.

Introduction

Between 1994 and 1996, the Arabian Sea became the focus of a multinational effort directed at studying ocean biological and physical processes and their links to the global carbon cycle [1,2]. The results of this comprehensive, multi-disciplinary effort known as the Joint Global Flux Study (JGOFS) program provided important indications of the role of the reversal of the monsoons and extremes in wind forcing in causing the greatest seasonal variability of primary production and vertical flux of carbon observed in any of the world's oceans. Since the end of the JGOFS program large-scale field ocean biogeochemical studies in the Arabian Sea have been few. Most contemporary investigations of primary productivity and biogeochemical possesses in the region have based on data collected during small programmatically focused shipboard cruises which have been largely regional in scope [3]. Over the past few years, large basin-scale studies have relied largely on coupled physical-biological models [4] and on satellite based observations [5,6]. Several of these studies have suggested that biological productivity within the Arabian may be on the rise.

In our satellite based study focused on the Arabian Sea using SeaWiFS data alone [5], we were able to conclude that the increase in chlorophyll in the Arabian Sea between 1998 and 2003 was largely the result of a year-on-year increase in summer-time phytoplankton blooms in the western Arabian Sea. With the aid of other satellite data products, we were able to demonstrate that the increase in summer-time phytoplankton blooms was not occurring in isolation but was part of a systematic response to the warming trend over Eurasia. Over the period of nine years of SeaWiFS observations, we were able to observe that the decline in winter and spring time snow over the Himalayan-Tibetan Plateau region associated with the warming trend, was causing a secular increase in the intensity of the SWM winds and upwelling along the coasts of Somalia, Yemen and Oman. We showed that an increase in nutrients resulting from enhanced upwelling was fuelling the year-on-year increase in phytoplankton biomass.

In the present study, we have used satellite data to show that the warming trend is undermining winter cooling in the Arabian Sea. Despite the weakening of convective mixing, satellite data sets reveal that chlorophyll (Chl *a*) concentrations have been on the rise. We have used data from several shipboard studies undertaken in collaboration with colleagues in India that show that the increase in Chl *a* during the winter monsoon is being caused by unprecedented blooms of a mixotrophic dinoflagellate, *Noctiluca*. The presence of a large population of an endosymbiotic prasinophyte *Pedinomonas noctilucae* affords the Arabian Sea *Noctiluca* its green color which making *Noctiluca* easily visible from space. We present some examples that demonstrate the promise and potential of ocean color imagery to provide the necessary temporal and spatial resolution required to identify the origin and dynamics of this unusual bloom.

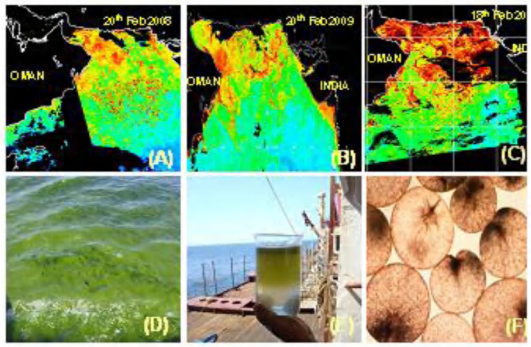

Fig. 1. Spatial extent of Noctiluca bloom as seen in Aqua-MODIS daily chlorophyll images of Feb. A) 2008, B) 2009 & C 2010. D) Blooms as seen from the ship-deck. E) Bucket sample transferred to a glass beaker shows thickness of bloom F) Bloom sample under a microscope showing individual Noctiluca cells.

Conclusions

Shipboard bio-optical measurements have been utilized to show that the large expanse of high Chl *a* seen in ocean color imagery is due to thick, surface dwelling blooms of *Noctiluca*. Large blooms of *Noctiluca* have become a regular feature of the Arabian Sea during the winter monsoon replacing diatoms as the dominant winter-bloom forming phytoplankton. Shipboard ecophysiological studies suggest that the growth of *Noctiluca* to bloom proportions in the open Arabian Sea is being facilitated by an unprecedented influx of oxygen deficient waters into the upper euphotic column. The extraordinary ability of its endosymbiont to photosynthesize more efficiently than other phytoplankton under reduced oxygen conditions also appears to offer *Noctiluca* a competitive growth advantage over other phytoplankton in a region of the world's oceans that appears to becoming increasingly hypoxic. Our observations also suggest that *Noctiluca* blooms may be causing a substantial loss of phytoplankton biodiversity, disrupting the traditional food chain of the Arabian Sea and effecting substantive shifts in carbon export.

References

[1] Burkill, P.H., (1999) ARABESQUE: an overview. *Deep-Sea Research II*, 46, 529-548. *Smith, 2001)*
[2] Goes, J.I., Thoppil, P.G., Gomes, H.do R., Fasullo, J.T., (2005) Warming of the Eurasian landmass is making the Arabian Sea more productive. *Science*, 308, 545-547.
[3] Kahru, M., and B. G. Mitchell, (2008) Ocean Color Reveals Increased Blooms in Various Parts of the World. *Eos Trans., AGU,* 89(18), doi:10.1029/2008EO180002. *Kahru and Mitchell, 2008*
[4] Parab, S., Matondkar, S.G.P., Gomes, H.d.R., Goes, J.I., (2006) Monsoon driven changes in phytoplankton populations in the eastern Arabian Sea as revealed by microscopy and HPLC pigment analysis. *Continental Shelf Research*, 26(20), 2538-2558.
[5] Smith, S.L., (2005) The Arabian Sea of the 1990s: New biogeochemical understanding. *Progress in Oceanography*, 65, 113-115.
[6] Wiggert, J.D., Hood, R.R., Banse, K., Kindle, J.C., (2005) Monsoon-driven biogeochemical processes in the Arabian Sea. *Progress in Oceanography*, 65, 176-213.

An improved FLH product for MERIS and OLCI

J.F.R. Gower[1], S.A. King[2], E. Young[3]

[1]Institute of Ocean Sciences, Fisheries and Oceans Canada, Sidney, BC, Canada
[2]Sea This Consulting, Nanaimo, BC, Canada
[3]University of Victoria, Geography Department, Victoria, BC, Canada
Email: jim.gower@dfo-mpo.gc.ca

Summary

ESA should make available a level 3 global MERIS FLH product, to provide new insight into productivity and blooms in coastal areas. MODIS ocean colour data, including fluorescence, are made widely available through the NASA Oceancolor and Giovanni web systems, but fluorescence does not appear to be widely used. We show problems with the Giovanni fluorescence data that may partly explain this. For fluorescence imaging, MERIS has the technical advantage over MODIS of better band placing (including the additional 709 nm band) and of higher spatial resolution (300m compared to 1000m). MERIS ocean colour data, including fluorescence, need to be made more easily available to encourage the work that needs to be done on FLH in preparation for OLCI.

Introduction

Both MERIS and MODIS were designed to map chlorophyll using FLH (Fluorescence Line Height) at wavelengths near 680 nm, as well as using the more standard green-to-blue ratio estimates based on measurements in the range 440 to 560 nm. The standard green-to-blue product has proven inadequate in many coastal areas, and we believe FLH to be a viable alternative. We have applied FLH in the coastal waters of Western Canada [1,2] and documented cases where FLH provides a superior result [3].

Discussion

We show here an example of the way fluorescence is made available by the Giovanni system developed and maintained by the NASA GES DISC, but note problems which probably contribute to its relative lack of use. We conclude that MERIS data should be made available using tools of this type. This applies to both fluorescence and the more conventional chlorophyll products. It will greatly improve global acceptance of OLCI data if such a system were tested and in place before launch of Sentinel 3

At present we notice two problems with Giovanni's fluorescence data. The first is the description of NFLH (Normalized Fluorescence Line Height) data as dimensionless. The normalization applied here is to scale the signal up to the radiance that would be observed under zenith sun, on the assumption that fluorescence increases proportional to incident solar irradiance. This will still have units of radiance. The second problem is the fact that the fluorescence data should not be normalized. The fluorescence data show that this is inappropriate (see Figure), and studies of the fluorescence mechanism [eg 4] confirm this. It has long been known that the fluorescence signal tends to saturate under high insolation. Data summarized in [4] support the conclusion that for all sun elevations over about 20 degrees, that is, when insolation is sufficient for ocean colour satellites to produce reliable results, fluorescence is fully stimulated, and the fluorescence signal is independent of the value of solar irradiance.

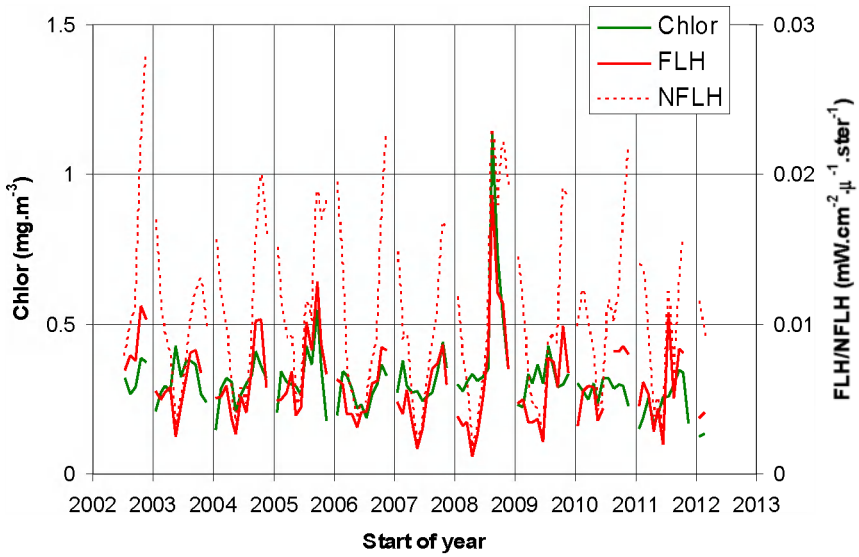

MODIS Aqua monthly average chlorophyll (green) and fluorescence (FLH, red), plotted as normalized fluorescence (NFLH, dotted red) and as FLH (solid red) for a 2-degree square centred on Ocean Station Papa in the NE Pacific. FLH values agree well with chlorophyll. NFLH data show a spurious annual cycle

Conclusions

We are finding successful applications of FLH data and believe that with more users, more successes would appear. We have found problems with the way fluorescence data are handled and believe that these are limiting their use. We note that MERIS data are not distributed using a simple, widely accessible web tool similar to NASA Giovanni. MERIS fluorescence data need to be made more widely available in this way. It would greatly improve international acceptance of OLCI data if such a system were tested with MERIS fluorescence and other data, and in place before launch of Sentinel 3.

Acknowledgements

This work has been supported by Fisheries and Oceans Canada and the Canadian Space Agency. The author thanks colleagues at IOS and the Universities of British Columbia and Victoria for useful discussions.

8. REFERENCES

1. Gower, J.F.R., Brown, L and Borstad, G.A., 2004. Observation of chlorophyll fluorescence in west coast waters of Canada using the MODIS satellite sensor. Can. J. Remote Sens. 30(1), 17-25.
2. Gower, J.F.R. and King, S.A., 2007. Validation of chlorophyll fluorescence derived from MERIS on the west coast of Canada. Int. J. Remote Sens. 28(3-4), 625-635.
3. Gower, J. and King, S., 2012. Use of satellite images of chlorophyll fluorescence to monitor the spring bloom in coastal waters. Int. J. Remote Sens. 33(23), 7469-7481. http://dx.doi.org/10.1080/01431161.2012.685979.
4. Behrenfeld, M.J., Westberry, T.K., Boss, E.S., O'Malley, R.T., Siegel, D.A., Wiggert, J.D., Franz, B.A., Mcclain, C.R., Feldman, G.C., Doney, S.C., Moore, J.K., Dall'Oolmo, G., Milligan, A.J., Lima, I., and Mahowald, N., 2009, Satellite-detected fluorescence reveals global physiology of ocean phytoplankton, *Biogeosciences*, **6**, pp. 779-794.

A hybrid MUMM NIR-Corrected algorithm for the atmospheric correction of turbid waters

C. Goyens[1], C. Jamet[1] and K. Ruddick[2]
[1]CNRS, UMR 8187, Univ Lille Nord de France, ULCO, LOG, F-62930 Wimereux, France
[2]MUMM | BMM | UGMM, B-1200 Brussels, Belgium
Email: clemence.goyens@univ-littoral.fr

Summary
In extremely turbid waters, the relation between water leaving reflectance ($\rho_w(\lambda)$) at two bands in the near infra-red (NIR) was shown to be well approximated by the polynomial function suggested by Wang et al. [1] for the atmospheric correction (AC) algorithm of GOCI. Accordingly, a new hybrid MUMM NIR-corrected AC algorithm is developed consisting to replace the constant NIR reflectance ratio in the MUMM AC algorithm [2,3] by the polynomial function of Wang et al. [1]. Based on a sensitivity study we conclude that the hybrid MUMM NIR-corrected AC algorithm results in improved $\rho_w(\lambda)$ retrievals in turbid waters.

Introduction

The use of satellites to retrieve $\rho_w(\lambda)$ requires effective removal of the atmospheric signal. This can be performed by extrapolating the aerosol optical properties to the visible from the NIR spectral region assuming that seawater is totally absorbent in this latter part of the spectrum, the so-called black pixel assumption. However, in turbid waters the scattering and absorption of coloured dissolved organic matter and non-algal particles result in non-zero $\rho_w(NIR)$. To extent the black pixel assumption AC algorithm, Ruddick et al. [2, 3] assumed a constant reflectance ratio, $\alpha(\lambda_{NIR1},\lambda_{NIR2})$, and spatial homogeneity in aerosol reflectance. Recently, Wang et al. [1] suggested a NIR-corrected AC algorithm for GOCI retrieving $\rho_w(\lambda)$ at two wavelengths in the NIR and including a polynomial function relating $\rho_w(\lambda_{NIR1})$ to $\rho_w(\lambda_{NIR2})$.

The polynomial function and the constant $\alpha(\lambda_{NIR1},\lambda_{NIR2})$, suggested by Wang et al. [1] and Ruddick et al. [3], respectively, are validated with 131 highly accurate *in situ* $\rho_w(\lambda)$ data. Next, a study is conducted to evaluate the sensitivity of the AC algorithm to the NIR marine reflectance model. *In situ* $\rho_w(\lambda)$ are therefore combined with a simplified power law model for aerosol reflectance. With the assumption that only single scattering occurs and that the diffuse atmospheric transmittance is equal to 1, we compute the Rayleigh corrected reflectance. The latter is than inverted using the AC algorithms to give the retrieved $\rho_w(\lambda)$, which for a perfect model should be equal to the *in situ* $\rho_w(\lambda)$. According to the results of the sensitivity test, a new AC algorithm is suggested to provide satisfactory $\rho_w(\lambda)$ retrievals over moderately, very and extremely turbid waters.

Discussion

The validation exercise shows that the polynomial function relating $\rho_w(748)$ to $\rho_w(869)$ [1] has a larger validity range compared to the constant reflectance ratio $\alpha(748,869)$ [3]. However, when evaluating the sensitivity of the AC algorithms to the NIR marine reflectance models, we observe that the NIR-corrected AC algorithm largely overestimate $\rho_w(\lambda)$ at all wavelengths and for all water types (median difference between *in situ* and retrieved $\rho_w(\lambda)$ ranging between 0.001 and 0.01, Fig.

1 (a-c)). With the MUMM AC algorithm and provided that the aerosol model is correctly retrieved, for moderate to very turbid waters the difference between observed and retrieved $\rho_w(\lambda)$ remains very small (median difference < -0.0001, Fig. 1 (a,b)). In contrast, for extremely turbid waters, $\rho_w(\lambda)$ are underestimated with a median difference between *in situ* and retrieved $\rho_w(\lambda)$ of about -0.003 (Fig. 1 (c)). Including an error of 40% on the angstrom coefficient for the selection of the aerosol model results in larger errors on the $\rho_w(\lambda)$ retrievals (not shown here). However, these $\rho_w(\lambda)$ retrievals are still closer to ground truth compared to the NIR corrected AC retrieved $\rho_w(\lambda)$ values.

To improve $\rho_w(\lambda)$ retrievals in extremely turbid waters, a hybrid MUMM NIR-corrected AC algorithm is suggested consisting to replace the constant NIR reflectance ratio in the MUMM AC algorithm [2,3] by the polynomial function of Wang et al. [1]. Indeed, this AC algorithm yields in median differences between retrieved and *in situ* $\rho_w(\lambda)$ below 0.001 in extremely turbid waters (Fig. 1 (c)). Nonetheless, for ρ_w(NIR) above 0.05, the hybrid MUMM NIR corrected AC algorithm still retrieves negative $\rho_w(\lambda)$ values in the blue suggesting a refinement of the polynomial function.

Conclusion

To improve $\rho_w(\lambda)$ retrievals in extremely turbid waters the constant NIR reflectance ratio suggested by Ruddick et al. [2,3] for the MUMM AC algorithm is replaced by the polynomial function used within the NIR-corrected AC algorithm of GOCI [1]. Future work will include a refinement of the polynomial function to account for the most turbid water masses and a validation of MODIS Aqua ocean color images processed with the new hybrid MUMM NIR-corrected AC algorithm.

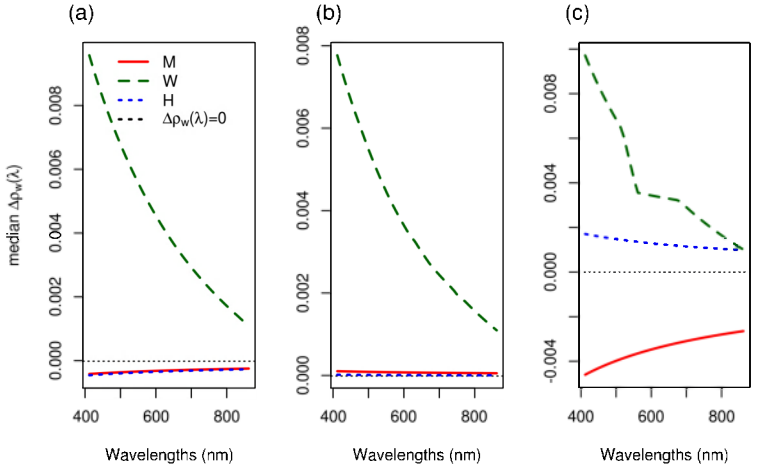

Fig.1: Median difference between in situ and retrieved $\rho_w(\lambda)$ for (a) moderately, (b) very and (c) extremely turbid water. M: MUMM AC algorithm assuming the correct aerosol model, W: NIR-corrected algorithm and H: Hybrid MUMM NIR-corrected AC algorithm assuming the correct aerosol model.

References

1. M. Wang, W. Shi and L. Jiang (2012). "Atmospheric correction using near-infrared bands for satellite ocean color data processing in the turbid western pacific region," Opt. Express, 20, 741-753.
2. K. G. Ruddick, F. Ovidio, and M. Rijkeboer (2000). "Atmospheric correction of SeaWiFS imagery for turbid coastal and inland waters, " Appl. Opt., 39, 897-912.
3. K. G. Ruddick, V. De Cauwer, Y. Park and G. Moore (2006). "Seaborne measurements of near infrared water-leaving reflectance: The similarity spectrum for turbid waters," Limnol. Oceanogr. 51, 1167-1179.

Applying a new method to measure phytoplankton carbon in the field for validating and constraining satellite-derived estimates of biomass

Jason R. Graff [1], Allen J. Milligan [1], Toby K. Westberry [1], Giorgio Dall'Olmo [2], Kristen M. Reifel [1], Virginie van Dongen-Vogels [1], Michael J. Behrenfeld [1]

[1] Oregon State University, Department of Botany and Plant Pathology, Corvallis, Oregon, USA
[2] Plymouth Marine Labs, Remote Sensing Group, Plymouth, UK
Email: jrgraff@science.oregonstate.edu

Summary

Chlorophyll is routinely used as a proxy for phytoplankton biomass, whether directly measured or estimated from fluorescence. This approach suffers from variability in cellular pigmentation due to physiological acclimation of phytoplankton to environmental conditions (e.g. light and nutrients). Over the last two years, we have developed and tested a method to directly assess phytoplankton carbon (C_{phyto}) using sorting flow-cytometry and elemental analysis. This method is independent of chlorophyll or fluorescence and, thus, provides a measure of phytoplankton biomass that is immune to the confounding effects of photophysiological variability. Two field campaigns to measure phytoplankton carbon were recently completed, one in the Equatorial Pacific and one as part of the Atlantic Meridional Transect. Direct assessments of phytoplankton biomass using this new method will be used to validate and constrain satellite-derived estimates of the standing stocks of microalgae. Preliminary results from the two cruises will be presented.

Introduction

Current methods for estimating phytoplankton carbon in the field rely on proxy measurements, such as chlorophyll (Chl), cell biovolume conversions, or regressions of particulate organic carbon (POC) with Chl. Other means of estimating C_{phyto} include remote-sensing applications that convert optical properties, such as Chl fluorescence or particulate backscattering, into biomass. These values, however, are not well constrained due to the variability of internal pigment concentrations and the lack of field data for validating C_{phyto} retrievals. Physiological variability results in pigment:C_{phyto} ratios that can span more than 1.5 orders of magnitude [1,2]. We developed a more direct method [3] to measure phytoplankton biomass. In contrast to methods that indirectly estimate C_{phyto}, the protocol provided in Graff et al. [3] employs sorting flow cytometry to separate phytoplankton cells from the background particle field; a particulate pool with non-linear relationships over time and space with phytoplankton biomass [4]. The sorted cell sample is then analyzed for its elemental composition through high temperature combustion techniques. This method alleviates effects of phytoplankton photophysiology and avoids filter artifacts which may include the loss of target cells or retention of non-target particulate carbon. The method has been applied in two recent field campaigns in the Equatorial Pacific and on an Atlantic Meridional Transect (AMT) cruise.

Discussion

Lab and field tests of this method showed that the community of cells in sorted samples matched that of the original sample. Most importantly, the C_{phyto} for laboratory cultures using the sort method agreed with published values for the same species using filter based CHN protocols (see Figure). The difference between the laboratory and the field, however, is an unknown background concentration of particles collected on a filter that muddle biomass estimates. Graff et al. [3] also showed that unwanted particles, e.g. bacteria, are efficiently removed from the sorted sample. Thus, the application of this method in the field alleviates the confounding variables of photophysiology and background particulate matter present in other methods.

Efforts during the Equatorial Pacific cruise provided >120 samples and the AMT cruise resulted in >150 samples for direct measurements of C_{phyto}. Continuous in-line optical measurements and discrete sampling for HPLC pigments and POC were also collected. The Equatorial Pacific cruise covered a narrower range of environmental parameters, waters numerically dominated by *Prochlorococcus* and *Synechococcus* (0.05 to 0.38 µg Chl a L^{-1}), while the AMT cruise covered a much larger gradient and included samples dominated by eukaryotic phytoplankton (up to 2.1 µg Chl a L^{-1}).

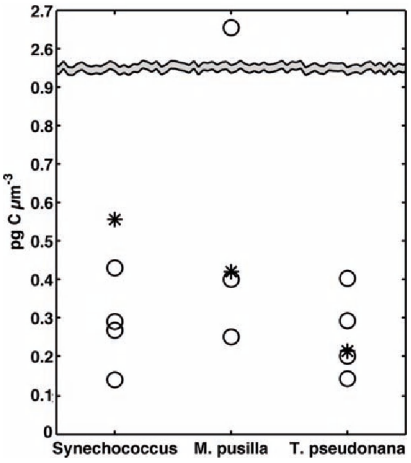

Figure from [3]: Comparison of carbon densities for three species of phytoplankton as determined by the sort method (*) compared to species-specific published values (o).

Conclusions

Results from these two cruises will be the first direct assessments of C_{phyto} that can be used to validate and constrain satellite estimates of phytoplankton biomass. Combined, these data will provide a unique validation of remotely determined C_{phyto} over the range of values that represents the vast majority of the world's oceans. Preliminary data from the two cruises will be presented.

References

[1] Behrenfeld, M., Boss, E., Siegel, D. and Shea, D. (2005). Carbon- based ocean productivity and phytoplankton physiology from space. Global Biogeochem. Cycles 19, GB1006.
[2] Geider, R. J. (1987). Light and temperature dependence of the carbon to chlorophyll a ratio in microalgae and cyanobacteria: implications for physiology and growth of phytoplankton. New Phytol. 106:1-34.
[3] Graff, J., Milligan, A., and Behrenfeld, M. (2012). The measurement of phytoplankton biomass using flow-cytometric sorting and elemental analysis of carbon. Limnol. Oceanogr. Meth. 10: 910-920.
[4] Banse, K. (1977). Determining the carbon-to-chlorophyll ratio of natural phytoplankton. Mar. Biol. 41:199-212.

Useful tools for geostationary ocean color satellite data processing: GDPS

Hee-Jeong Han, Jeong-Mi Ryu, Sun-Ju Lee, Hyun Yang, Young-Je Park, Joo-Hyung Ryu

Korea Institute of Ocean Science and Technology, Korea Ocean Satellite Center, Seoul, 425-600, Korea
Email: han77@kioat.ac

Summary

GOCI Data Processing System (GDPS) which is the standard data processing software for GOCI [1] has been improved with its products algorithms and user interfaces following the requests from ocean color colleagues. This software can support 64 bit windows operating system as well as 32 bit. It generates almost GOCI level 2/3 products including the Rayleigh corrected reflectance which is applied into land application and disaster monitoring. Image display/analysis functions are improved and GDPS batch processing functions are introduced for user convenience. GDPS new version install file is provided on the KOSC (Korea Ocean Satellite Center) website. For more reliable GOCI operation and data accuracy enhancements, the atmospheric correction algorithm and each products algorithms in GDPS will be improved continuously.

Introduction

GOCI is the world-first satellite to monitor the ocean environmental phenomena on geostationary orbits. For the data processing of GOCI, KOSC provides the GDPS as basic tools including atmospheric correction, L2/ L3 products generation, display, analysis like spectral profile, band math, etc since Sep. 2011. Band new version of GDPS is version 1.2 released in Mar. 2013.
New features of GDPS ver. 1.2 are composed to a. 64bit OS supported GDPS b. new products c. batch processing d. user-friendly interface. 64bit GDPS has improved processing speed and stability and has increasing number of opening windows because of extending memory available. This software can generate GOCI Level 2/3 products not only standard products as water leaving radiance, chlorophyll concentration, total suspended sediments, colored dissolved organic matter but also additional products like red-tide index, primary productivity, water current vector, fishing ground index, yellow dust over ocean, vegetation index, daily composite products, etc. It generates also the Rayleigh corrected reflectance which is applied into land application and disaster monitoring, for example, like green algal spread, oil spill movement. GDPS batch processing function can do various simultaneous works like to subset image, to generate L2, to generate L3, to export other format, to extract pixel information matching to *in-situ* measurement points from several GOCI input files. Improvement of the navigation window which treats displayed area size/location is syncing opening windows. The mouse point information window add the draw point button to show the red cross sign(+) for selected point on display window and arrow button(up, down, left, right) to move the draw point one pixel toward each direction. In data analysis field, spectral profile can overlay 20 points spectrum with conversion option to excel file and image file. Water current vector result can be shown on image display, also.

Discussion

GOCI has high temporal resolution to observe short-term ocean phenomena. Syncing and draw point function is very useful to detect the movement of interested something in time-series images. Draw point works as ground control point for all images opened in GDPS.

For GOCI products algorithm validation, it is necessary to generate match up information for comparison between in-situ measurement data and satellite derived data. If user uses the GDPS batch processing function, he can get match up result text files from all GOCI Level 1B files during in-situ observation periods and observation point information. If someone need to process fishery ground index or primary productivity in L3 processing, he should prepare the sea surface temperature (SST) like GHRSST from NASA Ocean Color web and photosynthetic active radiation (PAR) like MODIS PAR using Import L3 Aux of File menu beforehand. All result of match up point can be extracted with surrounding values by 3x3 or 5x5 and statistical information as minimum value, maximum value, average, standard deviation.

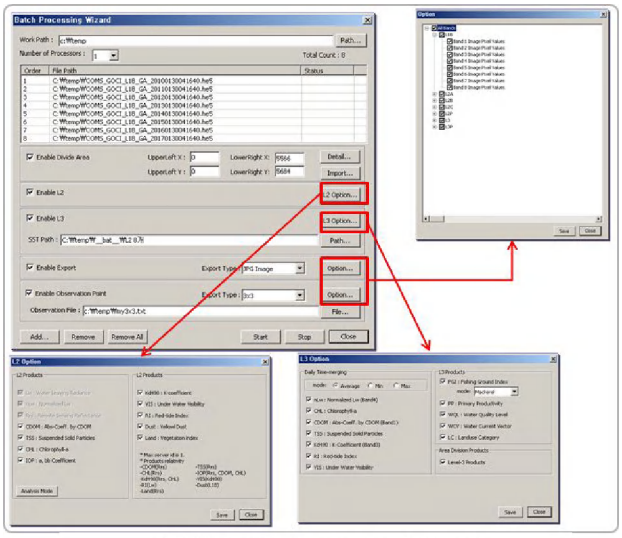

GDPS Batch Processing Wizard

Conclusions

GDPS new version can generates all L2 data. But it still remains many correction and validation work for data accuracy enhancements. This software will be improved consistently in processing algorithms and user interfaces. GDPS will have the functionality to open NOAA SST, MODIS SST, PAR, COMS MI SST to compare with GOCI at once. Also, KOSC will establish GOCI data reprocessing system for composite data generation applied new algorithms.

Reference

[1] Joo-Hyung Ryu, Hee-Jeong Han, Seongick Cho, Young-Je Park, and Yu-Hwan Ahn (2012). Overview of Geostationary Ocean Color Imager(GOCI) and GOCI Data Processing System(GDPS). Ocean Sci. J. 47(3):223-233.

Role of pigments in setting phytoplankton community structure and resulting effects on water leaving radiance

A. E. Hickman*[1], S. Dutkiewicz*[2], O. Jahn[2], M. J. Follows[2]

1. University of Southampton, National Oceanography Centre, Southampton, SO14 3ZH, U.K.
2. Massachusetts Institute of Technology, Earth Atmosphere and Planetary Sciences, Cambridge, MA 02139, USA

* These authors contributed equally to this work

Email: A.Hickman@noc.soton.ac.uk

Summary

We use a three-dimensional numerical model to explore how the species-specific pigment compositions of marine phytoplankton contribute to setting the observed horizontal and vertical phytoplankton distributions in the global ocean. The optical properties of each of several different phytoplankton "functional" types are prescribed from a representative species in culture [1,2]. We perform a series of sensitivity experiments where we impose uniform absorption spectra, uniform scattering spectra, as well as uniform growth parameters for the different phytoplankton. We find that the specific absorption spectra are very important in determining the competiveness of the different phytoplankton types, the ecosystem structure, and the feedback to biogeochemistry. We also explore the difference in model derived surface reflectance between these sensitivity experiments.

Introduction

Phytoplankton are a key part of the marine microbial community; the primary producers of organic carbon in the ocean, they mediate biogeochemical pathways including the export of organic matter to the deep ocean and ocean carbon storage. Their functional diversity has important biogeochemical implications. Motivated by these factors, recent efforts to observe the biogeography of marine phytoplankton from space, and to model these populations and their biogeochemical activity, have placed emphasis on resolving aspects of this diversity. Intracellular pigments are a key functional trait that differs between plankton types. Here we expand on an earlier study [1] to explore how the chromatic adaptation helps set the global biogeography of different species and assess the impact of the ecosystem optical characteristics on surface reflectance.

Model Description and Evaluation

The model resolves a three-stream radiative transfer of photosynthetically available radiation (PAR, 400-700nm), which is dependent on the spectral absorption and scattering properties of water, phytoplankton, detritus and coloured dissolved organic matter (CDOM). The model is described in more depth in companion abstract "Role of optical constituents in setting in water and water leaving optical properties". The optical properties for each phytoplankton type is prescribed from a representative species in culture [1,2]. Other traits such as growth rate and nutrient requirements are derived from relative size of the different species and from the literature. The phytoplankton types include *Prochlorococcus* (high and low light), *Synechococcus*, a generic pico-autotroph, coccolithophores,

diatoms and *diazotrophs*. We evaluate the model against data from the Atlantic Meridional Transect Programme AMT15 cruise. We capture the broad patterns of Chlorophyll-a, the 1% light level and the community structure distribution. In particular we find a well defined vertical distribution of the phytoplankton types. On a global scale the model also compares well to satellite derived products such as Chl-a, PIC, POC as well as the patterns of surface reflectance within the different spectral wavebands.

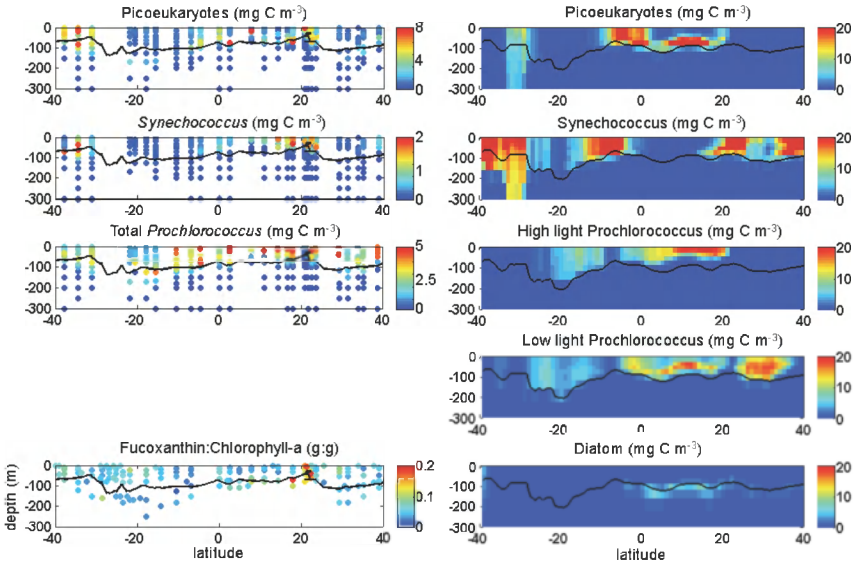

Atlantic Meridional Transect (AMT) community structure: (left) observation from AMT15 transect (Sep 2004) and (right) from MIT ecosystem, biogeochemical, and optical model. Black line indicates 1% light level for photosynthetically available radiation between 400-700. Flow cytometry data on Prochlorococcus, Synechococcus and a mixed group of picoeukaryotes courtesy of Jane Heywood and Mike Zubkov.

Sensitivity Experiments

We perform a series of sensitivity experiments to assess the role of pigments against other traits in setting community structure. We use the model to explore the mechanisms by which species selection takes place, the feedbacks on biogeochemistry and the impact on surface leaving irradiances. We sequentially impose uniform absorption spectra, uniform scattering spectra, and uniform growth parameters for the different phytoplankton types. When absorption spectra are the only trait that differs between functional groups we find that coccolithophores dominate the ecosystem. When all functional groups have the same optical properties, low light *Prochlorococcus* and pico-eukaryotes dominate. Thus, though important, the chromatic adaptation between species has co-evolved (or is energetically determined) along with their other traits. We find that while the scattering characteristics of the different phytoplankton types are of minimal importance for setting the community structure, they do impact the water leaving irradiances.

References

[1] Hickman, A.E., S. Dutkiewicz, R.G. Williams, and M.J. Follows (2010). Modelling the effects of chromatic adaptation on phytoplankton community structure in the oligotrophic ocean. *Mar. Ecol. Prog. Ser.*, 406, 1-17, doi:10.3354/meps08588

[2] Stramski D., A. Bricaud, A. Morel (2001). Modeling inherent optical properties of the ocean based on the detailed composition of the planktonic community. Appl. Optics, 40, 2929-2945

Satellite Phytoplankton Functional Type Algorithm Intercomparison and Validation

T. Hirata[1], R. J.W. Brewin[2], N. Hardman-Mountford[3], L. Crementson[4], R. Barlow[5], A. Bracher[6], T. Kostadinov[7], T. Hirawake[8], C. Mouw[9]

[1] Hokkaido University, Sapporo, 060-0810, Japan

[2] Plymouth Marine Laboratory, Plymouth, PL1-3DH, UK

[3] CSIRO, Floreat, 6010, Australia

[4] CSIRO, Hobart, 3195, Australia

[5] Bayworld Centre for Science and Education, CapeTown,7806, South Africa

[6] Alfred-Wegener Institute for Polar and Marine Research, Bremerhaven, D-28334, Germany

[7] University of Richmond,Richmond, 23173, USA

[8] Hokkaido University, Hakodate, 041-8611, Japan

[9] Michigan Technological University, 49931, USA

Email: tahi@ees.hokudai.ac.jp

Summary

A satellite phytoplankton functional type algorithm intercomparison project was launched in 2011. The project was tasked to: (i) produce a PFT algorithm user-guide; (ii) collect in situ data for use in algorithm testing; (iii) conduct an algorithm intercomparison; and (iv) conduct an algorithm validation. In this presentation, preliminary results of the intercomparison are presented. The algorithm comparison exercise showed that global micro- and picoplankton distributions did not diverge among algorithms, although some differences were found, notably between algorithms using input data obtained from different satellite sensors.

Introduction

A number of new ocean colour algorithms have been developed to derive global phytoplankton community structure for better understandings of biogeochemical cycles as well as food web structure and trophic energy efficiency of marine ecosystems. Improving the algorithms and obtaining a community consensus as to how phytoplankton community is composed and maintained in our planet, are necessary steps. Therefore, a satellite phytoplankton functional type algorithm intercomparison

project was organized in 2011. The project is composed of 4 working groups (WGs): (1) User guide WG, (2) In situ data compilation WG, (3) Intercomparison WG, (4) Validation WG. In this presentation, we show initial results of from the intercomparison and validation WGs.

Algorithm Comparison

Algorithms used in the current comparisons include: Alvain et al., 2012; Brewin et al., 2010; Bricaud et al., 2012; Bracher et al, 2009; Fujiwara et al., 2011; Hirata et al., 2011; Kostadinov et al., 2010; Roy et al., 2012; and Uitz et al., 2006. While Bracher et al. (2009) model is applicable only to the SCHYMACHY instrument, all other algorithms used SeaWiFS L3 9km data as inputs. The comparison was made for the 2003-2007 period. Monthly climatologies and average fields over the period were generated for comparison of global distributions of micro- and picoplankton as well as their seasonality.

Most algorithms showed a consistent distribution of microplankton (Fig.1). The largest differences were observed between the SCHYMACHY-based algorithm and SeaWiFS-based algorithms, partly because the SCHYMACHY-based algorithm estimates diatoms, not exactly same as "microplankton" defined in the other algorithms, and partly because input satellite data are different. In spite of providing a different output ("frequency of dominance" in Alvain et al., 2008, "% Chla" in others), the Alvain et al (2008) approach showed a distribution of relative abundance of pico-sized phytoplankton similar to these derived from other SeaWiFS-based algorithms However, in both microplankton and picoplankton distributions, the similarity among algorithms do not guarantee results are accurate, and a validation using in situ data is required to give a better understanding as to the accuracy of our current estimation of PFT distributions.

Ongoing validation efforts

In situ datasets (collected within the in situ data compilation WG) are to be matched in space and time with satellite observations. The satellite observations will be used by algorithm developers to process and estimate PFTs, meanwhile, in situ data will be also processed to estimate PFTs based on a method agreed by the community. An objective methodology to test the performance of the satellite algorithm is currently being developed. This includes simple statistical tests such as Type II regression, RMSE and bias, with reference to a similar methodology used in the ESA OC-CCI project.

Retrieval of size fractionated chlorophyll *a* concentration: an application of particle size distribution

Y. Arakawa[1], T. Hirawake[2]* and A. Fujiwara[3]

[1] Hokkaido University, Graduate School of Fisheries Sciences, Hakodate, Hokkaido 041-8611, Japan

[2] Hokkaido University, Faculty of Fisheries Sciences, Hakodate, Hokkaido 041-8611, Japan

[3] National Institute of Polar Research, Tachikawa, Tokyo 190-8518, Japan

***Email**: hirawake@salmon.fish.hokudai.ac.jp

Summary

We have developed an algorithm to estimate size fractionated chlorophyll *a* (chl *a*) concentration using inherent optical properties (IOPs). A function of particle size distribution based on the Junge distribution was applied to express the size fractionated chl *a* and a slope of power function was determined for each sample. This method can estimate three phytoplankton size classes (micro, nano and picoplankton) with root mean square errors less than 36 % when the IOPs were calculated from remote sensing reflectance. Advantage of applying the particle size distribution is possibility to represent other size factions. Algorithm developed in this study succeeded to derive a fraction of ultraplankton (< 5 μm) from *in situ* IOPs.

Introduction

Size of phytoplankton cells are strongly related to limitation factors of photosynthesis such as light and nutrients [1]. Meanwhile sinking speed of the cells and number of trophic levels in marine food web are strongly influenced by the size [2, 3]. Therefore, large spatio-temporal scale observation of the phytoplankton size distribution is important to understand the global carbon cycle and marine ecosystems. While the phytoplankton size distribution has been determined frequently by measuring size fractionated chlorophyll *a* (chl *a*) concentration using several kinds of filters with different pore or mesh size, pigments composition measured with the high performance liquid chromatography (HPLC) is utilized to estimate phytoplankton size class, particularly for development of ocean color algorithms recently [e.g. 4]. However, gaps between the two methods are expected and algorithm to derive phytoplankton size from the former method has not been developed. In this study, we provide a new way to estimate size fractionated chl *a* concentration using light absorption coefficient of phytoplankton and spectral slope of backscattering coefficient and evaluate the performance of algorithm.

Discussion

A function of particle size distribution based on the Junge distribution [5] was applied to express the size fractionated chl *a* concentraions of three size classes (pico, nano and microphtyoplankton defined as fraction of <2, 2-10, >10µm, respectively). For each sample, a slope of power function (η) was determined assuming the minimum and maximum size is 0.7 and 200 µm, respectively. The slope η was derived from spectral slope of backscattering coefficient (γ) and a ratio of absorption coefficients of phytoplankton (a_{ph}) at two wavelengths using a multiple linear regression (Fig. 1).

This method can estimate fraction of three phytoplankton size classes with root mean square errors (RMSE) less than 36 % when the IOPs were calculated from remote sensing reflectance. If η is possible to derive without error, RMSE in estimation of the fractions reduces to <10.5%. Although further improvements in derivation of η from IOPs, a fraction of ultraplankton (< 5 µm) was able to be estimated from *in situ* IOPs (RMSE = 18%). This algorithm is appropriate to compare with typically measured size fractionated chl *a in situ* for oceanographic and marine ecological studies.

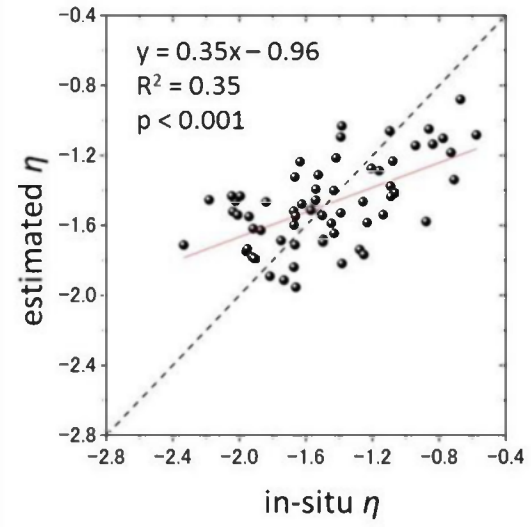

Fig. 1. Estimation of η using IOPs. Comparison between in situ and modeled values.

References

[1] Aiken, J., Pradhan, Y., Barlow, R., Lavender, S., Poulton, A., Holligan, P., and Hardman-Mountford, N. (2009). Phytoplankton pigments and functional types in the Atlantic Ocean: A decadal assessment, 1995-2005. Deep-Sea Res. II, 56: 899-917.

[2] Buesseler, K. O., et al. (2007). Revisiting carbon flux through the ocean's twilight zone. Science, 316: 567– 570.

[3] Lalli, C. M., Parsons, T. R. (1997). Biological Oceanography: An Introduction, Pergamon Press, Oxford.

[4] Hirata, T., Hardman-Mountford, N. J., Brewin, R. J. W., Aiken, J., Barlow, R., Suzuki, K., Isada, T., et al. (2011). Synoptic relationships between surface Chlorophyll-a and diagnostic pigments specific to phytoplankton functional types. Biogeosci., 8: 311-327.

Acknowledgement

This work was supported by JAXA GCOM-C program.

Multi-sensor ocean color in Greenlandic waters

E. Howe[1], J.L. Høyer[1], T.G. Nielsen[2], E.F. Møller[3]

[1]Danish Meteorological Institute, Center for Ocean and Ice, 2100 Copenhagen Oe, Denmark
[2]DTU- AQUA, Section for Oceanography and Climate, 2920 Charlottenlund, Denmark
[3]Aarhus University, Institute for Bioscience, 4000 Roskilde, Denmark
Email: eho@dmi.dk

Summary

This study spans five years and examine the spring phytoplankton dynamics in relation to break up of sea ice in Disko Bay, West Greenland using Chlorophyll *a* concentrations from satellite and in situ measurements. The in situ data were collected at a monitoring station 1 Nmile south of Qeqertarsuaq from February to June for the years 2008-2012. The satellite data used are Meris data from ENVISAT until April 2012 and Modis data from AQUA for the entire period.

Introduction

Disko Bay is located on the western coast of Greenland at the southern border of sea ice. This makes the bay an ideal test site for investigation of climate impacted changes of the ice plankton dynamics. In a period of five years in situ measurements of chlorophyll *a* have been collected during the spring bloom together with sea ice coverage. It is well documented that spring bloom in ice covered seas is impacted by advection and ice conditions.

These data are compared with satellite chlorophyll a values to extrapolate from point measurements off Disko Bay to the bay proper and thereby get an indication on how the blooms is impacted on bay scale by the changes in ice cover.

The satellite data used are from the medium-spectral resolution imaging spectrometer (Meris) onboard the ENVISAT satellite and the Moderate resolution imaging spectroradiometer (Modis) onboard the AQUA satellite. Both data sets have a resolution of approximately 1 km. The data sets cover the period February – June 2008 – 2012 except for Meris which stopped sending data on April 2012. The satellite data are from the operational setup at DMI covering several areas round Greenland.

Discussion

The sea ice cover is changing due to climate impact. This effects the primary production of phytoplankton. In situ measurements capture the spring bloom very precise but only in points. The spring bloom is intense and lasts for only a few weeks between April and June. After this interval the nutrients has been depleted. The satellites are able to see the spring bloom over a larger area and keep track of the spatial and temporal distribution regardless of the timing of the spring bloom, see Figure 1.

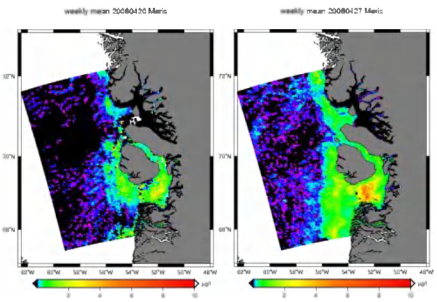

Figure 1Weekly means of satellite data from end April 2008 showing the spatial distribution of primary production

Ocean color data product uncertainty, consistency, and continuity: Evaluation with a new algorithm concept

Hu, Chuanmin[1]; Lee, Zhongping[2]; Franz, Bryan[3], Feng, Lian[4,1];
[1]University of South Florida 140 Seventh Avenue, S., St. Petersburg, FL, 33701, United States, huc@usf.edu;
[2]University of Massachusetts at Boston, Boston, Massachusetts, 02125, United States;
[3]NASA/GSFC, Greenbelt, MD, 20771, United States;
[4]State Key Laboratory of Information Engineering in Surveying, Mapping and Remote Sensing, Wuhan University, Wuhan 430079, China.

ABSTRACT

Studies of long-term ocean changes in response to climate variability call for the most accurate and consistent data products across multiple ocean color missions, and a thorough understanding of the uncertainties is the first step towards a seamless, multi-sensor data record. For a well-calibrated sensor, data product uncertainties result primarily from two sources: the sensor's signal-to-noise ratio (SNR) and the algorithms to derive the products. Using statistics and a recently developed chlorophyll-a (Chl) algorithm (the ocean color index (OCI) algorithm) to determine the highest-quality data, we quantified SNRs, uncertainties in the remote sensing reflectance (R_{rs}) products, noises in the band-ratio OCx Chl products and OCI Chl products from several ocean color instruments including SeaWiFS, MODIS/Aqua, MERIS, and VIIRS. MODISA ocean bands show 2-4 times higher SNRs than SeaWiFS and comparable SNRs to MERIS-RR (reduced resolution, 1.2-km) data. Correspondingly, MODISA Chl products show the least uncertainties when evaluated using a spatial homogeneity test. While MERIS and VIIRS data are still being analyzed, both SeaWiFS and MODISA showed R_{rs} uncertainties within mission specifications, with higher uncertainties in SeaWiFS R_{rs} data possibly due to its lower SNRs. When comparing the global and regionally monthly means for deep oceans, the sensors often showed significant differences (> 5-10%) in the OCx Chl products. These differences may overwhelm real ocean changes and may also bring questions to the fidelity of the global data when only one sensor is operational in orbit. The cross-sensor differences in the product uncertainties are believed to result primarily from different SNRs and imperfect atmospheric corrections. In contrast, the OCI Chl algorithm was designed to be much more tolerant to noises and atmospheric correction errors for clear waters (Chl $\leq$ 0.25 mg m^{-3}), which indeed led to a much more consistent multi-sensor Chl data record from all sensors evaluated (SeaWiFS, MODISA, MODIST, MERIS, VIIRS) for the deep ocean, with most of the cross-sensor differences reduced by more than half. While some of these uncertainties may be removed using empirical approaches (Fig. 1), the new OCI algorithm provides a solution to bring all sensors together to form a multi-sensor Chl data record (Fig. 2). As we are now entering a transition period to use VIIRS and to design several ocean color continuity missions, it may be time to change the 40-year band-ratio paradigm to a band-subtraction concept or other mechanistic algorithms in order to establish more consistent multi-sensor ocean color data records.

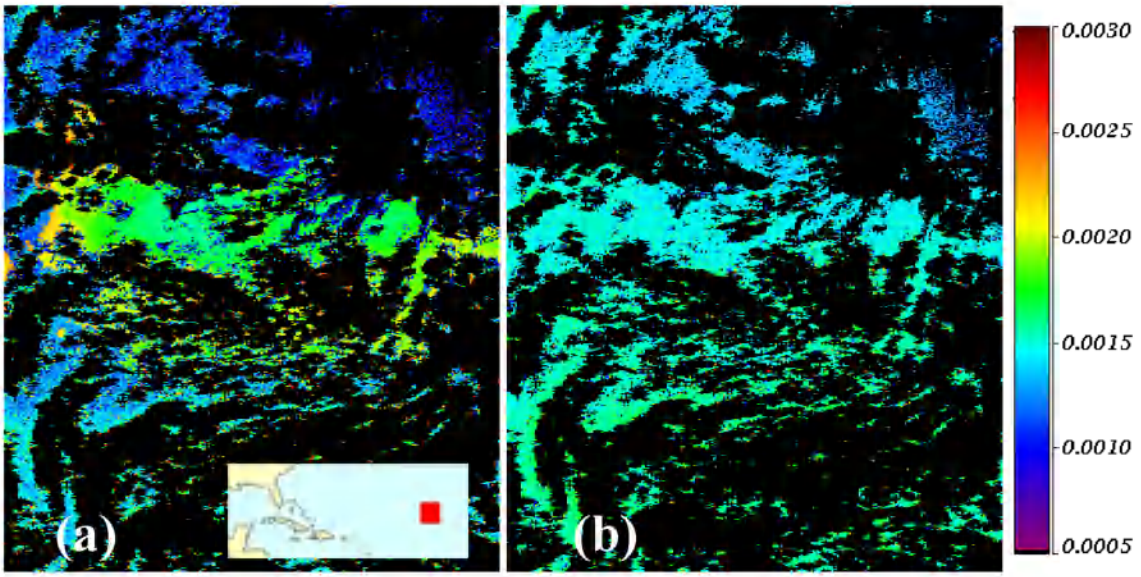

Fig. 1. SeaWiFS $R_{rs}(555)$ (sr^{-1}) in the North Atlantic Gyre (~1500 km x 1500 km centered at 23°N 47°W) on 27 December 2006 from the default SeaDAS processing (a) and after an empirical correction (b). In this oligotrophic gyre $R_{rs}(555)$ is expected to be homogeneous.

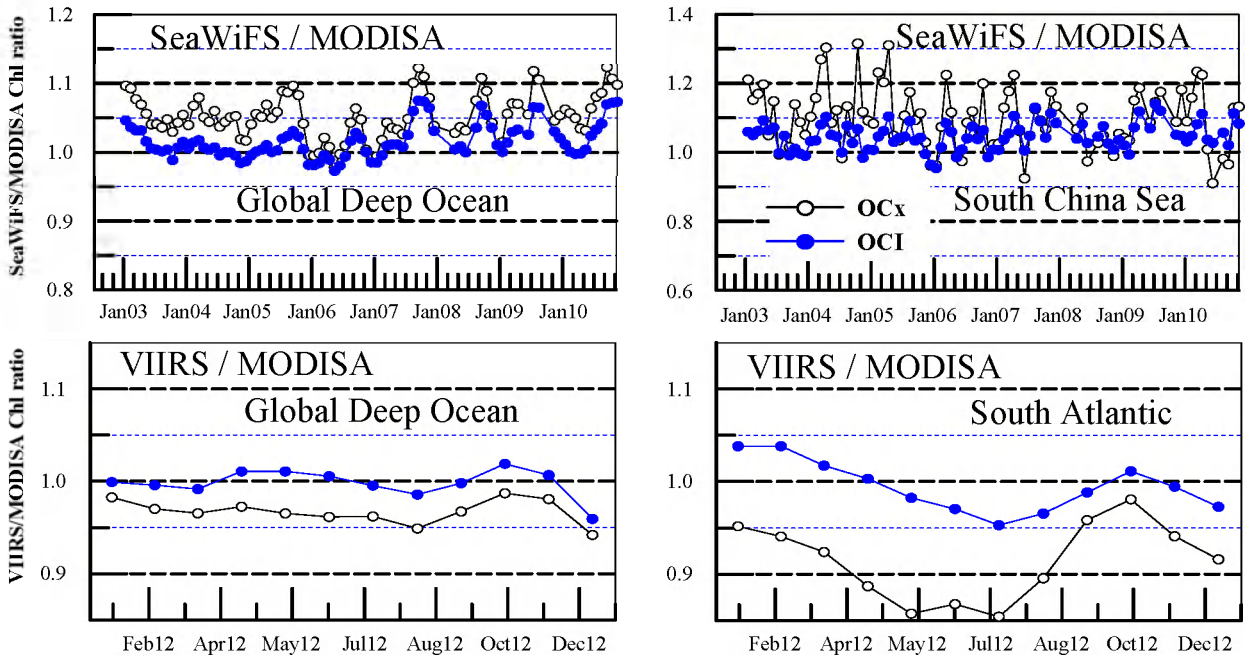

Fig. 2. Chl ratios between different satellite sensors using two algorithms: the default OCx band-ratio algorithm and the new OCI algorithm. The latter is shown to improve cross-sensor consistency significantly.

Particle Retention in the Moroccan Coastal Ocean

Dale A Kiefer[1] and Ian S F Jones[2]

[1] University of Southern California
[2] University of Sydney
Email: ian.s.f.jones@hotmail.com

Summary

Superpositioning of surface current vectors produced by a numerical model and the monthly chlorophyll concentration in the Atlantic ocean near Morocco have revealed a surface eddy trapped by the Canary Islands adjacent to the coast. Near the eddy chlorophyll concentrations are higher 100 km off shore that at more distant locations. There are implications for larvae retention of the northern sardine stocks.

Text

Pelagic fisheries are an important element in the Moroccan economy and the fluctuations in the magnitude and location of the stocks present difficulties for the management of the resource. Schooling small pelagic fish in an upwelling region such as the Moroccan coastal region are able to spawn in the Canary current and have the juveniles develop to adults in the same geographic region. The eggs provided by small pelagic fish float passively in the water column and take order 30 days to develop swimming skills able to counter in the prevailing current.

We used satellite ocean colour data [1] and 0.1 degree resolution hydrodynamic ocean model outputs fused by EASy [2] software to examine the Moroccan coastal ocean from the Gibraltar Straits to the Canary Islands. Monthly averages of the surface current from the hydrodynamic model ECCO2 was used. During the period 1997 to2007 a topographically trapped counter clockwise eddy north of the Canary Islands persistently provided recirculation of chlorophyll rich water. The time for a passive scalar to make one circuit of the eddy is order 40 days.

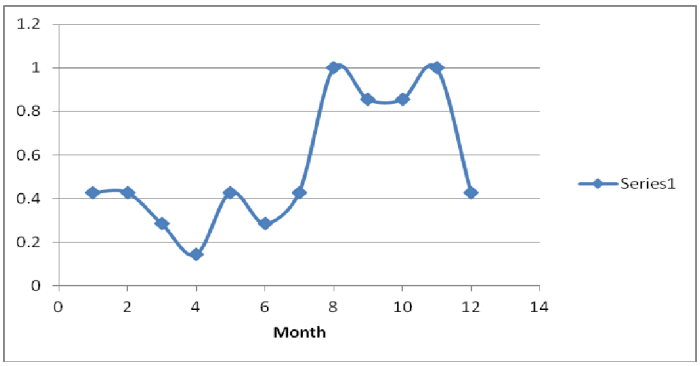

The probability of finding an eddy at 30 degrees N for the period 1997 to 2007.

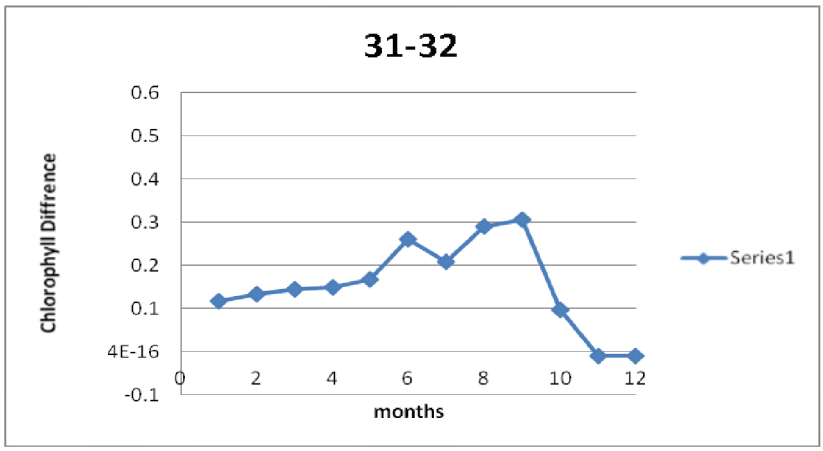

The difference in chlorophyll concentration mg/m^3 100 km from the coast at latitude 31 degrees N and 32 degrees N during the period 1997 to 2007.

Kifani [3] identified two reproduction areas on this portion of the Moroccan Coast and one is near latitude 32 degrees N where in autumn there is a very high probability of finding the counter clockwise rotating eddy. Chlorophyll levels at 100 km from the coast are higher near the eddy than further to the north providing potential food for larvae that remain within this eddy. The eddy probability of occurrence and the larger chlorophyll concentration is shown as a function of the month of observation.

Key words:

Fisheries, Morocco, recruitment, small pelagic

References

[1] Jones, I S F, Y. Sugimori & R. W. Stewart (1993) *Satellite remote sensing of the oceanic environment*. Seibutsu Kenkyusha, Tokyo, pp 528, 1993.

[2] Tsontos, V.M.; Kiefer, D.A. (2000). Development of a dynamic biogeographic information system for the Gulf of Maine *Oceanography 13(3)*: 25-30.

[3] Kifani, S (1998) Climate Dependent Fluctuations of the Moroccan Sardine and their Impact on Fisheries.

Optimized multi-satellite merger to create time series of inherent optical properties in the California Current

M. Kahru[1], Z. Lee[2], R.M. Kudela[3], M. Manzano-Sarabia[4]
B.G. Mitchell[1]

[1]University of California San Diego, Scripps Institution of Oceanography, La Jolla, CA 92093, USA
[2]University of Massachusetts, Dept. of Environmental, Earth and Ocean Sciences, Boston, USA
[3]University of California Santa Cruz, Ocean Sciences Department, Santa Cruz, CA 95064, USA
[4]Universidad Autónoma de Sinaloa, Mazatlán, Sinaloa, México

Summary

We have developed empirically optimized versions of the QAA semianalytic algorithm for 4 ocean color sensors (OCTS, SeaWiFS, MODIS-Aqua and MERIS) by applying a complex optimization process that minimizes the differences in estimated inherent optical properties (IOPs) between match-ups of *in situ* and satellite data and also between the estimated IOPs of the overlapping satellite sensors (SeaWiFS, MODIS-Aqua, MERIS). We then apply the algorithms to standard satellite remote sensing reflectance (*Rrs*) estimates and create merged multi-sensor time series of the near-surface optical characteristics in the California Current region for a time period of over 16 years (November-1996 to December-2012).

Introduction and Results

Satellite observations of ocean color have become the most important method of monitoring global distributions of phytoplankton and ocean productivity, and validating various models. However, the primary output product, the concentration of chlorophyll-a (*Chla*), when estimated with the standard band ratio algorithms primarily represents a change in the total absorption coefficient at the blue wavelength (~440 nm) and is often biased compared to *in situ Chla*. Here we estimate the following set of IOPs using a tuned version of the QAA semianalytic algorithm [1]: the total absorption coefficient at 490 nm (*a490*), phytoplankton absorption coefficient at 440 nm (*aph440*), absorption by dissolved and detrital organic matter at 440 nm (*adg440*) and particle backscattering coefficient at 490 nm (*bbp490*). By tuning the coefficients of the QAA models we were able to remove most of the bias when compared to the *in situ* measurements and between individual sensors (Fig. 1). However, due to the limited number of *in situ* match-ups and their uneven distribution as well as the large errors in the satellite-derived *Rrs*, the uncertainty in the retrieved IOPs is still significant and the differences between the IOPs derived from different sensors cannot be completely eliminated. The merged time series show the dominant annual cycle (Fig. 2) but also significant variability at interannual time scales. The ratio of *adg440* to *aph440* is around 1 in the transition zone of the California Current (100-300 km from coast), is >1 in the coastal zone (0-100 km from coast) and generally <1 offshore (>300

km from coast). *adg440* decreases towards south and towards offshore.

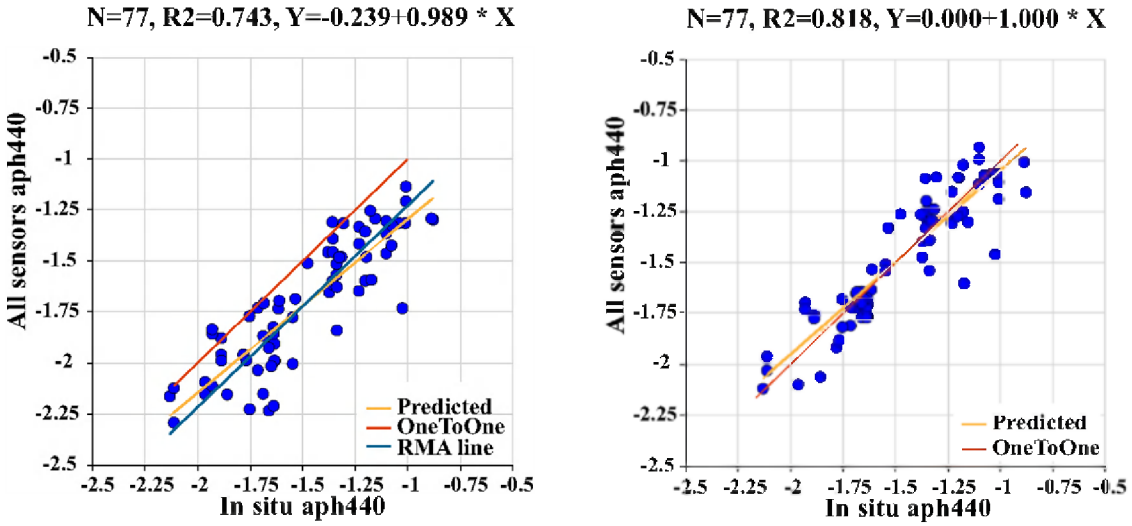

Fig. 1. Combined (OCTS, SeaWiFS, MODISA, MERIS) match-ups (blue dots) of *aph440* between satellite estimates and *in situ* using the standard QAA model (left) and the tuned QAA (right).

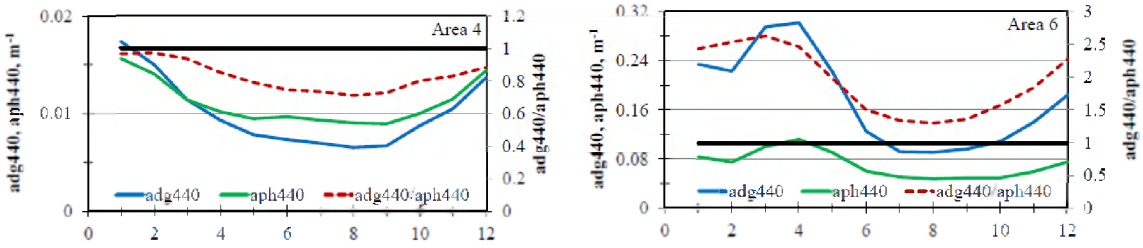

Fig. 2. Mean annual cycle of the merged multi-sensor *adg440*, *aph440* (left axis) and the ratio of *adg440* to *aph440* (right axis) for offshore (left panel, 300-1000 km from coast) and coastal (right panel, 0-100 km from coast) of Southern California. The horizontal black line shows where *adg440/ aph440* = 1.

Conclusions

We created a consistent multi-sensor time series of the surface IOPs in California Current region. The merged 16-year time series (1996-2012) show an increasing trend until 2012 in the proxies of phytoplankton biomass in the California Current which is consistent with some observations [2] and model predictions of either increased upwelling or increased nutrient content in the upwelled waters. Also, a trend of decreasing phytoplankton biomass in the oligotrophic subtropical Pacific was shown. However, uncertainties in our estimates of IOPs are still large and require further work.

References

[1] Lee, Z. P., et al. (2002). Deriving inherent optical properties from water color: A multi-band quasi-analytical algorithm for optically deep waters. Applied Optics, 41, 5755-5772.

[2] Kahru, M., Kudela, R., Manzano-Sarabia, M., Mitchell, B.G. (2009). Trends in primary production in the California Current detected with satellite data. J. Geophys. Res., 114, C02004.

MODIS/AQUA Ocean Color Validation in the Amundsen Polynya, Southern Ocean

Hyun-cheol Kim

Division of Polar Climate Research
Korea Polar Research Institute
Email: kimhc@kopri.re.kr

Summary

Two Years (January of 2011 and 2012) Amundsen Polynya survey for ocean color validation were conducted as part of the Amundsen expedition of KOPRI by Icebreaker ARAON because of the polynya have shown unusually high amount of satellite retrieved chlorophyll-a. On both expedition periods *in-situ* chlorophyll-a and suspended sediments were measured and at the same time absorptions by an organic and inorganic matters and a colored dissolved organic matters were measured for understand of the Inherent optical properties on Amundsen Polynya. In-water profiler (HPRO II/Satlantic Inc.) and above water reflectance acquisition system (HSAS/Satlantic Inc.) were operated for understand of the apparent optical properties as well. The results showed that In-situ chlorophyll-a showed quite different amounts on the both years, even if the MODIS showed similar pattern with amount showed on the both years. The major reason of this difference was due to the suspended sediments amount between the both years. The suspended sediments might be linked with sea ice melting, but the source of suspended sediments are still not know well, because continuous time based survey were not performed much on the Amundsen Polynya. The estimation of primary production on the Amundsen Polynya should be considered after validation of ocean color comparing with in-situ amount. The validation also should be conducted, as possible as, during several years of field survey on the same region.

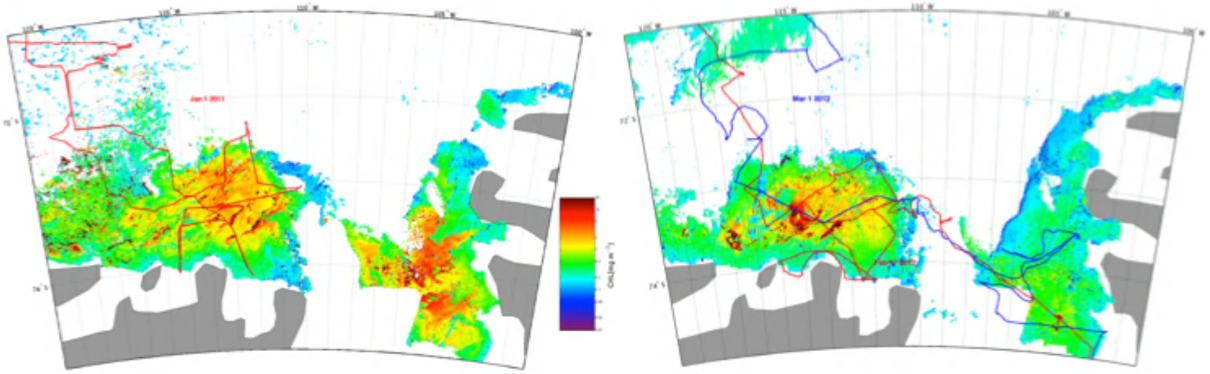

Figure 1. Daily 1km MODIS mosaic on the both expeditions (January of 2011: left, and 2012: right) and the lines on the images indicate the each expedition track by icebreaker ARAON.

Ocean Colour in Australia's Integrated Marine Observing System

E A King[1], V E Brando[2], LA Clementson[1], J L Lovell[1], H Franklin[3], J M Anstee[2], L Besnard[4]
[1]*CSIRO Marine & Atmospheric Research, Hobart, 7001, Australia.*
[2] *CSIRO Land and Water, Canberra, 2601, Australia*
[3] *CSIRO Land and Water, Brisbane, 4001, Australia*
[4] *IMOS, Hobart, 7001, Australia.*
Email Edward.King@csiro.au

Summary

Satellite ocean colour data play an important part in Australia's flagship program to provide infrastructure to support marine research, the Integrated Marine Observing System (IMOS). The program includes multiple activities aimed at improving the availability and quality of ocean colour data in the Australasian region. The work involves the development of a bio-optical database of Australian waters, the deployment of two autonomous radiometers on research vessels to continually acquire underway spectra of above water-leaving radiance, sky radiance and downwelling irradiance, and also support for the operation of Lucinda Jetty Coastal Observatory. In addition, an ocean colour production system, based on SeaDAS software, has been developed using national eResearch infrastructure and used to process the Australian 1km SeaWIFS archive and MODIS Aqua archives to standard products. This system, together with the growing collection of in-situ data provides the capability to support characterization of globally sourced ocean colour products in the Australian bluewater ocean, and the development of regionally tuned products in optically complex waters.

Introduction

IMOS is part of a major government investment since 2007 intended to provide science-driven research infrastructure. It is a collaborative national system aimed at sustained observing at ocean-basin and regional scales, and including physical, chemical and biological variables. It includes coastal radar installations, gliders, coastal and deep-water moorings, an AUV, animal tagging, support for Australia's contribution to ARGO, and a remote sensing component. All data collected with IMOS funding is made freely available via a data management facility and portal.

The remote sensing facility within IMOS supports production and validation of SST and ocean colour for the Australian region, satellite altimetry/calval activity, the operation of parts of a direct broadcast reception network, and a capability for the storage and management of large remote sensing data sets. The ocean colour investment is further comprised of a set of activities designed to pursue a strategy of providing quality characterized products for Case 1 waters around Australia, and progressively building the capacity to support customized regional product development in Case 2 waters.

Bio-Optical Database of Australian Waters

The development of a bio-optical database of Australian waters, bringing together both historical and contemporary in-situ measurements, is a critical step in improving the capability to characterize the quality of ocean colour products around Australia, and to develop new regional products. Data collected by several agencies and institutions since late 1990s is being organized into a consistent framework for this purpose [1]. In addition to local research use, where the observations conform to the requirements of NASA and ESA, they are being provided to SEABASS and Mermaid databases to help improve global algorithm development.

Underway Radiometers on Ships

Radiometers are being deployed on research vessels to autonomously acquire underway spectra of above water-leaving radiance, sky radiance and downwelling irradiance, adding to the in-situ data pool [2]. These enable testing of atmospheric correction algorithms and, whenever bio-optical sampling is performed on the vessels, provide a full characterization of the light field. The first instrument has been operating successfully since late 2011.

Lucinda Jetty Coastal observatory

The 5km long Lucinda Jetty is located in NE Australia and protrudes into the lagoon of the Great Barrier Reef [3]. The coastal observatory is equipped with instrumentation to regularly acquire above water radiometry, in-water optics and information on weather, sky and sea conditions. The observatory is intended as a long term monitoring site, a platform for instrument cross calibration, and as a source of match-up data for cal/val. In 2011, the instrumentation was removed from the site the day prior to its destruction by cyclone Yasi. The observatory is expected to return to operation in the first half of 2013.

National Ocean Colour Production Facility

IMOS supports a national archive of MODIS and SeaWIFS Level-0 data based at the National Computational Infrastructure eResearch facility. This system permits ocean colour data production to take place locally in Australia, enabling reprocessing as calibration evolves, and full time and space resolution to be retained in products. Users can obtain data easily without having to download it from overseas or process it themselves. Furthermore, a match up database for cal/val work is readily available, and the storage and management of the entire data set and processing chain in one location facilitates development and testing of regionally tuned products.

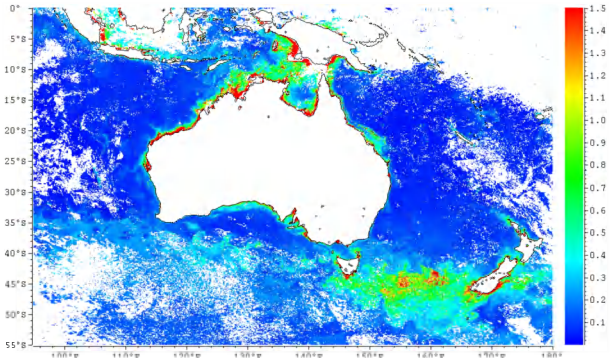

7 day mosaic of MODIS Chl from the IMOS facility

Conclusion

The IMOS investment in ocean colour is enabling a national approach, leading to efficiencies in data management and processing supporting research in the Indian and Southern Oceans. Multiple research projects are now making use of this capability which is unique within Australia. By improving support for in-situ data acquisition and management, IMOS is simplifying the task of undertaking further research and development in ocean colour in the Australian region.

Acknowledgement

IMOS is supported by the Australian Government through the National Collaborative Research Infrastructure Strategy and the Super Science Initiative.

References

[1] Clementson, L.A. *et.al.* (2012), Australia's Integrated Marine Observing System delivering bio-optical datasets to the global community, Ocean Optics XXI, Glasgow.

[2] Brando, V.E. *et.al.* (2013), Autonomous Ship Based Ocean Color Observations on Australian Research Vessels, this symposium

[3] http://imos.org.au/lico.html

Carbon-based Phytoplankton Functional Types and Productivity via Remote Retrievals of the Particle Size Distribution

Tihomir S. Kostadinov[1], Svetlana Milutinović[2], Irina Marinov[2]

1. Department of Geography and the Environment, Univ. of Richmond, Richmond, VA, USA
2. Department of Earth and Environmental Science, Univ. of Pennsylvania, Philadelphia, PA, USA

E-mail: tkostadi@richmond.edu

Assessment of the ocean's role in biogeochemical cycling and climate formation requires characterization of oceanic ecosystems' structure and function. This can be accomplished by understanding the spatio-temporal variability of phytoplankton functional types (PFTs) and its physical drivers. Satellite remote sensing of ocean color is the best available tool for sustained continuous oceanic ecosystem observation. Various algorithms for the retrievals of PFTs have been developed in recent years, using different theoretical bases and PFT definitions [1]. The algorithm of Kostadinov et al. [2,3] defines the PFTs in terms of percent contribution to biovolume of three size-based PFT groups: picophytoplankton (here, cell diameter between 0.2 and 2 μm), nanophytoplankton (2–20 μm) and microphytoplankton (20–50 μm). This method is based upon retrievals of the parameters of an assumed power-law particle size distribution (PSD), using existing spectral backscattering retrievals [4] and a theoretically derived look-up table.

Phytoplankton carbon biomass (rather than biovolume) is more closely related to biogeochemical cycling and climate and it is needed for deriving carbon-based phytoplankton productivity from ocean color [5]. Here, we develop a procedure to recast the PFTs in terms of relative contribution to carbon biomass, rather than volume. We start with the same PSD retrievals as the volume-based approach (here, derived from monthly SeaWiFS r2010.0 imagery), but convert cell volumes in each size class to carbon biomass before PFT calculation. We use the allometric relationships of Menden-Deuer and Lessard [6], as in the initial effort by [7]. Fig. 1 illustrates the SeaWiFS mission climatology for picoplankton (A) and microplankton (B). As expected, picoplankton dominate oligotrophic areas and microplankton are abundant only in eutrophic areas.

Partitioned carbon biomass estimates were also uses as input to the vertically-integrated version of the carbon-based productivity algorithm (CbPM) [5] in order to estimate PFT-specific NPP. PFT-specific maximum growth rates were based on [8], and PFT-specific chlorophyll concentrations were based on SeaWiFS chlorophyll (r2010.0) and the size fractions of Uitz et al. [9]. Results for the August 2007 image are presented in Fig. 1C for picoplankton and Fig. 1D for microplankton.

At this stage the presented products are preliminary and retrieved variables may not be necessarily geophysically accurate. While this especially applies to the absolute values of carbon biomass and productivity, carbon-based PFTs (Fig. 1A-B) are defined by ratios of biomass. Our goal is to assess the feasibility of using ocean color-based retrievals of the particle size distribution parameters to estimate size-partitioned carbon-based biomass and productivity. Next steps will focus on further methodology

improvements, comparison to existing algorithms [1, 10, see also 7], and validation of these novel satellite ocean color products.

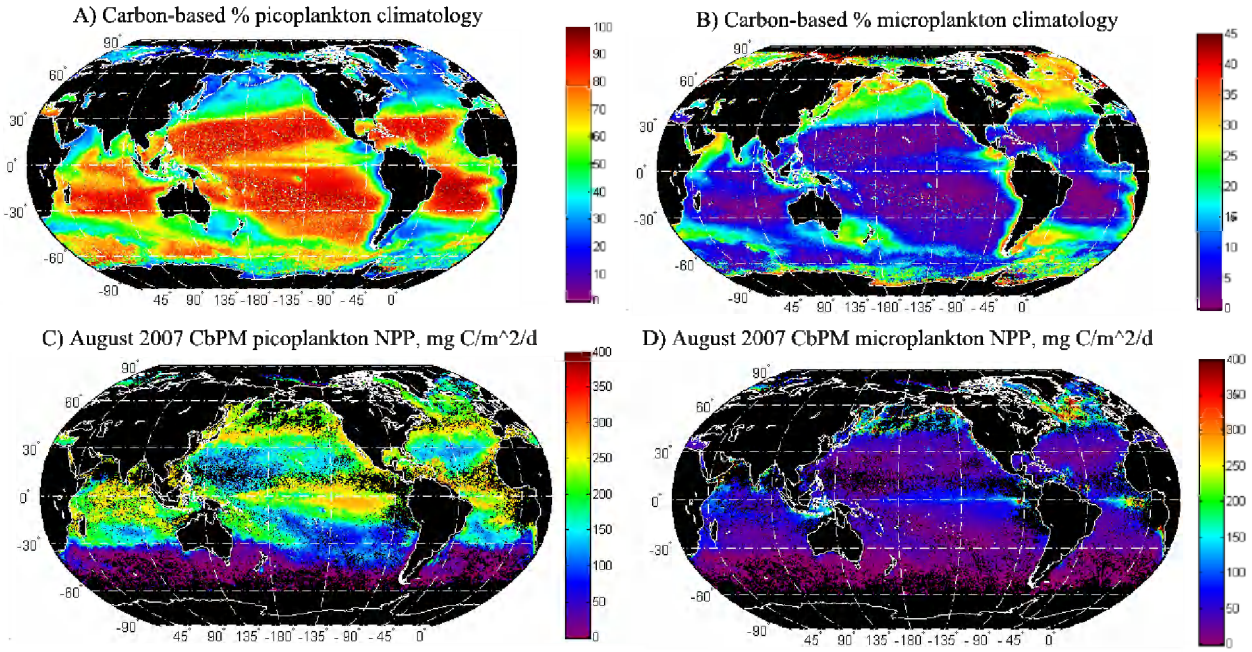

Figure 1. *SeaWiFS mission climatology (1997-2010) of percent allometric carbon biomass due to (A) picoplankton (0.2 -2 μm) and (B) microplankton (20-50 μm). Note the different colorbar scales. August 2007 CbPM net primary productivity due to (A) picoplankton (0.2-2 μm), and (B) microplankton (20-50 μm), using allometric PSD-based carbon estimates.*

References

[1] Hirata, T., et al. (2012), Comparing satellite-based phytoplankton classification methods, Eos Trans. AGU, 93(6).

[2] Kostadinov, T. S., D. A. Siegel, and S. Maritorena (2009), Retrieval of the particle size distribution from satellite ocean color observations, *Journal of Geophysical Research-Oceans*, *114*, 22.

[3] Kostadinov, T. S., D. A. Siegel, and S. Maritorena (2010), Global variability of phytoplankton functional types from space: assessment via the particle size distribution, *Biogeosciences*, *7*(10), 3239-3257.

[4] Loisel, H., Nicolas, J.-M., Sciandra, A., Stramski, D., and Poteau, A. (2006), Spectral dependency of optical backscattering by marine particles from satellite remote sensing of the global ocean, J. Geophys. Res., 111, C09024, doi:10.1029/2005JC003367.

[5] Behrenfeld, M., E. Boss, D. Siegel, and D. Shea (2005), Carbon-based ocean productivity and phytoplankton physiology from space, *Global Biogeochemical Cycles*, *19*(1), GB1006.

[6] Menden-Deuer, S., and E. Lessard (2000), Carbon to volume relationships for dinoflagellates, diatoms, and other protist plankton, *Limnology and Oceanography*, *45*, 569–579.

[7] Kostadinov, T. S. (2009), Satellite Retrieval of Phytoplankton Functional Types and Carbon via the Particle Size Distribution, Ph.D. thesis, 217 pp, University of California, Santa Barbara, CA, USA.

[8] Ward, B. A., S. Dutkiewicz, O. Jahn, and M. J. Follows (2012), A size-structured food-web model for the global ocean, Limnology and Oceanography, 57(6), 1877-1891.

[9] Uitz, J., H. Claustre, A. Morel, and S. B. Hooker (2006), Vertical distribution of phytoplankton communities in open ocean: An assessment based on surface chlorophyll, Journal of Geophysical Research-Oceans, 111(C8).

[10] Uitz, J., H. Claustre, B. Gentili, and D. Stramski (2010), Phytoplankton class-specific primary production in the world's oceans: Seasonal and interannual variability from satellite observations, Global Biogeochem. Cycles, 24, GB3016, doi:10.1029/2009GB003680.

ROBUST $K_d(490)$ AND SECCHI DEPTH ALGORITHMS FOR REMOTE SENSING OF OPTICALLY COMPLEX WATERS DOMINATED BY CDOM

Alikas, Krista[1]; Kratzer, Susanne[2,3]; Reinart, Anu[1]
[1]Tartu Observatory, Tartumaa, Toravere, 61602, Estonia; e-mail: alikas@ut.ee
[2]Stockholm University, Stockholm, Stockholm, SE-106 91, Sweden
[3]Brockmann Consult GmbH, Max-Planck-Str. 2, 21502 Geesthacht, Germany

ABSTRACT

We developed and compared different empirical and semi-analytical algorithms for optically complex waters to retrieve the diffuse attenuation coefficient of downwelling irradiance, $K_d(490)$, and tested them against an independent data set, in order to ultimately suggest a robust algorithm that is valid for optically complex water bodies with high concentrations of CDOM.

In the first approach, developed by Austin and Petzold (1981), revisited by Mueller (2000), $K_d(490)$ was estimated from the empirical relation between $K_d(490)$ and the ratio of remote-sensing reflectance at two wavelengths within the visible spectrum. Due to MERIS characteristics, several bands in the longer wavelengths (560, 620, 660, 710 nm) were available to retrieve better reference conditions over CDOM dominated coastal waters. Various sets of band ratios were tested to achieve the best estimate for *Kd*(490) where reflectance data was retrieved either using MERIS standard algorithms (ODESA) or an alternative processor for atmospheric correction and water quality parameters (FUB WeW). In the second approach, $K_d(490)$ was expressed as a function of inherent optical properties (IOP) after the algorithms by Lee et al. (2005b) and Kirk (1994). The IOPs needed as an input for these algorithms were retrieved from MERIS level 2 products (algal_2, total_susp and yellow_subs) or taken from the literature.

We compared the MERIS derived $K_d(490)$ values by various algorithms with values measured in optically complex coastal waters in the Baltic Sea which showed very good estimates for both methods. The results indicate that for empirical algorithm, the RMSE (%) decrease and the coefficients of determination (R2) increase when using the longer wavelengths in the visible spectrum as reference band. The best estimates were retrieved by using the reflectance ratio of MERIS bands *Rrs*(490)/*Rrs*(710), which provides a promising approach (RMSE 14%, R2=0.98, N=14) for estimating $K_d(490)$over a wide range of values (0.2 - 2.5m^{-1}). Figure 1 shows $K_d(490)$ for the Baltic Sea on 22 May 2002 using the best algorithm.

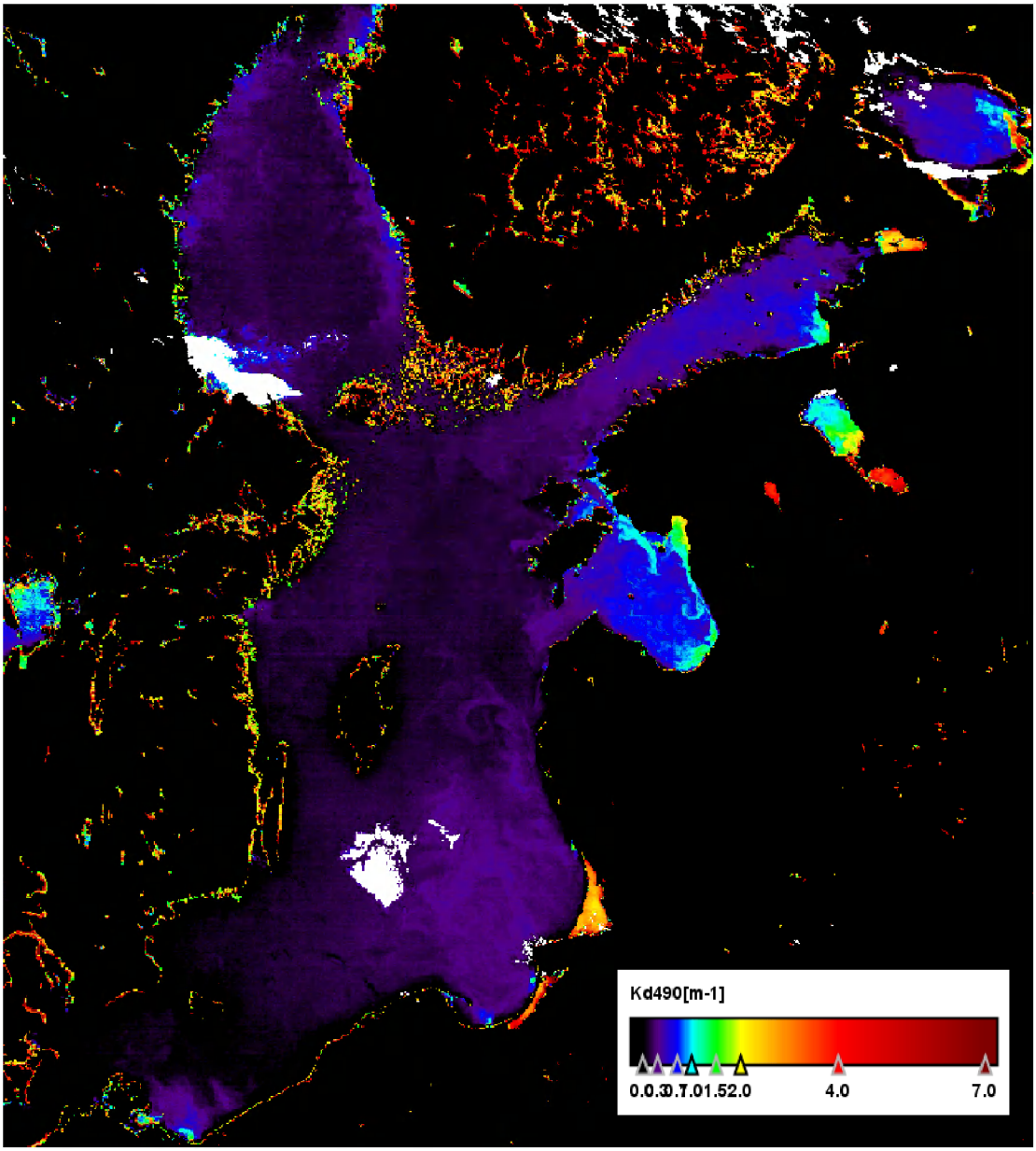

Figure 1 $K_d(490)$ image of the Baltic Sea on 22 May 2002 using MERIS bands *Rrs*(490)/*Rrs*(710).

Data Assimilation and Numerical Simulation of Storm Surges Along Bay of Bengal and Bangladesh Coast

***Mohan K. Das[1, 2] and Sujit K. Debsarma[1]**

[1]SAARC Met. Research Centre, Theoretical Division, Dhaka, 1207, Bangladesh
[2]Jahangirnagar University, Department of Physics, Dhaka, 1342, Bangladesh
E-mail: mohan28feb@yahoo.com, mkdas@saarc-smrc.org

Summary

Bangladesh is situated at the northern tip of the funneling Bay of Bengal (BoB). The long continental shelf, shallow bathymetry, and complex coastal geometry with many kinks and islands with the overall funneling shape of the Bay of Bengal are well-known features of the highest storm surge of the longest duration. IIT Kharagpur Model (2002) for storm surge is used for numerical simulation of storm surges near Orissa, West Bengal, and Bangladesh coasts. High resolution (Δx = 3.7 km, Δy = 3.5 km, Δt = 60 sec) IIT Model has been used for the simulation. Three or six hourly positional data of several severe storms that hit Bangladesh and West Bengal coasts have been used for making gradual changes in the storm surge scenario. A Generic Mapping Tool (GMT) has been employed with a view to imaging surges. 3D view of the peak surges during landfall has also been made by incorporating geo-referenced peak surge data into WinSurfer. Doppler Weather Radar (DWR) Data are used to study the BoB cyclone through 3-dimensional variational (3DVAR) data assimilation technique within the WRF-ARW modeling system. The mean track error at the time of landfall of the cyclone is 66.6 km. The distribution and intensity of rainfall are well simulated by the model as well and were comparable with the TRMM estimates. Using this model, numerical experiments are performed to simulate the storm surge heights associated with past severe cyclonic storms which struck the coastal regions of Bangladesh. The model results are in agreement with the limited available surge estimates and observations.

Introduction

Cyclone Aila-2009 was of moderate intensity it ravaged southwestern part of Bangladesh badly. Alongside it ravaged West Bengal of India, eastern Nepal and southern Bhutan. Due torrential rain these four countries had flooding effects. Advanced Research WRF (ARW) Model with horizontal resolution of 9 km x 9 km, 50s time step and 27 vertical levels has been used to simulate the nature of cyclone Aila and its associated wind, rainfall etc.

Hydro-dynamical/ Numerical Storm Surge Model with Air Bubble Entrainment is a vertically integrated semi-implicit forward with time, centred with space numerical/ Hydro-dynamical storm surge model based on Indian Institute of Technology (IIT) Model [1]. Entrainment of air-bubble is made in the Model. The required meteorological and hydrological inputs are (1) three hourly storm centres of Cyclone Aila, (2) three hourly radii of maximum winds, (3) three hourly pressure drop and (4) topographic and bathymetric data (USGS ETOPO2). Domain of the Storm surge model is model is 18 - 23°N, 83.5 - 94.5°E with horizontal resolution of 3.7 km x 3.5

km, and time step of 60s. Generic Mapping Tool (GMT) is used for visualization of surge.

Discussion

The strong low level heating and a cooperative positive vorticity in the wind field acts as a triggering mechanism for the initial rise and growth of the thermal energy [2]. Vorticity field moved more or less northwards with the movement of the cyclone and is distorted when the cyclone approached the hilly areas of Nepal, Bhutan and northeast India.

3-D and 2-D storm surge scenarios of Aila during landfall are shown in Fig. (a) and Fig. (b) respectively.

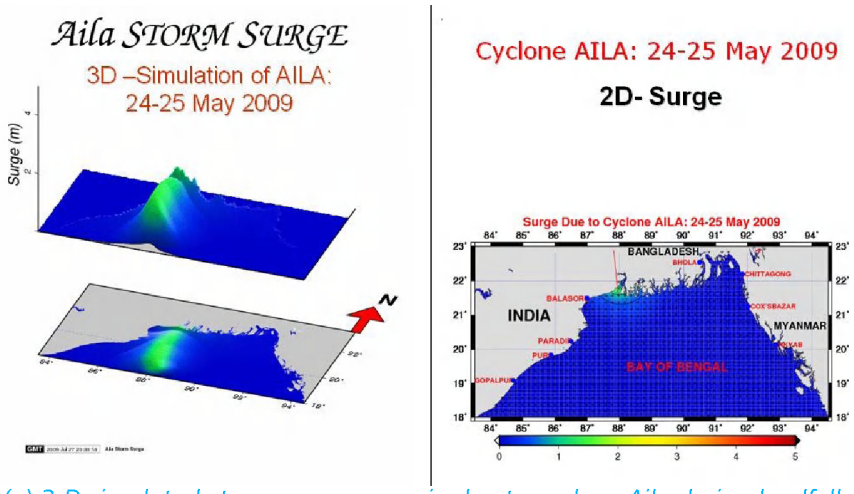

(a) 3-D simulated storm surge scenario due to cyclone Aila during landfall,
(b) 2-D simulated storm surge scenario due to cyclone Aila during landfall.

Conclusions

The tropical cyclone (Aila), developed over the North Indian Ocean, is selected to simulate the characteristics such as structure, intensity and movement. Model simulated rainfall is over estimated over hilly region like Bhutan and neighbourhood and also over West Bengal and Bangladesh except for Chittagong region where it was under estimated. Simulated lowest ECP, before the landfall is 7 hPa higher than observed or satellite derived observations and the maximum simulated wind is 4 m/s lower than the satellite estimated wind. SYNOP, AWS and TEMP data of STORM Field Exp. 2009 and Khepupara DWR Radial Wind have been used in 3DVAR DA (Cold and Warm start). There is some spatio-temporal shift in rainfall which is minimized by 3DVAR DA. Very high resolution topographic data is needed for making better predictions.

References

[1] Debsarma, Sujit Kumar, (2009). Simulations of Storm Surges in the Bay of Bengal, *Marine Geodesy*, 32:2, 178-198.
[2] Mohanty, U.C., M. Mandal and S. Raman, (2004). Simulation of Orissa super cyclone (1999) using PSU/NCAR meoscale model, *Natural Hazards*, 31, 373-390.

Interannual variation of Phytoplankton Production in the southern Benguela upwelling system

T. Lamont[1,3], R. Barlow[2,3]

[1]Oceans & Coasts Research, Department of Environmental Affairs, Cape Town, 8012, South Africa
[2]Bayworld Centre for Research & Education, Oceanography Unit, Cape Town, 8012, South Africa
[3]Marine Research Institute, University of Cape Town, Rondebosch, 7701, South Africa
Email: tarron.lamont@gmail.com

Summary

Satellite-derived SST, Chl*a* and primary production (PP) was investigated in order to describe the large scale spatial and temporal variability in phytoplankton biomass and production rates in the southern Benguela at seasonal and interannual timescales, and to explore the relationship between PP and environmental variability. In general, above-average biomass and PP corresponded to negative SST anomalies that tended to be associated with La Niña conditions. In contrast, positive SST anomalies associated with El Niño conditions generally coincided with below-average biomass and PP.

Introduction

The southern Benguela upwelling system is a highly dynamic environment with significant seasonal and interannual variability in oceanography and meteorology which drives the variability in PP. This environment supports a rich pelagic ecosystem, as well as numerous top predators such as seals, gannets and penguins [1]. Understanding the spatial and temporal patterns and trends in PP in the southern Benguela is important for the effective management of the economically and ecologically significant pelagic ecosystem. Warming trends observed in most LME's [2] have resulted in large spatial changes in phytoplankton distribution and a reduction of global PP since the early 1980s [3]. The predicted decrease in global PP has important consequences for the sustainability of fisheries ecosystems like the southern Benguela. The primary aim of this study was to investigate the large scale spatial and temporal variability in phytoplankton biomass and production at seasonal and interannual timescales, and to explore the relationship between PP and environmental variability.

Discussion

Standard monthly-averaged ocean colour data from SeaWiFS and MODIS-Aqua, with a spatial resolution of 9.26 km, was obtained from the OBGP at NASA's GSFC. SeaWiFS data covered the period from September 1997 to June 2002, while MODIS-Aqua data covered the period from July 2002 to February 2012. The VGPM model was applied to the SeaWiFS and MODIS-Aqua data in order to obtain PP estimates [4]. Monthly-averaged SST from AVHRR Pathfinder and MODIS-Aqua, with a spatial resolution of 4 km, was used to explore the relationship between PP and environmental variability. Monthly time series of latitudinally-averaged SST, Chl*a* and PP were constructed along the coast between 29 °S and 34.3 °S, and used to investigate temporal patterns and latitudinal differences. Anomalies were computed by subtracting the monthly climatic mean from each month in the time series.

The seasonal variation in SST was described by higher temperatures during spring and summer, and lower temperatures in autumn and winter. The seasonality in chlorophyll *a* concentrations and PP was

generally in phase with periods of maximum upwelling during spring and summer. Throughout the time series, SST varied between 13-21°C and PP typically ranged from 0.5-6 g C m^{-2} d^{-1}. Considerable interannual variations were evident, with the highest summer temperatures being observed during 2002 and 2003, while the lowest were noted in 2006. A clear decreasing trend in the summer maxima is evident for the period from 2003 to 2006. Although the exact timing did not always coincide on a month to month basis, above-average SSTs generally corresponded to El Niño events, while negative SST anomalies were associated with La Niña events. A clear decreasing trend in the maximum summer PP was observed from 1997 to 2003 and again from 2007 to 2010, while PP during 2004 and 2005 was typically above-average and was associated with higher than normal biomass and SST, and also corresponded to a prolonged period of El Niño conditions.

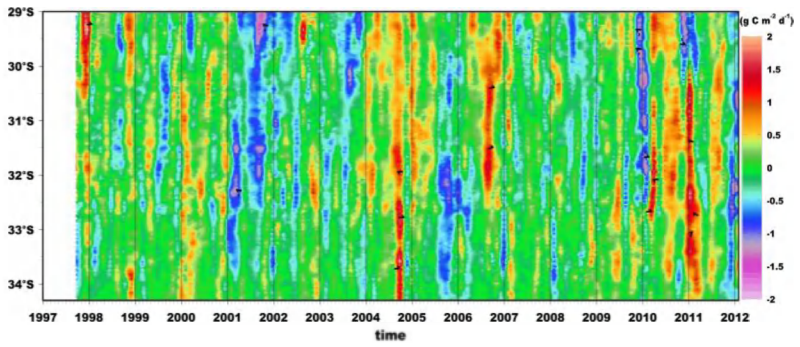

PP anomalies in the Southern Benguela

Conclusions

Over the long term, temporal variations in PP were observed to be larger than the spatial differences. This was opposite to the findings of [5], who showed that spatial variations were generally greater. Similar to the findings of [3], the long term variations in SST, Chl*a* and PP were linked to variations in climate, with increasing temperatures related to a decrease in phytoplankton biomass and PP, and vice versa. These variations are likely to have a significant impact on ecosystem functioning by driving changes in the physiological state of phytoplankton, taxonomic composition of zooplankton populations, and ultimately influencing the trophic structure of pelagic food webs [3]. In the southern Benguela, this pattern is not straight-forward and is complicated by regionally-driven events.

References

[1] van der Lingen, C.D., Shannon, L.J., Cury, P., Kreiner, A., Moloney, C.L., Roux, J-P., Vaz-Velho, F. (2006) Resource and ecosystem variability, including regime shifts in the Benguela Current System, In: Benguela: Predicting a Large Marine Ecosystem, Large Marine Ecosystems 14, Shannon, V., Hempel, G., Malanotte-Rizzoli, P., Moloney, C.L., Woods, J. (Eds), Elsevier, Amsterdam.

[2] Belkin, I.M. (2009) Rapid warming of Large Marine Ecosystems. Prog Oceanogr 81: 207-213.

[3] Behrenfeld, M.J., O'Malley, R.T., Siegal, D.A., McClain, C.R., Sarmiento, J.L., Feldman, G.C., Milligan, A.J., Falkowski, P.G., Letelier, R.M., Boss, E.S. (2006) Climate-driven trends in contemporary ocean productivity. Nature 444: 752-755.

[4] Behrenfeld, M.J., Falkowski, P.G. (1997) A consumer's guide to phytoplankton primary productivity models. Limnol Oceanogr 42: 1479-1491.

[5] Chassot, E., Bonhommeau, S., Dulvy, N.K., Mélin, F., Watson, R., Gascuel, D., Le Pape, O. (2010) Global marine primary production constrains fisheries catches. Ecol Lett 13, 4: 495-505.

A New Paradigm for Interpreting Remotely Sensed Phytoplankton Fluorescence

S. R. Laney

Woods Hole Oceanographic Institution, Biology Department, Woods Hole MA, 02543, USA
Email: slaney@whoi.edu

Summary

Introduction

Over the past four decades there has been considerable progress in satellite approaches for mapping global distributions of phytoplankton biomass. Now, new algorithms for phytoplankton functional types are bolstering our ability to assess the composition of surface ocean phytoplankton assemblages. Yet ocean color approaches and algorithms for assessing the photosynthetic state of phytoplankton – the third pillar of marine phytoplankton biogeochemistry and ecology – remain notably underdeveloped. Since the early 1970s sun-stimulated fluorescence has been considered an ocean color property with considerable potential for examining phytoplankton's photosynthetic state, but there have been only a few examples where ecologically meaningful results have been derived using fluorescence products from ocean color satellites. *New, innovative efforts are needed in order to advance our ability to use ocean color from space – especially fluorescence – to assess photosynthetic state in phytoplankton.*

Discussion

The attraction of sun-stimulated fluorescence F_{sun} (or passive, solar, or natural fluorescence F_{nat}) as a remotely sensed property is that it is sensitive to a wide range of environmental changes. This makes it ideal for identifying situations in the ocean when photosynthesis is perturbed (e.g., responses to changing nutrient conditions). This sensitivity is also the main drawback of sun-stimulated fluorescence because different environmental perturbations affect phytoplankton F_{sun} differently, in both time scales and magnitude. The daily variability in F_{sun} is highly complex, even in idealized, highly constrained conditions when only one environmental parameter is changed (Fig. 1, top). Phytoplankton physiology has a 'memory' and its current state reflects past events in a strongly nonlinear fashion [1]. As a result, simple linear, correlative, or statistical approaches for interpreting F_{sun} variability may not be appropriate for deciphering these complex dynamics [2, 3].

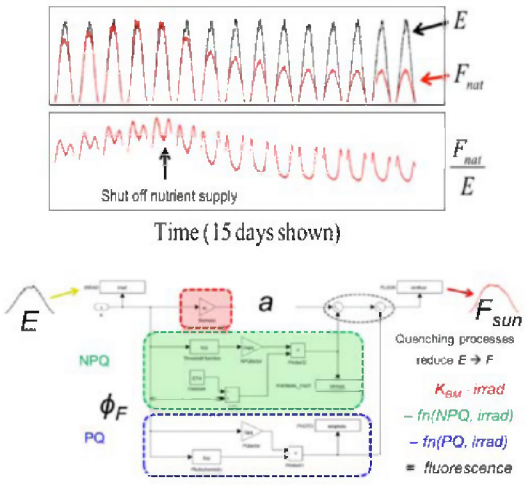

Fig. 1. Top: Laboratory data showing the degree of dynamical complexity in daily F_{nat} *for 15 days before & during nutrient starvation. Daily trends in* F_{nat}/E *can be explained by a dynamical model (bottom) of daily irradiance* E *which predicts daily* F_{sun} *trajectories with only a few parameters.*

Sun-stimulated fluorescence is a remotely sensed ocean color property for which a new, dynamical approach can lead to considerable advances. A dynamical model for F_{sun} (Fig. 2, bottom) shows how observed daily changes in F_{sun} and its apparent yield can be described using only a few basic physiological

factors, which works because the model is constructed in a dynamically appropriate fashion. Current quantitative frameworks for interpreting variability in F_{sun} rely on equations that directly relate measured fluorescence to a multiplicative function of factors such as irradiance, chlorophyll, absorption, and so-called 'quantum yield'. Such equations have limits as to the types of dynamical behaviors that they can reproduce. A properly constructed dynamical model can take the complex daily trajectories of F/E (the apparent fluorescence yield) and interpret them to generate day-to-day time series of basic photosynthetic properties, providing insight into photosynthetic saturation (e.g., E_K) and nonphotochemical quenching. Day-to-day changes in these basic aspects of photosynthetic state will reflect acclimations to perturbations in the ocean environment, such as that caused by nutrient availability or insolation. Thus, fed with appropriately resolved within-day measurements of irradiance and F_{sun}, a proper dynamical framework can be used in algorithm development to generate remote sensing products for basic aspects of the photosynthetic state of phytoplankton.

Nonanalytical models for examining the dynamics of complex systems have not yet become part of the mainstream of phytoplankton ecophysiology, but those few that have been developed and examined to date (e.g., [4]) show considerable promise for describing the types of dynamical variability we see in the ocean's sun-stimulated fluorescence. Ocean color measurements of F_{sun} have been historically been used as single-point observations but approaches that consider the within-day variability have been proposed from laboratory studies [2]. The twin MODIS sensors aboard EOS-Terra and -Aqua can provide data for very crude metrics of within-day variability in F_{sun}, but the most significant advances in the use of remotely sensed ocean color to assess photosynthesis in the ocean will likely come from geosynchronous ocean color satellites [5] that collect data for driving such dynamical algorithms.

Conclusions

Oceanic chlorophyll and functional types do not change appreciably over the course of the day but photosynthetic state does, and so appropriate interpretation of sun-stimulated fluorescence from space requires an approach that takes this within-day variability into account. Geosynchronous ocean color observations could provide the data needed for algorithms that generate ecologically useful remote sensing products that track aspects of photosynthetic state from space. Such an approach is equally useful for ocean color sensing by high-altitude AUVs that repeat observations locally within a day.

References

[1] Laney, S.R., et al. (2001). *Measuring the natural fluorescence of phytoplankton cultures.* J. Atmos. Ocean. Tech, 18: 1924-1934.
[2] Laney, S.R., Letelier R.M., and Abbott, M.R. (2005). *Parameterizing the natural fluorescence kinetics of Thalassiosira weissflogii.* Limnol. Oceanogr., 50: 1499-1510.
[3] Morrison, J.R. (2003). *In situ determination of the quantum yield of phytoplankton chlorophyll a fluorescence: A simple algorithm, observations, and a model.* Limnol. Oceanogr 48: 618-631.
[4] Laney, S.R., Letelier, R.M., and Abbott, M.R. (2009). *Using a nonanalytical approach to model nonlinear dynamics in photosynthesis at the photosystem level.* J. Phycol 45: 298-310.
[5] IOCCG, ed. *Ocean-Colour Observations from a Geostationary Orbit.* ed. D. Antoine. Vol. 12. 2012.

Estimation of spectral attenuation coefficient of downwelling irradiance: from oligotrophic to coastal waters

Zhongping Lee[1], Chuanmin Hu[2], Shaoling Shang[3], Keping Du[4], Marlon Lewis[5], Robert Arnone[6]

[1] University of Massachusetts Boston

[2] University of South Florida

[3] Xiamen University

[4] Beijing Normal University

[5] Dalhousie University

[6] University of Southern Mississippi

The attenuation coefficient of downwelling irradiance at 490 nm (Kd490) is a standard product for satellite ocean color missions. Presently Kd490 is derived from the ratio of remote sensing reflectance (Rrs) at ~490 nm and ~555 nm, and it is limited to this single spectral band. Studies from photosynthesis to heat transfer, however, require spectral Kd, where empirical band ratios could be cumbersome for its generation. In principle, Kd is a function of sun angle and water's inherent optical properties (IOPs) including absorption and backscattering coefficients. Because these IOPs products are also generated routinely from satellite measurements, it is logical to evolve the empirical Kd product to semi-analytical Kd product that is not limited to one wavelength but flexible for hyperspectral data. The semi-analytical Kd product also explicitly accounts for the impact of sun angle and the contribution of backscattering coefficient. Furthermore, the analytical nature makes it straightforward to quantify the product uncertainty pixel-by-pixel. Here, using field data collected from oligotrophic ocean to coastal waters covering >99% of the range of global oceans, we evaluate the semi-analytical Kd product and demonstrate the applicability of the algorithm as well as the quality of the product. Data products generated from ocean-color sensors are also presented to provide a global perspective.

ProVal

A new Argo profiler dedicated to the validation of ocean color remote sensing data

E. Leymarie[1], C. Penkerc'h[1], H. Claustre[1], D. Antoine[1], J.F. Berthon[2], S. Bernard[3], M. Babin[4], S. Bélanger[5]

[1] CNRS/UPMC, Laboratoire d'Océanographie de Villefranche (LOV), Villefranche-sur-mer, France.
[2] Joint Research Centre (JRC), Ispra (VA), ITALY.
[3] CSIR – NRE, Stellenbosch, South Africa.
[4] Univ. Laval/CNRS, UMI Takuvik, Québec, Canada.
[5] UQAR, Rimouski, Canada
Email: leymarie@obs-vlfr.fr

Summary

We present here a new profiling float dedicated to the validation of ocean color remote sensing data. This new autonomous platform, equipped for high quality radiometric acquisition, has a lot of advantages to sample distant areas all year round, but requires also major developments. Specifications of the new ProVal float as well as new opportunities and advantages over other methods to acquire radiometric data will be presented here. The ProVal float development and operations are part of the newly formed Sentinel-3 validation team (S3VT) activities. Intercalibration of ProVal floats with the BOUSSOLE program is planned in this frame.

Introduction

In the late 1990's the physical community designed and implemented the Argo program [1], the aim of which being to develop an array of vertically profiling floats that measure temperature and salinity throughout the world's ocean upper 2000m. After a decade of operation, this program has succeeded in attaining its initial objective of 3000 floats actively profiling (once every 10 days) and providing data with improved accuracy. These data are used by a large array of agencies, researchers and are assimilated into global circulation models. With more than 100,000 Temperature-Salinity profiles during 2008 alone, the Argo array accounts for ~ 95% of the vertical profiles ever measured.

The aim of the ProVal project is to take advantage of the dynamics surrounding Argo floats to develop a profiler dedicated to Ocean Color data validation. This kind of instrument does not have the accuracy of permanent installations (like the Moby or Boussole moorings) but is strongly recommended by the Bio-Argo group of the International Ocean Color Coordinating Group [2]. Advantages of using validation floats are:

- High measurement frequency augmenting the probability of matching-up satellite records: several measurements of surface quantities can be expected every day around solar noon for each float;
- Global distribution of floats allowing year-round the validation of satellite products in a variety of trophic areas of the world ocean: in particular, polar zones or oceanic gyres presently undersampled in database;
- Access through profiling to the vertical dimension of the radiometric quantities, thus facilitating in some environment the extrapolation of the signal to the surface: flexibility is kept for the selection of the extrapolation layer with respect to fixed-depth measurements.
- Consistency of carried radiometric sensors and of calibration and processing methods: this will lead to a reduction of the uncertainty presently found in radiometric data sets gathered from multiple instrumentation/processing measurements carried out during various ship campaigns;

- Near real-time transmission, data processing and distribution: a modification of the sampling strategy in a near real-time mode will allow an extra-sampling of particular areas (for example during a clear sky day in a frequently cloudy region);
- Relatively low cost with respect to ship campaigns.

The ProVal float

The ProVal float is a new profiling float developed by the Laboratoire d'Océanographie de Villefranche (LOV) thanks to a CNES funding. It is based on a new version of the PROVOR float (CTS5, NKE company) equipped with a new acquisition board (developed by Osean company in collaboration with the LOV). This board allows the acquisition of 8 independent sensors and has sufficient CPU capabilities to process recorded data in real time. It is interfaced with a new navigation board (used to drive the float) developed by NKE. This navigation board allows a more complex definition of the float mission and is able to receive navigation commands from the acquisition board. This dialog allows retroactive programming of the float's mission based on scientific measurements, which could be extremely useful for a large number of applications including adapted sampling in function of weather conditions.

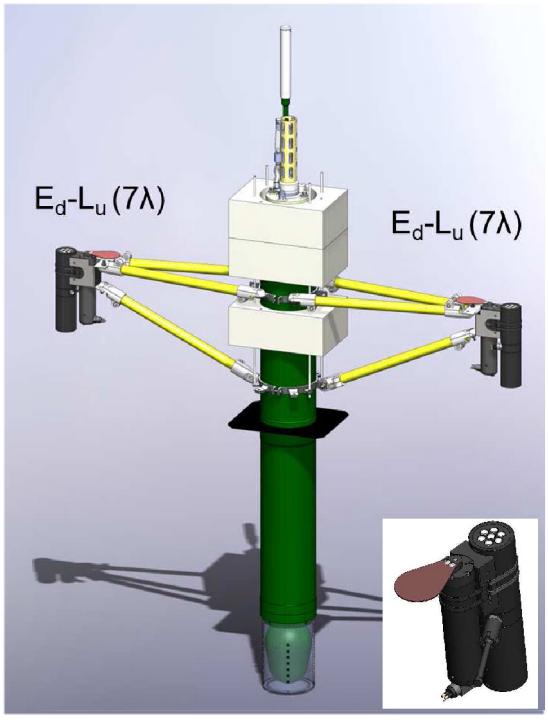

The ProVal float with 2 E_d-L_u(7λ) combo

Regarding sensors, the ProVal float is equipped with two identical radiometric combos (E_d-L_u) from Satlantic. Each sensor has the same seven wavelengths (currently 400, 412, 443, 490, 510, 560, 665 nm). Top sensor (Ed) is protected from "marine snow, i.e. particles" by a bioshutter. This configuration with two identical sensors is used to avoid self-shading (one sensor is always on the sunny side of the float) and to allow a monitoring of sensors drift by comparing data from both sensors. The ProVal float is also equipped with a tilt sensor to record the tilt of the profiler during the acquisition. Other sensors, like Chla-fluorescence or backscattering, could be also easily added to the float.

Acknowledgments

The ProVal project is funded by the CNES-TOSCA. This project also takes advantages of other programs oriented on profiling floats: the project remOcean (ERC advanced grant N°246777) and the project NAOS (ANR-10-EQPX-40).

References

[1] Roemmich D, Boebel O, Freeland H, King B, Le Traon P-Y et al. (1999). On the design and Implementation of Argo - An initial plan for a global array of profiling floats. International CLIVAR project Office ICPO Report No21 GODAE Report No 5 Published by the GODAE International Project office, c/o Bureau of Meteorology, Melbourne, Australia, 32pp.

[2] IOCCG (2011). Bio-Optical Sensors on Argo Floats. Claustre, H. (ed.), Reports of the International Ocean-Colour Coordinating Group, No. 11, IOCCG, Dartmouth, Canada.
http://www.ioccg.org/reports/IOCCG_Report11.pdf

Characterization of in-situ multi-angle reflectance for turbid productive inland waters: a case study in Meiliang Bay, Taihu Lake, China

J. S. Li, B. Zhang , Q. Shen, H. Zhang
Center for Earth Obeservation and Digital Earth, Chinese Academy of Sciences, Beijing 100094, China
Email: jshengli@ceode.ac.cn

Introduction

The optical field above water surface is anisotropic [1]. It is important to study the directional reflectance properties of the optical field above water, which is useful for investigating the parameters of the model for retriving water quality from remotely sensed data. The bidirectional reflectance distribution function for oceanic waters has been well studied [2]. However, the function for inland waters is still challenged partly due to the lack of in-situ multi-angle remote sensng reflactance. A device equipped with a spectrometer has been designed for measuring multi-angle remote sensing reflectance, which is valueable for sdudying the directional reflectance properties for waters and was used in the cruise over Meiliang Bay, Taihu Lake, China. Using the multi-angle remote sensing reflectance collected during the cruise, the bidirectional reflectance properties have been characterized.

Methods and Results

A cruise was carried out over Meiliang Bay on October 17-18, 2012. It was measured in the cruise the multi-angle remote sensing reflectance and the concentrations of cholorophyll-a, total suspended matter, and colored dissolved organic matter for a total of 9 observation sites. It should be noted that the reflectance data was collected at 17 angles using a specialized device equipped with a spectrometer, as shown in Fig. 1.

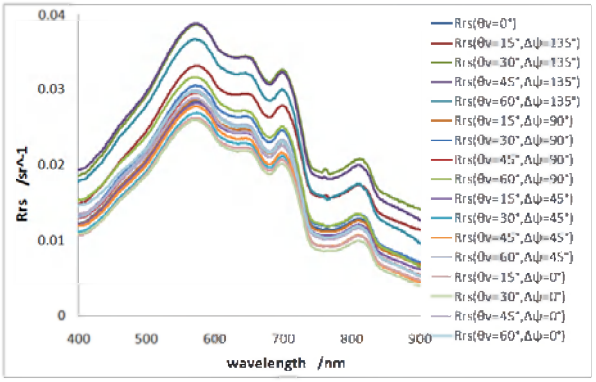

Fig. 1 Multi-angle remote sensing reflectance spectra on a typical sampling site. (Where θ_v is viewing zenith angle; $\Delta\psi$ is relative azimuth angle, which is the difference between viewing azimuch angle and solar azimuch angle, and $\Delta\psi$ is 0° if the sensor and the sun are in the same direction from the target.)

Discussion and Conclusion

Based on the statistics (shown in Fig.2) calculated using the in situ multi-angle remote sensing reflectance, the directional reflectance properties are characterized as follows. (1) The average values of Rrs(400-900nm) in the forward direction of sunlight ($\Delta\psi$=135°) are much higher than those in opposite and side directions of sunlight ($\Delta\psi$=0°, 45°, 90°). (2) All the values of the average correlation coefficients for remote sensing reflectance at each two observation angles on each sampling site are higher than 0.986, which means that the spectral shapes of the multi-angle reflectance do not change much with the observation angles. (3) The standard deviations divided by average values of Rrs(400-900nm) range from 7.8% to 41.3%, indicating

that the average values of the multi-angle reflectance change much with the observation angles. (4) The standard deviations divided by average values of R_{rs}(645nm/628nm) and R_{rs}(706nm/676nm) range from 0.4% to 2.9%, which means that some band ratios of the multi-angle reflectance do not change much with the observation angles.

In short, the average values of the multi-angle reflectance change much with the observation angles, but the spectral shapes and some band ratios do not change much. Therefore, spectral shapes and some band ratios can be used in models to reduce the directional effects of optical field above inland waters.

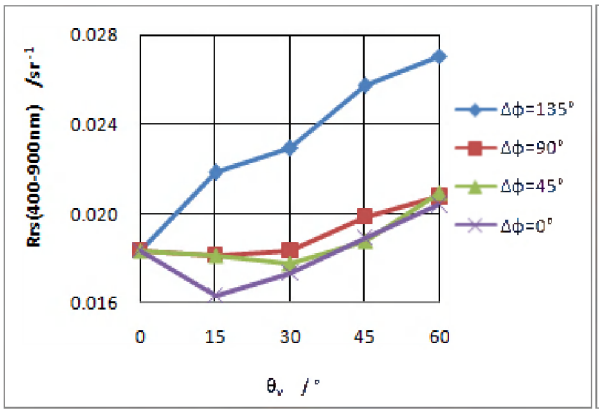

(a) Average values of R_{rs}(400-900nm) in each observation angle

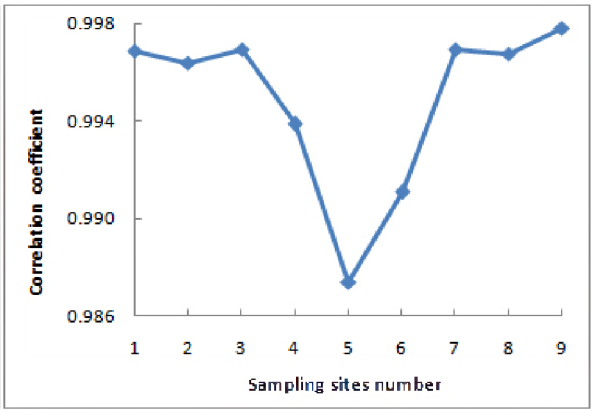

(b) Average values of correlation coefficients between every two observation angles on each sampling site

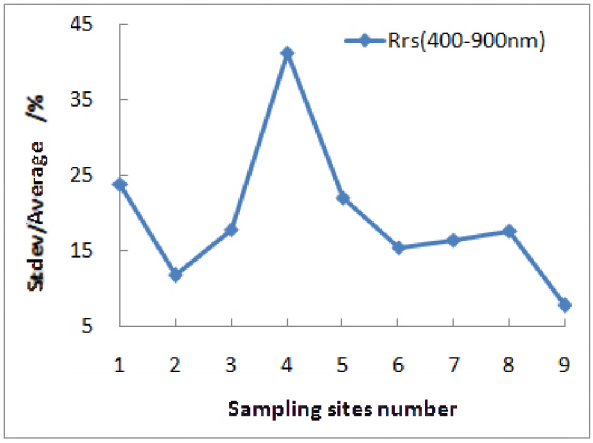

(c) Standard deviation value of R_{rs}(400-900nm) divided by average value of R_{rs}(400-900nm) on each sampling site

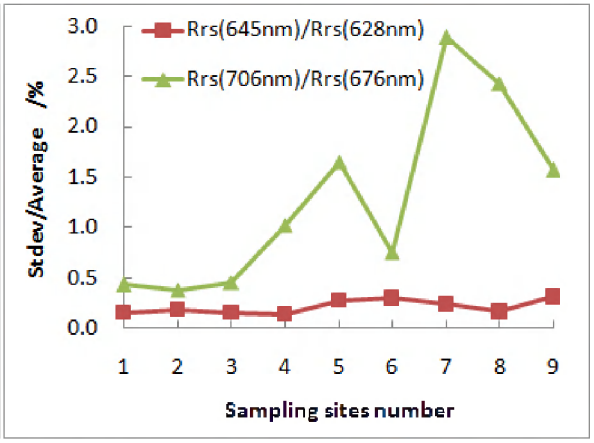

(d) Standard deviation value of two band ratios divided by average value of the two band ratios on each sampling site

Fig. 2 The statistics derived from the in situ multi-angle remote sensing reflectance spectra

References

[1] Voss K J, Morel A, Antoine D. (2007). Detailed validation of the bidirectional effect in various Case 1 waters for application to ocean color imagery. Biogeosciences, 4(5): 781-789.

[2] Morel A and Gentili B. (1996). Diffuse reflectance of oceanic waters .3. Implication of bidirectionality for the remote-sensing problem. Applied Optics, 35(24): 4850-4862.

Deriving suspended sediment and turbidity products from remote sensing reflectance in turbid coastal waters

Soo Chin Liew, Chew Wai Chang and Boredin Saengtuksin

National University of Singapore, Centre for Remote Imaging, Sensing and Processing,
Singapore 119260, Singapore
Email: scliew@nus.edu.sg

Summary

Remote sensing reflectance measured by high resolution satellite sensors is used to map water turbidity and total suspended sediment concentration (TSS) in turbid coastal waters. Empirical relations between water turbidity, backscattering coefficient and TSS were derived using in-situ measurement data. These relations were applied to satellite derived backscattering coefficient to produce maps of turbidity and TSS.

Introduction

Water reflectance depends on the intrinsic optical properties, primarily the absorption and scattering coefficients. Hence, it is possible to derive the water turbidity and TSS, both related to scattering by suspended particles, from remote sensing reflectance measured by satellite sensors. In this paper, we describe our experience in providing a user service for mapping water turbidity and TSS in turbid coastal waters using high resolution SPOT-5 satellite. The service was provided in conjunction with the environmental impact assessment of a bridge construction project. The visible bands have considerable penetrating power through water. Hence, the signals from these bands are likely to be influenced by water depth. We used the NIR band to derive water turbidity and TSS to minimize this problem.

Method

The SPOT satellite data were converted to the top-of-atmosphere reflectance, and corrected for Rayleigh scattering and molecular absorption using routines in the 6S package [1] with considerations of the sensor spectral response. The SWIR band is used to correct for surface glints. The water reflectance is converted to sub-surface remote sensing reflectance and the backscattering coefficient was computed using an algorithm based on the Quasi-Analytical Algorithm (QAA) [2] [3]. In-situ measurements of water reflectance, suspended sediment concentration and water turbidity were performed to establish the relations between water backscattering coefficient, turbidity and TSS. The relations were applied to convert the satellite measured water backscattering coefficient to water turbidity (in nephelometric turbidity unit, NTU) and TSS.

Results and discussion

Results of in-situ measurements conducted during seven field trips indicate that the backscattering coefficient has a linear relation with water turbidity (R^2 = 0.93). The backscattering coefficient values were derived from above-water reflectance spectra measurement by a hand-held spectroradiometer using a spectral matching method [4]. TSS (in mg/l, measured by the filtration method) was found to

have a power-law relation with turbidity (R^2 = 0.84) (see Fig. 1). The field trips were conducted over a period of 3 years from Sep 2009 to Sep 2012 at twenty sampling locations. The turbidity values ranged from about 1.5 NTU to over 100 NTU. Only samples with turbidity below 70 NTU (136 out of 140 samples) were used in establishing the regression relations. These relations were applied to the backscattering coefficient derived from satellite data to produce maps of water turbidity and TSS at about half yearly interval.

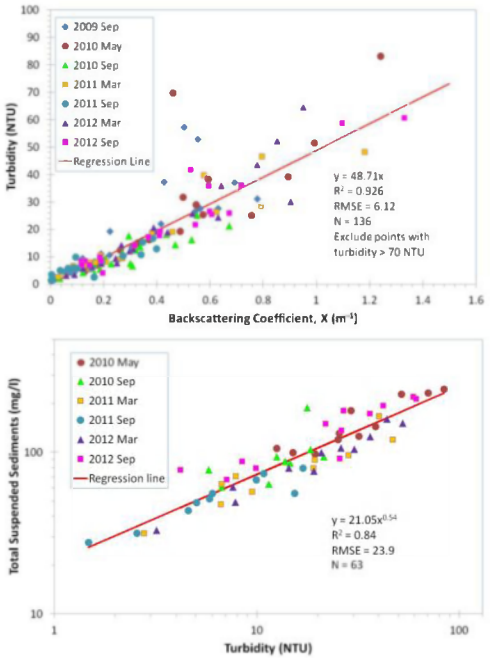

Fig. 1: Relations between backscattering coefficient and turbidity (top), turbidity and TSS (bottom).

Due to prevalence of cloud covers in the region, most of the field trips did not coincide with satellite data acquisition dates. In one occasion (13 March 2012), the satellite derived values of backscattering coefficient were found to agree quite well with those derived from in-situ spectral reflectance measurements collected within an hour of the satellite pass (bias = 0.07 m^{-1}, R^2 = 0.50)

Conclusion

We demonstrated that water turbidity and TSS maps can be derived from high resolution satellite data such as those acquired by the SPOT and Landsat satellites. Our experience with measurements across different water types seem to indicate that the relation between turbidity and backscattering coefficient is quite robust. This is probably due to the fact that turbidity and backscattering coefficient are both determined by the scattering properties of suspended particles. Our method of deriving backscattering coefficient does not require the availability of external data and hence can be used for routine operational applications in monitoring water turbidity for different water types. On the other hand, The relation of TSS with turbidity is expected to depend on the bulk density, refractive index and size distribution of the suspended particles. This relation needs to be established before TSS can be derived from remote sensing measurements.

References

[1] Vermote, E., Tanre, D., Deuze, J. L., Herman, M., Morcette, J. J. (1997). Second simulation of the satellite signal in the solar spectrum: An overview. IEEE Transactions on Geoscience and Remote Sensing, 35: 675-686.

[2] Lee, Z. P., Carder, K.L., Arnone, R. (2002). Deriving inherent optical properties from water color: A multiband quasi-analytical algorithm for optically deep waters. Applied Optics, 41: 5755-5772.

[3] Liew, S. C., He, J. (2008). Uplift of a coral island in the Andaman Sea due to the 2004 Sumatra earthquake measured using remote sensing reflectance of water. IEEE Geoscience and Remote Sensing Letters, 5: 701-704.

[4] Lee, Z. P. et. al. (1999). Hyperspectral remote sensing for shallow waters. 2. Deriving bottom depths and water properties by optimization. Appl. Opt. 38: 3831–3843.

Climate and Human Influences on Land-Ocean Fluxes in a Large River System

S.E. Lohrenz[1], W.-J. Cai[2], H. Tian[3], R. He[4], Z. Xue[4], K. Fennel[5], C. Hopkinson[2], and S. Howden[6]

[1] Univ. of Massachusetts Dartmouth, School for Marine Science and Technology, New Bedford, MA 02744, U.S.A.

[2] Univ. of Georgia, Dept. of Marine Sciences, Athens, GA, 30602, U.S.A. (wcai@uga.edu)

[3] Auburn Univ., School of Forestry and Wildlife Sciences, Auburn, AL, U.S.A.

[4] North Carolina State Univ., Dept. of Marine Earth and Atmospheric Sciences, Raleigh, NC 27695, U.S.A.

[5] Dalhousie Univ., Oceanography Department, Halifax, Nova Scotia, Canada

[6] Univ. of Southern Mississippi, Dept. of Marine Science, Stennis Space Center, MS 39529, U.S.A.

Email: slohrenz@umassd.edu

Changing climate and land use practices have the potential to dramatically alter coupled hydrologic-biogeochemical processes and associated movement of water, carbon and nutrients through various terrestrial reservoirs into rivers, estuaries, and coastal ocean waters. Consequences of climate– and land use–related changes will be particularly evident in large river basins and their associated coastal outflow regions. Here, we describe a NASA Interdisciplinary Science project and complementary Carbon Monitoring System project that employ an integrated suite of models (Figure 1) in conjunction with remotely sensed as well as targeted in situ observations with the objectives of describing processes controlling fluxes on land and their coupling to riverine, estuarine and ocean ecosystems. The objectives of these efforts are to 1) assemble and evaluate long term datasets for the assessment of impacts of climate variability, extreme weather events, and land use practices on transport of water, carbon and nitrogen within terrestrial systems and the delivery of materials to waterways and rivers; 2) using the Mississippi River as a testbed, develop and evaluate an integrated suite of models to describe linkages between terrestrial and riverine systems, transport of carbon and nutrients in the Mississippi and Atchafalaya rivers and tributaries, and associated cycling of carbon and nutrients in coastal ocean waters; 3) evaluate uncertainty in model products and parameters and identify areas where improved model performance is needed through model refinement and data assimilation; and 4) establish and populate geospatial portals for sharing and analysis of carbon datasets and products. This research will provide information that will contribute to determining an overall carbon balance in North America. Results would also benefit efforts to describe and predict how land use and land cover changes impact coastal water quality including possible effects of coastal eutrophication and hypoxia.

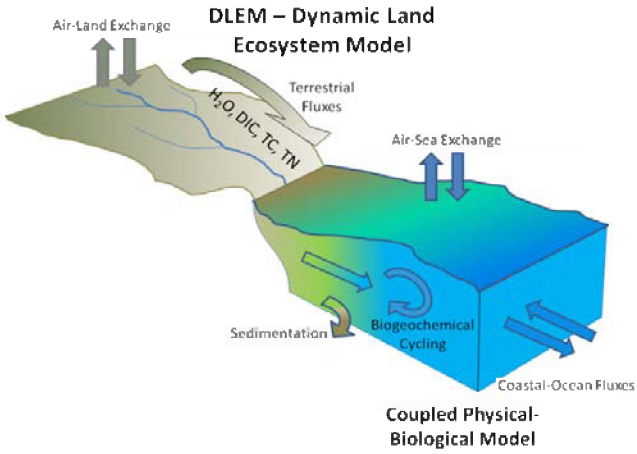

Figure 1. Integrated land-ocean modeling suite.

Examining dissolved organic carbon transport by rivers using satellite imagery: the Orinoco River case study

by

Ramón López[1], Carlos E. Del Castillo[1], Richard L. Miller[2], Joseph Salisbury[3] and Dominik Wisser[3]

[1]The Johns Hopkins University Applied Physics Lab, Laurel, MD 20723, USA
[2]East Carolina University, Greenville, North Carolina, USA.
[3]Institute for the Study of Earth, Oceans and Space, University of New Hampshire, Durham, New Hampshire, USA.

Summary

We examined the seasonal transport of dissolved organic carbon by the Orinoco River into the eastern Caribbean using the conservative relationship of colored dissolved organic matter (CDOM) and dissolved organic carbon (DOC) in low salinity coastal waters influenced by river plumes. In situ measurements of CDOM absorption, DOC, and salinity were used to develop an empirical model for DOC concentration at the Orinoco River Plume. Satellite remote sensing reflectances were used with empirical models to determine DOC river transport. Our estimates of CDOM and DOC significantly correlated with in situ measurements and were within the expected ranges for the river. Average DOC transport by the Orinoco River during the period of 1998 to 2010 was 5.29 Tg C y^{-1} of DOC, a ~ 6% increase to previous published estimates.

Introduction

The Orinoco River is the fourth largest in the world in terms of water discharge and organic carbon export to the ocean. River export of organic carbon is a key component of the carbon cycle and the global carbon budget. Dissolved organic carbon (DOC) is a major component of terrestrial carbon transported by rivers, comprises most of the organic carbon found in the coastal ocean, and is one of the largest global carbon pools [1].

Accurate assessments of the global ocean carbon concentration and understanding of ocean carbon cycle dynamics is limited in large-part by the availability of in situ data. In contrast, the easily accessible, large sets of ocean color data obtained from satellite instruments such as the Sea-Viewing Wide Field-of-View Sensor (SeaWiFS) and the Moderate Resolution Imaging Spectroradiometer (MODIS) may provide a means to obtain global estimates of land-ocean carbon fluxes of DOC.

DOC concentration cannot be measured directly using ocean color sensors because not all the organic carbon is colored. However, colored dissolved organic matter (CDOM) is a major component of the total dissolved organic carbon pool in coastal waters influenced by rivers. CDOM is often the major absorber and provides a direct approach to determining DOC concentration in coastal waters particularly those environments influenced by rivers [2]

In this study we hypothesize that the conservative behavior of CDOM and DOC in river plume influenced coastal waters, along with the possibility of detecting CDOM with Ocean Color remote sensing allows for a globalize approach in the estimation of organic carbon export by large rivers. A general goal was to expand and generalize the previous approach of Del Castillo and Miller [3] by incorporating the use of the QAA semi-analytical algorithm to estimate CDOM and to estimate river discharge using hydrological models and data from NASA's Tropical Rainfall Measuring Mission (TRMM). Unlike the Mississippi River system which is instrumented and there exists a large set of field measurements, the Orinoco River is not instrumented. Therefore, as a large river, the Orinoco River is an ideal system in which to develop a remote sensing approach to estimate terrestrially derived flux and dynamics of DOC coastal waters.

Results and Conclusions

The distribution of CDOM determined by surface patterns of a_g443 indicates that CDOM concentration changes as the ORP mixes with oceanic waters throughout the eastern Caribbean. The direct relationship of DOC and a_g443 in this region and constant spectral slope throughout the Gulf of Paria suggests that CDOM and DOC concentration is governed in large-part by the concentration and mixing of river waters indicating a conservative behavior throughout the plume[2,4]. An empirical model to estimate DOC was then developed based on the relationship between measured in situ CDOM, salinity and DOC, from samples of the Orinoco River Plume (ORP) and Mississippi River Plume (MRP). This model is defined by:

$$\text{Salinity} = 36.65 - 26.1 * a_g443 \quad (1)$$

$$DOC_P = 5.3 - 0.12 * \text{Salinity} \quad (2)$$

Subsequently, using a two end-member mixing model *Del Castillo and Miller* [3] we extrapolated DOC_P these modeled concentrations to the expected concentrations at the river itself. These estimates were then multiplied by the modeled river flow to obtain the DOC transport per day, with an average of 0.0143 Tg C day^{-1}. These estimates correlated those calculated using in situ DOC concentrations measured in situ[1], and integrated to yearly transports rates of 5.29 Tg C y^{-1} of DOC for the 1998 to 2010 period. Reflecting a 6.1 % increase in DOC transport over the previous estimates.

Despite image variability and methodology biases, our analysis captured the dynamics of organic carbon in the Orinoco River plume. The variability in organic carbon fluxes responded mostly to the seasonality of the river flow, and not to variations in the DOC concentrations within the river waters. The collection of ORP and MRP into a single data set favored a decrease in the variability and into conservative DOC estimates.

In conclusion our results corroborates the possibility of estimating organic carbon transport by large rivers, using remote sensing data and hydrological models. We propose that, because river flow is the dominant term in organic transport, a global CDOM-DOC relationship can be used to estimate carbon export in rivers with sparse or no field data. Our methodology here applies only to river plumes where there is a conservative behavior between salinity, CDOM, and DOC. At global scales the transport by large rivers such as the Orinoco River outweigh the impact of these areas to the global carbon cycle, our estimates of total organic carbon flow into the eastern Caribbean by the Orinoco River represent a 3.1 % of the total continental discharge.

References

[1] Hedges, J. I. 2002. Why Dissolved Organics Matter, p. 1-33. *In* A. H. Dennis and A. C. Craig [eds.], Biogeochemistry of Marine Dissolved Organic Matter. Academic Press.

[2] Del Castillo, C. E., P. G. Coble, J. M. Morell, J. M. Lopez, and J. E. Corredor (1999), Analysis of the optical properties of the Orinoco River plume by absorption and fluorescence spectroscopy, *Marine Chemistry*, *66*(1-2), 35-51.

[3] Del Castillo, C. E., and R. L. Miller (2008), On the use of ocean color remote sensing to measure the transport of dissolved organic carbon by the Mississippi River Plume, *Remote Sensing of Environment*, *112*(3), 836-844.

[4] Blough, N. V., O. C. Zafiriou, and J. Bonilla. 1993. Optical Absorption Spectra of Waters From the Orinoco River Outflow: Terrestrial Input of Colored Organic Matter to the Caribbean. J. Geophys. Res. **98:** 2271-2278.

[1] By the Environmental Research Observatory (ORE) HYBAM (http://www.ore-hybam.org/)

OSS2015 - Ocean Strategic Service beyond 2015

Odile Fanton D'Andon[1]; Antoine Mangin[1]; Kathryn Barker[2]; John Hedley[2]; Pierre Brasseur[11]; Charles Trees[5]; Isabelle Carslake[6]; Hubert Loisel[3]; Ned Dwyer[9]; Andreas Oschlies[8]; Sukru Besiktepe[10]; Julie Maguire[7]; Lionel Arteaga[8]; Murat Gunduz[10]; David Antoine[4]; Hervé Claustre[4]; Clément Fontana[4]. ([1]ACRI-ST; [2]ARGANS; [3]ULCO; [4]LOV(UPMC); [5]NURC; [6]Frontiers Economics; [7]DOMMRC; [8]IFM-GEOMAR; [9]UCC; [10]DEU; [11]LEGI)

OSS2015 Objectives

OSS2015 is a FP7 R&D project focused on nowcast, forecast and climatology of the biogeochemical properties of the ocean mixed layer. OSS2015 addresses the fusion of satellite ocean colour data (multispectral radiance of the sea surface) and in situ measurements from autonomous platforms (buoys, drifters, gliders, …) through assimilation into biogeophysical models.

R&D activities are performed in order to improve the nowcast, the forecast and the estimation of the spatial and temporal variability of biogeochemical variables in the ocean mixed layer, the development and validation of new tools for integration and assimilation of EO and in situ data into biogeochemical models as well as of new products relevant to the biogeochemistry of the ocean. Development and demonstration of new prototype service lines towards scientific and operational users are also in the scope of OSS2015 activities.

The OSS2015 project aims to carry out R&D activities for the development of marine biogeochemistry products and services not currently available through the precursor service of the operational forecast and analysis component of the European Marine Core Service (MCS)- the upstream marine service of GMES/Copernicus.

Main scientific topics of the project

1. Exploitation of in-situ and satellite data in bio-geochemical and bio-optical models:
   - ❖ For **direct assimilation** of bio-optical parameters in the Ligurian sea (and in parallel assimilation of EO-Chl-a in a pilot site in the North-Atlantic)

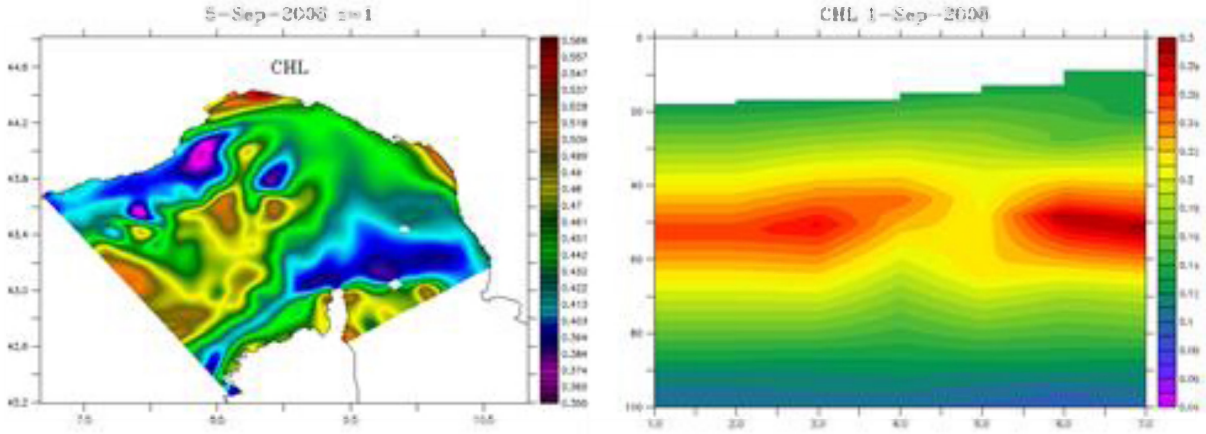

- For **optimisation** of deployment of bio-argo profilers in North Atlantic

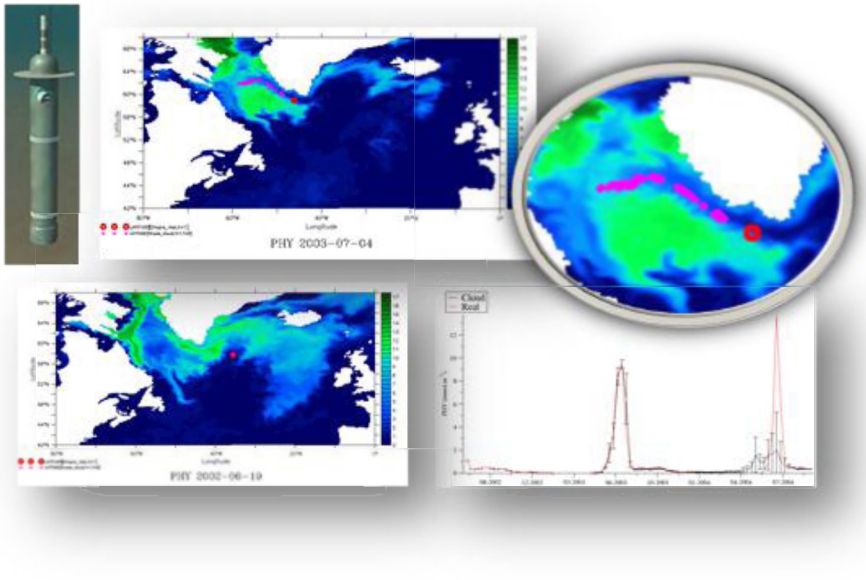

2. Definition and test **production of bio-geochemical information** (POC, NPP, PFT, PSD) relevant to Climate Science and Ecosystem Health assessment

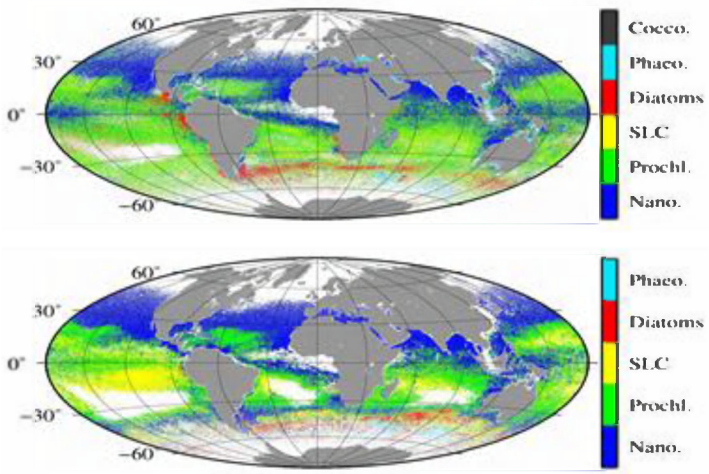

3. Prototyping **"on-demand" services of data processing**, information formatting and delivery

Present project results

The project has started in November 2011 and will last until October 2014. Latest results obtained at the time of the meeting IOCS will be presented.

Acknowledgment

The research leading to these results is receiving funding from the European Community's Seventh Framework Programme FP7/2007-2013 under grant agreement n° FP7-SPA.2011.1.5-03 / Collaborative project N° 282723 (OSS2015)

Development and Analysis of Ocean Color Satellite DOM Products for Studies in Coastal Ocean Dynamics

Antonio Mannino[1], Rachael Dyda[2], Peter Hernes[2], Michael Novak[1], Stan Hooker[1], Kim Hyde[3]
[1]NASA Goddard Space Flight Center, [2]UC-Davis, [3]NOAA NEFSC

In the coastal ocean, multiple source inputs and removal processes yield variable distributions of colored dissolved organic matter (CDOM), dissolved organic carbon (DOC) and particles on a seasonal to inter-annual basis. Our objectives entail development and validation of regional ocean color satellite algorithms for the CDOM absorption coefficient (a_{CDOM}), DOC and lignin phenols (as proxies for terrigenous DOM), and application of these algorithms to quantify seasonal to interannual distributions, inventories, cross-shelf fluxes and study the processes that contribute and remove organic matter from coastal zone. Field measurements of remote sensing reflectance (Rrs) and a_{CDOM} are used to develop regional satellite algorithms to retrieve a_{CDOM} and CDOM spectral slope (S). Empirical relationships of a_{CDOM} and S with DOC and lignin phenols from field observations will be applied to retrieve DOC and lignin phenols from ocean color satellite data. We have demonstrated strong linear relationships between a_{CDOM} and discrete measurements of DOC throughout the northeastern U.S. continental margin and between lignin phenols and a_{CDOM} or S within the southern Middle Atlantic Bight and Chesapeake Bay. The correlations between DOC and CDOM vary seasonally and between regions requiring variable coefficients for each region (southern Middle Atlantic Bight, Hudson estuarine plume and western Gulf of Maine). Nevertheless, the regional and seasonal a_{CDOM} to DOC correlations enable satellite retrieval of DOC through the a_{CDOM} algorithm.

Overview of NASA's Geostationary Coastal and Air Pollution Events (GEO-CAPE) mission

Antonio Mannino
NASA Goddard Space Flight Center, USA

The science objectives and technical requirements for the coastal ecosystems component of the Geostationary Coastal and Air Pollution Events (GEO-CAPE) mission will be presented. GEO-CAPE is a Tier 2 Earth Science Decadal Survey mission recommended by the U.S. National Research Council (NRC) in 2007 that focuses on measurements of tropospheric trace gases and aerosols and aquatic coastal biogeochemical properties from geostationary orbit (35,800 km altitude; Fishman et al. 2012). The main advantage afforded by an ocean color radiometer on a geostationary platform versus a low-earth polar orbit is the capability to image the same regions multiple times per day. Such a capability is necessary to study coastal oceans where the physical, biological and chemical processes react on short time scales from seconds to a few days. From a geostationary vantage point, a sensor can stare at an instantaneous field-of-view (iFOV) to gain sufficient signal-to-noise to retrieve ocean reflectance during low light conditions (early morning and late afternoon) and at high satellite view angles (e.g., high northern or southern latitudes). Compared to open oceans, satellite retrievals from coastal waters pose additional challenges including the need for increased signal-to-noise ratios (SNR), correcting for a more complex array of atmospheric constituents (absorbing and non-absorbing aerosols, ozone, nitrogen dioxide, etc.) and difficulties in calibration and validation efforts. Two sets of requirements are presented which represent the minimum (threshold) and fully capable (baseline) mission for achieving the stated science objectives. Current technological and financial realities weigh heavily on the requirement recommendations such that a mission with achievable science objectives and feasible sensor capabilities has been put forward.

A new approach to estimate the aerosol scattering radiance for Case 2 waters

Zhihua Mao, Delu Pan, Difeng Wang , Fang Gong

State Key Laboratory of Satellite Ocean Environment Dynamics,

Second Institute of Oceanography, State Oceanic Administration

36 Bochubeilu, Hangzhou, 310012, China

ABSTRACT

The atmospheric correction of satellite remote sensing data for turbid waters meets some problems in which the aerosol scattering reflectance is the most uncertain term to be determined. The standard method of the atmospheric correction is based on the dark pixel assumption of the water-leaving reflectance in the two NIR bands and this assumption usually becomes invalid for turbid coastal waters. A new approach was developed to accurately estimate the aerosol scattering reflectance for the turbid coastal waters. This approach is based on the idea that the aerosol scattering reflectance can be obtained from the known water-leaving reflectance of the satellite measured reflectance at the top of the atmosphere. The water-leaving reflectance is determined from the choice of a look-up table of in situ measurements based on the Angstrom law of the candidate aerosol scattering reflectance using the best non-linear least squares fit function. The performance of the approach was evaluated using the simulated reflectance at the top of the atmosphere, the Sea-viewing Wide Field-of-view Sensor (SeaWiFS) imagery, and in situ measured aerosol optical thickness. This approach is based on the assumption of the aerosol scattering reflectance following the Angstrom law instead of the standard dark pixel assumption, providing a new approach of the atmospheric correction of satellite remote sensing data.

Keywords: Atmospheric correction; Aerosol scattering reflectance; Satellite remote sensing; Coastal waters

Detecting dominant Phytoplankton Size Classes (micro-, nano- and pico-phytoplankton) from SeaWiFS data in the Mediterranean Sea: spatial and temporal variability

A. Di Cicco[1,2], M. Sammartino[3,4], S. Marullo[1], R. Santoleri[4] , [1]F. Artuso

[1]ENEA - Technical Unit Development of Applications of Radiations - Diagnostic and Metrology Laboratory – Frascati (Italia)
[2]Università degli Studi della Tuscia - DEB - Laboratorio di Oceanologia Sperimentale ed Ecologia Marina, Civitavecchia (Italia)
[3]Università di Pisa, facoltà di scienze Ambientali, Dipartimento di Scienze della Terra, Pisa (Italia)
[4]Istituto di Scienze dell'Atmosfera e del Clima – CNR – Gruppo Oceanografia da Satellite – Roma (Italia)
Email: salvatore.marullo@enea.it

Summary

In this paper we present the analysis of the spatial and temporal distribution of the Phytoplankton Size Classes in the Mediterranean Sea derived from a SeaWiFS satellite dataset produced using a Mediterranean regional algorithms for case 1, case 2 and transition waters. The results show the open Mediterranean water are mainly dominated by picoplankton all around the year with a maximun during summer and minima in autumn and winter in open sea regions not affected by intense spring blooms. Coastal and intense bloom regions, instead, show the dominance of nano and micro plankton.

Introduction

In recent years several models have been proposed to identify the contribute of different Phytoplankton Size Classes (PSCs) and Phytoplankton Functional Types (PFTs) to the total phytoplankton chlorophyll-*a* biomass or to estimate Particle Size Distribution from remote sensing Ocean Color data. These bio-optical algorithms can provide an important instrument for a synoptic studies of the Phytoplankton community structure and its spatial and temporal variability and then improve our knowledge about the ecological and biogeochemical dynamics connected with it. Validation exercises performed at global scale using data representative of a variety possible situations have shown that the models are able to capture the general trend of the size-specific chlorophyll-a concentration [1], [2], [3]. Of course, at regional scale deviation from this trends agreement can be observed.

Discussion

In this work we concentrated our investigation over the Mediterranean an Black Seas region applying two models, based on biological and ecological approaches , proposed by Brewin and co-authors [2] and by Hirata and co-authors [3] to the SeaWiFS mission data from 1998 to 2010. The regional

Mediterranean case 1 and case2 merged product were provided by MyOcean Ocean Colour Thematic Assembling Centre.

The two models were tested using a Mediterranean subset of the NOMAD SeaBASS *in-situ* dataset [4],[5],[6] and HPLC data collected by the authors group in several cruises in the West Mediterranean Sea. The matchup analysis indicates that the first model [2] tends to slightly to underestimate the concentration of nanoplakton chlorophyll and overestimate the concentration of picoplankton chlorophyll. In the second model [3] the nanoplankton underestimation is less evident as well as the picoplakton overestimation.

The analysis of the spatial and temporal distribution of the three PSC components, derived from satellite data, indicates that Picoplankton dominates all around the year with a maximum during summer and minima in autumn and winter in open sea regions not affected by intense spring blooms. Coastal and intense bloom regions, instead, in general show the dominance of nano and micro plankton.

Figure 1 shows an example of the yearly cycle for Pico, Nano Micro-planktonin the Ligurian Sea. The yearly cycle of the three components is well marked by a minimum of picoplankton concentration in spring (March - April) and maximum in summer. Microplankton dominated from March to April. In the Ionian Sea, where the spring bloom is less intense, the picoplankton maximum occurs from December to February.

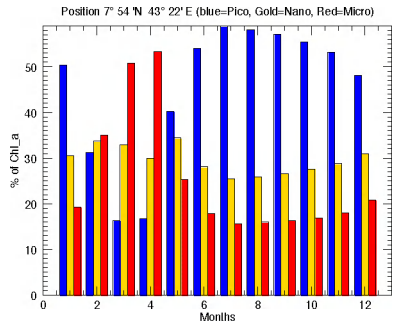

Figure 1. Mean monthly PSC distribution in the Ligurian Sea (NW Mediterranean). Picoplakton percent (blue), Nanoplankton percent(yellow), microplankton percent (red)

References

[1] Brewin R. J. W.. An intercomparison of bio-optical techniques for detecting dominant phytoplankton size class from satellite remote sensing (2011). Remote Sensing of Environment 115 (2011) 325–339

[2] Brewin R. J.W., E. Devred E, S. Sathyendranath, S. J. Lavender, and N. J. Hardman-Mountford. Model of phytoplankton absorption based on three size classes (2011), App. optics ,Vol. 50, No. 22.

[3] Hirata, T., Hardman-Mountford, N. J., Brewin, R. J. W., Aiken, J., Barlow, R., Suzuki, K., Isada, T., Howell, E., Hashioka, T., Noguchi-Aita, M., and Yamanaka, Y.: Synoptic relationships between surface Chlorophyll-*a* and diagnostic pigments specific to phytoplankton functional types (2011), Biogeosciences, 8, 311-327

Autonomous observations of arctic phytoplankton activity: The first annual cycle in ice-covered waters

P. Matrai[1], M. Steele[2], D. Swift[2], S. Riser[2], K. Johnson[3] and L. Breckenridge[1]

[1]Bigelow Laboratory for Ocean Sciences, Newcastle, ME, 04544, USA
[2]University of Washington, Seattle, WA, 98105, USA
[3]MBARI, Monterey, CA, 95039, USA
Email: pmatrai@bigelow.org

Arctic bio-floats survive stratification and sea ice! We examine the weekly variability of phytoplankton biomass and primary production as a function of changes in sea ice cover, stratification, and temperature measured in the Greenland Sea over an annual cycle for the first time, using ARGO profiling bio-floats. The Greenland Sea offers an arctic sea with weaker stratification relative to the Beaufort Sea, which allows for a more "standard" ARGO float profiling strategy (i.e., full profiling to 1000 m depth). Delicate buoyancy management is required to overcome the extreme stratification observed in the Arctic Ocean as well as ice avoidance. Each float has a CTD (warming; stratification), a dissolved oxygen sensor (primary production), fluorometer/backscattering sensors (phytoplankton biomass, primary production, particulate organic carbon) and a nitrate sensor (new and net community production), cycling every 5 days under sea ice and in open water.

The float herein was deployed in the north-central Greenland Sea in late summer 2011, where it circulated slowly cyclonically until the end of that year. At that time, it was entrained into the outer limb of the southward-flowing East Greenland Current, keeping very close to the ice edge but generally able to surface and report data. Within a few weeks it arrived at the northern edge of the Jan Mayen Ridge, where it followed the bathymetry and moved quickly eastward and away from the ice edge. Then it stalled, which allowed the eastward-advancing winter ice pack to overtake it. No positions were reported from March-July 2012, evident in Figure 1 as a straight line interpolation of positions at the start and end of this period. Preliminary analysis of drift speeds over the entire deployment to date indicates that the true trajectory over March-July 2012 was probably more circuitous than a straight line: in part, the float likely followed the isobaths westward and then back eastward. Nonetheless, the float remained in a circumscribed region in March-December 2012. In late summer 2012, the sea ice pack began its northward retreat and the distance to the ice edge increased. By the end of January 2013, the float had wandered southward over the central Jan Mayen Ridge, still relatively far away from the ice pack. The course of this float has remained near to or under sea ice providing a unique set of continuous biophysical observations at the ice edge.

A time series of various *observed* (temperature, nitrate, chlorophyll, O_2) and *derived* (NPP, POC) quantities obtained from the float so far will be presented. The float was deployed in the north-central Greenland Sea in late summer 2011, when the surface was warm and fresh (salinity was obtained but is not shown in this figure), oxygen, chlorophyll, and backscatter (POC) values were moderately high, and nitrate concentration was high. Fall and early winter 2011 brings low biological activity and convective deepening and cooling as the float travels southward toward the Jan Mayen Ridge, characteristic of central Greenland Sea conditions. From March-July 2012, on the other hand, the float is overtaken by the ice pack and its associated cold, fresh surface conditions. In July 2012 the ice pack begins to retreat, and the float begins to intermittently surface. This is also when biological activity accelerates and a

strong summer bloom follows with elevated biomass, trapped near the surface by high stratification probably associated with ice melt. Fall and early winter 2012 brings a cessation of biological activity and deepening mixed layers.

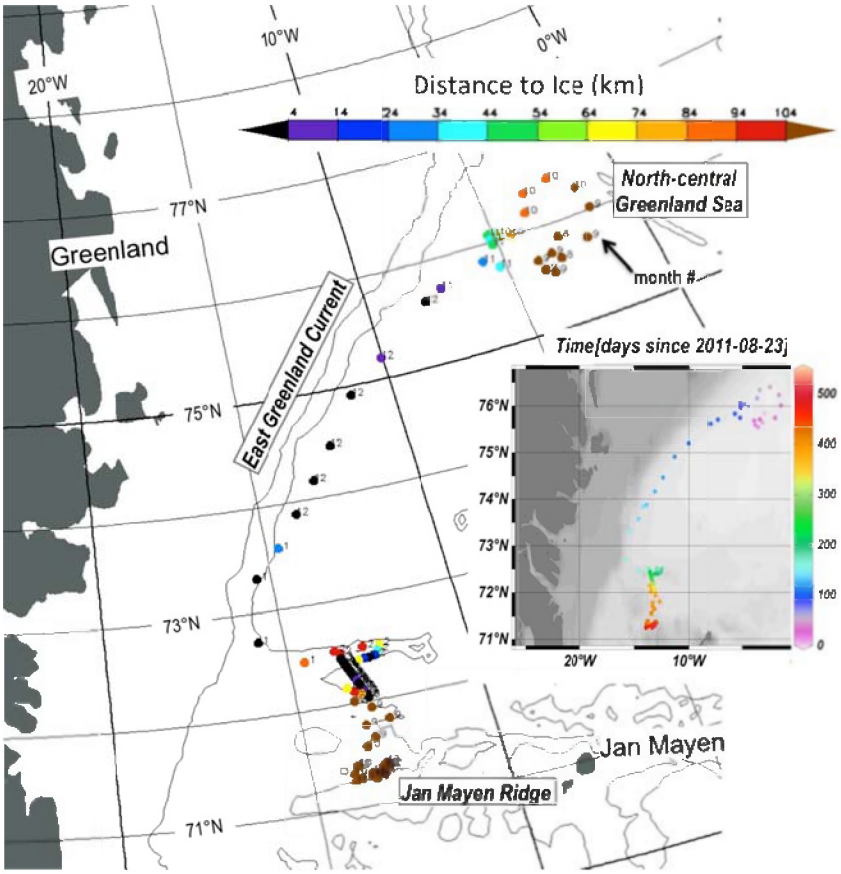

Figure 1. *Drift track of APPSS float deployed in the Greenland Sea in summer 2011. "Distance to ice" was determined using the multi-sensor MASIE sea ice data set (http://nsidc.org/data/masie/). The straight section over the northern Jan Mayen Ridge was made by interpolating positions before and after the float was under the ice pack.*

Total NPP over the 2012 growth season was also computed, using an arctic-specific chlorophyll – primary productivity relationship and also using fall minus spring nitrate values[1,2]. The results compare favorably with historical values for this region, which are generally averages over large space and time scales. However, a more informative comparison might be obtained with some further "re-analysis" of the historical observations, in order to better determine the ice and water mass regimes that they sampled, relative to those sampled in 2012.

[1] Codispoti, L. A., V. Kelly, A.Thessen, P. Matrai, S. Suttles, V. J. Hill, M. Steele, B. Light, Synthesis of primary production in the Arctic Ocean: III. Nitrate and phosphate based estimates of net community production, *Prog. Oceanogr., in press,* **2013**.

[2] Matrai, P. A., E. Olson, S. Suttles, V. J. Hill, L. A. Codispoti, B. Light, and M. Steele, Synthesis of primary production in the Arctic Ocean: I. Surface waters, 1954-2007, *Prog. Oceanogr., in press,* **2013**.

Distinguishing cyanobacteria from algae in eutrophic near-coastal and inland waters from space: theory and applications

M.W. Matthews[1], S. Bernard[12]

[1]Marine Remote Sensing Unit, Department of Oceanography, University of Cape Town, Cape Town, South Africa

[2] Earth Systems Earth Observation, Council for Scientific and Industrial Research, 15 Lower Hope Street, Rosebank, 7700, Cape Town, South Africa

Email: MTTMAR017@myuct.ac.za

Summary

Cynobacteria may be distinguished from eukaryotic algae on the basis of the magnitude of the peak near 709 nm from top of atmosphere MERIS FR data. A new approach called the maximum peak height (MPH) algorithm is presented for estimating trophic status (chlorophyll a), surface scums and floating vegetation in inland and near coastal waters. Evidence is presented from a two-layered sphere model for enhanced backscattering from cyanobacteria due to intracellular gas vacuoles. Cyanobacteria dominant waters may be distinguished from those dominated by eukaryotes using a flagging procedure based on the unique pigmentation and fluorescence features of cyanobacteria.

Introduction

Cyanobacterial blooms in marine and fresh waters represent an increasing and substantial global health threat. A new approach is presented which enables cyanobacteria-dominant waters to be distinguished from those dominated by eukaryotic algae from space [1]. A dataset consisting of 74 coincident top-of-atmosphere reflectance spectra from the Medium Resolution Imaging Spectrometer (MERIS) and *in situ* chlorophyll-a (chl-a) observations is used to derive an algorithm for estimating phytoplankton biomass (chl-a) over a wide trophic range (0.5 mg/m^3<chl-a<362 mg/m^3). The algorithm makes use of the chl-a fluorescence and backscatter/absorption features in the red/NIR MERIS wavebands to calculate the maximum-peak height. By plotting the MPH variable in chl-a space, waters dominated by *Microcystis* cyanobacteria may be distinguished from those dominated by diatom/dinoflagellate eukaryotes on the basis of the magnitude of the MPH variable. This, we hypothesize, is due to an enlarged chl-a specific backscatter in the red/NIR associated with vacuolate cyanobacteria.

Results: Distinction of cyanobacteria and eukaryotic phytoplankton

Using a two-layered sphere model to simulate the optical properties of algae and cyanobacteria, evidence is presented for enhanced backscatter resulting from internal vacuoles in prokaryote species as opposed to eukaryotes and non-vacuolate prokaryotes. Two layered sphere population model results and radiometry are used to provide some evidence for the increased magnitude of the 709 nm reflectance observed in *Microcystis* dominant waters. Furthermore, a new flagging procedure based on cyanobacteria-specific spectral pigmentation and fluorescence features between 620 and 681 nm enables cyanobacteria-dominant waters to be further distinguished.

Applications: Time series analysis

Time-series applications of the MPH algorithm and the cyanobacteria-flag to South African and global study areas demonstrate how these techniques might be applied for effective monitoring and frequency analysis of high-biomass cyanobacterial blooms. The MPH algorithm also provides a suitable alternative when targeting high-biomass (chlorophyll-a > 20 mg/m^3), turbid and spatially constrained waters since conventional ocean colour algorithms are generally poorly parameterised for use in these environments.

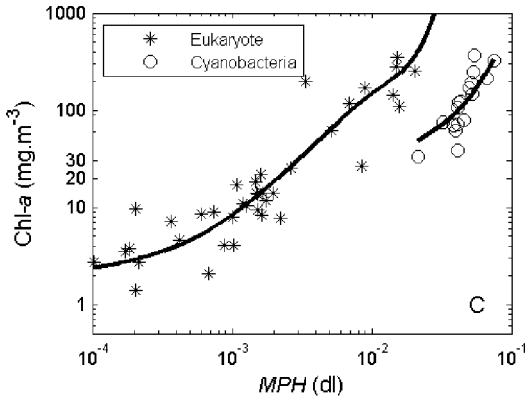

Figure 1 Chl-a versus MPH variable showing separation of cyanobacteria and eukaryotic algae

References

[1] Matthews, M. W., Bernard, S., & Robertson, L. (2012). An algorithm for detecting trophic status (chlorophyll-a), cyanobacterial-dominance, surface scums and floating vegetation in inland and coastal waters. Remote Sensing of Environment, 124, 637–652. doi:10.1016/j.rse.2012.05.032b

MARINE COLLABORATIVE GROUND SEGMENT: OVERVIEW OF THE OCEAN COLOUR RADIOMETRY PLATFORM

Constant Mazeran[1], Odile Fanton d'Andon[1]

[(1)]ACRI-ST, 260 route du Pin Montard, BP 234, Sophia-Antipolis, France

Email: constant.mazeran@acri-st.fr

MCGS (Marine Collaborative Ground Segment) is a project aimed at making the most of ESA Sentinels satellites' potential for users driven services based on high level products. MCGS addresses the need of the European Space Agency to build up data processing centers in conjunction with the Copernicus Program for the provision of services to local and national, public and private European institutions or entities involved in marine activities. For its innovative content, MCGS has been nominated by the professional clusters "pole Mer PACA", "pole Mer Bretagne" & "Aerospace Valley".

Lead by ACRI-ST and involving 8 French organisations specialised in space oceanography (ACRI-ST, CLS, IFREMER, SHOM, GIS-COOC/LOV, GIS-BRETEL, LEGOS, AS+), MCGS is developing satellite-based services through three dedicated processing centres, complementing the Sentinel "core products", in a collaborative approach with ESA/EUMETSAT: an ocean colour radiometry platform (Sentinel-3 and Sentinel-2), a topography platform (Sentinel-3), and a wind/wave/current platform (Sentinel-1). It will provide environmental information for operational monitoring & support, optimisation of human and material means, respect of regulation at sea and coastal areas.

This presentation will give an overview of the ocean colour radiometry platform, in term of data management, complementary and tailored processing, targeted services and demonstration products.

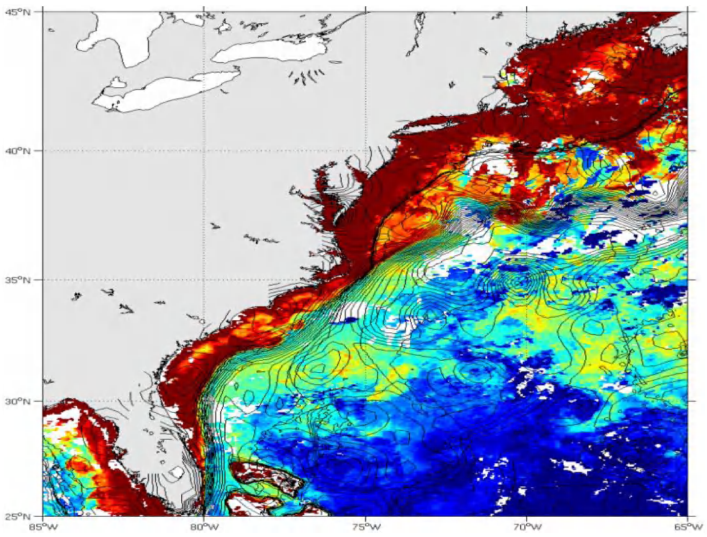

Example of MCGS precursor service in support to oceanographic campaign: chlorophyll map from GlobColour off the US East coast in 2012, with overlaid Sea surface height from AVISO, as used for Tara Oceans

ODESA, A TOOL FOR THE IMPLEMENTION AND VALIDATION OF OCEAN COLOUR ALGORITHMS

Christophe Lerebourg[1], Nicolas Gilles[1], Julien Demaria[1], Olivier Sardou[1], Constant Mazeran[1], Véronique Bruniquel[2], Ludovic Bourg[1], Odile Fanton d'Andon[1], Philippe Goryl[3], Henri Laur[3]

[(1)]ACRI-ST, 260 route du Pin Montard, BP 234, Sophia-Antipolis, France

[(2)]ACRI-ST, 8 esplanade Compans-Caffarelli, Toulouse, France

[(3)]ESA/ESRIN, Via Galileo Galilei CP 64, Frascati, Roma, 00044, Italy

Email: christophe.lerebourg@acri-st.fr

Summary

ODESA is the Optical Data processor of the European Space Agency. Its main feature is ODESA software (*Figure 1*) which has been developed to provide the scientific community with a complete level 2 processing environment for MERIS data. Three additional and complementary facilities are also available through ODESA system: ODESA online processing facility, a validation and qualification tool linked to MERMAID facility and a dedicated forum to help and foster ESA optical sensor community. All ODESA features are accessible through a single web page: http://earth.eo.esa.int/odesa/.

ODESA software provides users with the binary codes and the source codes of MERIS level 2 Ground Segment prototype processor (MEGS) in a user friendly environment (Java GUI). ODESA software basic feature allow users to process level 1 to level 2 images, access all intermediate variables of MERIS level 2 processing chain, select region of interest, able or disable land, cloud or water branches, modify Auxiliary Data File (ADF) configuration. Alternative products like fully normalized water leaving reflectance or GSM products are already implemented in ODESA software. Level 2 outputs can be generated either in native ENVISAT or NetCDF format, readable in BEAM. Advanced features allow users to implement custom product in the processing chain. MEGS is written in C language but any routine developed in a compiled language like C++ or Fortran can be implemented in the processing chain. A quick start guide and a detailed tutorial are available to beginners on ODESA webpage. Training sessions are regularly proposed to users in addition to support provided on ODESA forum. An essential feature of the software is it capacity to process text file and notably MERMAID level 1 data files. It is unique and fundamental aspect of ODESA since it provides users with the capacity to validate a remote sensing product against a representative among of consolidated in situ measurements. In situ measurements available include AOPS, IOPs and biogeochemical measurements. Last but not the least, ODESA software is evolving to offer the capacity to process next generation of ESA optical sensors, namely OLCI and SLSTR on-board sentinel-3.

ODESA online is as a web based facility that provided MERIS level 1 and level 2 products on user selected regions. Data are available in 2nd and 3rd reprocessing versions.

The validation and qualification tools allow users to access MERMAID database and assess the performance of new algorithms against in situ measurements. Qualified algorithms can be implemented on a dedicated cluster for mass processing and comparison against nominal ESA processing.

Finally ODESA forum provide users with a tool to resolve any issue related to ODESA, MERIS data and MERIS data processing.

ODESA system therefore provide comprehensive tools to process, implement, analyse and validation remote sensing optical data.

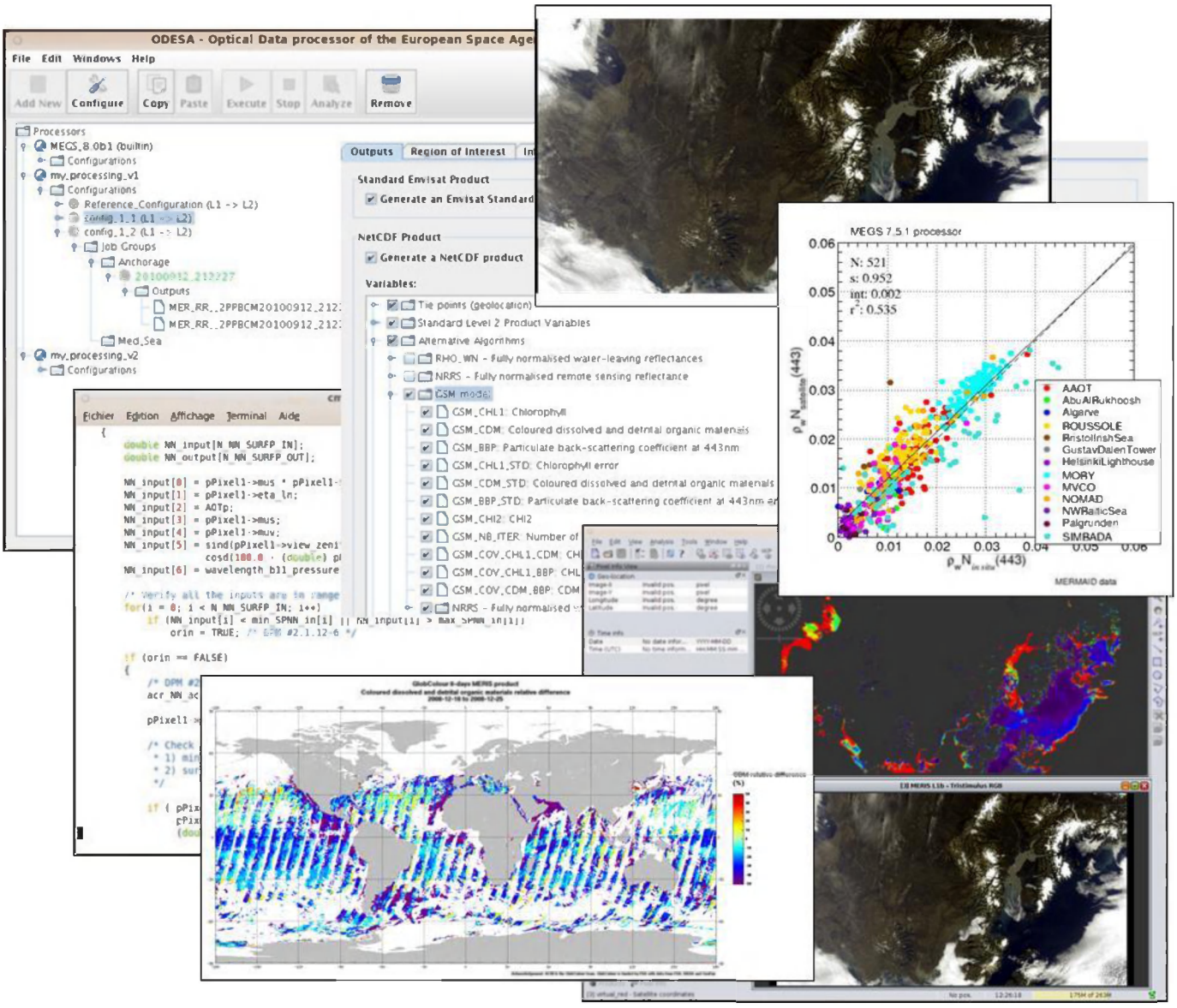

Figure 1: Screenshot from ODESA facility

KALICOTIER: A DEMONSTRATION DATA SERVER TOWARD DEDICATED EARTH OBSERVATION SERVICES IN THE COASTAL ZONE

Christophe Lerebourg[1], Arnaud Selle[2], Constant Mazeran[1], Patrice Henry[2], Hélène de Boissezon[2]

[(1)]ACRI-ST, 260 route du Pin Montard, BP 234, Sophia-Antipolis, France
[(2)]CNES, 18 avenue Edouard Belin, Toulouse, France
Email: christophe.lerebourg@acri-st.fr

Around 44% of the world's population lives within 150km of the coast. Therefore, an important part of economic activities take place in the coastal zone: marine related activities (fisheries, fish farming, shipping, mining, leisure …) as well as terrestrial activities concentrated around urban centres. Being at the interface between land and ocean, the coastal zones are under the influence of a complex mixture of natural and anthropogenic phenomena originating from both oceans and lands. For the latest, river discharge which carries pollution originating from agricultural, industrial and domestic activities of the entire river basin is a major contributor on coastal environment. As a consequence, the coastal zone is the major place of interest for environmental and safety monitoring. This complexity leads to an important need of integrated coastal management in which remote sensing can play an important part from long term monitoring to fast analysis and response to natural or industrial hazards.

In order to address these needs, the Kalicotier demonstration data server has been funded by CNES as part of the GIS COOC data portal (French Scientific group in Ocean colour). This portal, dedicated to coastal satellite data and available at http://kalicotier.gis-cooc.org is an ocean colour data server providing extensive remote-sensing datasets for the study of coastal regions of major oceanographic interest. Kalicotier so far provides an easy and fast access to MERIS Full Resolution data (300m) on five coastal sites: Ligurian Sea, English Channel, Bay of Biscay, New Caledonia and Vanuatu Islands and the South Vietnam region. Each site is managed in partnership with a researcher of the scientific community locally involved in the region, who insures relevance and update of the information. The objective of Kalicotier is to demonstrate on a limited number of coastal sites the utility of providing comprehensive satellite time series. If relevant, data from other sensors will be added to the data portal. This could include other ocean colour sensors (SeaWiFS, MODIS, VIIRS, OLCI) as well as other data type (SST, SSH, wind speed, broad band high resolution radiometric sensors). Ultimately, the concept would be extended and integrated in operational services with a focus on NRT and RT data dissemination.

The specificity of the coastal zone regarding atmospheric correction has put forward the need to provide to users an improved algorithm SAABIO (Semi Analytical Atmospheric and BIO-optical processor), described hereafter. Together with the satellite data, Kalicotier provides validation plots for each selected area thanks to long term in situ acquisition systems (notably BOUSSOLE, AERONET-OC and SOMLIT) and oceanographic cruises provided by institutional partners. Main features of Kalicotier portal are (figure 1):

1. Access to full time series of MERIS FR Level 1 and Level2 products (NetCDF format) over five coastal regions.

2. Access to two processing version (MERIS 3rd reprocessing and an experimental processor, SAABIO, described hereafter)
3. Extraction capability of single Level 2 products from NetCDF files to reduce storage volume in users facilities
4. Fast and easy visualization of all MERIS products
5. Visualization tool to select none cloudy images
6. Validation plots of satellite data against in situ measurements
7. Data are restricted to research and educational

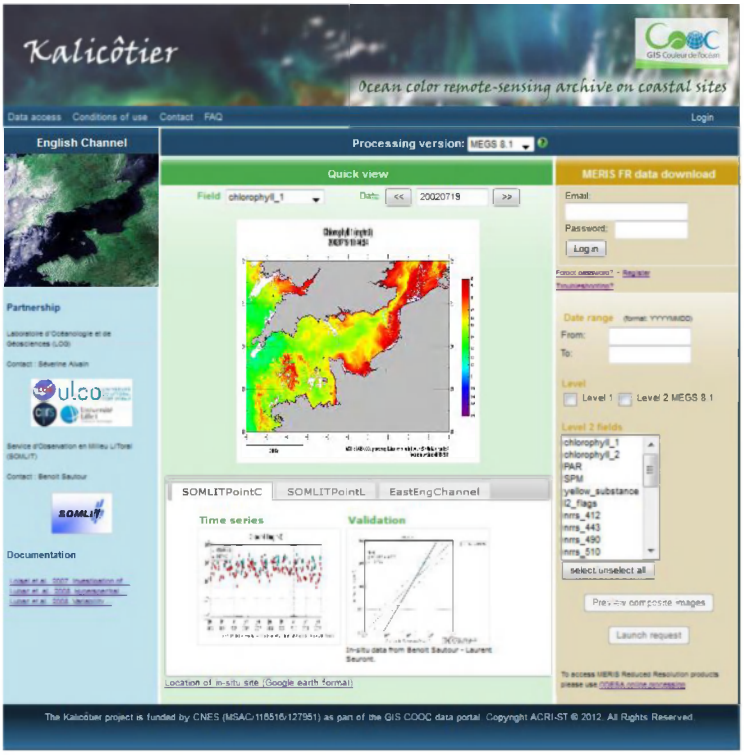

Figure 1 Kalicotier web page, http://kalicotier.gis-cooc.org

SAABIO is an experimental processor developed by CNES and ACRI-ST, alternative to the Case 2 neural network of the MERIS 3rd reprocessing. It is based on:

1. An alternative Bright Pixel Atmospheric Correction, using a semi-analytical approach to retrieve residual marine reflectance in the red and near-infrared;
2. The GSM, semi-analytical bio-optical model to retrieve Chl, bbp and cdm;

Kalicotier is foreseen to evolve in the near future and users are invited to express their needs for evolution, providing other alternative algorithms, requiring for other EO data as well as suggesting evolution of the data portal itself. The purpose of the presentation is the description of the SAABIO algorithms and the main outcomes of the reprocessing as well as the usages carried out from the Kalicotier datasets.

Past Observations and Future Challenges for Ocean Color Remote Sensing

Charles McClain

[2]NASA Goddard Space Flight Center, Ocean Ecology Laboratory, Greenbelt, MD, USA

Summary

About 40 years ago, an ocean color sensor to be flown on the NASA Nimbus-7 earth observation satellite was proposed and approved. The sensor was called the Coastal Zone Color Scanner (CZCS). The CZCS was a technology demonstration as the only previous remote sensing measurements had used simple airborne sensors, e.g., nadir viewing only. The CZCS proved much more successful than ever anticipated, particularly over the open ocean ironically, in providing quantitative estimates of pigment concentrations (chlorophyll-a + phaeophytin) and diffuse attenuation coefficients. As a result of this success, a variety of sensors with ocean color measurement capabilities have been launched by a number of space agencies. Those providing global observations include the Sea-viewing Wide Field-of-View Sensor (SeaWiFS, US), the Ocean Color and Temperature Scanner (OCTS, Japan), the Moderate Resolution Imaging Spectroradiometer (MODIS, US), the Medium Resolution Imaging Spectrometer (MERIS, Europe), the Global Imager (GLI, Japan), and the Visible and Infrared Imaging Suite (VIIRS, US). A number of future global ocean color missions are in the planning or development phases, e.g., the Second Generation Global Imager (SGLI, Japan), the Ocean and Land Colour Imager (OLCI, Europe), and the Ocean Ecology Sensor (OES, US). As requested by the IOCS planning committee, this presentation focuses on a "top ten" list of specific projects, events, and developments that this presenter feels played a major role in advancing the field of ocean colour remote sensing. The selections emphasize activities initiated and lead by members of the research community that reflect outstanding team work, initiative, and vision. An "honorable mention" list is also included, but not discussed in any detail, because of the numerous noteworthy contributions. Certain publications are highlighted as related to the particular entries in the top ten list, but no single publication is listed as a "top ten" entry because of the huge volume of outstanding research.

Selecting the "top ten" accomplishments is indeed challenging and the presenter spent much time deliberating on the list and will discuss the rationale for the selections, identifying key individuals involved in each as best possible. The order is intended to be chronological rather than a ranking of importance so as to "tell the story" of satellite ocean color remote sensing to date.

The conveners also asked for a perspective on the challenges that lay ahead for our community. There are a number of political, financial, and technical hurdles before us and the presenter will outline a number of these.

Towards Improved Scattering Correction for In Situ Absorption and Attenuation Measurements.

David McKee[1], Rüdiger Röttgers[2], Jacek Piskozub[3] and Rick Reynolds[4]

[1]University of Strathclyde, Physics Department, Glasgow, G4 0NG, Scotland
[2]Helmholtz-Zentrum Geesthacht, Centre for Materials and Coastal Research, Geesthacht, 21502, Germany
[3]Institute of Oceanology PAS, Sopot, 81-712, Poland
[4]Scripps Institution of Oceanography, University of California San Diego, La Jolla, California, 92093-0238, USA
Email: david.mckee@strath.ac.uk

Summary

The performance of several scattering correction schemes for reflecting tube absorption and beam attenuation measurements is evaluated with data collected in European shelf seas. Standard scattering correction procedures for absorption measurements perform poorly due to non-zero absorption in the near infrared and wavelength-dependent scattering phase functions. Two new approaches to correct in situ ac-9 absorption and attenuation are presented. The first is an empirical approach based upon observations of non-zero NIR absorption using a Point Source Integrating Cavity Absorption Meter (PSICAM). The second is a revised iterative correction method based upon Monte Carlo simulations of the optical layout of the ac-9 instrument, and uses coincident backscattering measurements to estimate scattering phase function for correction of scattering losses for both absorption and attenuation measurements. The updated Monte Carlo scattering correction provides excellent agreement with independent absorption and attenuation measurements made with a Point Source Integrating Cavity Absorption Meter (PSICAM) and a LISST (Laser In Situ Scattering and Transmissometry; Sequoia Sci.) respectively. Implications for historic data sets and requirements for application to future data sets are discussed.

Introduction

The propagation of light through seawater is regulated by the effect of the optical properties of the water itself and of materials suspended and dissolved within the medium. The spectral absorption, $a(\lambda)$, and attenuation, $c(\lambda)$, coefficients are fundamental optical characteristics of the medium. Measuring the absorption of dissolved substances is normally straightforward and can be easily achieved for normal practical error expectation levels using simple spectrophotometric methods. However, measuring the absorption of turbid media is considerably more complicated due to the effect of scattering on measured signals [1]. Various approaches to resolve this issue have been attempted, with the reflecting tube absorption meter (WET Labs ac-9/-s) becoming a widely adopted instrument within the optical oceanography community for measuring in situ absorption. This method uses total internal reflectance at the flow-tube walls to redirect a portion of the scattered light towards a diffuser in front of a large area receiver with the aim of minimising scattering losses. Even with this setup, it is necessary to perform a scattering correction to account for residual scattering losses [2]. These residual scattering losses can be quite substantial in turbid waters. To date there has not been a thorough validation of the efficacy of the various proposed scattering correction methods for WET Labs ac-9 absorption data using field data. The attenuation of seawater is measured by focusing a transmitted collimated beam of light

onto a small aperture and detecting the photons that have not been absorbed or scattered, b(λ), with c(λ)=a(λ)+b(λ). As a result of the aperture having a finite diameter, the optical arrangement has a characteristic collection angle, ψ_c, which is a source of scattering error for the attenuation measurement. Boss et al. [3] recently demonstrated that uncorrected WET Labs ac-9 attenuation values are approximately 50 – 80% of equivalent LISST attenuation data, with the two instruments having in water scattering collection angles of ~0.9 and ~0.027° respectively.

Discussion

The development of a functional PSICAM by Röttgers *et al.* at HZG has provided a new opportunity to validate in situ ac-9 absorption measurements. Two new scattering error approaches are presented here. The first stems from observation of an empirical relationship between the measured ac-9 absorption signal in the NIR and corresponding PSICAM data. This permits calculation of a non-zero NIR offset correction which, together with additional weighting of attenuation values reflecting the observations of Boss et al., provides a new simple empirical scattering correction equation

$$a_{ac9}(\lambda) = a_m(\lambda) - (a_{m715} - a_{715})\left[\frac{(1/e_c)c_m(\lambda) - a_m(\lambda)}{(1/e_c)c_{m715} - a_{715}}\right] \quad (1)$$

The second ac-9 correction method is based upon a revised Monte Carlo simulation of the absorption flowtube optical layout and uses backscattering measurements in an iterative process to estimate the scattering phase function, enabling correction of both absorption and attenuation data. As well as requiring additional b_b information, this method requires PSICAM validation data to select an appropriate wall reflectance for the absorption flowtube. This parameter is found to vary between ac-9 instruments. ac-9 data corrected using this method matches PSICAM values over a very wide range of IOP conditions.

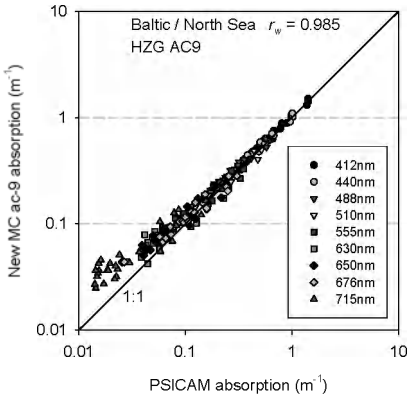

MC corrected ac-9 data matches PSICAM values

Conclusions

Accurate inherent optical property measurements are essential for interpretation of ocean colour remote sensing signals and for full exploitation of radiative transfer simulation capabilities. We are working towards new correction methods for ac-9 data in the hope that both new and historic data sets can be improved, particularly in turbid coastal waters. Initial results are very encouraging though further work is required to fully establish the extent to which the new methods can be applied across the field.

References

[1] Stramski, D. and Piskozub, J. (2003) Estimation of scattering error in spectrophotometric measurements of light absorption by aquatic particles from three-dimensional radiative transfer simulations. Appl. Opt., 42: 3634-3646.

[2] Zaneveld, J. R. V., Kitchen, J. C. and Moore, C. M. (1994) The scattering error correction of reflecting-tube absorption meters. Proc. SPIE 2258: 44-55.

[3] Boss, E., Slade, W. H., Behrenfeld, M. and Dall'Olmo, G. (2009) Acceptance angle effects on the beam attenuation in the ocean. Opt. Expr., 17: 1535-1550.

In search of long-term trends in the ocean colour record

F. Mélin[1]

[1] E.C. Joint Research Centre, Institute for Environment and Sustainability, Italy
Email: frederic.melin@jrc.ec.europa.eu

Summary

The use of ocean colour data records for trend detection and climate research is presented, particularly in terms of requisites and challenges. A major concern is the existence of significant differences between mission-specific data sets that need to be properly accounted for before these data sets can be combined for time series analyses. The cases of the remote sensing reflectance and the chlorophyll-a concentration are illustrated and their quality as consistent multi-mission data records is discussed.

Introduction

Constructing a long-term record of ocean colour data suitable for monitoring activities or climate research necessitates a suite of successive satellite missions, considering that missions may have a typical life time of 5-10 years. But flying a continuous suite of missions is obviously not sufficient to allow quantitative temporal analyses such as trend detection. First, each mission-specific series needs to possess certain characteristics minimizing the possibility that variations in the data record be the result of changes in the processing environment: a fully characterized calibration history of the instrument, a consistent set of ancillary data, a stable set of algorithms, etc... Then, combining data records from various ocean colour missions for time series analyses may introduce spurious temporal artifacts resulting from inter-mission systematic differences. Eventually, constructing a consistent multi-mission data record requires a thorough knowledge of each mission-specific series, and complete inter-mission comparisons. A direct implication is that this effort is fundamentally connected to, and dependent on, mission temporal overlaps.

The presentation will focus on the two ocean colour variables considered as essential climate variables (ECV) by GCOS [1], the spectrum of water-leaving radiance (or remote sensing reflectance, R_{RS}) and the concentration of chlorophyll-a (Chla). In both cases, the emphasis is on inter-comparison results and the implications in terms of data set consistency and trend detection.

Analysis of the remote sensing reflectance data record

A complete inter-mission comparison is conducted on the SeaWiFS, MODIS-Aqua and MERIS R_{RS} data sets. This is done by accumulating the matching pairs of R_{RS} spectra for each spatial bin and day over the periods of mission overlaps. Before comparison, differences in spectral band specifications between sensors are also accounted for using a bio-optical model.

The inter-comparison statistics document two major characteristics of the R_{RS} data sets. First, a spatially resolved estimate of the random error of the R_{RS} uncertainty budget for SeaWiFS, MODIS and MERIS is computed through an analysis of variance and covariance terms over the comparison ensemble. Then, it

is particularly important to assess, and correct for, inter-mission biases since they can lead to artificial trends in combined data sets that would lessen the usefulness of the series for climate studies. Inter-mission biases vary with wavelength, time and space, but they show well defined spatial patterns that are discussed using a new optical classification. The development of inter-mission bias models is introduced.

Time series analysis of chlorophyll-a concentration

Differences existing between the monthly time series of Chla from SeaWiFS, MERIS, MODIS-Aqua and MODIS-Terra are also analyzed through various statistical indicators like average differences, correlation, or their inherent variances. The trends displayed by each mission are also illustrated, showing significant differences between them (example on figure; updated from [2]).

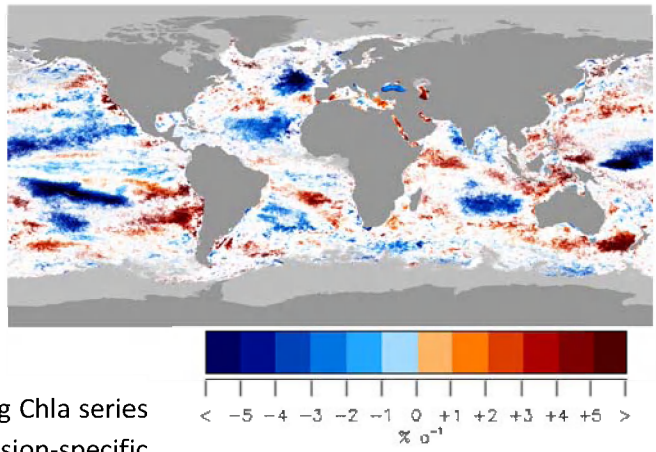

Trends for SeaWiFS Chla, 1998-2007 (non-parametric seasonal Kendall, statistics, p<0.05). Only statistically significant trends are shown. Grey areas show points with not enough data for analysis.

Trends are then computed on data sets combining Chla series from different missions, and compared with mission-specific trends. The part of these trends resulting from biases between missions is analyzed using artificial series made of climatologies. Finally, the level of inter-mission biases that can be tolerated for trend detection is discussed.

Conclusion

Ideally, the field of ocean colour should move from a mission-centric stance to a variable-centric distribution more attractive for users. Besides the continuous presence of ocean colour instruments in space, this requires a continued effort to produce a multi-mission consistent data record and appropriate statistical approaches to account for remaining inter-mission differences.

Acknowledgements

NASA and ESA are duly acknowledged for the distribution of satellite data. This work has been supported by various colleagues, the contributions of which are warmly recognized.

References

[1] GCOS (2011). Systematic observations requirements for satellite-based data products for climate. Supplemental details to the satellite-based component of the Implementation Plan for the Global Observing System for Climate in Support of the UNFCCC.

[2] Vantrepotte, V., and Mélin, F. (2011). Inter-annual variations in the SeaWiFS global chlorophyll *a* concentration (1997-2007). Deep-Sea Res., I, 58, 439-441.

A SATELLITE NET PRIMARY PRODUCTION (NPP) ALGORITHM FOR THE SOUTHERN OCEAN BASED ON A VARIANT OF THE VGPM FRAMEWORK - PERFORMANCE EVALUATION AND TIME-SERIES APPLICATIONS

B. Greg Mitchell[1], Rick Reynolds[1], Mati Kahru[1], Christopher Hewes[1], Brian Schieber[1], John Wieland[2], Brian Seegers[2], Osmund Holm-Hansen[1]

[1]Scripps Institution of Oceanography, La Jolla, CA 92037, USA
[2]University of Southern California, Los Angeles, CA 90089

Summary

We present a synthesis and analysis of Southern Ocean in situ data for chlorophyll a (chl-a) and net primary production (NPP). Due to differentiation in the bio-optical properties of the Southern Ocean, we have developed the OC4ANT chl-a ocean color algorithm and the VGPMANT NPP algorithm. Implications for the quantitative differences between our approach based on a synthesis of data from more than 20 cruises to the Southern Ocean over 15 years, and the standard algorithms developed with low latitude data will be discussed.

Introduction

The Southern Ocean (SO) has bio-optical properties that are differentiated from lower latitudes, as first demonstrated by Mitchell and Holm-Hansen (1991). An alternative Southern Ocean chl-a algorithm has been developed by Mitchell and Kahru (2009; Figure 1A). Behrenfeld and Falkowski (1997) developed the Vertically Generalized Productivity Model (VGPM) for net primary production (NPP) that has proven relatively robust for much of the global oceans at lower latitudes. However, we find that some of the parameterizations of the VGPM NPP algorithm require tuning. Specifically our VGPMANT model differs in the estimate of Zeu from chl-a. We also optimized the estimate of Pbopt from SST. These new revisions were based on data from 12 SO cruises we carried out to diverse parts of the SO resulting in our modified model, VGPMANT. We evaluate VGPMANT using an in situ data set of 672 ship observations of NPP, PAR, chl-a and SST.

Discussion

The differences in bio-optical properties, in particular low concentrations of colored dissolved organic matter (CDOM) and larger phytoplankton with significant pigment packaging lead to differentiation in the reflectance vs chl-a relationship in the Southern Ocean. Backscattering differences are also noted but do not play a large role in the band ratio off sets which are dominated by absorption differences of the Southern Ocean compared to low latitude data sets. This also affects the penetration of PAR and hence the estimated depth of the euphotic zone, a parameter in the VGPM model framework for NPP. Figure 1A summarizes our data and algorithm for chl-a and Figure 1B shows the performance of VGPMANT with a large in situ validation data set we have synthesized.

Applying our algorithms to the Southern Ocean satellite time series reveals that the standard algorithms can underestimate chl-a and NPP by up to a factor of 2. OC4ANT performs better than the original VGPM and several other models we have tested. We apply OC4ANT and VGPMANT to time-series of the SO with a primary focus on the Drake Passage region. Major interannual variations in NPP will be discussed in relation to regional forcing including sea ice and bathymetry-steered circulation of the Drake Passage.

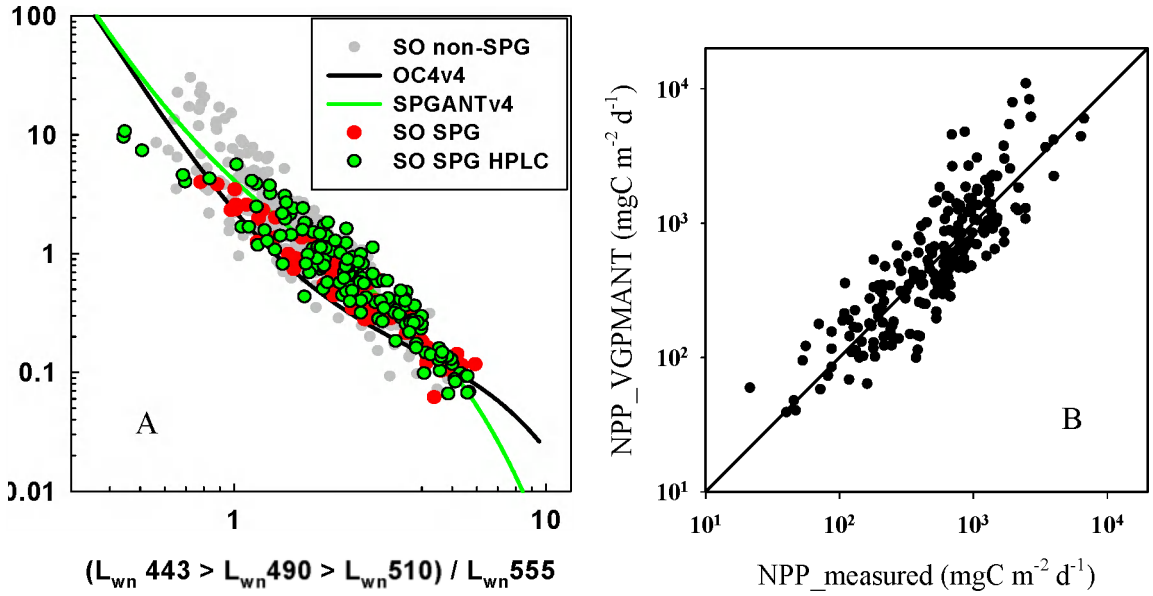

Figure 1. A. Chlorophyll plotted vs an OC4 Maximum Band Ratio for our Southern Ocean data (red fluorometric chl-a, green HPLC chl-a) and NOMAD Southern Ocean data from other groups (gray). The black line is NASA standard OC4v4 fit and the green line is our OC4ANT fit to our data sets. There is large divergence with the NASA standard underestimating chl-a by up to 2-3x for chl-a values in the range 0.5-5 mg m^3. **B.** Net primary production (NPP) measured at sea using 14C bicarbonate methods (our data merged with data of Saba et al. 2012) compared to the estimate using our VGPMANT algorithm. Our VGPMANT has slope of 1 and almost no bias compared to in situ data and agreed better than the standard VGPM or other models we tested with our merged in situ validation data set.

Conclusions

Using a synthesis of optics, chl-a and NPP data from more than 20 cruises over 15 years, we validate the original concepts of bio-optical differentiation in the Southern Ocean reported first by Mitchell and Holm-Hansen (1991) . The data are used to develop OC4ANT and VGPMANT, Antarctic variants of the classic maximum band ratio approach for chl-a (OC4) and VGPM for NPP. There is a need to explore how best to implement these Southern Ocean algorithms in global processing of ocean color data.

References

[1] M. J. Behrenfeld and P. G. Falkowski, (1997). A consumer's guide to phytoplankton primary productivity models, Limnol Oceanogr 42(7), 1479.

[2] Mitchell, B. G. & Holm-Hansen, O. 1991. Bio-optical properties of Antarctic Peninsula waters: Differentiation from temperate ocean models. *Deep-Sea Research I*, 38(8/9): 1,009-1,028.

[3] Mitchell, B. G. & Kahru, M. 2009. Bio-optical algorithms for ADEOS-2 GLI. *J.Remote Sensing Soc.of Japan*, 29(1): 80-85.

Analysis of recent dust storm over the Indian region using real time multi-satellite observations from direct broadcast receiving system at IMD

A.K MITRA and A.K SHARMA

National Satellite Meteorological Center, India Meteorological Department, New Delhi
ashimmitra@gmail.com

Summary

In this study, observations from microwave satellites, visible and infrared instruments have been analyzed to detect dust storm over north and north-west part of India during 18 to 23 March 2012. This study investigated the approaches to utilize the multi satellite data of Moderate Resolution Imaging Spectroradiometer (MODIS) onboard Terra and Aqua satellite and the Advanced Microwave Sounding Unit (AMSU) onboard NOAA satellite to study the characteristics of dust storms from real time direct broadcast (DB) receiving system installed at three places of India Meteorological Department (IMD). Microwave measurements are used to detect the dust storm underneath clouds and ice clouds, while visible and infrared measurements are utilized for delineating the cloud-free dust systems. The dust storm detection is based on infrared brightness temperature (BT) difference between channels at 11 and 12 μm and polarized BT difference between two channels of 89 GHz and 23.8 GHz. It is found that the significant differences between the BT of channel 89 and channel 23.8 can be used as a discriminator of identifying dust storm. Finally, the occurrence of dust outbreaks has also been validated with skyradiometer of IMD, which confirms the presence of a dust storm over the Indian region.

Introduction

Dust storms are common in the northwest part of the Indian sub-continent covered by Thar Desert, which is a primary source of dust storms in south Asia. The dust outflow over the region exhibits a marked seasonality with higher frequency and intensity during dry pre-monsoon season between March to May. As a consequence, dust strongly affects the aerosol characteristics over these regions as it is mixed with local anthropogenic pollution. Several techniques have been proposed for detecting dust and volcanic ash using thermal–infrared observations (Ackerman, 1997; Singh et al.,2008). Ackerman (1997) suggested in his study that a combination of three IR channels near the 8, 11, and 12 μm band is likely to provide a more robust way to identify dust. He also outlined the usefulness of BT differences either in two or three channels for detecting the dust storms. However, the most common dust storms are those caused by strong winds behind a cold front and generally coexist with cirrus. Because the visible–infrared radiance is primarily sensitive to the upper cirrus cloud layer, especially when the upper-layer cirrus is thick, the temperature difference approach is not very useful to detect dust under cirrus areas whereas the microwave radiation is not significantly scattered or absorbed by ice clouds.

Discussion

Dust screening using AMSU channel 23.8 and 89 GHz BT from NOAA satellite

The microwave region of the electromagnetic spectrum has longer wavelengths compared to the visible and ultraviolet regions. However, the dimension of dust particles is larger than that of the normal aerosol particulates, but is similar to the incident wavelength of microwave radiation. Therefore, Mie scattering is dominant when sand particles are about the same size as the radiation wavelength. This type of scattering takes place in the lower atmosphere less than 4.5 km, where larger particles are more abundant. The shorter the wavelength of the incident radiation in the microwave range, the greater the scattering and hence the BT is lower (El-Askary et al., 2003). AMSU-A on-board the NOAA satellite is primarily a temperature sounder operating in 15 frequency channels ranging from 23.8 to 89 GHz and has 40 kms horizontal spatial resolution at Nadir. The first and last channels, 23.8 and 89 GHz respectively, provide the surface information. In the present study, we have used the 23.8 GHz and 89 GHz frequency channel (vertically polarized - horizontal polarized) from AMSU-A. The

difference between polarized channels of 23.8 and 89 GHz could represent the scattering signature of dust aerosols because the scattering in Mie regime tends to depolarize the surface polarization. Huang et al., (2007) have shown that the difference (ΔBT) between lower frequency (23.8 GHz) and higher frequency (89 GHz) can be used as a benchmark to detect dust regions. Figure-6 (a, b, c) shows the polarized difference of scatter plot of Tb89 GHz (AMSU Channel 15) and Tb23.8 GHz (AMSU Channel 15) for three dust storm cases during March, April and June 2012. It can be seen from the figures that the Tb of channel 89 and channel 23.8 is much larger in the dusty region (shown in the red color) but for other than dust such as cloud, water cloud and precipitation particles the difference is much lower (<273K, shown in the yellow and off blue color). This large difference arises due to the presence of clouds since microwave radiation emanates from much lower dust layers than the top ice cloud radiance. These results suggest that significant differences between the Tb of channel 89 and channel 23.8 can be used as a discriminator of identifying dust storm.

Conclusions

This paper investigated the integrated approach to use the multi satellite data of thermal IR bands from MODIS on-board Terra and Aqua satellite and the microwave data of AMSU on-board NOAA satellite to study the characteristics of dust storms over the Indian region from real time direct broadcast (DB) receiving systems at IMD during March to June 2012. It is found that the thermal IR band difference between channels at 11 and 12 µm, can discriminate against pure dust regions with appropriate thresholds, but it is not so useful for the dust covered by the clouds or water droplets because sometime the BT of the pixels over the water and ice cloud may also scatter emitted radiance with the same peak as dust and complicate the discrimination process. Since microwave radiation can penetrate the ice and clouds, the polarized BT difference between two channels of 89 and 23.8 GHz from NOAA satellite has been analyzed and found that the significant differences between the BT of channel 89 and 23.8 GHz can be used as a discriminator for identifying the dust storm.

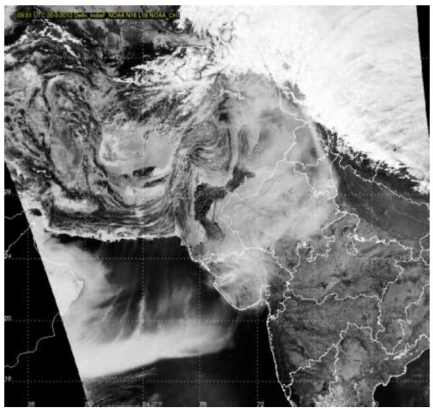

NOAA Channel-1 (1 Km resolution) at 09:31 UTC

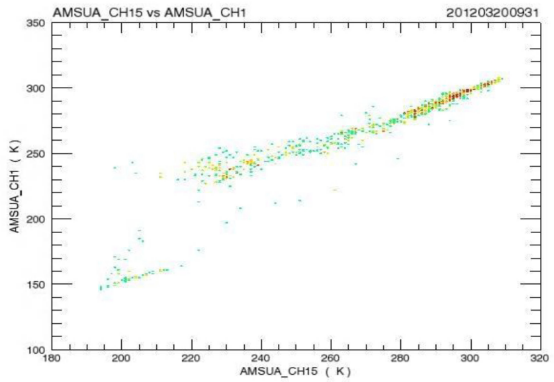

The microwave brightness temperature difference (in K) between BT 89 – BT23.8 on 20/03/2012. The red color represents the cloud free dust region.

References

[1] Ackerman, S. A. Remote sensing aerosols using satellite infrared observations. *Journal of Geophysical Research*, 102(D14), 17,069–17,080. 1997

[2] Singh, RP; Prasad, AK; Kayetha, VK, et al., Enhancement of oceanic parameters associated with dust storms using satellite data, JOURNAL OF GEOPHYSICAL RESEARCHOCEANS Volume: 113 Issue: C11 Article Number: C11008

[3] El-Askary, H., Gautam, R., Singh, R. P., & Kafatos, M. Dust storms detection over the Indo-Gangetic basin using multi sensor data. Advances in Space Research Journal, 37, 728–733. 2006

A hybrid halo-optical remote sensing model for characterizing particulates in the Saint Lawrence Estuary

Montes-Hugo, M.A., Seneville S., St-Onge Drouin S., Mohammadpour G.

Institut des Sciences de la Mer de Rimouski, Université du Québec à Rimouski, 310 Allée des Ursulines, Office P-216, G5L 3A1, Rimouski, Québec, Canada

*corresponding author (e-mail : martinalejandro_montes@uqar.ca, phone: 418-723-1986, ext. 1961)

Abstract

Light attenuation in the St Lawrence estuary (SLE) can be mainly attributed to changes on chromophoric dissolved organic matter and detritus. Thus, the use of optical remote sensing for estimating algal abundance indicators (e.g., chlorophyll a concentration, Chl) or second-order attributes of particulates in the SLE is anticipated to be inadequate unless it is complemented with ancillary environmental information linked to distribution of optical components. A preliminary inversion technique (hereafter, ocean color salinity inversion, OCSI) for estimating Chl and the spectral slope of particulate backscattering (γ) was constructed by combining two remote sensing reflectance ratios in the visible range ($R_{rs}(440)/R_{rs}(510)$, $R_{rs}(670)/R_{rs}(550)$) and concurrent surface (average 0-20 m depth) salinity estimates computed using a regional circulation model. Daily OCSI products at 5 km resolution were obtained from SeaWiFS (Sea-viewing Wide Field-of-view Sensor) imagery and validated with field data collected during May 2000. Preliminary results support the use of OCSI-derived Chl in the lower estuary (relative error up to 25%). In the most productive regions of the SLE (i.e., upwelling zone and north shore), OCSI-derived γ had a direct covariation with a proxy of particle size distribution (the spectral slope of beam attenuation coefficient).

The performance of globally-tuned bio-optical algorithms have been shown to vary in different oceanic basins (Szeto et al, 2011) and different optical environments (Moore et al, 2009). As a consequence, the uncertainties of ocean color products based on these algorithms also vary spatially and are not uniform. Single, bulk statistics without regard to optical environment do not realistically represent how the products are performing spatially. It is important to capture the spatial variation in product uncertainty for assimilation models and for gaining a deeper understanding in how to focus improvements of algorithms to reduce errors in ocean color products. In this work, we present our results of uncertainty analysis on ocean color products for select semi-analytic algorithms. We compare the distribution of uncertainty from matchup data sets for different ocean colors satellites from the viewpoint of optical water types. We also examine these results in the context of how the uncertainties are spread over optical water types using the NOMAD data set. While using matchup data sets has its own sources of error, these comparisons shed light on how algorithms and satellite products are faring for different water types and different sensors. The approach allows for a mapping of product uncertainty by water type for different satellites. These are companion (yet independent) products associated with their corresponding ocean color geophysical products.

HICO-Based NIR-red Algorithms for Estimating Chlorophyll-*a* Concentration in Inland and Coastal Waters – the Taganrog Bay Case Study

W. J. Moses[1], A. A. Gitelson[2], S. Berdnikov[3], J. H. Bowles[1], V. Povazhnyi[3], V. Saprygin[3], and E. J. Wagner[1]

[1]Naval Research Laboratory, Remote Sensing Division, Washington, D.C., USA.
[2]Center for Advanced Land Management Information Technologies (CALMIT), University of Nebraska-Lincoln, USA.
[3]Southern Scientific Center of the Russian Academy of Sciences, Rostov-on-Don, Russia.
E-mail: wesley.moses@nrl.navy.mil

Summary

The results presented here demonstrate the strong potential of the spaceborne hyperspectral sensor HICO as a reliable tool for monitoring coastal water quality, which is critically relevant for coastal ocean color research, especially with the recent demise of MERIS. Two-band and three-band NIR-red algorithms, which have been used very successfully with MERIS data for estimating chlorophyll-*a* (chl-*a*) concentration in coastal waters, yielded accurate estimates of chl-*a* concentration when applied to HICO images. Given the uncertainties in the radiometric calibration of HICO, the results illustrate the robustness of the NIR-red algorithms, validate the radiometric corrections applied to HICO data as they relate to estimating chl-*a* concentration in productive coastal waters, and provide an indication of what could be achieved with future spaceborne hyperspectral sensors.

Introduction

Algorithms that use reflectances in the red and near infrared (NIR) regions of the spectrum are suitable for estimating chl-*a* concentration in optically complex coastal waters (e.g., [1]). NIR-red algorithms based on the spectral channels of MERIS have been shown to yield consistent, highly accurate estimates of chl-*a* concentration for inland and coastal waters from various geographic locations (e.g., [2,3]. The recent demise of MERIS has caused a potentially serious gap in the availability of reliable coastal ocean color data, considering the limitations of MODIS for coastal water quality analysis and the fact that no multispectral or hyperspectral sensor with characteristics that are similar to or better than those of MERIS is scheduled to be launched in the immediate future. In this study, we have used data collected from multiple campaigns on the Taganrog Bay to test the ability of the space borne Hyperspectral Imager for the Coastal Ocean (HICO) to provide accurate estimates of chl-*a* concentration and serve as a reliable tool for coastal water quality analysis.

Discussion

Four *in situ* data collection campaigns were undertaken on the Taganrog Bay between July and Sep 2012, resulting in data from 31 stations, with chl-*a* concentrations ranging between 27.06 and 172.77 mg m^{-3}. The following two-band [4] and three-band [1] NIR-red models were applied to HICO images acquired concurrently with *in situ* data collection:

$$\text{Two-Band HICO NIR-red Model: Chl-}a \propto \left[R_{665}^{-1} \times R_{708}\right] \quad (1)$$

$$\text{Three-Band HICO NIR-red Model: Chl-}a \propto \left[\left(R_{665}^{-1} - R_{708}^{-1}\right) \times R_{754}\right] \quad (2)$$

where, *Rx* is the reflectance at *x* nm and $\overline{R}_{665}$ is the average of the reflectances at 662 nm and 668 nm. Both NIR-red models had close linear relationships with chl-*a* concentrations (Fig. 1), with determination coefficients of 0.83 and 0.86. The NIR-red algorithms were validated by the leave-one-out cross validation procedure and found to yield accurate estimates of chl-*a* concentration. For the two-band NIR-red algorithm, the Root Mean Square Error (RMSE) and the Mean Absolute Error (MAE) were only 13.52% and 10.89% of the total range of chl-*a* concentration; the corresponding figures for the three-band NIR-red algorithm were 12.02% and 9.12%, respectively. The NIR-red algorithms were used to generate chl-*a* maps that accurately portrayed the spatial and temporal variation of chl-*a* concentration in the bay.

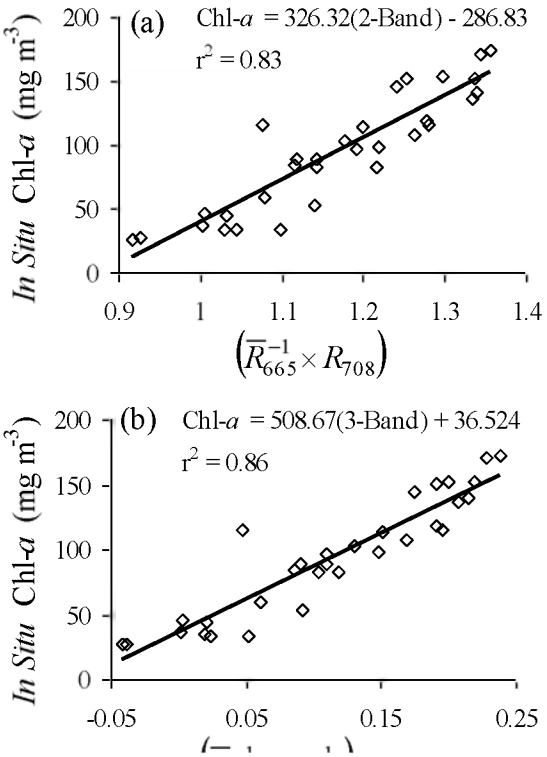

Fig. 1. Plots of chl-*a* concentrations measured in situ versus the (a) two-band and (b) three-band NIR-red model values.

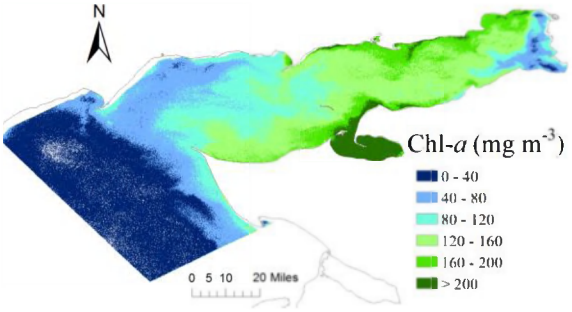

Fig. 2. Chl-*a* map generated from a HICO image using the two-band NIR-red algorithm.

Conclusion

The accuracy of the results obtained illustrates the robustness of NIR-red algorithms and the potential of HICO as a reliable tool for monitoring water quality in coastal waters. It also validates the radiometric and atmospheric corrections applied to HICO [5] as they relate to estimating chl-*a* concentration.

References

[1] Dall'Olmo, G. and Gitelson, A. A. (2005). "Effect of bio-optical parameter variability on the remote estimation of chlorophyll-a concentration in turbid productive waters: experimental results", *Appl. Opt.*, 44(3): 412-422.

[2] Moses, W. J., Gitelson, A. A., Berdnikov, S., Saprygin, V., and Povazhnyi, V. (2012). "Operational MERIS-based NIR-red algorithms for estimating chlorophyll-*a* concentrations in coastal waters – The Azov Sea case study", *Remote Sens. Environ.*, 121: 118-124.

[3] Gitelson, A. A., Dall'Olmo, G., Moses, W., Rundquist, D. C., Barrow, T., Fisher, T. R., Gurlin, D. and Holz, J. (2008). "A simple semi-analytical model for remote estimation of chlorophyll-a in turbid waters: Validation", *Remote Sens. Environ.*, 112(9): 3582-3593.

[4] Gitelson, A. (1992). "The peak near 700 nm on radiance spectra of algae and water - relationships of its magnitude and position with chlorophyll concentration", *Int. J. Remote Sens.*, 13(17): 3367-3373.

[5] Gao, B. -C., Li, R. -R, Lucke, R. L., Davis, C. O., Bevilacqua, R. M., Korwan, D. R., Montes, M. J., Bowles, J. H., and Corson, M. R. (2012). "Vicarious calibrations of HICO data acquired from the International Space Station", *Appl. Opt.*, 51(14): 2559-2567.

Phytoplankton size variability in the global ocean

C. B. Mouw[1]
[1]Michigan Technological University, Houghton, 49931, USA
Email: cbmouw@mtu.edu

Summary

Phytoplankton groups are important to biogeochemical and food web processes. They can be determined based on their ecological role or cell size and are able to be optically differentiated. In this study, the Mouw and Yoder (2010) approach that retrieves percent microplankton (> 20 µm) within a phytoplankton community is utilized. Variability of satellite-derived percent microplankton across the global ocean is explored in the context of the chlorophyll concentration record from the SeaWiFS and MODIS missions. Empirical orthogonal function analysis is used to identify dominant statistical modes in the phytoplankton size and chlorophyll concentration imagery time series. There is evidence of temporal and spatial decoupling between chlorophyll and phytoplankton size. These cases over broad regions of the global ocean are explored in depth. Implications of the observed variability are investigated in the context of biogeochemistry, carbon cycling and flux.

Introduction

The ecology and biogeochemistry of the world's oceans are tightly interconnected. The physical and chemical environment shape microbial community structure which, in turn, mediates biogeochemical pathways including the export of organic matter to the deep ocean and ocean carbon storage. Phytoplankton are a key part of this community and their functional diversity has biogeochemical implications. Motivated by these factors, recent efforts to observe the abundance and activity of the marine phytoplankton from space have placed emphasis on resolving aspects of this diversity; notably broad functional and size classes. Satellite-based observations are revealing the variability of phytoplankton populations on inter-annual to decadal scales. Satellite retrieved estimates of percent microplankton in the phytoplankton assemblage (S_{fm}) [1] and semi-analytical inversion retrieval of chlorophyll concentration ([Chl]) [2] are considered together to understand the relationship between phytoplankton size and [Chl]. This work provides a quantitative comparison of the temporal and spatial relationship between these parameters for near-surface global ocean waters through the use of empirical orthogonal function analysis.

Discussion

Monthly mean percent microplankton [1] and [Chl] [2] imagery time series were investigated with empirical orthogonal function (EOF) and trend analysis. EOF analysis is used to simultaneously examine both temporal and spatial variability. It is useful for compressing the spatial and temporal variability of time series data into a series of orthogonal functions or statistical modes. The temporal variance of the data can be partitioned into modes, revealing spatial functions having time-varying amplitudes, also known as principle components. Prior to EOF analysis, temporal gaps in the data were filled and the data were temporally demeaned. EOF analysis was run on global images of S_{fm} and [Chl] individually and jointly (figure 1). The individual EOF indicates, that with the exception of ENSO, [Chl] mode 1 amplitude time series displays adjustments to the seasonal cycle. However, the S_{fm} amplitude time series suggests a decreasing trend. An advantage of the joint EOF is that both variables will have the same principle components (time-varying amplitudes), thus making it easy to detect and interpret common temporal (seasonal) patterns. The mode 1 amplitude time series of the joint EOF (figure 1) is very similar to the

mode 1 S_{fm} individual amplitude time series, suggesting the dominant variance in time is related to S_{fm}. Spatially, the greatest variability in both parameters in the equatorial Pacific associated with ENSO. The locations of high variability in the S_{fm} individual and S_{fm} and [Chl] joint spatial patterns correspond to regions of the ocean identified [3] as having significant temporal trends. This spatial correlation suggests phytoplankton size structure plays an important role beyond biomass.

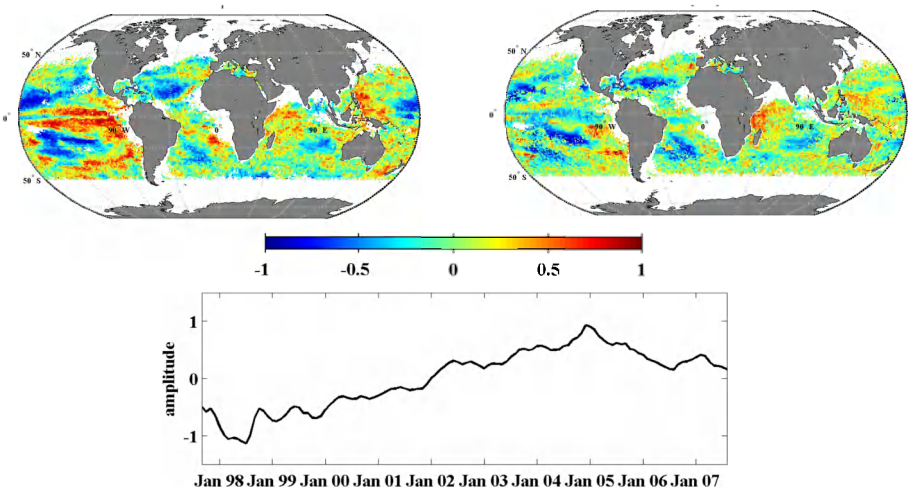

Figure 1. *Mode 1 empirical orthogonal function analysis performed on chlorophyll concentration ([Chl]) and phytoplankton percent microplankton (S_{fm}) jointly. Spatial eigenfunctions for S_{fm} (top left panel) spatial eigenfunctions for [Chl] (top right panel), and time varying amplitudes for both parameters. S_{fm} and [Chl] (bottom panel) both display substantial spatial variability associated with significant temporal variability. It is important to note that S_{fm} and [Chl] spatial variability are not identical, indicating phytoplankton size is not simply responding linearly with [Chl].*

Given ENSO plays such a large role in global spatial and temporal patterns, regional analyses were also carried out to understand emergent patterns at smaller spatial scales. EOF and The decadal climatology and demeaned trends of S_{fm} and [Chl] were determined for the North Atlantic, Equatorial Pacific and Southern Ocean regions.

Conclusions

The EOF analysis indicates S_{fm} and [Chl] spatial variability are not identical, indicating phytoplankton size is not simply responding linearly with [Chl]. In terms of climatology, phytoplankton size generally tracks chlorophyll over an annual cycle but deviations from a linear relationship are evident.

References

[1] Mouw, C., & Yoder, J. (2010). Optical determination of phytoplankton size composition from global SeaWiFS imagery. Journal of Geophysical Research, 115(C12018). doi:10.1029/2010JC006337.

[2] Maritorena, S., Siegel, D., & Peterson, A. (2002). Optimization of a semianalytical ocean color model for global-scale applications. Applied Optics, 41(15), 2705–2714.

[3] Gregg, W., Casey, N., & McClain, C. (2005). Recent trends in global ocean chlorophyll. Geophysical Research Letters, 32(3), L03606. doi:10.1029/2004GL021808.

[4] Alvain, S., Moulin, C., Dandonneau, Y., & Loisel, H. (2008). Seasonal distribution and succession of dominant phytoplankton groups in the global ocean: A satellite view. Global Biogeochem. Cycles, 22(GB3001), doi:10.1029/2007GB003154.

[5] Bricaud, A., Ciotti, A. M., & Gentili, B. (2012). Spatial-temporal variations in phytoplankton size and colored detrital matter absorption at global and regional scales, as derived from twelve years of SeaWiFS data (1998–2009). Global Biogeochemical Cycles, 26(1). doi:10.1029/2010GB003952.

GCOM-C SGLI calibration and characterization

H. Murakami

Earth Observation Research Center, JAXA
Email: murakami.hiroshi.eo@jaxa.jp

Summary

Evaluation tests of the Engineering Model (EM) of the Second-generation Global Imager (SGLI) on the Global Change Observation Mission (GCOM) is being reviewed in this winter-spring. The tests included radiometric gain, linearity, spectral response, stray light, polarization sensitivity, geometric characterization and so on. Manufacturing of the Pre-Flight Model (PFM) reflects the results of EM design and its evaluation. SGLI has multiple on-board calibration methods using a solar diffuser, LED lamps, a thermal black body, and monthly pitch-maneuver operation for the lunar observation at the same phase angle.

1. SGLI sensor system and onboard calibration system

The Second-generation Global Imager (SGLI) on the Global Change Observation Mission -Climate (GCOM-C) is a multi-band optical imaging radiometer in the wavelength range from 380nm to 12000nm. It consists of two main components, the Visible and Near Infrared Radiometer (SGLI VNR) and the Infrared Scanning Radiometer (SGLI IRS) [1].

SGLI VNR is a push-broom scanning type radiometer (Fig. 1). VNR Non-Polarized observation sub unit (VNR-NP) has 11 bands in the wavelength range from 380nm to 865nm [2] with 250-m spatial resolution and 1150-km cross-track swath covered by three telescopes. Other two telescopes are mounted on the tilting bench (+/-45 degrees along track) and dedicated for the polarized light observation at two bands of red and NIR (VNR-PL). SGLI IRS is a whisk broom type scanner with a 45deg-folded scanning mirror rotating for 1400-km swath.

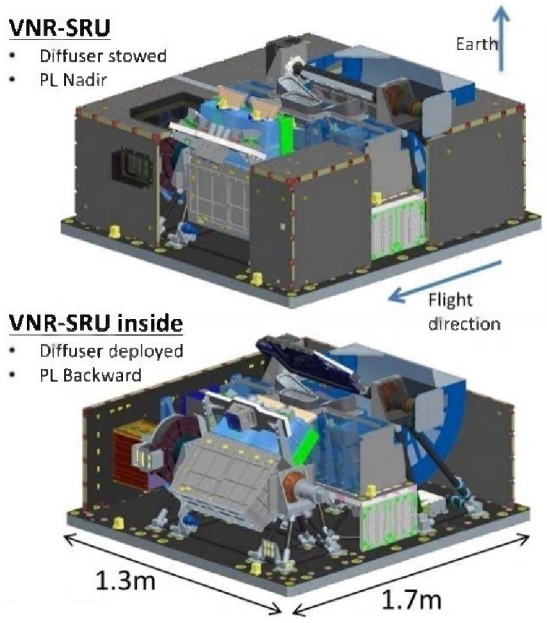

Figure 1 SGLI VNR sensor design. The calibration diffuser is deployed in the lower figure. Cited from [3].

SGLI-VNR has multiple on-board calibration functions, diffuser for solar irradiance and lamp (LED) calibration. SGLI-IRS also has a diffuser illuminated by the sun and lamps (LED and halogen), black body (for thermal infrared bands), and deep space window. Maneuver observation is planned for evaluating BRDF of the solar diffuser after the launch. SGLI is planned to see the moon at a constant phase angle monthly by pitch maneuver of GCOM-C satellite [3].

2. Pre-launch calibration and characterization

Sensor characterization (development of a sensor model) and radiometric gain calibration will be conducted by the similar way that has been done for the evaluation tests of EM [4].

(1) Gain calibration
Radiometric gain including non-linearity at each pixel (VNR and IRS) and scan angle (IRS) by using the integration sphere which have to be traceable to the national standard through transfer instruments, e.g., spectro-radiometer and blackbody radiators.
(2) Signal to noise ratio (SNR)
SNR at the standard radiance level (depend on application targets) is evaluated in the optical tests. Noise of the dark target is also evaluated. SNR and dark noise will be monitored by the lamp calibration data both before and after launch.
(3) Spectral response
Spectral response of band-pass filters and the total optical system will be measured. Field-Of-View (FOV) dependence of the line filters are carefully measured and characterized [2].
(4) Polarization sensitivity
Polarization sensitivity is measured at several points in the FOV for each band and sensor components, IRS and each telescope of VNR.
(5) Stray-light
Stray-light is often to be one of the serious problem for the imager. It can be caused by scatterings in the telescope and around the focal plane. Quantitative characterization and correction model will be investigated.
(6) Geometric model
The geometric model depends on the sensor geometric design and optical characteristics. It will be measured in the pre-launch tests and revised after launch by the GCP matching analysis. The GPS receiver and the star-tracker will be used for the geometric (position and angle) correction on orbit.

3. Calibration strategy integrating the calibration functions/methods

Multiple ways are planned for the SGLI calibration after launch. SGLI calibration team will use the solar-diffuser as the main calibrator, and lamp data for checking the launch shift, and moon observation for monitoring long-term change [3]. Vicarious adjustment will be conducted over both the land and the ocean, and the results will be compared to the on-board calibration methods and other satellite sensors in cooperation with international community and CEOS Cal/Val groups.

References:

[1] K. Tanaka, Y. Okamura, T. Amano, M. Hiramatsu, K. Shiratama , Development status of the Second-generation Global Imager (SGLI) on GCOM-C, Sensors, Systems, and Next-Generation Satellites XIII, Proc. of SPIE Vol. 7474, 74740N, 2009.
[2] A. Kurokawa, Y. Nakajima, S. Kimura, H. Atake, Y. Okamura, K. Tanaka, S. Tsuida, K. Ichida, T. Amano, High-precision narrow-band optical filters for global observation, ICSOS, 2012.
[3] Operation Concept of Second-generation Global Imager (SGLI), K. Tanaka, Y. Okamura, T. Amano and M. Hiramatsu,K. Shiratama, SPIE-AP, Incheon, Oct. 13, 2010.
[4] T. Hosokawa , K. Tanaka, Y. Okamura, T. Amano and M. Hiramatsu, Engineering model testing for SGLI IRS especially TIR radiometric data, Proc. SPIE 8528, Earth Observing Missions and Sensors: Development, Implementation, and Characterization II, 852818, Nov. 9, 2012.

Challenges and Opportunities for the operational use of Ocean Colour for Fisheries

Shailesh Nayak
Earth System Science Organization (ESSO), Delhi 110003, India

Satellite remote sensing affords monitoring of large spatial areas at very high temporal scales. The availability of food, feeding habits and environmental conditions play a key role in the distribution of fishery resources. The congregation of food on surface, water column and sea bed habitats, control the abundance, type and distribution of fish. The chlorophyll images from ocean colour data provide information on productivity and on oceanographic features such as colour boundaries, fronts, eddies, rings, gyres, meanders and upwelling regions. The next important aspect is physiologically suitable environment for fishery resource. Satellite-derived sea surface temperature (SST) partially explains suitability of fish to a habitat.

The SST images when used along with ocean colour images allowed identification of various oceanographic feathers as well as gradient in magnitude in productivity and temperature. This coincidence of chlorophyll and SST features indicate close coupling of the physical and biological processes. Sea surface wind provide information on the movement of oceanographic features and thus on circulation. The synergistic analysis of time series measurements of chlorophyll, SST and surface wind vector allows to understand the formation of productive grounds and its dynamics. Attempts are being made to assess fishery potential using ocean color data as the productivity is linked to physical processes. It has been now realized that sardine fishery is closely linked to onset of monsoon. The use of ocean colour in ecosystem modelling has been taken up. The prediction of seasonal productivity will help assessment of fishery resources.

High-resolution IOP measurements for ocean color algorithm development support

N B Nelson[1], D A Siegel[1], E Aghassi[1], E Stassinos[1]
[1]University of California, Santa Barbara
Earth Research Institute
Santa Barbara, 93106-3060, USA
Email: norm@eri.ucsb.edu

Summary

We developed an alongtrack system that measures particle inherent optical properties with high temporal (therefore spatial) sampling frequency, for studies of the links between optical properties and biogeochemical processes on the submesoscale and for applications to ocean color algorithm development for microbial community parameters. We report on several applications of the system for a long transect across the South Pacific and across frontal zones at the edge of mesoscale features in the subtropical Sargasso Sea. Potential applications of the data for developing new algorithms for connecting ocean color to microbial community structure and the limitations of the data will be discussed.

Introduction

In recent years, new capabilities have been developed to assess phytoplankton community structure and organic carbon cycling from satellite ocean color observations. However, validation of these novel remote sensing retrieval approaches and their further development is limited by scarcity of field observations over the variety of biogeochemical provinces of the global ocean. We have developed a flow-through system that measures surface inherent optical properties (IOPs) such as spectral absorption, backscattering and particle size spectra, in whole water and 0.2 micron filtered water. Our field effort is closely coupled to our ongoing collaborative efforts in developing new ocean color products useful for assessing global productivity and carbon cycling. The combination of field and satellite data analyses will enable us to understand the controls on plankton community structure allowing an understanding of the processes by which phytoplankton community structure affects open ocean IOPs and how one can best assess community structure characteristics from IOPs.

The alongtrack IOP system has several main optical instruments (WETLabs BB3 and AC-s, Sequoia LISST) and ancillary sensors including a Sea-Bird CT and flow meters, integrated with the ship's GPS feed for location and time information. The system also includes a Satlantic FIRe fluorescence kinetics system for measuring photosynthetic physiological parameters. The principal feature of the alongtrack system is a 0.2 micron filter cartridge which can be switched in and out of the flow. Under computer control the water is filtered two or three times per hour while the system is running. Under standard conditions the 'filtered' water can be used as a baseline, in which phenomena such as variable CDOM, calibration drift, and uncompensated temperature effects are integrated. When an interpolated 'filtered' record is subtracted from the 'unfiltered' data stream the resultant data are characteristic only of the >0.2 micron particles in the flow.

On the first deployment of the system, a section across the South Pacific at approximately 32 degrees south latitude from Australia to Chile, we observed large-scale changes in particulate backscattering coefficient consistent with the overall ecosystem structure. In the ultra-oligotrophic eastern South Pacific central gyre, the stability of the background allowed observations of daily excursions of b_{bp} and b_{bp} slope parameter, suggesting we were observing diel cycles of cell division.

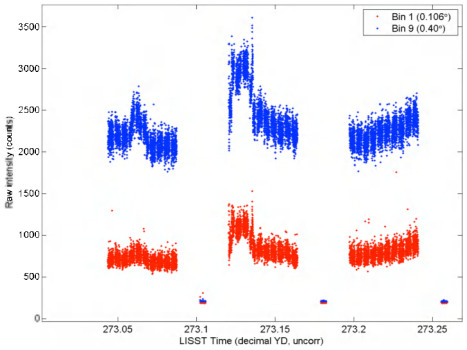

Figure 0: Example raw LISST data collected while crossing Lagrangian coherent structure features in the northern Sargasso Sea, September 2011. The data are raw scattered light intensity at two angle. Individual data are sampled at 1Hz in five minute blocks. Blanks (filtered seawater) can be seen in the gaps. Distance covered is approximately 30 km.

On subsequent deployments of the system in the Sargasso Sea between the Gulf Stream and Puerto Rico, we focused on submesoscale features identified by inferring Lagrangian coherent structures from satellite-altimetery derived circulation. In these studies we ran the system collecting data at 1Hz for 30-40 km crossing features of interest. Data are still in the preliminary stages of analysis, but temperature/salinity fronts were identified in almost all cases. We were also able to observe features in most cases in the inherent optical property data as well, but instrument noise was typically large relative to signal changes (Fig. 1). Changes in the IOPs across the observed temperature fronts could reflect changes in the microbial community structure driven by small-scale patterns of circulation and ephemeral nutrient supply. Instrument calibration drift was significant over the course of all the cruises.

Discussion

Understanding the connections between IOPs, the community structure, biogeochemical processes, and ocean color are goals for our ongoing research. Studies such as these, combined with other physical and relevant biological observations, can allow us to validate future products and determine how much of the variability observed at the submesoscale in satellite imagery is attributable to actual ecosystem variability. At present our ability to do this is limited by the precision of the instruments and the procedures and data processing algorithms required. In the ocean-basin scale studies, the large spatial baselines allowed us to reduce data appropriately and observe ecosystem gradients in helpful ways.

Conclusions

Upcoming ocean color sensors will be able to retrieve IOP and community structure parameters via existing and new algorithms, but these will be difficult to validate. Technological improvement in inherent optical property sensors will be essential for developing and validating the next generation of ocean color algorithms. Instrumental stability needs to be improved and facilities for simple field calibration of sensors should be developed.

Comparison of atmospheric corrections of HICO images of a subtropical estuarine region in Brazil.

M.A. Noernberg[1,3], S. Lavender[2,3], J.D. Hedley[4], R. Gould[5]
[1] Federal University of Paraná, Center for Marine Studies, Pontal do Paraná, 83255-976, Brazil
[2] Pixalytics Ltd, Tamar Science Park, Plymouth, Devon, PL6 8BX, UK
[3] Plymouth University, School of Marine Science & Engineering, Plymouth, Devon, PL4 8AA, UK
[4] Environmental Computer Science Ltd., Tiverton, Devon, EX16 6LR, UK
[5] Naval Research Laboratory, Stennis Space Center, Mississippi, USA
Email: m.noernberg@ufpr.br

Summary

The quality of ocean color retrieved products depends on accurate atmospheric correction, and this remains a challenging task. Despite the huge scientific contribution of Hyperspectral Imager for the Coastal Ocean (HICO) the spectral quality of this rapidly developed proof of concept instrument also presents challenges. The work presented here investigated different atmospheric correction approaches and the consequences for bio-optical algorithms when retrieving products such as absorption coefficient curves. The results from the approaches are of mixed quality, illustrating that HICO presents challenges for current off-the-shelf atmospheric correction algorithms. However, undertaking this ensemble approach where this is limited *in situ* data provides a greater understanding of the environmental optics and suggests future research that will ultimately lead to a solution that can be applied in an operational monitoring context.

Introduction

The Hyperspectral Imager for the Coastal Ocean (HICO) sensor is the first spaceborne hyperspectral imager designed specifically for the coastal environment. It became operational on the International Space Station in September 2009 and combines high signal-to-noise ratio, contiguous 10 nm wide spectral channels over the range 400 to 900 nm, and a scene size of 42 × 190 km, designed to capture the scale of coastal dynamics. The quality of ocean color retrieved products depends on accurate atmospheric correction, and this remains a challenging task. It has been demonstrated that assuming that sea-water absorbs all the light in the red and near-infrared (NIR) region of the spectrum, referred as the black-pixel assumption (Gordon & Wang, 1994 – GW94), introduces significant errors when applied in turbid waters. Numerous algorithms have been developed with alternative hypotheses taking into account non-negligible NIR ocean contribution to the measured signal. Further, the challenge of atmospheric correction is greater when the need is to retrieve products from areas with few *in situ* measurements. This is the case of the Paranaguá Estuarine Complex, located in south-eastern Brazil, which is a large interconnected subtropical estuarine system, hence frequently turbid and in an area with little resources for in situ radiometric data collection.

Despite the huge scientific contribution of HICO the spectral quality of this rapidly developed proof of concept instrument also presents challenges. The near infra-red (NIR) wavelengths are noisy, which hinders the atmospheric correction. The work presented here investigated different atmospheric

correction approaches and the consequences for bio-optical algorithms when retrieving products such as absorption coefficient curves.

Since Jun 2011, 46 HICO images were acquired over the area or interest; 13 were largely free of clouds. For the same period 24 campaigns for monitoring the absorption coefficients of the three major optically active substances: colored dissolved organic matter, non-algal particles and phytoplankton were realized. At least five sample points were visited near the inlet giving a total of 105 samples. The atmospheric correction required for retrieving the bio-optical absorption coefficients was implemented using four different approaches:

1) Convolution of the hyperspectral bands to "MODIS-like" multispectral bands, and then applying standard GW94 [1] atmospheric correction routines that NASA use for SeaWiFS and MODIS, with near-IR iteration turned on for coastal radiances, to reduce negative water-leaving radiance retrievals. This is processed by the NRL Automated Processing System (APS).
2) An approach originally designed to correct Compact Airborne Spectrographic Imager (CASI) [2], which has the MERIS Bright Pixel approach included [3].
3) The Fast Line-of-sight Atmospheric Analysis of Spectral Hypercubes (FLAASH) available in the ENVI software. Unlike the previous atmospheric corrections that interpolate radiation transfer properties from a pre-calculated database of modeling results, FLAASH incorporates the MODTRAN4 radiation transfer code.
4) An image-driven approach in which the atmosphere reflectance (L_a) is calculated from a pair of adjacent pixels that are in and out of a cloud shadow, with the transmittance and irradiance estimated using the reflected radiance from the top of clouds [3]. The limitation of this method is that it requires distinctive cloud shadow in a near uniform water area, and this shadow cannot be from thin clouds. Also, it does depend on the assumption that L_a is nearly uniform for the study area.

The results from the approaches are of mixed quality, illustrating that HICO presents challenges for current off-the-shelf atmospheric correction algorithms. However, undertaking this ensemble approach where this is limited *in situ* data provides a greater understanding of the environmental optics and suggests future research that will ultimately lead to a solution that can be applied in an operational monitoring context.

References

[1] Gordon, H.R. & Wang, M. (1994). Retrieval of water-leaving radiance and aerosol optical thickness over the oceans with SeaWiFS: A preliminary algorithm. App. Optics, 33:443-452.
[2] Lavender, S.J. & Nagur, C.R.C. (2002). Mapping coastal waters with high resolution imagery: atmospheric correction of multi-height airborne imagery. J. Opt. A: Pure Appl. Opt., 4:S1–S.
[3] Moore, G.F., Aiken, J., Lavender, S.J., (1999). The Atmospheric correction of water colour and the quantitative retrieval of suspended particulate matter in case 2 waters: application to MERIS. Int. J. of Remote Sens., 20:1713–1733.
[4] Lee, Z.P., Casey, B., Arnone, R.A. Weidemann, A.D., Parsons, A.R., Montes, M., Gao, B.C., Goode, W.A., Davis, C., Dye, J. (2007). Water and bottom properties of a coastal environment derived from Hyperion data measured from the EO-1 spacecraft platform. J. Appl. Remote Sens., 1(1):011502.

The multivariate *Partial Least Squares* regression technique for the retrieval of algal size structure from particle and phytoplankton light absorption spectra

E. Organelli, A. Bricaud, D. Antoine, J.Uitz

Laboratoire d'Océanographie de Villefranche, UMR 7093,
CNRS and Université Pierre et Marie Curie, Paris 6, 06238 Villefranche sur Mer, France
Email: emanuele.organelli@obs-vlfr.fr

Summary

The *Partial Least Squares* (PLS) regression technique is here used for the retrieval of the three phytoplankton size classes (micro-, nano- and pico-phytoplankton) from a nine-year time series of *in situ* particle and phytoplankton absorption measurements in the Mediterranean Sea (BOUSSOLE site). PLS models were established for the quantification of concentrations of total chlorophyll *a* (Tchl *a*), of the sum of 7 bio-markers pigments (DPs) and of pigments associated with micro-, nano- and pico-phytoplankton separately. When training PLS models with a dataset including light absorption and HPLC pigment measurements from the Mediterranean Sea only, good accuracy in predicting the algal community structure and its temporal changes at the BOUSSOLE site was observed. A lower accuracy of prediction of phytoplankton size classes over the BOUSSOLE time series was instead revealed by PLS models trained with data from various locations of the world's oceans. Similar performances between PLS models trained with both particle and phytoplankton absorption measurements open the way to an application of this approach also to absorption spectra derived from inversion of field or satellite radiance measurements.

Introduction

The PLS is a multivariate analysis technique that relates a data matrix of predictor variables to a data matrix of response variables by regression. Thus, the PLS method can be used for the prediction of one or several dependent variables from several independent variables [1]. This method is frequently used in chemistry for spectroscopy analysis but only scarcely applied in oceanography, e.g. for the retrieval of information concerning algal populations. An application performed by Stæhr and Cullen [2] showed, however, remarkable skills of PLS in predicting the fraction of chlorophyll biomass of the harmful algae *Karenia mikimotoi*. This led to hypothesize a potential PLS application also for the detection of other phytoplankton types in natural environment.
Two extensive datasets of *in situ* light absorption and HPLC pigment measurements were used for training the PLS technique in order to retrieve concentrations of pigments associated with the three phytoplankton size classes (micro-, nano- and pico-phytoplankton). The fourth-derivatives of particle ($a_p(\lambda)$) or phytoplankton ($a_{phy}(\lambda)$) absorption spectra were selected as the predictor variables while concentrations of Tchl *a*, of the sum of 7 bio-markers pigments (DPs) and of pigments associated with the three phytoplankton size classes [3] were selected as the response variables. A first training dataset consisted of 716 simultaneous HPLC pigment and light absorption measurements collected during several cruises across the world in different years and seasons (hereafter denoted GLOCAL). A second training dataset comprised only data from the Mediterranean Sea (n=239, hereafter denoted MedCAL). The PLS trained models were tested using the nine-year time series (January 2003-May 2011) of absorption measurements at the BOUSSOLE site (n=484; Mediterranean Sea) and the predicted pigment concentrations were compared with those retrieved from HPLC pigment measurements.

Discussion

GLOCAL PLS trained models revealed good accuracy only in predicting Tchl *a* and total DPs content at the BOUSSOLE site. Predicted values of pigments associated with the three size classes separately were actually correlated with HPLC measured values (r^2>0.42) but predictions were systematically overestimated for micro-phytoplankton and underestimated for nano- and pico-phytoplankton. Algal biomass and concentrations of pigments associated with the three size classes were predicted with very good accuracy by the MedCAL trained PLS models. Predicted values were significantly correlated with the measured ones (r^2>0.52) and the points were very close to the 1:1 line. More importantly, $a_p(\lambda)$ and $a_{phy}(\lambda)$ trained models showed similar performances. MedCAL PLS-predicted pigment concentrations reproduced satisfactorily HPLC pigment temporal changes over the entire BOUSSOLE time series (Fig.1).

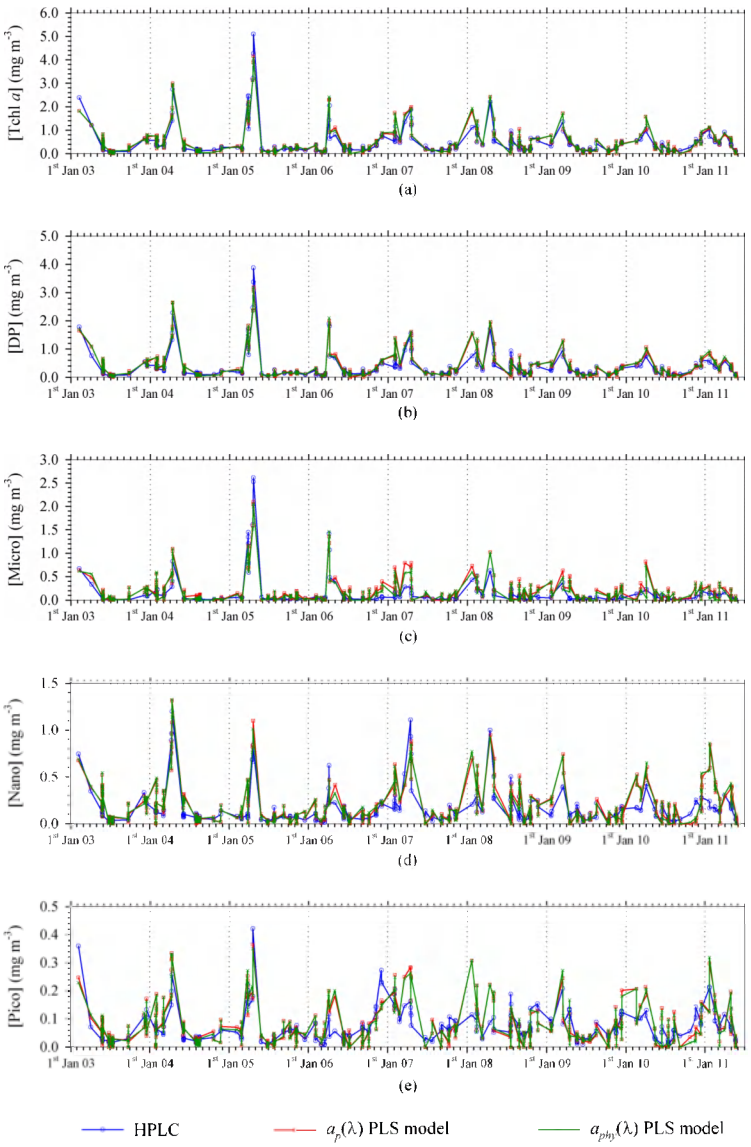

Figure 1 BOUSSOLE time series of pigment concentrations as derived from HPLC pigment measurements and from MedCAL trained PLS models.

Conclusions

The PLS technique represents an encouraging method for retrieving algal biomass and size structure from *in situ* absorption properties especially when models are trained with a regional dataset. Similar performances of $a_p(\lambda)$ and $a_{phy}(\lambda)$ trained models open the way to the application of the PLS method to absorption spectra derived from hyperspectral *in situ* or satellite radiances.

References

[1] Martens, H. and Næs, T. (1989). Multivariate Calibration, Wiley & Sons.

[2] Stæhr, P.A. and Cullen, J.J. (2003). Detection of *Karenia mikimotoi* by spectral absorption signatures. J. Plankton Res., 25: 1237-1249.

[3] Uitz, J., Claustre, H., Morel, A. and Hooker, S.B. (2006). Vertical distribution of phytoplankton communities in open ocean: an assessment based on surface chlorophyll. J. Geophys. Res., 111: C08005.

A novel algal discrimination algorithm based on first principles of aquatic optics and applied to hyperspectral remote sensing imagery of the coastal ocean

Sherry L. Palacios[1], Heidi M. Sosik[2], Tawnya D. Peterson[3], Liane S. Guild[1], Raphael M. Kudela[4]

[1]NASA Ames Research Center, Biospheric Science Branch, MS 245-4, Moffet Field, CA 94035 USA
[2]Woods Hole Oceanographic Institute, MS 32, Woods Hole, MA 02543 USA
[3]Oregon Health and Science University, Science & Technology Center for Coastal Margin Observation and Prediction, Beaverton, OR 97006 USA
[4]University of California – Santa Cruz, Ocean Sciences, 1156 High St., Santa Cruz, CA 95064 USA
Email: sherry.l.palacios@nasa.gov

Summary

A new hyperspectral bio-optical algorithm was developed to discriminate phytoplankton taxa in optically complex, case 2 waters. The semi-analytical, phytoplankton detection with optics (PHYDOTax) algorithm is based on first principles of bio-optics with applications to biogeochemical modeling, testing phytoplankton functional type (PFT) models, and detecting and monitoring harmful algal blooms (HABs). PHYDOTax can presently differentiate among diatoms, dinoflagellates, haptophytes, chlorophytes, cryptophytes, and cyanophytes with its existing signature library. PHYDOTax is unique as it discriminates between dinoflagellates and diatoms, a distinction historically considered challenging using chlorophyll-*a*, other pigments, or light absorption spectra alone. With increased availability of hyperspectral imagery from existing satellites, and the launch of new satellites, PHYDOTax holds promise for validating PFT models, modeling biogeochemical cycles, and monitoring harmful algae in optically complex coastal waters. The feasibility of applying the algorithm to other imaging spectrometers (e.g. the AVIRIS simulation of Hyperspectral Infrared Imager- HyspIRI and the Hyperspectral Imager for the Coastal Ocean –HICO) of the Monterey Bay is explored.

Introduction

An initial goal of ocean color remote sensing was to estimate global phytoplankton chlorophyll-a biomass in case 1 waters to address questions related to the ocean's role in carbon uptake and the global carbon budget. Over time, sophisticated algorithms evolved to address more than just chlorophyll-a concentrations in case 1 waters to include: deriving inherent optical properties, cell bio-volume, red-tide indices, water mass detection, and primary productivity in both case 1 and case 2 waters. The bulk chlorophyll-a pool has been further differentiated to quantify the incumbent taxa using pigment-based [1] and ocean color remote sensing algorithms [e.g. 2]. These phytoplankton discrimination algorithms are varied and address specific questions related to carbon flow through aquatic ecosystems, PFTs, and the detection and monitoring of HABs.

The Monterey Bay, CA (USA) is an open bay located along an eastern boundary current. Physical forcing drives nutrient availability to phytoplankton and two of the three oceanographic seasons are characterized by dominant phytoplankton taxa: Upwelling (Mar – Aug)- diatoms and Oceanic (Sep – Oct)- dinoflagellates. This climatological pattern can be disrupted within-season resulting in blooms of mixed assemblages of phytoplankton. This is of particular interest in northern Monterey Bay as extensive dinoflagellate blooms occur in the "red-tide incubator" and may mask co-occuring toxic diatom blooms that pose a threat to ecosystem and human health. The objective of this study was to discriminate phytoplankton taxa contained within algal blooms in case 2 waters using first principles of

bio-optics to identify both the presence of a taxon and to quantify the relative proportions of taxa contained within a bloom to address the need to detect and monitor HABs over a large spatial scale. The algorithm we developed can also be applied to questions related to validating PFT models and carbon uptake within the coastal zone, a region where the understanding of carbon flux is not yet well characterized.

Results and Discussion

PHYDOTax is composed of three parts: 1) a signature library of R_{rs} for phytoplankton taxa found in the coastal ocean derived from measured inherent optical properties (IOPs) of algal cultures and radiative transfer equations, 2) an inverse-matrix approach to deconvolve the signature library from R_{rs} spectra collected from natural waters, and 3) the computation of relative proportions of the total chlorophyll-a pool represented by the constituent taxa. Like its conceptual predecessor, CHEMTAX, the predictions from PHYDOTax are dependent on the taxa represented in the input signature library. The library was developed using IOPs of cultures from thirteen phytoplankton species, representing six taxa commonly found in Monterey Bay: diatoms, dinoflagellates, haptophytes, chlorophytes, cryptophytes, and cyanophytes. Validation with synthetic mixtures confirmed correlation between algorithm predictions and known mixture proportions for all taxa except *Emiliana huxleyi*. Field validation in Monterey Bay, CA in 2006 and 2010 demonstrated a strong correlation between measured and modeled taxon-specific biomass for all taxa except cryptophytes (cyanophytes could not be field validated). PHYDOTax was applied to hyperspectral imagery of Monterey Bay from 2006 and it predicted a bloom with proportions of >60% dinoflagellates and ~20% diatoms; a pattern confirmed with *in situ* cell counts.

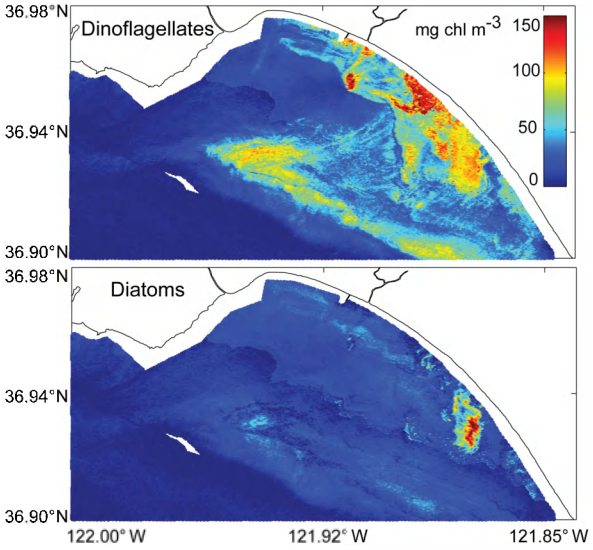

Fig. 1. Predicted taxon-specific biomass: dinoflagellates and diatoms during a major red-tide in northern Monterey Bay, CA (USA). In-water measurements of taxon assemblage validated predictions by PHYDOTax. SAMSOM Hyperspectral airborne sensor (Sep 12, 2006).

Conclusions

PHYDOTax is one of the first bio-optical algorithms to discriminate between dinoflagellates and diatoms in the coastal ocean, a distinction historically considered challenging. It is now possible to track carbon flow through either diatom- or dinoflagellate-dominated ecosystems using hyperspectral remote sensing imagery. PHYDOTax is being evaluated in calibration and validation efforts for the NASA Coastal and Ocean Airborne Science Testbed (COAST) mission in Oct. 2011 and the HyspIRI satellite simulations (AVIRIS airborne imager) in 2013 and 2014, and with other satellite imagers such as HICO.

References

[1] Mackey, M. D., Mackey, D. J., Higgins, H. W. & Wright, S. W.(1996).CHEMTAX - A program for estimating class abundances from chemical markers: Application to HPLC measurements of phytoplankton. Mar Ecol-Prog Ser 144, 265-283.

[2] Alvain, S., Moulin, C., Dandonneau, Y. & Breon, F. M.(2005). Remote sensing of phytoplankton groups in case 1 waters from global SeaWiFS imagery. Deep-Sea Research Part I-Oceanographic Research Papers 52, 1989-2004, doi:10.1016/j.dsr.2005.06.015.

Validation of the WISP algorithm for 9 years of MODIS observations on Dutch monitoring stations

S. Peters [1], K. Poser [1], N. deReus [1], M. Laanen [1], A. Hommersom [1]

Water Insight BV, Wageningen, 6709 PG, The Netherlands

Email: Peters@waterinsight.nl

Summary

Time series of MODIS derived Chl-a and TSM at the locations of Dutch monitoring stations from 2003-2011 were compared to in-situ observations. The MODIS results were obtained by applying the MUMM atmospheric correction and the Water optics Iterative Semi-analytical Processing suite of algorithms (WISP-algorithm). Within this algorithm choices can be made which spectral bands contribute to one of the subalgorithms for Chl-a, TSM and CDOM.

Introduction

Ocean Colour remote sensing in coastal zones with complex waters requires dedicated sensors with high radiometric accuracy, a dedicated spectral band set, specific atmospheric correction methods and algorithms that are able to separate Chlorophyll-a from TSM and CDOM in waters with highly variable concentrations of these components. Between MERIS and SENTINEL, the only usable sensor for this region is MODIS (and VIIRS in the near future). Therefore we have investigated the optimal combination of atmospheric correction and an semi-analytical algorithm to be able to continue providing these services. Using the MUMM atmospheric correction and an adapted version of the WISP algorithm we now are able to prove that Chl-a retrieval with MODIS at elevated TSM concentrations is possible; and that TSM retrieval is at least as good with MODIS as with MERIS.

Discussion

The WISP algorithm (Peters, in preparation) is a semi-analytical approach that uses an iterative scheme to calculate Chl-a, TSM, CDOM. Within the iterative scheme use is made of separate algorithms for each parameter. This allows the use (within the scheme) of band ratio's for Chl-a determination and single band algorithms for TSM and CDOM calculation. The calculation is based on [1] LUTs and the 4^{th} degree polynomial formulation for the reflectance function proposed by these authors. One other attractive aspect of the iterative approach is that per iteration a determination can be made if the water seems to contain high or low concentrations of Chl-a and TSM and to adapt the sub-algorithms (in terms of band choices) automatically to these concentration ranges. From literature we know that low Chl-a concentrations in waters with low TSM are best detected using blue-green band ratio's, while in other cases the red-NIR band ratio provides better results. Similar choices for spectral bands are known for TSM algorithms. The WISP algorithm is therefore one of the first algorithms that adapts itself to various conditions. The algorithm is very successful in case-2 waters using the MERIS band set because of the presence of the 705 nm reference band. Since this band is missing in MODIS alternatives had to be investigated. For Chl-a estimations a value is calculated from the blue green band ratios (443/531,

469/531, 488/531) in the cases that Chl-a is the only important optical active component in the water. In other cases either the band ratio 645/667 or 667/678 is used. Our investigations indicate that the ratio 645/667 contains a clear Chl-a signal for stations close to the coast, while the ratio 667/678 contains the information on high biomass blooms in open waters. For TSM a green band was used in case of low concentrations; in case of higher concentrations we used a red band such as the 678 band. The WISP algorithm is semi-analytical; its parameterization is formulated based on generally accepted SIOP functions according to the SIOP models used in Hydrolight and e.g. in the Coastcolour Round Robin Simulations [2]. Phytoplankton absorption is based on the Bricaud functions; but for the North Sea the absorption at the Chlorophyll-a red absorption band (667 nm) is elevated based on earlier observations. Compared to the CoastColour simulations settings we chose a lower value for the scaling factor for the specific backscattering of mineral particles (0.31).

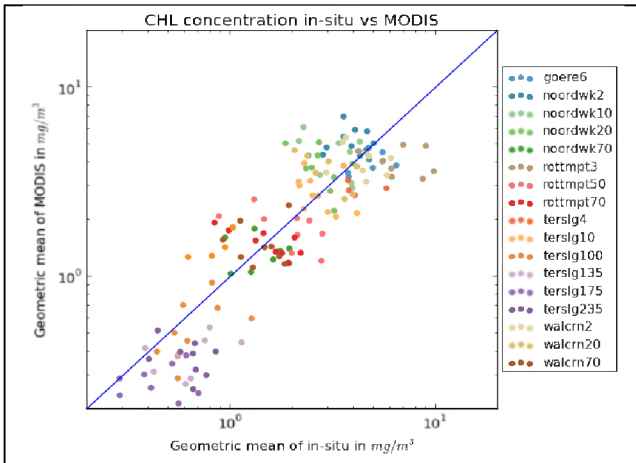

Yearly Chl-a averages at the MWTL stations for MODIS versus in-situ for 2003-2011: R2: 0.78 Slope: 1.02, Intercept: -0.03, RMSE: 0.2, MEA: 0.17

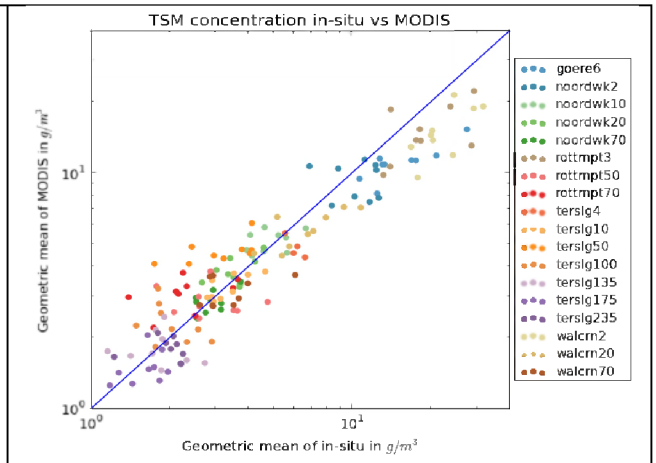

Yearly averages at the MWTL stations for MERIS versus in-situ for 2003-2011: R^2: 0.89, Slope: 0.81, Intercept: 0.11, RMSE: 0.13, MEA: 0.1

Conclusions

The correlation for the yearly geometric mean values is good, both for Chl-a and TSM, although the in-situ station has about 10-20 observations per year while MODIS realizes between 200 and 800 observations per station per year. We can conclude that this version of the WISP algorithm with the optimized selection of MODIS bands provides an effective determination of concentration both at the low end and high end of the values. Even at a distance of 2 km to the coast the values are still reasonable. We find that to improve the results even further, we need stripe removal algorithms and improved cloud flagging, especially at cloud edges.

References

[1] Y. Park and K. Ruddick, "Model of remote-sensing reflectance including bidirectional effects for case 1 and case 2 waters," Appl. Opt. 44, 1236-1249 (2005).

[2] Nechad, B. and Ruddick, K.: DUE CoastColour Round Robin – Harmonized comparison of algorithms Version 2.1 November 2012

A new oil spill detection methodology for MODIS and MERIS satellite imagery: an application to the Mediterranean Sea

A. Pisano[1], S. Colella[1], F. Bignami[1], R. H. Evans[2], R. Santoleri[1]

[1]CNR, ISAC, Rome, 00133, Italy
[2]University of Miami, RSMAS, Miami, 4600, USA
E-mail: andrea.pisano@artov.isac.cnr.it

Summary

We present an innovative automated methodology developed to detect and classify oil spills and look-alikes in MODIS high resolution (250 m) and MERIS full resolution (300 m) top of atmosphere reflectance images. Oil spill detection in optical satellite imagery is very recent and there is a lack of detection algorithms in literature. Our aim is to provide an efficient tool for this detection and thus an additional and complementary cost-effective support to SAR oil spill monitoring of the marine environment. This OS detection procedure was developed within the Italian PRIMI project, as part of the PRIMI operational oil spill monitoring and an oil slick forecasting system.

Introduction

MODIS and MERIS sensors, thanks to their increased spatial resolution, large swath and short revisit time, are now able to resolve small oil spills [1] which represent a prime source of marine hydrocarbon pollution resulting from illegal discharge. Also, these optical sensors, with their near-real time data and availability free of charge, can complement SAR sensors routinely used in oil spill (OS) detection and thus provide a more cost-effective and timely detection approach.

The mechanism behind MODIS (MERIS) oil feature detection mainly depends on the spectral information between oil and surrounding water (e.g. oil-water contrast) and illumination-view geometry of the incident light and satellite (e.g. sun glint condition). Experimental results proved the detectability and observability of oil films on the sea surface with the MODIS sensor [2,3] but there is still a lack of automated detection procedures.

Our oil spill detection procedure first determines where sun glint contamination is present in the image, since the relative oil/water contrast switches depending on the presence of glint. Then, a correction procedure ("image flattening") is applied to the image to remove or at least minimize atmospheric and oceanic natural variability from top of the atmosphere radiances, so as to enhance oil-water contrast. Next, the flattened image is fed to a segmentation algorithm to obtain "oil spill candidate" cluster regions in the image, by discarding non-slick cluster regions. Finally, a set of "feature parameters", defined to discriminate between slicks and look-alikes, are calculated for each OS candidate, leading to further non-slick pruning and to the assignment of a probability score to the remaining, most probable, OS candidates, the score expressing the likeliness of being a true OS.

This OS detection procedure was also used pre-operationally and validated in the framework of the oil spill detection and forecast system developed during the Italian PRIMI project (PRogetto pilota Inquinamento Marino da Idrocarburi/ marine hydrocarbon pollution pilot project).

Discussion

This detection methodology was developed using a set of MODIS and MERIS images of oil spill cases in the Mediterranean Sea for which *in situ* validation observations are available. We built an OS database, consisting of 15 images and 161 slicks. The OS database can be considered representative of the

Mediterranean oil slicks, given the variety of OS geometric (large and small illegal discharge OSs) and illumination/view characteristics.

The definition of feature parameters (e.g. OS area, perimeter, oil-water contrast etc.) and scores is based on the spectral, geometric and statistical analysis carried out on the OS dataset, in which both slicks and look-alikes are known. This analysis has also allowed to estimate the threshold values associated to each feature. These parameters are used to eliminate most non-slick or look-alike cluster regions in an image and to assign a score to the remaining probable oil spills.

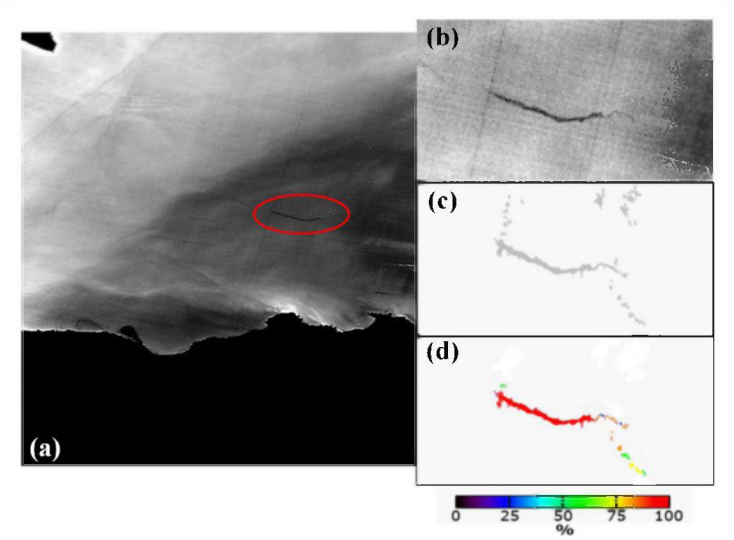

Figure 1. (a) Input flattened image from MERIS (865nm band, August 7 2008 09:50 UTC, off Algeria), oil spill in red ellipse; (b) zoom of the OS area; (c) cluster image; (d) oil spill candidate image after pruning, with color-coded associated scores.

The figure shows the representative steps of the OS detection methodology. The input image, containing the oil spill (in red ellipse of Fig. 1a and enlarged in Fig. 1b) to be detected, is the flattened 865 nm reflectance band relative to the MERIS sensor. By applying the OS detection algorithm to the input band, we obtain the cluster image shown in Fig. 1c, where grey regions represent both candidate oil spill and look-alikes. Finally, Fig. 1d shows the oil spill candidate image, after pruning and score assignment, where slicks are classified with score around 90%.

The method has been tested over the entire OS dataset and demonstrated its capability to detect also small slicks coming from illegal discharges. Validation showed that the method was able to detect 85% of the known slicks of the database. Preliminary validation was also performed on OS cases outside the OS database with encouraging results.

Conclusions

We have developed a methodology for the automatic detection and characterization of oil spills in MODIS and MERIS satellite top of atmosphere reflectance bands, using a set of in situ certified oil spills (OS database) in the Mediterranean Sea. This OS detection procedure was also used pre-operationally and validated in the framework of the oil spill detection and forecast system developed during the Italian PRIMI project (PRogetto pilota Inquinamento Marino da Idrocarburi/ marine hydrocarbon pollution pilot project).

References

[1] Hu, C., Li, X., Pichel, W. G. and Muller-Karger, F. E. (2009). Detection of natural oil slicks in the NW Gulf of Mexico using MODIS. Geophys. Res. Lett., 36, L01604.

[2] Bulgarelli, B. and Djavidnia, S. (2012). On MODIS Retrieval of Oil Spill Spectral Properties in the Marine Environment. IEEE Geoscience and Remote Sensing Letters, 9(3), 398-402.

[3] Adamo et al. (2009). Detection and tracking of oil slicks on sun-glittered visible and near infrared satellite imagery". International Journal of Remote Sensing Vol. 30, No. 24, 6403-6427.

Changing trend of Arabian Sea Productivity

Prince Prakash[1,2], Satya Prakash[2], Hasibur Rahaman[2], M. Ravichandran[2], and Shailesh Nayak[3]
[1] National Centre for Antarctic and Ocean Research, Goa
[2] Indian National Centre for Ocean Information Services, Hyderabad
[3] Earth System Science Organization, Ministry of Earth Sciences, New Delhi
Email:prakash@ncaor.org

Summary

Analysis of 13 year (1997-2010) record of satellite ocean color showed that summer monsoon chlorophyll concentration in the south-western Arabian Sea has been decline after 2003. Based on the analysis of possible physical parameter (wind, sea surface temperature (SST), Sea Level Anomaly (SLA) and thermocline depth), we attributed the declining chlorophyll concentration during summer monsoon to increasing SLA. This led to deepening of thermoclione and subsequently limits the supply of nutrients to the euphotic zone. This result suggests that changes are occurring in the biology of the south-western Arabian Sea not only due to local wind but also due to remotes forcings.

Introduction

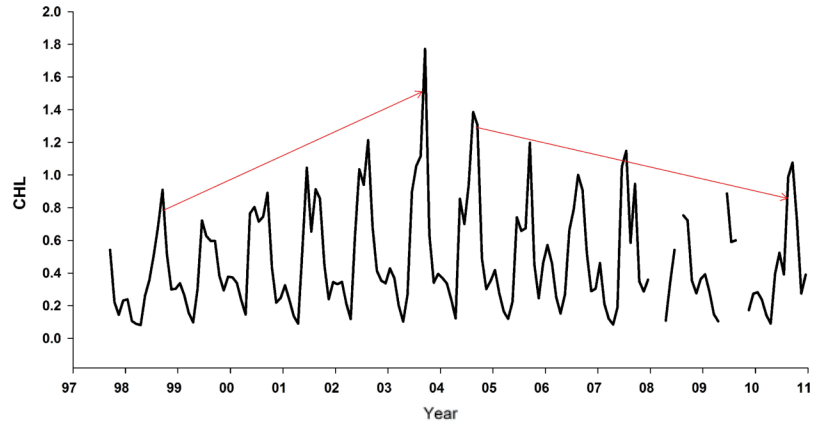

Figure 1 Figure 1Area averaged monthly time series of Chlorophyll -a for south-western Arabian Sea (47-55°E&5-10°N). The trend lines shown depict the increasing and decreasing trends during 1998–2003 and 2004–2010, respectively

South-western Arabian Sea is the most productive region in the Indian Ocean. The biogeochemistry of the Arabian Sea is mainly driven by seasonally reversing monsoons: Southwest (summer) and Northeast (winter) monsoons. Both the monsoons trigger high biological production but the underlying mechanisms are different: during summer south westerly monsoon wind causes an intense coastal and open ocean upwelling in Somalia and Oman coasts convective mixing during the northeast monsoon bring ample nutrient into the upper layer and triggers high biological production. Some of the recent observations on the basis of ocean color data have shown contradicting trends in ocean productivity for the Arabian Sea; it has increased by more than 350% over the last 6 years in the western Arabian Sea due to strengthening of the monsoonal winds [1] whereas no such trend is seen in the eastern Arabian Sea [2].The present study analyses satellite derived surface chlorophyll data for the past 13 years to investigate the long term changes in the in the south-western Arabians Sea (area identified by [1]) and delineates mechanism that explains the observed change.

Discussion

Our analysis of Satellite derived (9-km spatial resolution SeaWIFS) Level-3 monthly chlorophyll-*a* concentration data for the period of 1997-2010 shows a decreasing trend in the summer chlorophyll-*a* for the south-western Arabian Sea (Somali Coast,47-55°E & 5-10°N) after 2003. The trend analysis revealed that there was an increase in the summer peak chlorophyll-*a* concentration from 1998 to 2003 (slope: 0.24 ± 0.06; r^2 = 0.85; p = 0.02) but decreased after that (slope: -0.06± 0.03; r^2 = 0.44; p = 0.10). In order to understand the responsible mechanism for the observed Chlorophyll-*a* change in the region, we analysed wind, sea surface temperature (SST), Sea Level Anomaly (SLA) and thermocline depth data. Analysis of winds (Cross Calibrated Multiplatform wind and QuickSCAT) strength and wind stress curl from 1997 to 2003 and from 2004 to 2009 does not show any appreciable change. During the period 1997 to 2003 Satellite derive SLA along the Somalia coast shows a decreasing trend (Slope = -0.06 cm/month, P-value = 0.02) while in between 2004 to 2010 the SLA increases (slope = 0.07 cm/month, P-value = 0.03). The sea level change generally reflects thermocline variation. Increase

(decrease) in sea level associated with deepening (shallow) of thermocline. We also choose to show the depth of the 23°C (D23) isotherm, which is a proxy for thermocline depth. Summer (June to September) average of D23 during 1997 was 130 meter which gradually decreases and shoaled upto 85 meter in 2003 and then reached 71 meter in 2004, but after 2004 it again gradually increases and deepens up to 109 meter in 2010. As the nutricline and thermocline are closely associated in the Arabian Sea there for change of thermocline directly affects the supply of nutrient to the surface layer. Thus the deepening of the thermocline during 2003 to 2010 reduced the supply of nutrients to the euphotic zone and thus causing a decrease in surface chlorophyll-*a*.

Conclusions

Our analysis reveals a remarkable change in trend in the chlorophyll concentration of the South-western Arabian Sea after the year 2003. Our finding raises the possibility that the south-western Arabian Sea could witness increase/decrees in bloom of phytoplankton not only due to the strengthening/weakening of local wind but sea level anomaly also play a crucial role in strength of bloom. So the bloom in the south-western Arabian Sea is not only due to atmospheric effect but it is the manifestation of oceanic effects. The observed variability in productivity is not an effect of the global warming but may be a part of the decadal oscillation. The changes observed in the SLA may be due to the local or remote forcing.

Reference

[1]Goes, J. I., P. G. Thoppil, H. do R Gomes, and J. T. Fasullo (2005), Warming of the Eurasian landmass is making the Arabian Sea more productive, Science, 308, 545–547, doi:10.1126/science.1106610.

[2] Prakash, S., and R. Ramesh (2007), Is the Arabian Sea getting more productive?,Curr. Sci., 92, 667– 671.

Sensor-centric calibration and near-real-time in-situ validation of VIIRS Ocean color bands using Suomi NPP operational data

Patty Pratt, Systems Engineering Architect

Northrop Grumman Aerospace Systems, Redondo Beach, California 90230, USA

Email: patty.pratt@ngc.com

Summary

After the launch of Suomi NPP (SNPP) VIIRS, the next generation ocean color sensor would never return to the testing facility. Capturing any existing calibration errors or those created by the space environment can be elusive and validation with in-situ data is sparse. A novel system of tools has been developed with a key acquisition tool installed on the NOAA NSIPS server that enables automated analysis of remote-sensing data from an on-orbit sensor perspective. This allows ocean color products to be tested, calibrated (including polarization residuals) and optimized post launch. It also supports in-situ validation field efforts by allowing scientists to obtain near-real-time data of only the valid retrievals.

Introduction

The automated system was developed to capture daily granules over targeted regions, apply data reduction sorting of good pixels and produce various products that assist ocean color scientists with calibration and validation and granule identification. Results from this automated tool are then ingested by a calibration tool that sorts the data from a sensor-centric approach and subsequently a third tool trends the data by days. Any anomaly, feature or characteristic inherent in the sensor, or algorithm can be identified before analysis of the in-situ match up data.

Discussion

There are two distinct ways to use the automated data. For sensor-centric calibration we used the automated results from the Ocean Overlap Matchup Tool (OMT) and then applied the other two tools, Polarization Verification Tool (PVT) and PVT Analysis and Trending Tool (PATT). The tool design was originally developed to support the verification of the polarization LUT that were tested on the ground and are applied per detector per band per HAM side for all SNPP outputs; however, it proved to be useful in detecting *any* out-of-character feature in the sensor and ocean color algorithm as the results presented here will show. Once these features are investigated and mitigated, the tool will then assess the higher detail characterization including polarization sensitivity residual.

For in-situ validation only the OMT results are necessary to do the matchups though the sensor calibration analysis will provide valuable insight into variations that appear to be in the in-water data that are in actuality introduced by the sensor. These matchups will then be critical in determining the vicarious calibration that is necessary for the optimal ocean color products.

Summary

This presentation shows the results from a recent 100 day study revealing potential sensor artifacts and algorithm features. Features and artifacts are verified through independent analysis from scientists working with in-situ data.

An Underway IOP System for Southern Ocean Observation

S. Thomalla[1], E. Rehm[2], D. Needham[3]

[1]Council for Scientific and Industrial Research (CSIR), Cape Town, South Africa
[2]University of Washington, Applied Physics Laboratory, Seattle, WA 98105, USA
[3]Sea Technology Services, Cape Town, South Africa

Email: erehm@earthlink.net

Summary

Gaps in our understanding of the regional characteristics of the sensitivity of biological production in the Southern Ocean are being addressed by high spatial and temporal resolution sampling during the course of a season. A ship-based system for continuous underway measurement of inherent optical properties has been developed to link seasonally-variable bio-optical properties to biogeochemical variables such particle size distribution, phytoplankton pigments, particulate organic and inorganic carbon.

Introduction

The Southern Ocean is arguably the main source of medium-term uncertainty in terms of the effectiveness of global CO_2 mitigation plans. The Southern Ocean Seasonal Cycle Experiment (SOSCEx) is designed to address gaps in our understanding of the regional characteristics of the sensitivity of biological production in the Southern Ocean to changes in spatial and temporal atmospheric forcing. SOSCEx includes numerous underway and autonomous observations that aim to link physical forcing mechanisms with biogeochemical responses over an entire annual cycle.

One component of SOSCEx is a series of underway observations of bio-optical properties of the surface ocean that aim to link water column inherent optical properties (IOPs) to outgoing-satellite visible irradiance as well as in-water biogeochemical properties such as particle size distribution, particulate organic carbon (POC), particulate inorganic carbon (PIC), chlorophyll concentration and phytoplankton accessory pigments. To establish these links, CSIR and Sea Technologies have developed an underway IOP observational system that provides calibration-independent hyperspectral measurements of spectral particulate absorption $a_p(\lambda)$ and attenuation $c_p(\lambda)$ as well as simultaneous measurement of multispectral backscattering $b_{bp}(\lambda)$ using a ship's uncontaminated seawater supply. This system also supports the in-line acidification of seawater, supporting PIC estimates.

Discussion

The CSIR underway IOP system consists of a number of components. To remove optically-troublesome bubbles, the ship's uncontaminated seawater supply is plumbed to a vortex debubbler. Sample water is then distributed to the optical instruments via a series of manual and electronically controlled valves. To provide calibration-independent estimates of $a_p(\lambda)$ and attenuation $c_p(\lambda)$, seawater is periodically diverted through an electronically controlled valve to a large surface area 0.2 μm cartridge filter to a WET Labs AC-S hyperspectral absorption and attenuation meter [1, 2]. Best results were found by plumbing the AC-S absorption and attenuation tubes in series as shown in [2]. The plumbing supports continuous higher quality measurements of 0.2 μm-filtered seawater using a TriOS OSCAR integrating

sphere absorption meter and also allows simultaneous AC-S and OSCAR measurements unfiltered seawater measurements.

A WET Labs BB-9 measures the volume scattering function at 117° at nine wavelengths and is configured with increased instrument gain for the low biomass waters found in the Southern Ocean. The BB-9 is mounted in a flow-through chamber that provides separate (non-baffled) chambers for each three-wavelength instrument face. Backscattering of the chamber walls has been characterized (see [1]). Glacial acetic acid can be added to the BB-9 flow, ahead of a mixing tube and in-line pH probe, to lower the pH to 5 and dissolve any suspended calcium carbonate. In post-processing, the stabilized acidified reading is subtracted from the unacidified, raw reading [3, 4]. The difference in readings represent acid-labile scatter which is subsequently calibrated to suspended calcite in the laboratory.

Flow routing is controlled by a microcontroller that switches two three-way ball valves and one on-off ball valve using a single RS-232 interface. Flow meters are mounted at the plumbing outlets leading to the AC-S, OSCAR and three BB-9 flow chambers. A second microcontroller provides continuous calibrated flow rate information via a USB/RS-232 interface, assisting in the quality assurance of the flow-through data. Additional plumbing outlets support continuous measurements of multispectral fluorescence and fast-repetition-rate fluorometry. A single eight-port RS-232 to USB converter is used to aggregate data onto a single logging computer. For the AC-S and BB-9, serial data for each instrument is hard-wired to two serial ports to support simultaneous data logging (via Python scripts) and data visualization (via WET Labs software). Python scripts control valves and record AC-S, BB-9, valve position and flow rate data streams; all logging is time aligned with support for flexible sampling periods. TriOS software also supports flexible interval sampling and simultaneous GPS coordinate recording.

Conclusion

By taking the difference between temporally adjacent samples of total and filtered seawater, $a_p(\lambda)$ and $c_p(\lambda)$ spectra within the resolution of the AC-S are being obtained. Together with water sample measurements of chlorophyll, POC, PIC and particle size distribution, high temporal and spatial resolution underway estimates of biogeochemical variables in the Southern Ocean are possible.

References

[1] Dall'Olmo, G., T.K. Westberry, M.J. Behrenfeld, E. Boss, and W.H. Slade, *Significant contribution of large particles to optical backscattering in the open ocean.* Biogeosciences, 2009. **6**(6): p. 947-967.

[2] Slade, W.H., E. Boss, G. Dall'Olmo, M.R. Langner, J. Loftin, M.J. Behrenfeld, and C. Roesler, *Underway and Moored Methods for Improving Accuracy in Measurement of Spectral Particulate Absorption and Attenuation.* J. Atmos. Oceanic Technol., 2010. **27**(10): p. 1733-1746.

[3] Balch, W.M., D.T. Drapeau, J.J. Fritz, B.C. Bowler, and J. Nolan, *Optical backscattering in the Arabian Sea—continuous underway measurements of particulate inorganic and organic carbon.* Deep Sea Res., Part I, 2001. **48**(11): p. 2423-2452.

[4] Balch, W.M. and D.T. Drapeau, *Backscattering by coccolithophorids and coccoliths: Sample preparation, measurement and analysis protocols*, in *Ocean Optics Protocols For Satellite Ocean Color Sensor Validation, Revision 5: Biogeochemical and Bio-Optical Measurements and Data Analysis Protocols*, J.L. Mueller, G.S. Fargion, and C.R. McClain, Editors. 2004, NASA Goddard Space Flight Space Center: Greenbelt, Md. p. 27-36.

Towards Improved Measurements of Absorption by Particulate and Dissolved Matter

Rüdiger Röttgers[1] and David McKee[2]

[1]Helmholtz-Zentrum Geesthacht, Centre for Materials and Coastal Research, Geesthacht, 21502, Germany
[2]University of Strathclyde, Physics Department, Glasgow, G4 0NG, Scotland

Email: rroettgers@hzg.de

Summary

Improvements of laboratory methods to determine the light absorption coefficient of dissolved and particulate matter are presented. The main improvements are related to an increase of sensitivity and a decrease of susceptibility of methods to light scattering effects. The new methods e.g. allow avoiding correction for scattering. These corrections are necessary in common techniques and rely on assumptions that are not valid in coastal waters, like the assumption that particle absorption at near infrared wavelength is negligible. Recommendations will be given to improve the common practice of absorption determinations.

Introduction

Determinations of light absorption by particulate and dissolved matter in water are essential for developing and validating ocean colour remote sensing algorithms. However, measurements, especially of particulate absorption, are difficult to perform due to often low particle concentrations and the interference of light scattering in common measurement techniques. The absolute error in these methods, e.g. that of the quantitative filter technique (QFT), can be large. Reasons are 1) the common practice to subtract signals in the near infrared to correct for scattering errors, assuming that absorption of natural particles at these wavelengths is negligible and that the scattering influence is wavelength independent, and 2) the variability in the path length amplification of optical measurements with diffuse filters. In measurements of absorption by dissolved matter the main problem is the very low absorption in most oceanic waters.

Discussion

Measurements of dissolved matter in water, known as gelbstoff, are typically done in spectrophotometers with cuvettes of 1 - 10 cm path length. This methods is sufficiently sensitive in inland and coastal waters, but not in clear oceanic waters. Since a few years liquid wave guide capillary systems with path length of up to 2 m are in use and improved the sensitivity of the determination by a factor of 2 to 10, in addition offering the possibility to perform measurements immediately after sampling and filtration at sea. Measurement errors arise from optical changes induced by **differences in salinity between reference and sample water, i. e. proper correction or avoidance of temperature and salinity difference between sample and reference are necessary. Measurements with a point-source integrating cavity absorption meter and such a capillary system are shown to describe the range of methodological errors.**

Particulate absorption is often measured after the particles have been concentrated on filters to increase sensitivity and avoid interference of absorption by water and dissolved matter. This technique (QFT) is used since 50 years and had been improved in different ways (e.g. in the

transmission-reflectance technique [1]). However, problems are unknown scattering losses and amplification of the path length by multiple scattering inside the filter. This amplification has to be corrected by independently determined amplification factors. These determinations of the amplification factor were done with highly concentrated particle suspension (e.g. algal cultures), assuming that the independent method used gives accurate absorption. Scattering errors are often corrected by subtracting the measured signal at infrared wavelengths, assuming that natural particles do not possess significant absorption at these wavelengths, and that the scattering error is wavelength-independent. Both assumption might not be valid, and would then lead to significant systematic errors. Recently methods were developed that are not susceptible to scattering but sensitive enough to be used with natural samples: a point source integrating cavity absorption meter (PSICAM) was shown to accurately determine absorption by particles [2] and dissolved matter [3], a QFT technique measuring a filter inside a large integrating sphere was shown to have as well insignificant scattering errors [4]. Both techniques are combined to obtain accurate absorption coefficients even for very clear oceanic waters. The PSICAM measurements are used to determine amplification factors individually for each filter, reducing the error related to the variability of the amplification factor. These methods were compared to common QFT determinations. The comparison revealed that variability of the amplification factor can lead to errors as high as 30 % in case a general amplification factor is used, and that absorption in the near infrared spectral region is substantial in coastal waters, making a subtraction of near infrared signals inappropriate, as it would induce an underestimations of the particulate absorption at 442 nm of up to 70 %.

Conclusions

Common methods to determine absorption by dissolved and particulate matter suffer from low concentrations in oceanic waters, significant errors induced by light scattering, invalid assumptions in the correction of this scattering errors, and variability in the amplification factor for the QFT. Recent developments in these techniques lead to more accurate determinations and offer the possibility to determine the measurement errors. Similar improvements can be made for in situ measurements of inherent optical properties.

References

[1] Tassan, S. and G. M. Ferrari, "An alternative approach to absorption measurements of aquatic particles retained on filters," Limnol. Oceanogr. 40, 1358-1368 (1995).

[2] Röttgers, R., C. Häse, and R. Doerffer, "Determination of particulate absorption of microalgae using a Point Source Integrating Cavity Absorption Meter," Limnol. Oceanogr. Methods 5, 1-12 (2007).

[3] Röttgers, R. and R. Doerffer, "Measurements of optical absorption by chromophoric dissolved organic matter using a point-source integrating-cavity absorption meter, " Limnol. Oceanogr. Methods 5, 126-135 (2007).

[4] Röttgers, R. and S. Gehnke. Measurement of light absorption by aquatic particles: improvement of the quantitative filter technique by use of an integrating sphere approach. Appl. Opt. 51, 1336-1351 (2012).

The saturation reflectance in turbid waters

K.G. Ruddick[1], A.I. Dogliotti[2], D. Doxaran[3], B. Nechad[1]

[1] Royal Belgian Institute for Natural Sciences (RBINS), 100 Gulledelle, 1200 Brussels, Belgium
[2] Instituto de Astronomía y Física del Espacio (IAFE), CONICET/UBA, P.O: 67 Suc. 68 (C1428ZAA), Buenos Aires, Argentina
[3] Laboratoire d'Océanographie de Villefranche (LOV), CNRS/UPMC, B.P. 8, Quai de la Darse, Villefranche-sur-Mer, 06238, France
Email : K.Ruddick@mumm.ac.be

Summary

It is well-known that for turbid waters there is a maximal value for the marine reflectance, termed here the "saturation reflectance". As suspended particulate matter concentration increases, marine reflectance tends asymptotically towards this "saturation reflectance" limit. This limit has previously been considered as not useful for remote sensing purposes and, for example, suspended particulate matter retrieval algorithms generally avoid exploiting data close to the saturation reflectance. In the present study it is shown that important new information can be extracted from the saturation regime. The saturation reflectance is analysed here using radiative transfer simulations, satellite data and in situ reflectance measurements in highly turbid waters.

Introduction

Ocean colour remote sensing is now well-established as a method for mapping of concentrations of optically active water constituents. Satellite-based ocean colour sensors provide daily maps of parameters such as suspended particulate matter (SPM) concentration by inversion of models relating marine reflectance to inherent optical properties such as absorption, a, and backscattering, b_b , coefficients. It is relatively well-established [1] that the marine reflectance tends towards an asymptotic limit, termed here "saturation reflectance", for infinitely increasing SPM concentration. As this limit is approached the marine reflectance for a given wavelength becomes less and less sensitive to changes in concentration. For example, the in situ measurements of [2] (see Figure) show almost no variability of water reflectance for the wavelength range 400-550nm while SPM varies between 39 and 527 mg/l, whereas significant variation is found for wavelengths 700-1000nm, monotonically increasing with SPM.

Because of the reduction in sensitivity to SPM concentration it is sometimes recommended that the asymptotic limit be avoided for ocean colour remote sensing applications, for example by preferentially using wavelengths with higher pure water absorption where the saturation effect is only reached for correspondingly higher concentrations [3, 4]. While it is true that as reflectance approaches the saturation reflectance there is less and less information on particulate concentration, there is conversely more and more information relating to particulate type or, more specifically, b_{bp}/a_p, the backscatter:absorption ratio of particles. This is in turn related to the refractive index and size distribution of particles. This information is valuable and is currently not adequately exploited in ocean colour remote sensing data.

Discussion

Investigation of the saturation reflectance is beyond the scope of most analytical marine reflectance models. Models, which are based on the quasi-single scattering assumption, typically express reflectance as a linear or quadratic function [5] of $b_b/(a+ b_b)$, and do have an asymptotic limit for high

b_b/a. However, the limit given by such models is simply incorrect, by a factor that can exceed two. Better modelling of the saturation reflectance can be achieved by the use of a two-flow irradiance approximation, as used for example by [4], since this model is more appropriate for highly diffusive media with strong multiple scattering.

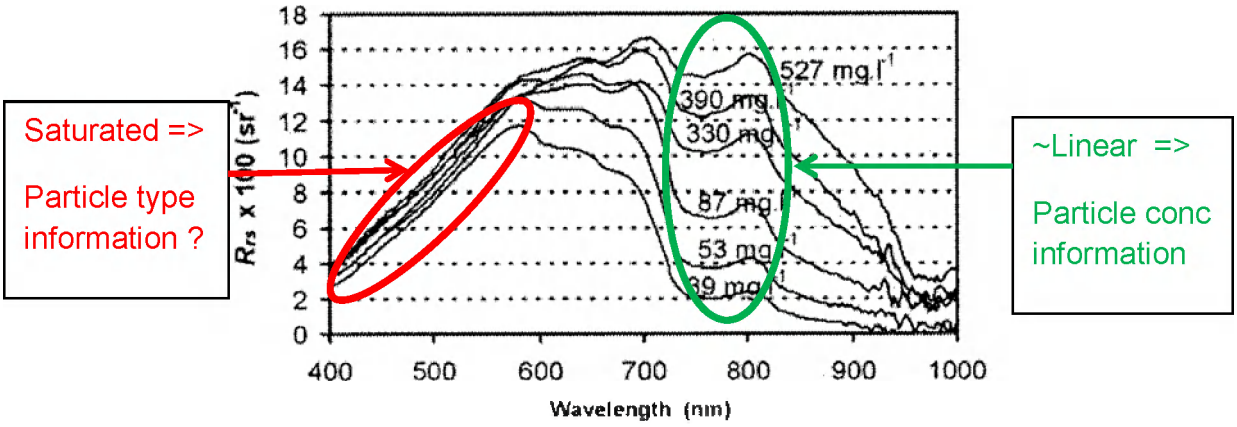

Reflectance spectra measured in the Loire Estuary for different SPM concentrations. Background figure reproduced from [2].

In this study radiative transfer simulations are made to investigate how the saturation depends on optical properties of particulate matter. Approximate analytical models are tested against the radiative transfer simulations. In situ reflectance measurements and satellite data for extremely turbid waters are used to validate the findings of the radiative transfer simulations.

Conclusions

Water reflectance in turbid waters is limited by a maximal value, termed here saturation reflectance. This saturation reflectance cannot be modelled using typical analytical models giving marine reflectance as a linear or quadratic function of $b_b/(a+ b_b)$. The value of saturation reflectance depends on b_{bp}/a_p and the particle volume scattering function. This suggests that remote sensing for saturated wavelengths will provide information on particle type to complement the information on particle concentration that can be retrieved from unsaturated wavelengths.

References

[1] Bowers, D.G., Boudjelas, S. and Harker, G.E.L. (1998), The distribution of fine suspended sediments in the surface waters of the Irish Sea and its relation to tidal stirring. Int J Rem Sen 19(14): p. 2789-2805.
[2] Doxaran, D., Froidefond, J.-M. , and Castaing, P. (2003). Remote-sensing reflectance of turbid sediment-dominated waters. Reduction of sediment type variations and changing illumination conditions effects by use of reflectance ratios. Applied Optics 42(15): p. 2623-2634.
[3] Nechad, B., Ruddick, K.G. , and Park, Y. (2010). Calibration and validation of a generic multisensor algorithm for mapping of Total Suspended Matter in turbid waters. Rem Sens Env 114: p. 854-866.
[4] Shen, F., et al. (2010). Satellite estimates of wide-range suspended sediment concentrations in Changjiang (Yangtze) estuary using MERIS data. Estuaries and Coasts. 33: p. 1420-1429.
[5] Gordon, H.R., et al. (1998). A semianalytical radiance model of ocean color. J Geophys Res 93(D9): p. 10909-10924.

FIELD VALIDATION OF THE PORTABLE REMOTE IMAGING SPECTROMETER: COASTAL HYPERSPECTRAL REMOTE SENSING IN ELKHORN SLOUGH

Heupel, E. E.[1], Dierssen, H. M.[1]Gao, B.[2], Green, R. O.[3], Mouroulis, P.[3], Russell, B.J. [1]
[1] Department of Marine Science, University of Connecticut
[2] Remote Sensing Division, Naval Research Laboratory
[3] Jet Propulsion Laboratory, California Institute of Technology
Corresponding Author: heidi.dierssen@uconn.edu

ABSTRACT

Hyperspectral imagery is a useful tool in mapping and monitoring coastal, benthic habitats [1,2]. Factors including high turbidity and fine spatial variability, however, continue to pose challenges in many coastal areas [3]. The turbid, sediment-laden estuarine waters and diverse habitats of Elkhorn Slough terminating in Monterey Bay, California present an excellent study site for testing the limits of hyperspectral imaging spectroscopy. This region was selected for field validation of the Portable Remote Imaging SpectroMeter (PRISM), a new imaging sensor package optimized for coastal ocean processes. PRISM provides spatial resolutions up to 30 cm and spectral resolutions of 3 nm [4]. *In-situ* sampling was conducted concurrent to the PRISM flights to measure inherent optical properties of the water column and sample selected benthic and coastal habitat spectral targets, including eelgrass and salt marsh. Here, we compare spectra obtained from the orthorectified and calibrated imagery using initial atmospheric correction of the imagery from the ATREM model with those collected from sampling locations within Elkhorn Slough. The corrected imagery matched well to *in-situ* remote sensing reflectance (R_{rs}) in magnitude and spectral shape over both the turbid optically deep channel and optically shallow eelgrass dominated targets. These successful results allow us to proceed with processing the imagery for chlorophyll and suspended sediment in the water column, as well as to begin to map the coastal habitats in this diverse area using a variety of radiometrically-based classification approaches. The PRISM sensor data from this validation will be used to address two ecological case studies in the slough, including a shallow water assessment of eelgrass beds and a deep water assessment of the Elkhorn Slough sediment plume. Excellent agreement between the PRISM and in-situ validation spectra provide the foundations for using PRISM to discriminate marine and coastal habitats. With very high spatial resolution the PRISM promises to be a valuable tool in coastal management to map, characterize and monitor coastal ecosystems.

References

[1] A. Dekker, V. Brando, J. Anstee, S. Fyfe, T. Malthus, and E. Karpouzli, "Remote sensing of seagrass ecosystems: use of spaceborne and airborne sensors," in Seagrasses: Biology, Ecology, and Conservation, Larkum AWD, Orth RJ, Duarte CM (eds.)., Springer, 2005, pp. 347–359.

[2] H. M. Dierssen, R. C. Zimmerman, R. A. Leathers, T. V. Downes, and C. O. Davis, "Ocean color remote sensing of seagrass and bathymetry in the Bahamas Banks by high resolution airborne imagery," Limnol. Oceanogr., vol. 48, no. 1, part 2, pp. 444–455, 2003.

[3] H. M. Dierssen and A. E. Theberge, "Bathymetry: Assessing Methods," in Encyclopedia of Ocean Sciences, vol. In press, New York, NY: Taylor and Francis, 2012.

[4] P. Mouroulis, B. E. Van Gorp, R. O. Green, M Eastwood, D. W. Wilson, B. Richardson, and H.M. Dierssen, "The Portable Remote Imaging Spectrometer (PRISM) Coastal Ocean Sensor," *Optical Remote Sensing of the Atmosphere,* 2012.

Calibration and validation of ocean color bio-optical models

M. S. Salama[*1,2], R. Van der Velde[1], H. Van der Woerd[3], J. Kromkamp[2], C. Philippart[2]

[1]University of Twente, ITC, The Netherlands
[2]Royal Netherlands Institute for Sea Research (NIOZ), The Netherlands
[3]Amsterdam Free University, IVM, The Netherlands
Email: s.salama@utwente.nl

Summary

We present a method to calibrate and validate bio-optical models that interrelate derived ocean color products to the governing bio-geophysical variables.

The match up set of ocean color observations and measurements is subdivided into calibration (Cal) and validation (Val) data sets. Each Cal/Val pair is used to derive the coefficients (from the Cal set) and the accuracy (from the Val set) of the bio-optical model.

Combining the results from all Cal/Val pairs provides probability distributions of the model coefficients and model errors. The results demonstrate that the method provides robust model coefficients and quantitative measure of the model uncertainty. This approach is easily scalable to different model structures and can be applied to infer the accuracy of ocean color algorithm products.

Introduction

In this paper we present the stochastic approach of Salama et al. [1] for selecting calibration and validation (Cal/Val) sets and demonstrate its use for ocean color bio-optical models. The approach combines the bootstrapping method of Efron and Tibshirani [2] with the Jackknife technique (which leaves out one, or more, observation) and adapts the sample size at each iteration. Bootstrapping and Jackknife methods are usually used to provide the standard error of the derived "plug in" estimates and have been employed for validating ocean color models. However, the combination of bootstrapping without replacement with Jackknife sampling and changing the sample size, at each iteration, is novel and provides not only the accuracy of regressed estimates, but also the underlying probability distribution of regressed estimates and their errors. The developed method samples from a complete matchup set to populate many sets of Cal/Val pairs. Each pair is used to derive the model coefficients and their associated errors, from which the probability distributions of the calibration and validation result is determined.

The method is demonstrated for matchups of chlorophyll-a (Chl-a) concentrations and derived absorption coefficients obtained from the NASA bio-Optical Marine Algorithm Data (NOMAD, version 2a [3]). The general practice is to derive the absorption coefficients from the observed radiance spectra using semi-analytical ocean color models (e.g. Salama and Shen 2010). Lambert-Beer law is then employed to estimate the absorption per unit mass from derived absorption coefficients and measured concentrations as:

$$a_{chla} = a^*_{chla} \times C_{chla} + \epsilon \qquad (1)$$

Where a_{chla} is the absorption coefficient of Chl-a in m^{-1}, a^*_{chla} absorption per unit concentration of Chl-a in $m^2.mg^{-1}$, C_{chla} the concentration of Chl-a in $mg.m^{-3}$ and ϵ is an offset term in m^{-1}. The presented method is applied on the n (424) match-up data points to derive a^*_{chla} and ϵ from Eq. (1) using the GeoCalVal model [1].

Discussions

The determination coefficients, R^2, of the Cal set are plotted against those of the Val set in Fig. 1-a for all possible combinations. The data point position with respect to the x-axis is an indication for the ability of the model to fit the matchups of the Cal set, whereas its position with respect to the y-axis represents the model's performance in deriving Chl-a absorption coefficient. NOMAD matchup produces a narrow region of Cal/Val pairs, for which the calibration R^2 is similar to validation R2, about 0.75–0.85 (light-grey coloured data points in Fig. 1-a. In other words, within these Cal/Val subdivisions the model validity and the accuracy assessment are balanced. This region defines the optimal setups for subdividing matchups into Cal/Val sets. The underlying mechanisms of the data points in this region are investigated further. We found that the optimal Cal/Val sets are obtained when the arithmetic mean and dispersion of each set are equal to those of the original data set. Figures 1-b,c show the derived probability distributions (PD) of model coefficients, and the associated uncertainties, for the NOMAD matchup set. The resulting PD of model's slope a^*_{chla} have high kurtosis (acute peak around the mean) values and flat tails, i.e. more prone to outliers. The reason for having flat tails is due to the fact that the accuracy of model coefficients depends on the size of the Cal set. In other words, for a large Cal set we expect to have higher accuracy as most data points are used; however, this makes them also sensitive to outliers in the Val set, because most of the data points have been used to create the Cal set. The proposed method reveals the shape of the underlying probability distribution without any a priori assumption on its parameters (e.g. degree of freedom). In the shown example (linear model of Eq.1), the t-probability density function (fitted black lines in Fig. 1-b and c) should be employed to describe the distributions of model coefficient and uncertainties. For non-linear models there is no straightforward theoretical approximation of the expected probability distribution. If we would follow the theory, we would have no means to justify our assumption on the underlying probability distribution and its parameters.

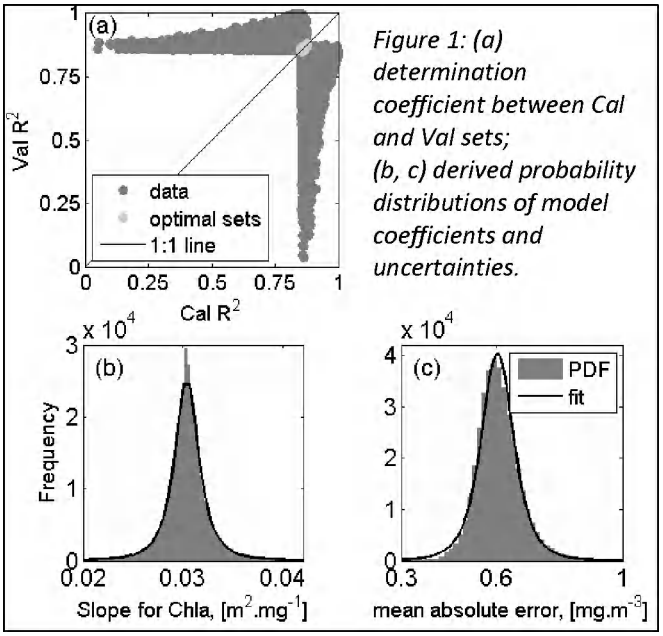

Figure 1: (a) determination coefficient between Cal and Val sets; (b, c) derived probability distributions of model coefficients and uncertainties.

Conclusions

i– The method provides an optimal setup for subdividing matchups into Cal/Val sets; ii– The coefficients and associated uncertainties of linear observation models follow the t-location scale distribution; iii– the optimal Cal/Val sets are obtained when the arithmetic mean and dispersion of the Cal/Val sets are equal to those of the original data set; iv– the presented method is applicable to any data set and can be adjusted to any observation model regardless of the application area.

References

[1] Salama M. S, van der Velde, R., van der Woerd, H.J., Kromkamp, J.C., Philippart, C.J.M., Joseph, A.T., O'Neill, P.E., Lang, R.H., Gish, T., Werdell, P.J. and Su, Z. (2012) Technical notes : Calibration and validation of geophysical observation models. Biogeosciences, 9,6, 2195–2201.

[2] Efron, B. and Tibshirani T. (1993) An introduction to the Bootstrap, 57, Monographs on Statistice and Applied Probability, Chapman & Hall/CRC.

[3] Werdell, J. and Bailey, S.: An improved in-situ bio-optical data set for ocean color algorithm development and satellite data product validation, Remote Sens. Environ., 98, 122–140, 2005.

Current Advances in Uncertainty Estimation of Ocean Color Products

M. S. Salama[*1,2]

[1]University of Twente, ITC, The Netherlands
[2]Royal Netherlands Institute for Sea Research (NIOZ), The Netherlands
Email: s.salama@utwente.nl

Summary

In this talk I review recent advances in uncertainty estimation methods for ocean color products and inter-compare their results. Both deterministic and stochastic methods are presented and their results are inter-compared. The stochastic method is more appropriate to estimate actual uncertainty of ocean color derived products than the deterministic methods. Stochastic methods, however, are still limited to few studies and require prior information. The uncertainties in inherent optical properties (IOPs) could be decomposed only if additional information is provided a priori. Using a simple exercise it is shown that atmospheric-induced errors are major contributors to the total error, whereas model-induced errors are intrinsic to the derived IOPs and depend on the used parameterization and number of spectral bands. A self-consistent and operational method is, however, still required to estimate the uncertainties of IOPs.

Introduction

Ocean color radiometric data are related to the physical and biological properties of water constituents through inherent optical properties (IOPs). These IOPs characterize the absorption and scattering of the water column and are used as proxies to water quality variables. The scientific procedure to derive IOPs from ship/space borne remote sensing data can be divided into three steps: i- *forward modeling*, relates the radiometric data to the IOPs of the water column; ii-*parametrization*, defines the minimal set of IOPs whose values completely characterize the observed radiance; iii- *inversion*, derives the values of IOPs, and hence water quality variables, from radiometric data.

Ocean color derived IOPs have an inherent stochastic error component. This is due to the dynamic nature of aquatic biogeophysical quantities, intrinsic sensor fluctuations, model approximations, correction schemes and inversion methods. Due to stochasticity of the measurements, as well as model approximations and inversion ambiguity, the retrieved IOPs are not the only possible set that caused the observed spectrum. Instead, many other IOPs sets may be derived. The probability distribution functions of the estimated IOPs provide, therefore, all the necessary information about the variability and uncertainties. Generally, uncertainty assessment of ocean color data falls under one of two methods, namely deterministic or stochastic methods. Deterministic methods are based on gradient techniques and have been used to assess the uncertainty of IOPs [1, 2]. The main drawback of gradient-based methods is that they depend on the used ocean color model to derive the IOPs and on the radiometric uncertainty. On the other hand, stochastic methods are less dependent on the used ocean color model but need *a priori* information on the errors to do the inference [3]. The problem arises when we attempt to validate these uncertainty models. The uncertainty here is estimated as the difference between ground truth measurement and satellite derived products. Direct matching between ocean color products and field data imbed, however, an inherent scale difference. This scale difference between *in-situ* measurements and a pixel of ocean color satellite is at least three to four orders of magnitude for nadir match-up sites and much larger for off-nadir ones. This huge scale difference adds up an extra uncertainty component when validating ocean color products. Therefore the validation of ocean color derived products should attribute the uncertainty to the scale difference, noise errors, correction errors and retrieval accuracy.

This talk is organized as follow: first I describe the ocean color paradigm, i.e. ocean color models, their parametrizations and inversion. Deterministic methods for error derivation are then described and followed by explanation of stochastic uncertainty methods. The results of both families (deterministic and stochastic) are inter-compared and complimented by an exercise to decompose the different sources of uncertainty. I finalize the talk by discussing the advantages and limitations of error estimation methods and initiate the thoughts for future developments.

Discussions

Figure 1 shows the errors obtained from deterministic model [1]. The model is applied to MERIS image acquired over the North Sea, Fig.1-i

The scatter plot (Fig.1-ii) of the red box shows on the X-axis the derived concentrations of chlorophyll-a (Chl-a) and on the Y-axis the associated errors.

Figure 1-iii shows the estimated uncertainties, expressed as standard deviation, against the known root-mean-square of errors (RMSE) using stochastic and gradient -based methods as applied to simulated IOCCG data set.

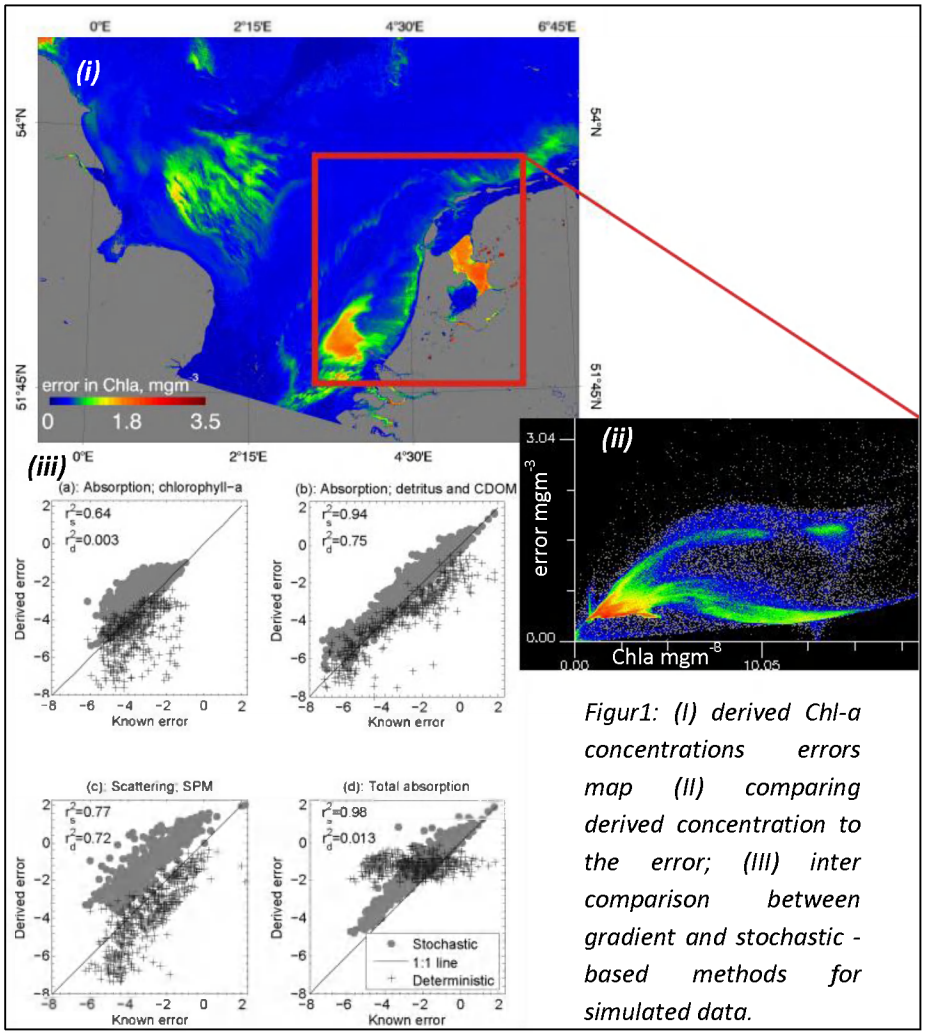

Figur1: (I) derived Chl-a concentrations errors map (II) comparing derived concentration to the error; (III) inter comparison between gradient and stochastic -based methods for simulated data.

Conclusions

Stochastic method has a better performance and is more appropriate to estimate actual errors of ocean-color derived products than the gradient based methods. The method, however, has a tendency to overestimate the values of errors and required prior information. A self-consistent and operational method is, therefore, still required to estimate the uncertainties of IOPs.

References

[1] Maritorena, S. and Siegel, D. (2005). Consistent merging of satellite ocean color data sets using a bio-optical model, Rem. Sens. Envi. 94, 4, 429–440.

[2] Lee, Z., Arnone, R., Hu, C., Werdell, J. & Lubac, B. (2010). Uncertainties of optical parameters and their propagations in an analytical ocean color inversion algorithm, Appl. Opt. 49,3, 369–381.

[3] Salama, M. and Stein, A. (2009). Error decomposition and estimation of inherent optical properties, Appl. Opt. 48, 26, 4947–4962.

Water typed merge of chl-a algorithms and the daily Atlantic (1km) and global (4km) chlorophyll-a analyses of MyOcean II.

Bertrand Saulquin (1), Francis Gohin (2), Garnesson Philippe (1), Odile Fanton-d'Andon (1)

(1) ACRI-ST, Sophia-Antipolis, France. (2) Ifremer Brest , France.

Contact: bertrand.saulquin@acri-st.fr

Summary

The provision of continuous (cloudless) daily fields of chlorophyll-a (chl-a) remains today a challenge. Such products are nevertheless of great interest for users and modellers. We propose here a simple methodology to merge the chl-a fields estimated using several algorithms depending on their validation results on determined water types. The merged fields of chl-a are then optimally interpolated to provide the global MyOcean II chl-a analysis at 4 km resolution and the Atlantic MyOcean II chl-a analysis at 1km resolution. The validation results performed using matchups show a clear added value of both, the merging of algorithms and the spatio-temporal interpolation. The level 4 chl-a analyses are available on a daily base using the MyOcean II facilities.

Introduction

Many algorithms are available for the community to estimate the chl-a concentration from satellite data. The OCx algorithms were calibrated for open ocean (case 1) waters, where the observed spectral shape is constrained by the water and the chl-a absorption spectrum. In coastal waters, the reflectance of the suspended matters and the absorption of the yellow substances influence also the observed spectrum. Today, many 'regional' algorithms have been derived by the scientists to estimate the chl-a locally. We propose here to determine reference water types from the shape of in-situ radiometric profiles. Once the reference water types estimated, we use the membership probability of the satellite derived spectrum to merge the chl-a fields in an optimal way for the end user, i.e. the 'best' algorithm is used on its better domain.

Discussion

We used 7952 in-situ spectra, extracted from the MERMAID database (http://hermes.acri.fr/mermaid) that gathers today more than 30 independent datasets including the NOMAD and AERONET-OC datasets. Each spectrum is defined using 6 wavelengths: 412, 442, 490, 510, 555 and 670 nm. These in-situ measurements have been gathered all over the word and the sampling is considered therefore as representative of the natural variability. The distance used in the segmentation procedure is the mean angle between a reference and the observed spectrum:

$$\boldsymbol{\theta = arcos}\left(\sum_{\lambda}\frac{sp(\lambda)*sp\_ref(\lambda)}{|sp|*|sp\_ref|}\right) \qquad (1)$$

We use and iterative procedure and after convergence, 3 reference spectra were defined: for clear waters, chl-a dominated waters, and coastal waters. The posterior probability of a spectrum i to belong to the water type k is estimated as:

$$P(i,k) = \frac{\left(\frac{1}{\theta(i,k)}\right)}{\sum_{k=1}^{N} 1/\theta(i,k)} \quad (2)$$

The most popular chl-a algorithms were validated on each water type and the 'better' chl-a algorithm is in the merging procedure. To ensure a continuous transition between the algorithms & the water types, the merging between the algorithms is obtained as a weighted sum, depending on, the probability P to belonging to the water types.

$$Chla(i) = \sum_{k=1}^{N} P(i,k) * Chla(i,k) \quad (3)$$

Once the chl-a merged (Figure 1, left), we use the simple kriging estimator with a regional estimation of the covariance structure to interpolate the chl-a fields (Figure 1, right):

$$V_K = -\sum_{i=1}^{n}\sum_{j=1}^{n} \lambda_i \lambda_j \gamma(x_i, t_i; x_j, t_j) + 2\sum_{i=1}^{n} \lambda_i \gamma(x_i, t_i; x_0, t_0). \quad (4)$$

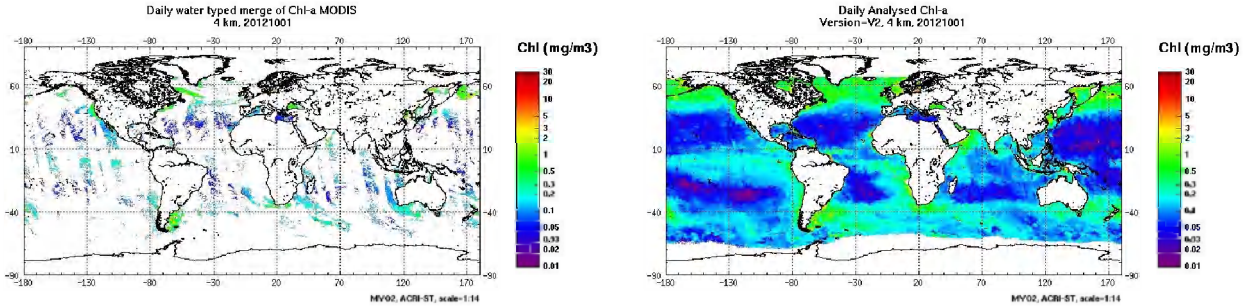

Figure 1: left, the water-typed merge of daily chl-a fields (here 3 different algorithms were used). Right, the corresponding daily optimal interpolation provided in MyOcean II.

Conclusions

The daily spatial coverage has increased from 14 % for the MODIS daily coverage at global scale, to 90 % for the analysed product and from 14% to 90% over the Atlantic. Results of the analyses validation show the same quality in term of bias and standard deviation compared to the merged fields of chl-a, with an increase of in mean X4.5 of the number of matchups. Using GSM only the results of the matchups were nb= 217, S= 1.23, R=0.74, Bias = 0.06, while for the merged chl-a fields the results were nb= 279, S= 1.13, R=0.79, Bias = 0.03 underlying the added value of the merging of chl-a fields derived from different algorithms approach adopted for MyOcean 2.

Acknowledgements

This research was supported by the European Community's Seventh Framework Programme FP7/2007-2013 under grant agreement FP7-SPACE-2009-1/ Collaborative project N° 241759 FP7. These research work is part of a national program on ocean color (GIS–COOC) supported by CNES.

Detection of linear trends in multi-sensor time series in presence of auto-correlated noise: application to the chlorophyll-a SeaWiFS and MERIS datasets and extrapolation to the incoming Sentinel 3 - OLCI mission.

Bertrand Saulquin (1, 2), Ronan Fablet (2, 3), Antoine Mangin (1), Grégoire Mercier (2, 3), David Antoine (4), Odile Fanton d'Andon (1).

(1) ACRI-ST, Sophia-Antipolis, France. (2) Institut Mines-Telecom Bretagne, Brest , France. (3) Université Européenne de Bretagne, Rennes, France. (4) Laboratoire d'Océanographie de Villefranche (LOV), France.

Contact: bertrand.saulquin@acri-st.fr

Summary

The detection of long-term trends in geophysical time series is a key issue in climate change studies. This detection is affected by many factors: the amplitude of the trend to be detected, the length of the available datasets, and the noise properties. Although the auto-correlation observed in geophysical time series does not bias the trend estimate, it affects the estimation of its uncertainty and consequently the ability to detect, or not, a significant trend. Ignoring the auto-correlation level typically leads to an over-detection of significant trends.

Satellite time series have been providing remote observations of the sea surface for several decades. Due to satellite lifetime, usually between 5 and 10 years, these time series do not cover the same period and are acquired by different sensors with different characteristics. These differences lead to unknown level shifts (biases) between the datasets, which affect the trend detection. We propose here a generic framework to address the detectability of a linear trend and its significance from multi-sensor datasets.

Introduction

From a methodological point of view, we extend the statistical analysis of linear trends in single-sensor time series in presence of auto-correlated noise [Tiao *et al.*, 1990; Weatherhead *et al.*, 1998] to multi-sensor time series. In particular we address both time overlaps and time gaps between time series. We report and discuss an application to the MERIS and the SeaWiFS chl-a datasets, which clearly demonstrate the gain of this joint analysis.

We investigate how also the time overlap between successive satellite missions could be optimized to improve the detectability of long-term trends and exploit the proposed statistical methodology to evaluate the duration of the S3-OLCI observation series required to improve the joint SeaWiFS-MERIS trend detection based on the hypothesis that the OLCI-MERIS level shift uncertainty will be of the same magnitude than the SeaWiFS-MERIS one.

Discussion

Given a two-sensor dataset, we assume that the two time series share the same long-term trend and seasonal patterns but involve an unknown level shift and correlated noise processes:

$$y_t = \mu + \omega.t + S_t + N_{1t},\ t = 1..n_1 \qquad \text{with} \qquad N_{1t} = \Phi_1 N_{1t-1} + \varepsilon$$

$$y_t = \mu + \omega.t + \delta.U + S_t + N_{2t},\quad t = T_0..n_2 \quad \text{with} \qquad N_{2t} = \Phi_2 N_{2t-1} + \varepsilon$$

where the time t is in any case relative to the start of the first time series, which is considered as the reference. T0 is the starting time of the second time series, and n1, n2, are respectively the length of the first and second time series. μ and ω are respectively the intercept term and the linear trend shared by the two time series. δ is the unknown level shift of the second time series compared to the first one, supposed here as constant in time and N_1 and N_2 the first order residuals (AR1). The trend uncertainty $\sigma_{\hat{w}}$ can then be expressed as a function of the weighted white noise variances and the trend coefficient uncertainty, $G = f(n_1, n_2, \Phi_1, \Phi_2, DT, \alpha)$ with DT the overlap or time interval between the two time series and α the correlation coefficient between the two white noise processes.

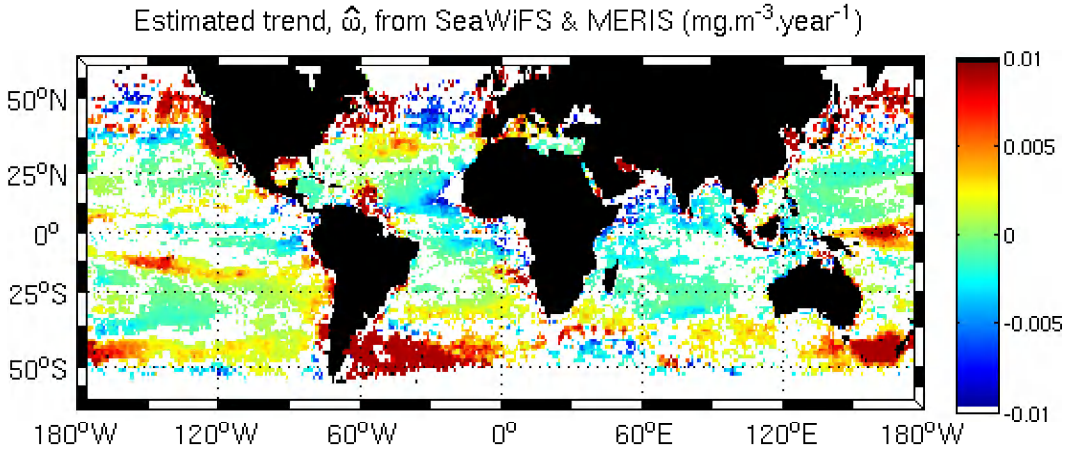

Figure 1: Estimated significant trend estimated from the multi-sensor model using the SeaWiFS and the MERIS dataset (1998-2011).

Conclusion

When two time series are available, the trend detection depends on the uncertainty on the level shift between the datasets. In case of an overlap, the shift uncertainty is diminished. The use of the joint chl-a SeaWiFS-MERIS dataset over the period 1998-2011 led to the detection of 60% of significant trends, compared to 41 % for the SeaWiFS dataset only and 50% for the MERIS dataset only, contributing to a better characterization of region-specific patterns in the detected trends. Using the same model, we estimated the minimal region-dependent duration of the Sentinel 3 - OLCI mission necessary to improve the detection of long-term linear trends issued from the SeaWiFS-MERIS dataset. We estimated a mean value of 53 months for the needed Sentinel 3 – OLCI observations, with some region-dependent fluctuations between 40 to 68 months. This simulation was carried out using an uncertainty level on the shift between OLCI and MERIS of the same magnitude than the one estimated between SeaWiFS and MERIS. These results are coherent with the expected lifetime of the Sentinel 3-OLCI mission, and suggest that the analysis of the global long-term patterns should actually benefit from the joint analysis of SeaWiFS, MERIS and Sentinel 3-OLCI datasets.

Satellite Derived Primary Productivity Estimates for Lake Michigan

Robert A. Shuchman[1], Michael Sayers[1], Gary L. Fahnenstiel [1], George Leshkevich[2]
[1]*Michigan Tech Research Institute (MTRI), Michigan Technological University* Ann Arbor, MI 48105
[2]*National Oceanic and Atmospheric Administration (NOAA)/Great Lakes Environmental Research Laboratory (GLERL)* Ann Arbor, MI 48108
Email: shuchman@mtu.edu

Summary
A new Case II water color satellite algorithm to estimate primary production (PP) has been generated and evaluated for Lake Michigan. The Great Lakes Primary Productivity Model (GLPPM) is based on a mechanistic model that utilizes remotely sensed observations as input for some variables. The Color Producing Agent Algorithm (CPA-A) [1] is a full spectrum three color component retrieval approach used to derive chlorophyll *a* values and the diffuse attenuation coefficient (K_d) for Photosynthetically Active Radiation (PAR). Satellite derived PP estimates were used to estimate a preliminary Lake Michigan annual primary production of 8.5 Tg C/year. The new algorithm can be used to generate PP time series estimates dating back to late 1997 and will contribute to improved assessment of Great Lakes primary productivity changes as a result of *Dreissenid* mussel invasions, climatic change and anthropogenic forcing.

Introduction
The rate of primary production (PP) is a fundamental property of aquatic systems and measurements of primary production are critical to our understanding of those ecosystems. The amount of primary production can determine the amount of matter and energy available to higher trophic levels and is thus an important measure for management decisions. While simulated in situ experiments provided accurate estimates of primary production in small volumes of water their application to large lakes was limited. Moreover, these in situ and simulated in situ experiments provide an integrated measure of production that is dependent of many variables, (e.g. phytoplankton biomass, light, temperature, etc.), thus limiting their predictive value. In the early 1970s, Fee [2] developed a mechanistic modeling approach that could provide estimates of primary production based on a limited number of input parameters, i.e., chlorophyll, incident irradiation, and photosynthesis-irradiance parameters. The Great Lakes Primary Production Model (GLPPM) is a satellite based implementation of the Fee model following the methods of Lang and Fahnenstiel [3]. The purpose of this program is to develop, evaluate and utilize a new remote sensing approach for estimating primary production in Lake Michigan. This method is an improvement over previous methods in that it requires less input than the wavelength resolving method of Lohrenz et al. (2004, 2008) and utilizes more robust satellite chlorophyll retrievals from ocean color sensors such as MODIS. Because high quality continuous remote sensing imagery exists back to 1997 (SeaWiFS), the application of remote sensing approaches allow one to determine lake-wide primary production in response to various stressors such as invasive species, climate change, oligotrophication, and anthropogenic forcing.

Discussion

The GLPPM was implemented in Lake Michigan using MODIS reflectance imagery along with Lake specific rates of photosynthesis as a function of irradiance. The GLPPM uses chlorophyll a concentrations estimated from the full spectrum three color component Color Producing Agent Algorithm (CPA-A) retrieval approach. The CPA-A uses lake specific Inherent Optical Property (IOP) cross sections as input to solve the inverse radiative transfer equation with respect to water constituent concentration. GLPPM production estimates were compared to in situ production observations for a single year to assess GLPPM accuracy. The GLPPM performs best in the spring and fall when the euphotic zone is well mixed, while it underestimates during periods of water column stratification in the summer. The GLPPM was applied to three dates in early April 2007, 2008, and 2009 to investigate the annual variation in Lake Michigan production. This analysis clearly showed that late winter/early spring primary productivity varies significantly in space and time at both nearshore and offshore regions. The new GLPPM enables, for the first time, estimates of lake-wide primary production. Using four dates in 2008 (Figure 1) and extrapolating to the shoreline for hatched areas, lake-wide production was calculated, excluding Green Bay, to be 9922 mt/d for March 20, 18846 mt/d for May 12, 33569 mt/d for July 5, and 32845 mt/day for September 1. Furthermore, if one assumes these individual dates to be representative of longer time periods, preliminary annual lake-wide primary production can be calculated. A preliminary estimate of annual lake-wide primary production is approximately 8.5 Teragrams (Tg) of carbon fixed per year. This annual production represents approximately 0.02% of the global oceanic annual carbon fixation.

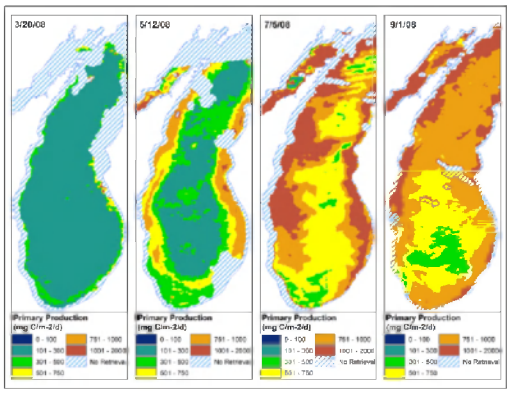

Figure 1. 2008 seasonal primary production estimated from the GLPPM

Conclusions

The satellite based GLPPM was developed for Lake Michigan using Great Lakes specific chlorophyll a concentrations and photosynthetic rates. The model compared well with in situ observations particularly in the spring and fall when the lake is not yet stratified. The GLPPM is able to provide, for the first time, accurate lake wide production estimates that can be used to examine spatial and temporal trends as well as derive yearly total carbon fixation estimates. These observations over time provide insight into the effects climate change, invasive species, and anthropogenic forcing have on Great Lake ecosystems.

References

[1] Pozdnyakov, D., Shuchman, R., Korosov, A., Hatt, C., 2005. Operational algorithm for the retrieval of water quality in the Great Lakes. Remote Sensing of Environment. 97, 353-370.

[2] Fee, E.J., 1973. A numerical model for determining integral primary production and its application to Lake Michigan. J. Fish. Res. Bd. Can. 30, 1447-1468.

[3] Lang, G.A., Fahnenstiel, G.L., 1996. Great Lakes primary production model - methodology and use. NOAA Tech. Memo. ERL GLERL-90, NOAA Great Lakes Environ. Lab, Ann Arbor, MI.

CDOM a useful surrogate for salinity: Mapping the extent of riverine freshwater discharge into the Great Barrier Reef lagoon from MODIS observations

Schroeder T.[1], Brando V.E.[2], Devlin M.J.[3], Dekker A.G.[2], Brodie J.E.[3], Clemenston L.A.[4], McKinna L.[5]

[1] CSIRO Land and Water, Brisbane, QLD 4102, Australia
[2] CSIRO Land and Water, Canberra, ACT 2601, Australia
[3] James Cook University, Townsville, QLD 4811, Australia
[4] CSIRO Marine and Atmospheric Research, Hobart, TAS 7001, Australia
[5] Curtin University, Perth, WA 8645, Australia
Email: Thomas.Schroeder@csiro.au

Summary

Daily ocean colour observations from MODIS-Aqua have been used to map the inter-annual extent of riverine freshwater flood plumes into the Great Barrier Reef (GBR) lagoon between 2002 and 2010. To enable a reliable mapping of low salinity waters we applied a regionally adapted physics-based coastal ocean colour algorithm [1],[2], that simultaneously retrieves chlorophyll-a, non-algal particulate matter and coloured dissolved organic matter (CDOM), from which we used CDOM as a surrogate for salinity (S) for mapping the freshwater plume extent.

Introduction

Riverine freshwater plumes are the major transport mechanism for nutrients, sediments and pollutants into the Great Barrier Reef (GBR) lagoon and connect the land with the receiving coastal and marine waters. Knowledge of the variability of the freshwater extent into the GBR lagoon is relevant for marine park management to develop strategies for improving ecosystem health and risk assessments. The inverse correlation between CDOM and S makes CDOM a useful tracer for lower salinity flood waters. In the open ocean, CDOM absorption originates predominantly from bacterial decomposition of phytoplankton cells, whereas in coastal waters, CDOM is dominated by humic and fulvic acids of terrestrial origin transported to the seas through freshwater runoff from the land as well as autochthonous CDOM from salt marshes, mangroves, inter- and sub tidal benthic microalgae, sea grasses, macro-algae and corals. Water types in the GBR, especially during the wet season, are a complex mixture ranging from clear blue oceanic waters to extremely turbid waters affected by river run-off and with high concentrations of suspended matter (up to 300 mg m^{-3}) and dissolved organic material (CDOM absorption at 443 nm up to 2 m^{-1}). River runoff in the GBR is highly seasonal and correlated with precipitation, with two-thirds of annual rainfall occurring during the wet season from December to April. In addition, there is a large inter-annual variability in precipitation and runoff observed depending on the intensity of the monsoon and the frequency of tropical cyclones.

The optical complexity of the GBR coastal waters especially during run-off conditions requires a model or physic-based inversion approach to distinguish the overlapping absorption features of phytoplankton, non-algal particulate matter and CDOM. In this study, CDOM absorption across the entire GBR World Heritage Area (coast line ~2,300 km) was estimated from a semi-analytical model with variable specific inherent optical properties [2]. Spatially coherent sampling of such a large area is not feasible with in-

situ methods. The application of remote sensing in the GBR however provides a fast and efficient tool for large scale monitoring.

Discussion and conclusions

For each wet season between 2002 and 2010 the freshwater extent was estimated from daily MODIS measurements (Fig. 1) by applying a threshold of 0.24 m^{-1} to maps of seasonally aggregated maximum CDOM absorption at 443 nm. The CDOM absorption threshold was derived from linear regression of 250 concurrent in-situ CDOM and salinity measurements covering the inner most GBR lagoon and corresponds to a salinity of S=30. This rather conservative threshold was established to enable robust automated image classification and to avoid mapping of any autochthonous CDOM production within the reef matrix. Further, the selected threshold is of ecological relevance as some coral species in the GBR have been reported to bleach at a salinity level of S=30 depending on exposure period and water temperature.

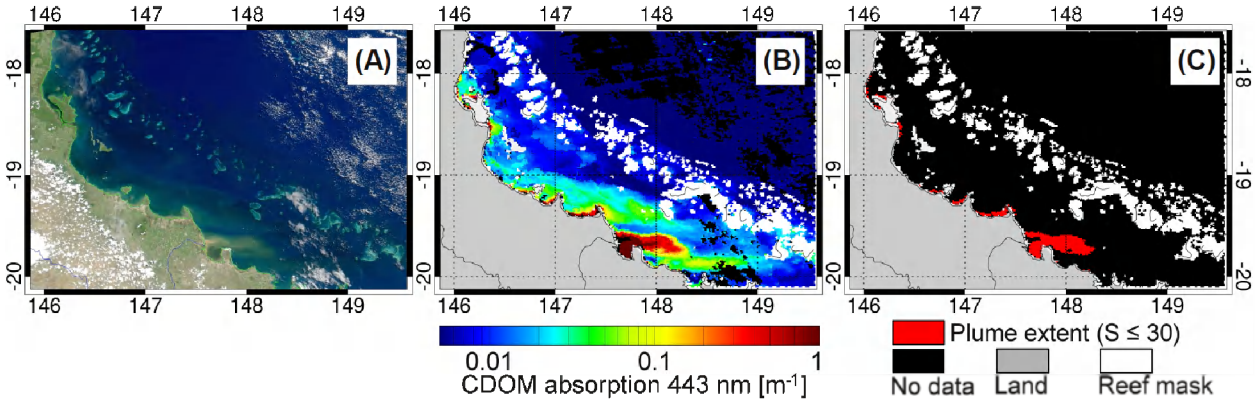

Fig. 1. Pseudo true-colour image of a sub-region in the central GBR (Burdekin) (A) captured by MODIS-Aqua on 02 Feb 2005 and associated CDOM absorption at 443 nm (B) and calculated freshwater plume extent with salinity values S≤30 (C).

The inter-annual extent analysis showed that lower salinity waters (S≤30) were found to reach a number of inner and mid-shelf reefs, but none of the outer shelf reefs located at the edge of the continental shelf. Across the entire GBR World Heritage Area the inter-annual variation in estimated freshwater plume areal extent was found to be highly correlated with flow data from stream gauges (R^2=0.73) and to a lesser degree with Southern Oscillation Index (SOI) data (R^2=0.66). The maximum freshwater extent over the entire GBR was observed in 2008 with an estimated area of approximately 22,000 km^2. Future applications of this method should provide additional information on coral reef exposure duration to various salinity levels, which in combination with sea surface temperature data, may assist Marine Park management in their risk assessment of coral health in the GBR.

References

[1] Schroeder, T., Behnert, I., Schaale, M., Fischer, J., and Doerffer, R. (2007). Atmospheric correction algorithm for MERIS above case-2 waters, International Journal of Remote Sensing 28 (7), 1469-1486.

[2] Brando, V.E., Dekker, A.G., Park, Y.J., and Schroeder, T. (2012). Adaptive semianalytical inversion of ocean color radiometry in optically complex waters, Applied Optics 51 (15), 2808-2833.

Vicarious Calibration Efforts for VIIRS Operational Ocean Color EDR

Menghua Wang[1], Wei Shi[1,2,*], Lide Jiang[1,2], Liqin Tan[1,2], Xiaoming Liu[1,2], and SeungHyun Son[1,2]

[1]NOAA/NESDIS Center for Satellite Applications and Research (STAR), E/RA3, 5830 University Research Ct., College Park, MD 20740, USA

[2]CIRA, Colorado State University, Fort Collins, CO, USA

[*]Presenter, Email: wei.1.shi@noaa.gov

Ocean color products have been routinely produced from the Visible Infrared Imaging Radiometer Suite (VIIRS) on the Suomi National Polar-orbiting Partnership (S-NPP) using the Interface Data Processing Segment (IDPS) since its launch in October of 2011. Recently, VIIRS ocean color Environmental Data Records (EDR), e.g., normalized water-leaving radiance spectra $nL_w(\lambda)$, chlorophyll-a concentration (Chl-a), have been declared as the Beta status. Thus, VIIRS ocean color EDR is now available to public through NOAA Comprehensive Large Array-data Stewardship System (CLASS). Although IDPS-produced ocean color EDR is quite reasonable compared with in situ data, on-orbit vicarious calibration has not been carried out for the IDPS ocean color products. There are some bias errors in the current IDPS-produced ocean color products. It is well known that, in order to derive accurate satellite ocean color products, post-launch on-orbit vicarious calibration is necessary [1]. In this presentation, we describe a vicarious calibration approach for deriving vicarious gains for VIIRS M1 to M7 bands for the IDPS operational ocean color data processing. The vicarious gains for VIIRS sensor are derived using the in situ $nL_w(\lambda)$ data that have been acquired with the Marine Optical Buoy (MOBY) system over oligotrophic waters off Hawaii [2]. With the vicarious calibration gains applied to the VIIRS M1 to M7 bands, ocean color products ($nL_w(\lambda)$ and Chl-a) from VIIRS IDPS operational data processing can be significantly improved.

Specifically, in the vicarious calibration approach, the gain coefficients for the VIIRS two near-infrared (NIR) bands (M6 and M7) at wavelengths of 745 and 862 nm are first derived and tested over the MOBY site and the South Pacific Gyre region. MOBY in situ $nL_w(\lambda)$ data for VIIRS spectral bands since January 2012 have been used to iteratively compute the vicarious gains for the VIIRS M1 to M5 bands. Based on results from iterative $nL_w(\lambda)$ matchup procedure, VIIRS vicarious gains are adjusted and derived for VIIRS bands M1 to M5 with the best matchups of satellite versus MOBY in situ measurements.

From results of extensive evaluations and assessments, we show that with the vicarious calibration VIIRS IDPS-produced ocean color products are significantly improved. In addition, some detailed analyses and discussions for the impact of vicarious calibration on ocean color products are provided. We show that, although there are still some important issues, VIIRS can potentially provide high-quality global ocean color products in support of the science researches and various operational applications.

References

[1] Gordon, H. R. (1998). In-orbit calibration strategy for ocean color sensors. *Remote Sens. Environ.*, 63, 265-278.

[2] Clark, D. K., H. R. Gordon, K. J. Voss, Y. Ge, W. Broenkow, and C. Trees (1997). Validation of atmospheric correction over the oceans. *J. Geophys. Res*, 102(D14), 17081-17106.

Sea ice properties in the Bohai Sea measured by MODIS-Aqua: Satellite Algorithm and Study of Sea Ice Seasonal and Interannual Variability

Wei Shi[1,2*] and Menghua Wang[1]

[1]NOAA/NESDIS Center for Satellite Applications and Research (STAR),
E/RA3, 5830 University Research Ct., College Park, MD 20740, USA

[2]CIRA, Colorado State University, Fort Collins, CO, USA
*Presenter, Email: wei.1.shi@noaa.gov

1. Satellite algorithm development (Shi and Wang, 2012a)

Based on the fact that sea ice reflectance drops significantly in the shortwave infrared (SWIR) wavelengths, black pixel assumption is assessed for three SWIR bands for the Moderate Resolution Imaging Spectroradiometer (MODIS)-at 1240, 1640, and 2130 nm-over the sea ice in the Bohai Sea in order to carry out atmospheric correction for deriving sea ice reflectance spectra. For the SWIR 1240 nm band, there is usually a small (but non-negligible) reflectance contribution over sea ice. Although there is a slight sea ice reflectance contribution at the MODIS 1640 nm band over sporadic land-fast or hummock ice, the black pixel assumption is generally valid with the MODIS bands 1640 and 2130 nm in the Bohai Sea. Thus, the SWIR-based atmospheric correction algorithm using MODIS bands at 1640 and 2130 nm can be conducted to derive sea ice optical properties in the region. Based on spectral features of the sea ice reflectance, a regionally optimized ice-detection algorithm is proposed. This regional algorithm shows considerable improvements in detecting sea ice over the Bohai Sea region, compared with a previous MODIS global sea ice detection algorithm. The sea ice coverage as identified in the new algorithm matches very well with the sea ice coverage from both the MODIS true color image and the imagery from the Interactive Multisensor Snow and Ice Mapping System (IMS).

2 Study of sea ice seasonal and interannual variability (Shi and Wang, 2012b)

During the 2009-2010 winter, the Bohai Sea experienced its most severe sea ice event in four decades, which caused significant economic losses, affected marine transportation and fishery, and impacted the entire marine ecosystem in the region. Measurements from the Moderate Resolution Imaging Spectroradiometer (MODIS) on the Aqua satellite from 2002 to 2010 and surface atmosphere temperature (SAT) data from the National Centers for Environmental Prediction (NCEP) are used to study and quantify the extreme sea ice event in the 2009-2010 winter and the interannual variability of the regional sea ice properties, as well as the relationship between sea ice and the climate variability in the Bohai Sea. The mean sea ice reflectance from MODIS-Aqua visible and near-infrared wavelengths are 933%, 13.26%, and 12.60% in the months of December 2009, January 2010, and February 2010, respectively, compared with the monthly average sea ice reflectance values (from 2002 to 2010) of 9.35%, 11.21%, and 11.41% in the same three winter months. The sea ice monthly average coverages are similar to 5427, similar to 27,414, and similar to 21,156 km(2) in these three winter months. These values are significantly higher than the averages of monthly sea ice coverage of similar to 2735, similar to 11,119, and similar to 10,287 km(2) in the Bohai Sea in December, January, and February between 2002 and 2010. Most of the sea ice coverage was located in the northern Bohai Sea. Both the intra-seasonal and interannual sea ice variability in the Bohai Sea is found to

be related closely to SAT. The mechanism of anomalous SAT and intense sea ice severity are also discussed and attributed to large-scale climate changes due to the variability of the Arctic Oscillation (AO) and Siberian High (SH).

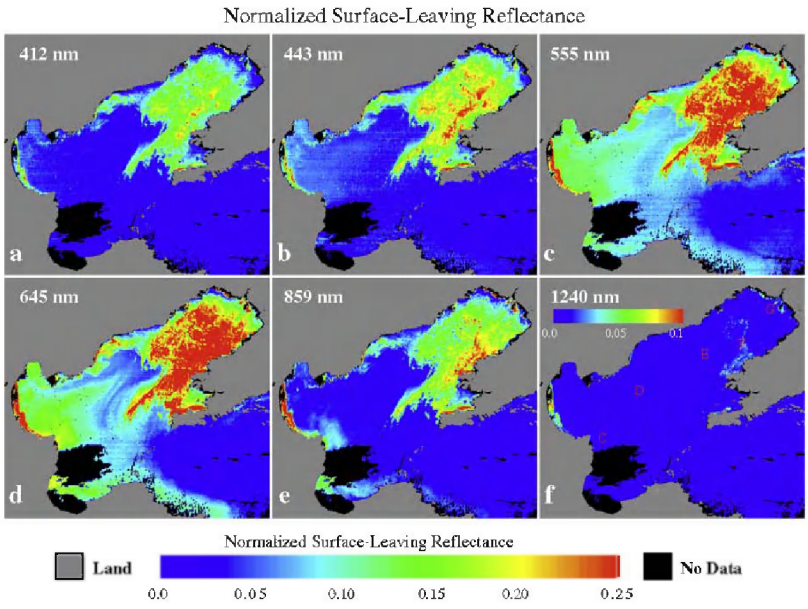

Figure caption:
Normalized surface-leaving reflectance at wavelengths of (a) 412 nm (deep blue), (b) 443 nm (blue), (c) 555 nm (green), (d) 645 nm (red), (e) 859 nm (NIR), and (f) 1240 nm (SWIR) derived from MODIS-Aqua measurements on February 12, 2010.

References

[1] SHI, W., and M. H. WANG. 2012a. Sea ice properties in the Bohai Sea measured by MODIS-Aqua: 2. Study of sea ice seasonal and interannual variability. Journal of Marine Systems **95:** 41-49, DOI 10.1016/j.jmarsys.2012.01.010.

[2] SHI, W., and M. H. WANG. 2012b. Sea ice property in the Bohai Sea measured by MODIS-Aqua: 1. Satellite algorithm development. J. Marine Systems **95:** 32-40.

Title: A Mechanistic Assessment of Global Ocean Carbon Export From Satellite Observation

Authors: D.A. Siegel[1], K.O. Buesseler[2], S.C. Doney[2], S. Sailley[2], M.J. Behrenfeld[3], P.W. Boyd[4]

1 – University of California, Santa Barbara, Santa Barbara, CA USA
2 – Woods Hole Oceanographic Institution, Woods Hole, MA, USA
3 – Oregon State University, Corvallis, OR, USA
4 – University of Otago, Dunedin, New Zealand

Abstract:

The biological carbon pump is thought to export anywhere from 5 to 12 Pg C each year from the surface ocean depth in the form of settling organic particles and its functioning is crucial for the global carbon cycle. Assessments of the global export flux have either been through the extrapolation of point measurements to global scales or the results of ocean system model experimentation. Satellites resolve relevant space and time scales providing guidance to the empirical extrapolation problem, but they do not quantify directly carbon export. Here, we introduce a mechanistic approach for assessing global carbon export by accounting for 1) the size distribution of phytoplankton leading to the direct sinking of algal carbon biomass and 2) upper ocean mass budgeting of phytoplankton carbon and the production of fecal export mediated by zooplankton grazing. The resulting export flux model does an excellent job reproducing regional export flux observations and it reproduces the basic patterns of export spatially and seasonally, predicting a global export of 5.9 (±1.3) Pg C per year. A sensitivity analysis shows a relatively weak dependence of the global flux summaries to large changes in the four model parameters. Our approach provides many insights for future research on carbon export and ecosystem trophic dynamics.

Ocean Diurnal Variations Measured by the Korean Geostationary Ocean Color Imager (GOCI)

Menghua Wang[1], SeungHyun Son[1,2,*], Lide Jiang[1,2], and Wei Shi[1,2]

[1]NOAA/NESDIS, Center for Satellite Applications and Research (STAR)
E/RA3, 5830 University Research Ct., College Park, MD 20740, USA

[2]CIRA, Colorado State University, Fort Collins, CO, USA
[*]Presenter, Email: seunghyun.son@noaa.gov

ABSTRACT

The first geostationary ocean color satellite sensor, Geostationary Ocean Color Imager (GOCI) onboard South Korean Communication, Ocean, and Meteorological Satellite (COMS), which was launched in June of 2010 and has eight spectral bands from the blue to the near-infrared (NIR) wavelengths in 412-865 nm, can monitor and measure ocean phenomenon over a local area of the western Pacific region centered at 36°N and 130°E and covering ~2500 × 2500 km^2. Hourly measurements during daytime (i.e., eight images per day from local 9:00 to 16:00) are a unique capability of GOCI to be used for the short- and long-term regional ocean environmental monitoring.

A recent study from a collaboration between NOAA Center for Satellite Applications and Research (STAR) and Korean Institute of Ocean Science and Technology (KIOST) showed that the GOCI ocean color products such as normalized water-leaving radiance spectra, $nL_w(\lambda)$, for GOCI coverage region derived using an iterative NIR-corrected atmospheric correction algorithm [1] were significantly improved compared with the original GOCI data products and have a comparable data quality as MODIS-Aqua in this region [2]. It is also shown that the GOCI-derived ocean color data can be used to effectively monitor ocean phenomenon in the region such as tide-induced re-suspension of sediments, diurnal variations of ocean optical and biogeochemical properties, and horizontal advection of river discharge.

In this presentation, we show some more results of GOCI-measured ocean diurnal variations in various coastal regions of the Bohai Sea, Yellow Sea, and East China Sea. With possibly eight-time measurements daily, GOCI provides a unique capability to monitor the ocean environments in near real-time, and GOCI data can be used to address the diurnal variability in the ecosystem of the GOCI coverage region. In addition, more in situ data measured around the Korean coastal regions are used to validate the GOCI ocean color data quality, including evaluation of ocean diurnal variations in the region. The GOCI results demonstrate that GOCI can effectively provide real-time monitoring of water optical, biological, and biogeochemical variability of the ocean ecosystem in the region. Finally, two-year GOCI ocean color data are used to characterize seasonal and interannual variations in water optical, biological, and biogeochemical properties in the western Pacific region.

References

[1] Wang, M., Shi, W., and Jiang, L. (2012). Atmospheric correction using near-infrared bands for satellite ocean color data processing in the turbid western Pacific region. *Opt. Express*, 20(2), 741-753.

[2] Wang, M., Ahn, J., Jiang, L., Shi, W., Son, S., Park, Y., and Ryu, J. (2013). Ocean color products from the Korean Geostationary Ocean Color Imager (GOCI). *Opt. Express*, 21(3), 3835-3849.

Seasonal to Interannual Variability in Phytoplankton Biomass and Diversity on the New England Shelf: In Situ Time Series to Evaluate Remote Sensing Algorithms

Heidi M. Sosik
Biology Department, MS 32
Woods Hole Oceanographic Institution
Woods Hole, MA 02540-1049
hsosik@whoi.edu

Hui Feng
Ocean Process Analysis Laboratory (OPAL)
University of New Hampshire
Durham, NH 03824
Hui.Feng@unh.edu

We are exploring and evaluating algorithms that can be applied to remotely sensed ocean color data, extending beyond phytoplankton biomass to the possibility of functional group or size-class-dependent biomass retrievals. We have approached this challenge with unique phytoplankton time series observations made possible by new sensor technology deployed at an ocean observatory on the New England Shelf near Woods Hole, Massachusetts. Observations of phytoplankton and optical properties are being made at the Martha's Vineyard Coastal Observatory (MVCO), with focus on the combination of automated submersible flow cytometry and automated above water ocean color radiometry (AERONET-OC) (Figure 1).

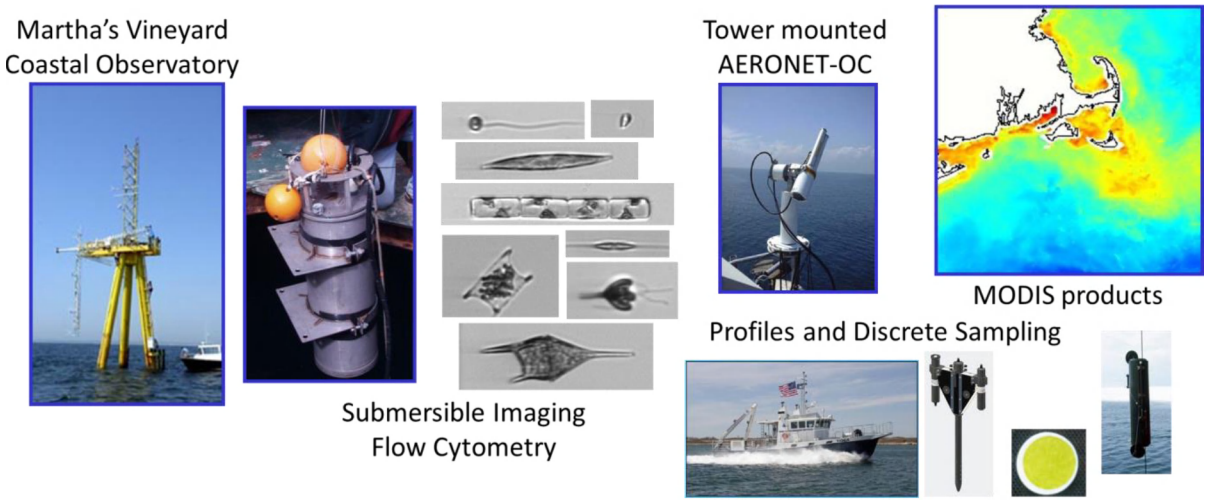

Figure 1. Autonomous sampling strategies at the Martha's Vineyard Coastal Observatory offshore tower site include an AERONET-OC SeaPRISM unit deployed on the rail of the tower, and Imaging FlowCytobot, shown here in its pressure housing ready for underwater deployment on the tower. Additional measurements and sample collection are conducted as part of water column profiles on trips to the site on a coastal vessel.

Our results show the MVCO study site is an excellent test case for a range of optical approaches to characterizing phytoplankton properties. The time series acquired to date emphasize that there are dramatic seasonal and some interannual fluctuations in the phytoplankton community, both

with respect to size structure (Figure 2) and taxonomic composition, thus providing a means to determine which types of algorithms can capture these changes.

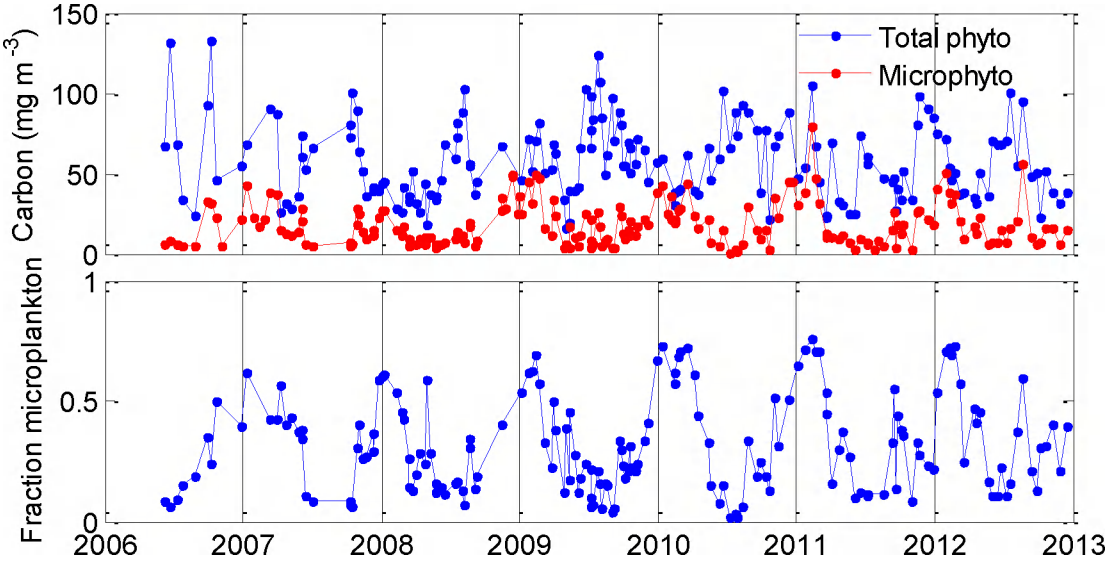

Figure 2. Time series of phytoplankton carbon biomass for the whole community and the microplankton (>20 μm) size fraction (upper panel) and the corresponding fraction of carbon in the microplankton (lower panel) at MVCO. Individual cell biovolumes are estimated from light scattering for small cells (Olson et al. 2003) and from 2D images for large cells and chains (Moberg and Sosik 2012); then carbon is estimated from cell volume according to published relationships (Menden-Deuer and Lessard 2000). Results shown here are for time points that include complete manual verification of image classification results ensuring highest quality estimates not affected by errors such as possible misidentification of detrital particles as plankton by automated classification approaches (Sosik and Olson 2007).

Efforts to date have focused primarily on evaluation of absorption- and pigment-based estimation of community cell size properties and pigment-based characterization of broad taxonomic groups. We find that published absorption- and pigment-algorithms both reproduce general patterns of seasonality, but tend to overestimate the contribution of microplankton in this system. In situ carbon-based taxonomic contributions are correlated with taxon biomass as Chl-a derived from published HPLC pigment algorithms, though relationships are non-linear and unexplained variance can be high, likely due in part to variation in carbon-to-Chl ratio with taxa and growth conditions. Preliminary assessment of published remote sensing algorithms for taxonomic indicator pigments shows they tend to underestimate at high concentrations such that retrieved seasonality is damped compared to in situ assessment.

Retrieval of aerosol and marine parameters in coastal environments: The need for improved bio-optical models

Stamnes[1], Knut, Li[1], Wei, Fan[1], Yongzhen, Stamnes[1], Snorre, Chen[1], Nan, and Stamnes[2], Jakob

[1]Stevens Institute of Technology, Hoboken, New Jersey 07030, USA
[2]University of Bergen, Bergen N-5000, Norway.

Simultaneous (one-step) retrieval of aerosol and marine parameters by means of inverse techniques based on coupled atmosphere-water radiative transfer modeling and optimal estimation can yield a considerable improvement in retrieval accuracy based on radiances measured by MERIS, MODIS, and similar instruments (Li et al., Int. J. Rem. Sens., 29, 5689-5698, 2008) compared with traditional (two-step) methods based on atmospheric correction which frequently lead to negative water-leaving radiances in turbid coastal waters. This one-step approach relies on adequate models describing the inherent optical properties (IOPs) of the atmosphere (aerosols) and the turbid water. However, recent experience (ftp://ccrropen@ftp.coestcolour.org/RoundRobin/CCRRreport.pdf with an annex: ftp://ccrropen@ftp.coastcolour.org/RoundRobin/CCRR_report_OCSMART.pdf) shows that IOPs produced by currently available bio-optical models do not match *in situ* measured IOPs very well, and give pigment absorption values that are smaller than the measured ones for high concentrations of pigmented particles found in turbid coastal waters. To remedy this problem we describe a different approach similar to that advocated by Stramski et al. (Applied Optics, 40, 2929-2945, 2001), and more recently by Zhang et al. (Applied Optics, 51, 5085-5099, 2012), in which we adopt two different groups of particles, one to mimic pigmented particles (characterized by its size distribution and refractive index with respect to water), and another group representing non-pigmented particles (characterized by its own size distribution and refractive index). Then we use the measured IOPs to determine that combination of size distributions, refractive indices, and mixing proportions of pigmented and non-pigmented particles which gives the optimum match between modeled and measured IOPs. This approach to IOP modeling of scattering and absorbing particles in the water is analogous to that currently used by NASA to describe aerosol IOPs (Ahmad et al., Applied Optics, 49, 5545-5560, 2010). It will be demonstrated that this consistent description of atmospheric and water IOPs leads to improved ability to retrieve aerosol and marine parameters in coastal environments through a one-step forward-inverse modeling approach based on coupled atmosphere-water radiative transfer modeling and optimal estimation.

Polymer: a new approach for atmospheric and glitter correction

F. Steinmetz, D. Ramon, P. Y. Deschamps
HYGEOS, Lille, 59000, France
Email: fs@hygeos.com

Summary

The POLYMER algorithm has been initially developed to process MERIS imagery, in particular in presence of intense sun glint. It has proven to be reliable, accurate and insensitive to many artifacts like light cloud contamination, improving greatly the usefulness of the MERIS data. Work is under progress to adapt the Polymer concept to other present ocean color sensors like MODIS and VIIRS. We are presenting preliminary results of application to VIIRS.

Introduction

The POLYMER algorithm [1] has been developed initially to improve atmospheric and glitter correction because of the two following rationales:

- The MERIS data exhibits large areas of sun-glint contamination that could not be treated correctly by the current atmospheric correction schemes extrapolating from the NIR
- The model of atmospheric scattering is simplified by using a polynomial of the wavelength, that allows to account for the multiple interactions between molecular and aerosol scatterings (and glitter) without reference to a specific aerosol model

It has been selected as the MERIS processor in the frame of the Ocean Colour Climate Change Initiative after an extensive comparison with other atmospheric correction algorithms [2].

MERIS processing

An example of the L2 product is given in Fig.1. The standard product processed by the standard MERIS Ocean Colour product (processed by MEGS) is also shown for comparison. Polymer allows retrieving effectively a consistent Chlorophyll pattern along the West Coast of Madagascar that is affected by an intense glitter pattern (up to 20% reflectance) and blacked out by the Megs processing. The POLYMER product is also less affected by the presence of clouds and less noisy than the Megs product. These merits are of paramount importance when compositing L3 products over a period.

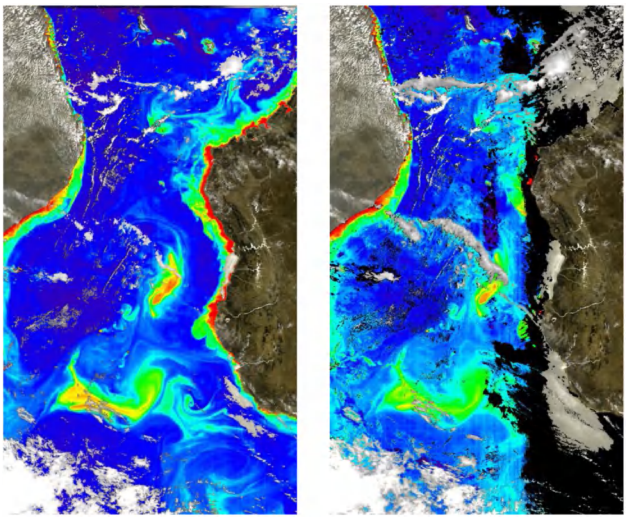

Fig.1: Example of level 2 chlorophyll-a concentration products from Dec. 21, 2003 over the Mozambique Canal, derived from MERIS data with Polymer (left) and MEGS (right) processors

VIIRS Processing

The POLYMER algorithm has been adapted to the processing of VIIRS data using its channels in the Visible and NIR. Preliminary results are shown in Fig.2 as well as the standard processing by NASA (processed by SeaDAS). We can see that the spatial coverage is higher for Polymer, and unlike the standard processing, do not show artifacts in the vicinity of the sun glint pattern.

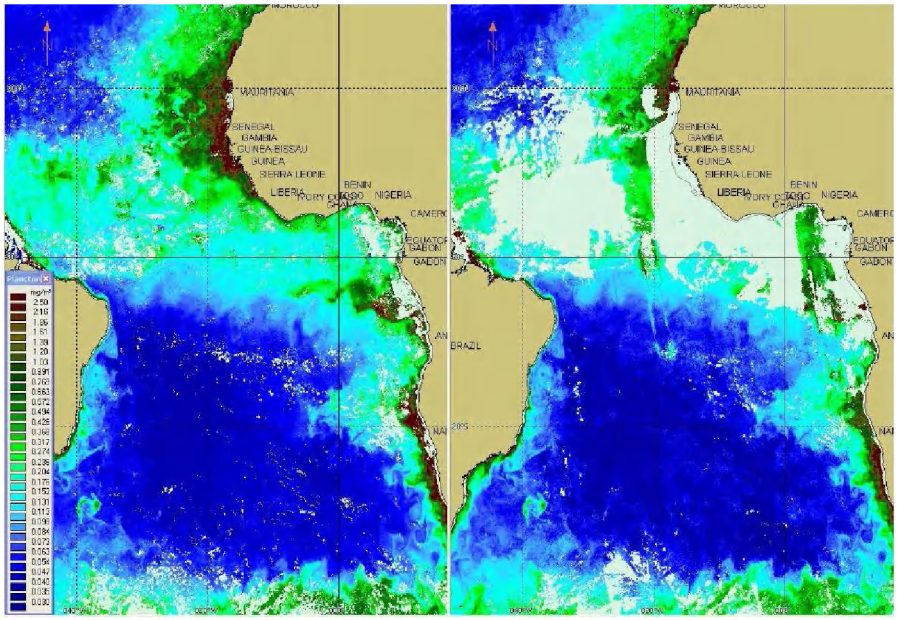

Fig. 2: example of level 3 composite of VIIRS chlorophyll-a concentration in the Atlantic Ocean from March 1-4, 2012, processed by Polymer (left) and SeaDAS (right).

Discussion

Due to a sensor-independent approach and an already successful application to multiple sensors, Polymer is an obvious candidate to the processing of OLCI data at Level 2. It performs best when applied to MERIS who has an excellent inter-band radiometric calibration thanks to its in-flight solar panel calibration and is less sensitive to the absolute radiometric calibration. It is a recommendation to the future to have a strong requirement on the specification of the inter-band radiometric.

References

[1] Steinmetz, F., Deschamps, P. Y. and Ramon, D. (2011). Atmospheric correction in the presence of sun glint: Application to MERIS. Optics Express, 19, 10, 9783-9800.
[2] Müller, D.; Krasemann, H.; Brewin, R.; Brockmann, C.; Deschamps, P-Y.; Doerffer, R.; Fomferra, N.; Franz, B.A.; Grant, M.G.; Groom, S.; Mélin, F.;Platt, T.; Regner, P.; Sathyendranath, S.; Steinmetz, F.; Swinton, J. (2012). The OC-CCI Assessment of Atmospheric Correction Processors. Sentinel-3 OLCI/SLSTR and MERIS/(A)ATSR workshop, ESRIN, Frascati, Italy.

Validation SIMEC adjacency correction for Coastal and Inland Waters?

S. Sterckx[1],E. Knaeps[1]
K.G. Ruddick[2], S. Kratzer[3,4], A. Ruescas[4]

[1] Flemish Institute for Technological Research (VITO), Boeretang 200, B-2400 Mol, Belgium
[2] Royal Belgian Institute for Natural Sciences (RBINS), 100 Gulledelle, 1200 Brussels, Belgium
[3]Stockholm University, Stockholm, Stockholm, SE-106 91, Sweden
[4]Brockmann Consult GmbH, Max-Planck-Str. 2, 21502 Geesthacht, Germany

Email: Sindy.Sterckx@gmail.com

Summary

In many coastal and inland waters environment effects hamper the correct retrieval of water quality parameters from remotely sensed imagery. SIMEC (SIMilarity Environment Correction), a new approach for the correction of adjacency effects is presented in this paper. SIMEC is applied to a MERIS match-up dataset over coastal and inland waters.

Introduction

Several new satellites such as Sentinel-2, Sentinel-3 and the hyperspectral satellites EnMAP and PRISMA will be launched in the near future. These EO sensors will provide a wealth of new data at increased spatial, spectral and temporal resolutions. Although not all conceived as being ocean colour missions, the inland and coastal water community could benefit considerably from these new data sources. A higher spatial resolution extends the existing monitoring efforts to cover even the first nautical mile from coast where the Water Framework Directive (WFD) is still in force or to lakes which are small and have irregular shapes and can not be monitored with the existing missions.

However for these nearshore coastal and inland waters adjacency effects complicate the atmospheric correction process. Light reflected from the nearby land can be forward scattered by the atmosphere into the sensor field of view. This causes a "blurring" of the signal and the effect, generally known as adjacency, background or environment effect, modifies the spectral signature of the observed pixel.

Here, we present a sensor-generic adjacency pre-processing method, the SIMilarity Environment Correction (SIMEC). This correction method was first proposed by Sterckx et al. (2010) [1] for the correction of airborne hyperspectral imagery. The correction algorithm estimates the contribution of the background radiance based on the correspondence with the NIR similarity spectrum [2]. A key aspect of the method is that no assumptions have to be made on the NIR albedo.

The objective of this paper is to validate SIMEC on MERIS images acquired from coastal and inland waters. SIMEC is applied to correct the TOA radiance signal for adjacency effects for a series of MERIS FR data covering the Belgian North Sea coastal waters, the turbid Scheldt estuary and a lake Vänern in Sweden, the third largest lake in Europe. Next, the standard MERIS processor (MEGS) is applied using the ODESA (Optical Data processor of ESA) software, in order to retrieve the water reflectance and to compare with in-situ measured water reflectance.

Discussion

The normalized water reflectance retrieved from ODESA-MEGS processing on MERIS FR images with and without first applying SIMEC are compared to the in-situ measured normalized water reflectance. For several sampling stations the MERIS retrieved normalized water reflectance is strongly underestimated

without SIMEC pre-processing with often negative water reflectance values for the first two MERIS bands (Figure 1). The correspondence between MERIS retrieved normalized water reflectance and in-situ measured normalized water are quantified on the basis of the Root Mean Square Error (RMSE) and the correlation coefficient (R^2). A significant decrease in RMSE and increase in R^2 is observed for several stations after SIMEC pre-processing.

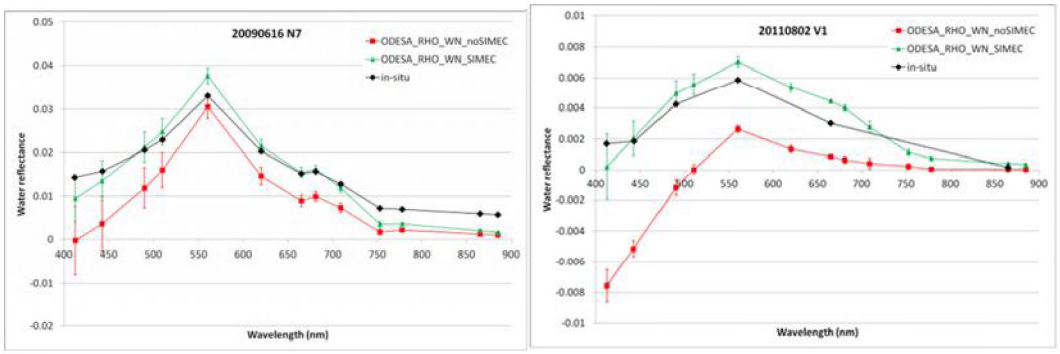

Fig. 1: Comparison between in-situ measured normalized water reflectance (black diamonds) and the normalized water reflectance extracted from MERIS FR within a 3x3 pixel box around the in-situ point derived from the ODESA-MEGS processor with (green triangles) and without (red squares) SIMEC pre-processing for North Sea (N) and Lake Vänern (V) sampling points. Error bars refer to the standard deviation calculated from the retrieved MERIS water reflectance for a 3 by 3 pixel window.

Conclusions

SIMEC is a sensor-generic approach and can therefore directly be applied to future. The performance of SIMEC was tested on MERIS FR images acquired over coastal areas, estuaries and lakes. SIMEC had a positive or neutral effect on the retrieved water reflectance calculated with the MERIS MEGS processor. A decrease in the RMSE up to 400 % was observed after SIMEC pre-processing.

References

[1] Sterckx, S., Knaeps, E., Ruddick, K., 2010, Detection and Correction of Adjacency Effects in Hyperspectral Airborne Data of Coastal and Inland Waters: the Use of the Near Infrared Similarity Spectrum. International Journal of Remote Sensing, 32(21), 6479-6505.

[2] Ruddick, K., De Cauwer, V., Park, Y., 2006, Seaborne measurements of near infrared water-leaving reflectance: The similarity spectrum for turbid waters, Limnol. Oceanogr., 51(2), 1167-1179.

Development of the Black Sea bio-optical algorithms: applications and some results based on ocean color scanner data sets

V. Suslin[1], T. Churilova[2]
[1]Marine Hydrophysical institute of National Academy of Sciences, Kapitanskaya str., 2, Sevastopol, 99011, Ukraine
[2]Institute of Biology of the Southern Seas of National Academy of Sciences, , 2 Nakhimov Ave. Sevastopol, 99011, Ukraine
Email: slava.suslin@gmail.com

Presently the Black Sea is the basin through which not only the transport streams of supply, metal and energy sources are passed, but also output of natural resources including hydrocarbon production takes place on shelf. The main wealth of the Black sea region is its recreational potential: comfortable weather conditions from May to October, unique natural landscape, properties of sea water (salinity ~ 17 ‰ and Secchi disk ~ 15 m on the southern coast of the Crimea) and a lot of historical places. So in near future its using will increase. Suitable tool is needed to track current ecological state of the Black Sea, to forecast and to calculate possible scenarios of various processes and events. Currently the cooperative operational hydrodynamical and ecological model of the Black Sea is this tool [1]. The models of such class induce development of regional algorithms which provides continuous stream of quantitative and qualitative information about biooptical characteristics of the upper layer of the Black Sea.

Main sources of these data are the measurements of the spectral radiances of the ocean-atmosphere system which are made by color scanners on the Earth orbit. Key element of regional biooptical algorithm for the Black Sea is the procedure of separation of the light absorption by phytoplankton and by colored detrital matter (sum of detritus and colored dissolved organic matter) [2, 3]. The example of this separation is shown on the figure. Biooptical characteristics of sea water such as particle backscattering coefficient in visible spectrum, spectral slope of particle backscattering coefficient [4], which is an integral part of inherent optical properties of seawater (*IOPs*), can be recovered, knowing the spectral characteristics of the coefficient of the light absorption by phytoplankton and by colored detrital matter and with remote sensing reflectance. Together with *in situ* measurements of taxonomic composition of phytoplankton they allows to analyze of links between *IOPs* and phytoplankton functional groups.

Based on the established features of the vertical distribution (statistics of field measurements of profiles) of concentrations of chlorophyll *a* and parameterization of the light absorption by all optically active components for the individual seasons and areas, it can restore the downward shortwave radiation field in the upper layer of the Black Sea [5]. This is necessary in the spectral approach to assess the primary production [6] and the contribution of short-wave radiation to the thermodynamic properties of seawater [7].

Acknowledgments

Source Data Credit: NASA/GSFC/OBPG, projects ODEMM, MyOcean-2, PERSEUS, DEVOTES, Russian-Ukrainian project “The Black Sea as a simulation model of the Ocean”, “Fundamental problem of operative oceanography” and “Riski” of

National Academy of Sciences of Ukraine.

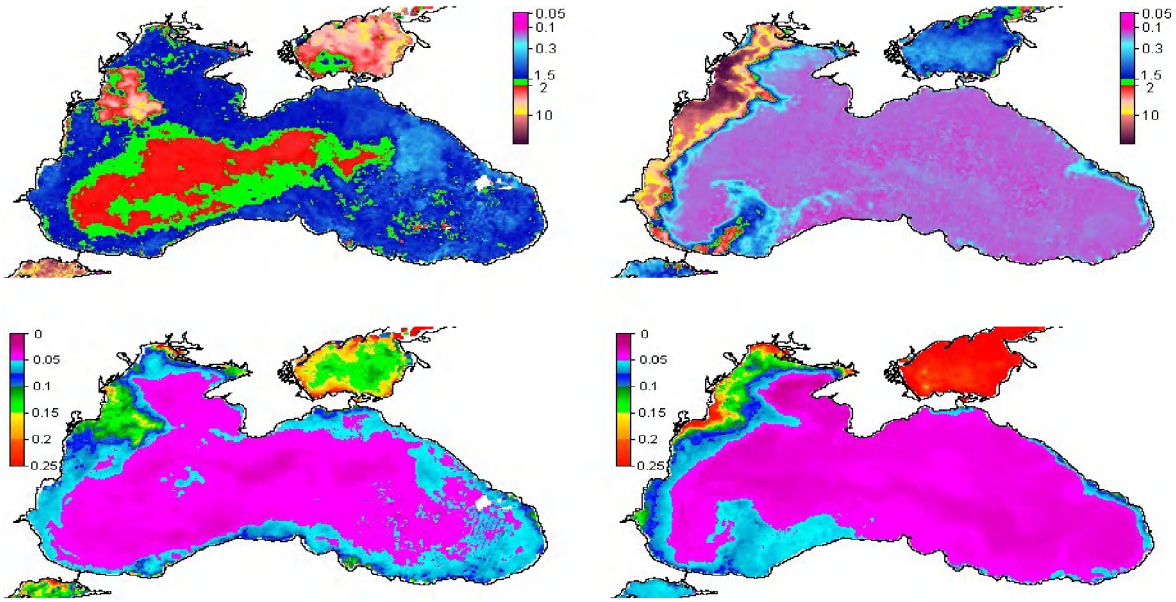

Figure. Example of merge products of chlorophyll a concentration (up, in mg m^{-3}) and absorption coefficient of colored detrital matter at 490 nm (bottom, in m^{-1}) in the 2nd half of March, 2004 (left) and in the 1st half of June, 2006 (right)

References

[1] Korotaev, G. K., Oguz, T., Dorofeyev, V.L., Demyshev, S. G., Kubryakov, A. I. and Ratner, Yu. B.: Development of Black Sea nowcasting and forecasting system, Ocean Sci., 7, 1–21, 2011.
[2] Suslin V., Churilova T., Sosik H. The SeaWiFS algorithm of chlorophyll a in the Black Sea // Marine Ecological J., 2008, Vol. VII, No. 2, p. 24-42, (in Russian)
[3] Suslin V., Sosik H., Churilova T., Korolev S. Remote Sensing of Chlorophyll *a* Concentration and Color Detrital Matter Absorption in the Black Sea: A Semi-Empirical Approach for the Sea-Viewing Wide Field-of-View Sensor (SeaWiFS) // Proceeding of XIX Ocean Optics conference, 6-10 October 2008, Tuscany, Italy, CD.
[4] Suslin V.V., Churilova T.Ya. The Black Sea *IOPs* based on *SeaWiFS* data // Ocean Optics XXI, Glasgow, Scotland, October 8-12, 2012, 9 p. OO121107_Suslin__Vyacheslav_Vladimirovich_OO121107.pdf
[5] Churilova T., Suslin V., Sosik H. Bio-optical spectral modelling of underwater irradiance and primary production in the Black Sea // Proceeding of XIX Ocean Optics conference, 6-10 October 2008, Tuscany, Italy, CD.
[6] Churilova T.Ya., Suslin V.V. Seasonal and inter-annual variability in waters transparency, chlorophyll a content and primary production in the Black Sea simulated by spectral bio-optical models based on satellite data (*SeaWiFS*) // Ocean Optics XXI, Glasgow, Scotland, October 8-12, 2012, 13 p. OO121251_Churilova__Tetyana_OO121251.docx
[7] Kubryakov A., Suslin V., Churilova T., Korotaev G. Effects of Penetrative Radiation on the Upper Layer Black Sea Thermodynamics // MyOcean Science Days, Toulouse, 1-3 December 2010, http://mercator-myoceanv2.netaktiv.com/MSD_2010/Abstract/ Abstract_KUBRYAKOVa_MSD_2010.doc

The Black Sea Color Website

N. Suslina[1], V. Suslin[2], T. Churilova[3]

[1]Sevastopol National Technical University, Sevastopol
[2]Marine Hydrophysical Institute of National Academy of Sciences, Sevastopol
[3]Institute of Biology of the Southern Seas of National Academy of Sciences, Sevastopol
Email: natsuslina@yandex.ru

Launched in the late 70's and early 80's satellite instruments (CZCS and MKS-BS) were the first ones which allowed to retrieve a quantitative information about the water-leaving radiances from the measurements of the spectral radiances of the ocean-atmosphere system with acceptable level of signal/noise [1, 2]. In the late 90's and early 2000's, the next generation of color scanners (OCTS, SeaWiFS, MERIS, MODIS-Terra/Aqua and etc.) began to accumulate to the daily global records of bio-optical products which is still going on [1]. However, as it has been shown in [3], the results of comparison between a global model processing and field measurements are unsatisfactory in different ocean areas. This stimulated the development of regional bio-optical algorithms and, accordingly, of regional websites where these results can be found, in particular, to the Black Sea color website [4]. The feature of this website is that web products were received with the use of regional bio-optical algorithms for the different color scanners during their lifetime period [5-8]. Some examples of presented on the website products are shown in Fig. 1 and 2.

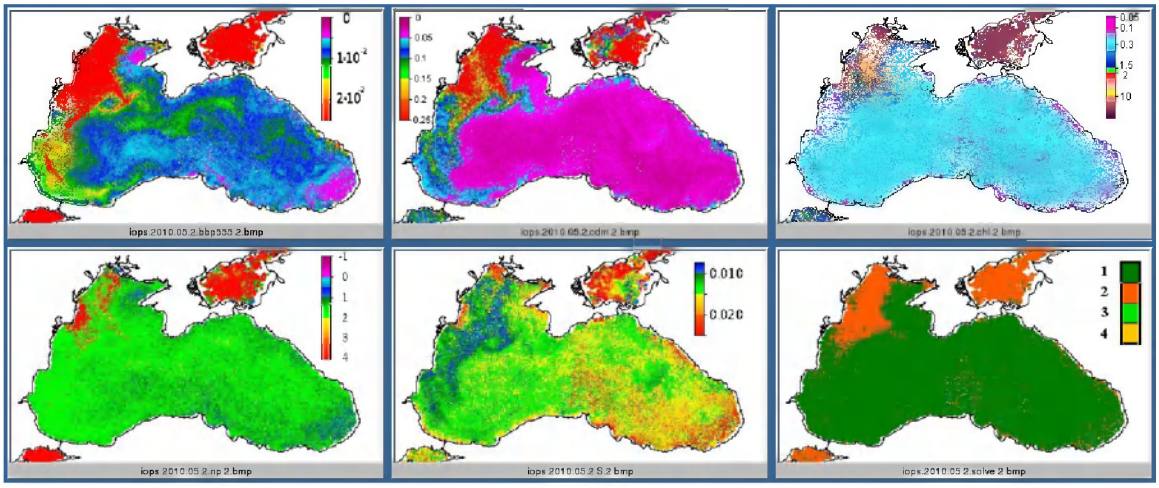

Fig. 1. Example of $IOPs$ *maps for second half of May, 2010.*

Top: (left) particle backscattering coefficient at 555 nm, $b_{bp}(555)$ *, m*$^{-1}$*, (center) absorption coefficient of sum of colored dissolved organic matter and non-algal particles (CDM) at 490 nm,* $a_{CDM}(490)$ *m*$^{-1}$*, and (right) chlorophyll a concentration,* C_a *, mg m*$^{-3}$
Bottom: (left) spectral slope of particle backscattering coefficient, n_p *dimensionless, (center) spectral slope of CDM absorption coefficient* S *, nm*$^{-1}$*, and (right) class of decision, dimensionless*

In addition, it is permanently updated (approximately once a month) in process

of receipt and processing/reprocessing of data set from existing scanners color.

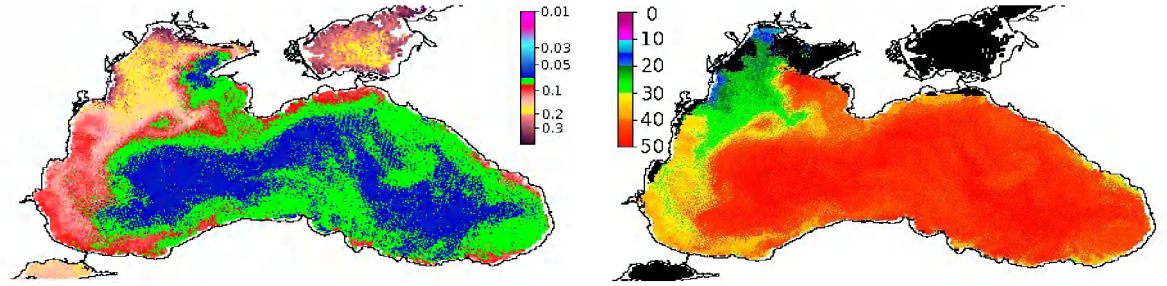

Fig. 2. Example of downwelling diffuse attenuation coefficient at 490 nm, $K_d(490)$ *, and depth of the euphotic zone,* Z_{eu} *,maps for 2nd half of May, 2010: (left)* $K_d(490)$ *is in* m^{-1} *and (right)* Z_{eu} *is in m*

Acknowledgments

Source Data Credit: NASA/GSFC/OBPG, projects ODEMM, MyOcean-2, PERSEUS, DEVOTES, Russian-Ukrainian project “The Black Sea as a simulation model of the Ocean”, “Fundamental problem of operative oceanography” and “Riski” of National Academy of Sciences of Ukraine.

References

[1] Feldman, G. C., C. R. McClain, Level 1 and 2 Browser, Ocean Color Web, Eds. Kuring, N., Bailey, S. W., Thomas, D., Franz, B. F., Meister, G., Werdell, P. J., Eplee, R. E., MacDonald, M., Rubens, M. 28 January 2013. NASA Goddard Space Flight Center. 28 January 2013. http://oceancolor.gsfc.nasa.gov/cgi/browse.pl?sen=am
[2] Bischoff K., Orlicek E., Schmelovsky K, Zimmermann G. (1983) First results of the Interkosmos satellite IK21// Acta Astronaut., Vol. 10, 3135.
[3] Gregg, W., Casey N. (2004). Global and Regional Evaluation of the SeaWiFS Chlorophyll Data Set. Rem. Sens. Environ., 93: (4) 463—479
[4] Black Sea Color Website: http://blackseacolor.com
[5] Suslin V., Churilova T., Ivanchik M., Pryahina S., Golovko N. (2011) A simple approach for modeling of downwelling irradiance in the Black Sea based on satellite data // *Proc. of VI International Conference «Current problems in optics of natural waters» (ONW'2011)*, St-Petersburg. Russia, September 6-9, 2011, Saint-Petersburg, Publishing house of «Nauka» of RAS, 199-203.
[6] Suslin V., Churilova T., Sosik H. The SeaWiFS algorithm of chlorophyll a in the Black Sea // Marine Ecological J., 2008, Vol. VII, No. 2, p. 24-42, (in Russian)
[7] Churilova T., Suslin V., Sosik H. Bio-optical spectral modelling of underwater irradiance and primary production in the Black Sea // Proceeding of XIX Ocean Optics conference, 6-10 October 2008, Tuscany, Italy, CD.
[8] Churilova T.Ya., Suslin V.V. Seasonal and inter-annual variability in waters transparency, chlorophyll a content and primary production in the Black Sea simulated by spectral bio-optical models based on satellite data (*SeaWiFS*) // Ocean Optics XXI, Glasgow, Scotland, October 8-12, 2012, 13 p.

The Felyx High Resolution Diagnostic Dataset System (HR-DDS)

Malcolm Taberner[1], Jean-Francois Piolle[2], David Poulter[3], Jamie Shutler[1],
Peter Walker[1], Shubha Sathyendranath[1]

Felyx is currently under development and is the latest evolution of a generalised High Resolution Diagnostic Data Set system funded by ESA. It draws on previous prototype developments and experience in the GHRSST, Medspiration, GlobColour and GlobWave projects.

Felyx is fundamentally a tool to facilitate the analysis of EO data: it is being developed by IFREMER, PML and Pelamis. It will be free open software written in python and javascript. The aim is to provide Earth Observation data producers and users with an open-source, flexible and reusable tool to allow the quality and performance of data streams from satellite, in situ and model sources to be easily monitored and studied. New to this project, is the ability to establish and incorporate multi-sensor match-up database capabilities. The systems will be deployable anywhere and even include interaction mechanisms between the deployed instances.

The primary concept of Felyx is to work as an extraction tool. It allows for the extraction of subsets of source data over predefined target areas(which can be static or moving). These data subsets, and associated metrics, can then be accessed by users or client applications either as raw files or through automatic alerts. These data can then be used to generate periodic reports or be used for statistical analysis and visualisation through a flexible web interface.

Felyx enables:

* subsetting - large local or remote collections of Earth Observation data over predefined sites (geographical boxes) or moving targets (ship, buoy, hurricane), storing locally the extracted data (reffered as miniProds). These miniProds constitute a much smaller representative subset of the original collection on which one can perform any kind of processing or assessment without having to cope with heavy volumes of data.
* generation of statistics - computing statistical metrics over these miniProds using for instance a set of usual statistical operators (mean, median, rmse), which is fully extensible and applicable to any variable of a dataset. These metrics are stored in a fast search engine which can be interrogated by humans and automated applications.
* generate reports or warnings/alerts - based on user-defined inference rules, through various media (emails, twitter feeds,..) and devices (phones, tablets).
* analysing – analysis of miniProds and metrics through a web interface allowing the data to be

explored and extracting useful knowledge through multidimensional interactive display functions (time series, scatterplots, histograms, maps).

There are many potential applications but important uses foreseen are :

* monitoring and assessing the quality of Earth observations (e.g. satellite products and time series) through statistical analysis and/or comparison with other data sources
* assessing and inter-comparing geophysical inversion algorithms
* observing a given phenomenon, collecting and cumulating various parameters over a defined area
* crossing different sources of data for synergy applications

The services provided by felyx will be generic, deployable at users own premises, and flexible allowing the integration and development of any kind of parameters. Users will be able to operate their own felyx instance at any location, on datasets and parameters of their own interest, and the various instances will be able to interact with each other, creating a web of felyx systems enabling aggregation and cross comparison of miniProds and metrics from multiple sources.

Initially two instances will be operated simultaneously during a 6 months demonstration phase, at IFREMER - on sea surface temperature and ocean waves datasets - and PML - on ocean colour.

1. Plymouth Marine Laboratory, Prospect Place, The Hoe, Plymouth, PL1 3DH, U.K.,
2. IFREMER
3. Pelamis Scientific Software Ltd, Pelamis Scientific Software Ltd, 4 Worcester Court, Bath BA1 6QT, U.K.

Accuracy assessment of satellite Ocean colour products in coastal waters.

Gavin Tilstone, Aneesh Lotliker[1], Steve Groom.

Plymouth Marine Laboratory, Prospect Place, West Hoe, Plymouth, PL1 3DH, UK
[1]Indian National Centre for Ocean Information Services (INCOIS), "Ocean Valley", P.B No.21, IDA Jeedimetla P.O, Hyderabad, 500 055, India

The use of Ocean Colour Remote Sensing to monitor phytoplankton blooms in coastal waters is hampered by the absorption and scattering from substances in the water that vary independently of phytoplankton. In this paper we compare different ocean colour algorithms available for SeaWiFS, MODIS and MERIS with in situ observations of Remote Sensing Reflectance, Chlorophyll-a (Chla), Total Suspended Material and Coloured Dissolved Organic Material in coastal waters of the Arabian Sea, Bay of Bengal, North Sea and Western English Channel, which have contrasting inherent optical properties. We demonstrate a clustering method on specific-Inherent Optical Properties (sIOP) that gives accurate water quality products from MERIS data (HYDROPT) and also test the recently developed ESA CoastColour MERIS products. We found that for coastal waters of the Bay of Bengal, OC5 gave the most accurate Chla, for the Arabian Sea GSM and OC3M Chla were more accurate and for the North Sea and Western English Channel, MERIS HYDROPT were more accurate than standard algorithms. The reasons for these differences will be discussed. A Chla time series from 2002-2011 will be presented to illustrate differences in algorithms between coastal regions and inter- and intra-annual variability in phytoplankton blooms

Coastal and Inland Water Data Product from the Hyperspectral Infrared Imager (HyspIRI)

Kevin R. Turpie[1]
on behalf of the HyspIRI Aquatic Data Products Working Group (HADPWG)

[1]University of Maryland, Baltimore County/JCET, Catonsville, USA, 20902
Email: kevin.r.turpie@nasa.gov

Summary

A team of about three dozen scientists in the coastal and inland water remote sensing community began a dialogue on how the upcoming HyspIRI mission could support the generation of coastal and inland data products and applications using its Visible to Short-wave Infrared hyperspectral (VSWIR) imager, eight thermal bands with high spatial resolution. This group, known as the HyspIRI Aquatic Data Products Working Group (HADPWG), demonstrated from the literature and their research with similar data sets that benefit of the HyspIRI mission of providing global remote sensing in these regions could be transformational. This report provides an overview of their conclusions and their vision for the future.

Introduction

HyspIRI is currently planned to include an imaging spectrometer with 213 spectral channels between 0.38 to 2.5 μm on 0.01 μm centers and a multispectral thermal infrared (TIR) instrument with eight spectral channels (one at 4 μm and seven between 7.5–12 μm) [1]. Both instruments will have a spatial resolution of 60 m at nadir. The spacecraft is also planned to be in an ascending polar orbit, crossing the equator at 10:30 AM local time. The equatorial revisit times will be 19 and 5 days for the VSWIR and TIR instruments, respectively [1]. The instrument will have 14bit radiometric resolution, 2% polarization sensitivity, and a 4° degree westward tilt to reduce solar specular reflectance. The projected SNR of HyspIRI is better than that of Hyperion, comparable to that of the Hyperspectral Imager for the Coastal Ocean (HICO) sensor on board the International Space Station (ISS), and is considered reasonably adequate for accurately retrieving hyperspectral reflectance from water surface for typical coastal conditions.

Discussion

Coastal ecosystems are amongst the most productive in the world, playing a major role in water, carbon, nitrogen, and phosphorous cycles between land and sea. Furthermore, coastal regions are home to about two thirds of the world's population [3]. Coastal counties in the USA alone produced nearly 40% of that country's GDP[4]. The wellbeing these human communities and their economies depends on the status of coastal ecosystems. Significant degradation and loss of wetlands [5], corals, submerged aquatic vegetation (SAV), have occurred [6]. Studies of coastal and inland water ecosystems structure and function, and how they interrelate, are critical to understand and protect these valuable resources.

These marginal regions between land and sea support valuable ecotones that are highly vulnerable to shifts in the environment, whether from climate change and its consequences (e.g., sea-level rise), human activities (e.g., eutrophication or changes to existing watershed hydrology), or natural

disturbances (e.g., storms or tsunamis). The so-called "Decadal Survey" (NRC 2008) [7], which defines the need for the HyspIRI mission, also identifies climate change as being more critical to coastal regions than any other. Establishing baseline maps and inventories for these ecosystems would be an important contribution to that end. Because these drivers of changes can occur on large scales or even globally, spaceborne remote sensing is a key tool for studying these environments. In particular, hyperspectral imagery is a valuable tool to assess coastal ecosystem status, distribution, and composition [8]. The HyspIRI mission in particular is well situated to produce global maps of coastal ecosystems and improve our understanding how these communities are distributed, structured, and function. This supports coastal ecosystem research and environmental conservation and management.

Conclusions

The HADPWG has pooled its resources and research, performed further analyses regarding specific technical issues, and synthesized the compiled information into a list of prioritized data products and applications. These are broken into five major areas:

1. Wetland Cover Classification and Mapping – e.g., tidal marshes, mangrove forests, fresh water wetlands, and boreal wetlands).
2. Water Surface Features and Floating Vegetation (Pleuston) – e.g., oil emulsions, kelp, sargassum mats, sea lettuce, floating debris)
3. Water Column Constituents – e.g., inherent and apparent optical properties, phytoplankton pigments, CDOM, and tripton.
4. Benthic Cover Classification and Mapping – e.g., coral and mollusk reefs, submerged aquatic vegetation, and algal mats.
5. Shallow Water Bathymetry

References

[1] Roberts, D.A., Quattrochi, D.A., Hulley, Hully, G.C., Hook, S.J., Green, R.O., (2012). Synergies between VSWIR and TIR dta for the urban environment: An evaluation of the potential for the Hyperspectral Infrared Imager (HyspIRI) Decadal Survey mission, *Remote Sensing of Environment*, 117, 83-101.

[3] Cracknell, A.P. (1999). Remote sensing techniques in estuaries and coastal zones – an update. International Journal of Remote Sensing, 19(3), 485-496. ISSN 0143-1161.

[4] Kildow, J.T., Colgan, C.S., Scorse, J. (2009). State of the U.S. Ocean and Coastal Economies – 2009. National Ocean Economics Program (NOEP). 60pp.

[5] Barbier EB; Hacker SD; Kennedy C; Koch EW; Stier AC, and Silliman BR., (2011). The value of estuarine and coastal ecosystem services. Ecological Monographs 81(2):169-193.

[6] Klemas, V .V ., (2001). Remote sensing of landscape-level coastal environmental indicators. Environmental Management 27(1): 47-57.

[7] National Research Council (2007). Earth science and applications from space: national imperatives for the next decade and beyond. Committee on Earth Science and Applications from Space: A Community Assessment and Strategy for the Future. 456 pp. (ISBN: 0-309-66714-3).

[8] Zomer, R. J., Trabucco, A. & Ustin, S. L., (2009). Building spectral libraries for wetlands land cover classification and hyperspectral remote sensing. *Journal of Environmental Management*, 90, 2170- 2177.

NASA Science Team Assessment of S-NPP VIIRS Ocean Color Products

Kevin R. Turpie[1], Barney Balch[2], Bruce Bowler[2], Bryan A. Franz[3], Robert Frouin[4], Watson Gregg[3], Charles R. McClain[3], Cecile Rousseaux[5], David Siegel[6], Menghua Wang[7]

[1]University of Maryland, Baltimore County/JCET, Catonsville, USA, 20902
[2]Bigelow Laboratory for Ocean Sciences, East Booth Bay, USA, 04544
[3]NASA Goddard Space Flight Center, Greenbelt, USA, 20771
[4]Scripps Institution of Oceanography, La Jolla, USA, 92037
[5]Universities Space Research Association, Greenbelt, USA, 20771
[6]University of California, Santa Barbara, USA, 93106
[7]NOAA/NESDIS/STAR, College Park, USA, 20742
Email: kevin.r.turpie@nasa.gov

Summary

Following the picture perfect launch of the Visible Infrared Imaging Radiometer Suite (VIIRS) aboard the Suomi National Polar-orbiting Partnership (S-NPP) spacecraft, the NASA S-NPP Science Team began an evaluation of the mission's ocean color data products to determine whether they could continue the existing NASA ocean color climate data record (CDR). To support this evaluation, evaluation products were generated using existing computation infrastructure at Goddard Space Flight Center and also at NOAA, the former having independent calibration and full, mission-level reprocessing capabilities. Members of the science team also investigated the use of algorithms for VIIRS that were not being applied operationally, including those that generated standard products for the Earth Observing System (EOS). Now, with over a year's worth of data, we present our assessment of both the operational ocean color data products and the NASA and NOAA evaluation data.

Introduction

VIIRS is being used by NOAA to routinely generate measurements of the Earth's surface and atmosphere, which are referred to as Environment Data Records (EDR). The ocean color EDR includes normalized water-leaving radiance, inherent optical properties (absorption and phytoplankton backscatter coefficients, a and b_b, at five wavelengths) based on an algorithm developed by Carder et al. [1], and chlorophyll a concentration using the three channel version of the empirical algorithm developed by O'Reilly et al. [2]. The science team needed to determine whether the NOAA ocean color EDR products would meet NASA science objectives, including continuity of the existing climate data record (CDR) established with earlier NASA ocean color missions, including the Sea-viewing Wide Field of view Sensor (SeaWiFS) and the MODerate resolution Imaging Spectroradiometer (MODIS) aboard the EOS satellite Aqua. Team members at the NASA/Goddard Space Flight Center (GSFC) evaluated the EDR products against NASA evaluation products, which were based on standard NASA ocean color algorithms, an independent calibration, and were generated with existing computational infrastructure with a full, mission-level reprocessing capability. Meanwhile, another team member (Wang) also compared the EDR products against those generate with NOAA research algorithms, based on the same standard NASA algorithms and the operational calibration. That investigation also looked at estimation of the diffuse attenuation coefficient at 490nm (i.e., $K_d(490)$), which is not part of the EDR suite, and the potential use of the VIIRS Shortwave Infrared (SWIR) bands to improve atmospheric correction over coastal waters.

Other members of the science team pursued data collection for product validation and for parameterization of other algorithms not currently in the operational processing stream. Data products considered that are part of NASA data record included an estimate of Particulate Inorganic Carbon (PIC) by Balch and an estimate of Photosynthetically Available Radiation (PAR), by Frouin. Experimental algorithms were also explored using *in situ* data. Gregg investigated a novel application that looked to improve the consistency of the chlorophyll *a* record using data assimilation. Siegel compared performance of the Garver, Siegel, Maritorena (GSM) semi-analytic model for VIIRS and MODIS in optically complex waters.

Discussion

The independent evaluation processing at GSFC demonstrated that a consistent, high quality color data could potentially be generated from S-NPP VIIRS using evaluation reprocessing. Indeed, the NASA evaluation chlorophyll *a* concentration from VIIRS agrees remarkably well with MODIS Aqua (see Figure 1). Likewise, VIIRS shows promise in supporting EOS standard products, such as PIC, PAR, and K_d(490). Validation analysis showed that operational and research evaluation surface reflectance showed relatively good comparisons with *in situ* data matching spatial and temporal criteria. However, biases in the radiometry, which a smaller than the uncertainty of the *in situ* regression analysis, are still sufficiently large to negatively impact the quality of the operational chlorophyll *a*.

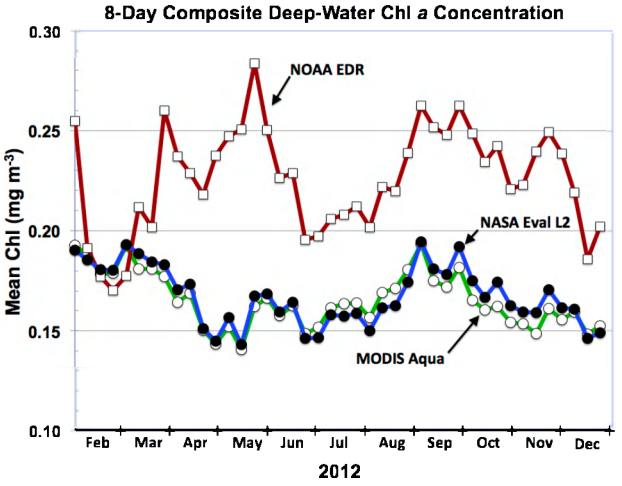

Figure 1 Comparison of Chlorophyll *a* Times Series - Averages were taken from 8-day global composites where depth was >1000m and bins existed for VIIRS EDR, evaluation products and for MODIS Aqua.

Conclusions

Operational and NASA evaluation surface reflectance are reasonable when compared with *in situ* data, however closer investigation indicates the significant biases still exist for the operational product and that this adversely affects derived product quality. Evaluation products show traditional EOS products currently not operationally carried by S-NPP can be generated can be continued with S-NPP at a quality level that is comparable to the NASA CDR. The first year of operational data demonstrates that reprocessing is critical to producing consistent and highly accurate VIIRS ocean color products required for continuity of the NASA CDR.

References

[1] Carder, K.L., Chen, F.R., Lee, Z.P., Hawes, S.K. (1999). Semianalytic Moderate- Resolution Imaging Spectrometer algorithms for chlorophyll *a* and absorption with bio- optical domains based on nitrate-depletion temperatures, Journal of Geophysical Research 104(C3), pp 5403–5421.

[2] O'Reilly, J.E., Maritorena, S., Mitchell, B.G., Siegel, D.A., Carder, K.L., Garver, S.A., Kahru, M., McClain, C.R., (1998). Ocean color algorithms for SeaWiFS, Journal of Geophysical Research 103(C11), pp 24937-24953.

Improving remote sensing water quality algorithms

Twardowski, M., H. Groundwater, J. Sullivan, N. Stockley, Z. Lee

Work on improving algorithms for determining suspended particulate matter (SPM) and chlorophyll concentration from inherent optical property (IOP) measurements will be presented, as this is a critical link to developing improved semi-analytical algorithms for determining these parameters from remotely sensed reflectance. Data collected in northern Lake Michigan in the summer of 2012 will be included in the analysis. One of the limitations of using IOPs such as attenuation or backscattering as proxies for a parameter such as SPM is those relationships are dependent on the composition of the particle population, most importantly variability in size distributions and bulk refractive index. Other techniques have been developed, however, to estimate these particle characteristics from certain IOPs, so that there is potential for combining algorithms to determine water quality parameters with a semi-analytical or fully analytical algorithm from a suite of IOPs with greater accuracy than current empirical relationships.

Atmospheric trace-gas dynamics and impact on ocean color retrievals in urban estuarine and coastal ecosystems

Maria Tzortziou [1, 2], Jay R. Herman [3, 2], Ziauddin Ahmad [4,2], Chris Loughner [1, 2]

[1]University of Maryland, Earth System Science Interdisciplinary Center, College Park, MD, 20742, USA
[2] NASA Goddard Space Flight Center, Greenbelt, MD, 20771, USA
[3]University of Maryland, Joint Center for Earth Systems Technology, Baltimore, MD, 21228, USA
[4] Science and Data Systems, Inc., Silver Spring, MD, 20906, USA

Summary

Spatial and temporal dynamics in trace gas pollutants were examined over urban estuarine and coastal ecosystems in the US, Europe and Korea, using a new network of ground-based Pandora spectrometers. Our measurements showcase the strong temporal and spatial gradients in atmospheric nitrogen dioxide (NO_2) typically observed in moderately to highly polluted coastal areas in both developed and developing countries. Ground based measurements were combined with satellite observations from Aura-OMI, air-quality model simulations, and radiative transfer calculations to assess impacts on ocean color atmospheric corrections and retrievals of coastal ocean biogeochemical variables.

Introduction

Among the largest sources of uncertainty for satellite ocean color retrievals in near-shore waters close to heavily polluted urban centers is the strong temporal variability and spatial gradients in atmospheric absorbing trace gases (e.g., NO2) associated with industrial emissions, traffic, construction, heating and other anthropogenic activities [1]. Atmospheric pollution over near-shore waters can be transported back inland through sea breeze circulations, and converge with freshly emitted pollutants, aggravating air pollution levels and deposition of atmospheric pollutants along the shoreline. Moreover, strong, prolonged sea breeze events can transport a large amount of urban air pollution into the free troposphere, where pollutants have longer lifetime and are susceptible to long range transport offshore and over adjacent shelf and open ocean environments [2]. If not adequately corrected, this variability in coastal atmospheric composition can impose a false impression of temporal and spatial variability on the coastal ocean optical and biogeochemical properties retrieved from space [3]. Consideration of these errors is important for measurements from polar orbiting ocean color (OC) satellite sensors, but becomes particularly critical for geostationary satellite missions that aim at providing higher frequency and higher spatial resolution observations of ocean dynamics from a geostationary orbit.

Discussion

High frequency (every 2 min) measurements from our network of ground-based Pandora spectrometers provided the capability to capture the strong temporal and spatial variability typically characterizing atmospheric composition in coastal urban areas [1] [4] [5]. Our measurements in US, European and South Korean coastal areas show that NO_2 changes frequently exceed 0.5 DU over a period of an hour and 1 DU over a period of less than 3 hours (Figure 1). Local maxima in $TCNO_2$ typically occur early in the morning with secondary peaks often observed later in the afternoon associated with rush-hour NO_x emissions. With a footprint of approximately 12 km x 24 km at nadir, and less sensitive to NO_2 concentrations near the surface where NO_x is emitted, Aura-OMI does not typically capture the strong

spatial and temporal variability in NO_2 observed by the Pandora network and predicted by air quality models such as CMAQ (Community Multi-scale Air Quality model). On a sun-synchronous polar orbit and with an overpass at around 13:30 local time, Aura-OMI misses the morning and late afternoon rush-hour peaks in $TCNO_2$ observed by the Pandoras and predicted by the air-quality model over urban areas, providing a satellite image of $TCNO_2$ under relatively low near-surface emission conditions. Pandora observations were combined with high-resolution CMAQ simulations, and detailed radiative transfer calculations to evaluate how the observed variability in NO_2 affects ocean color retrievals from polar orbiting or geostationary satellite sensors if not corrected, or if atmospheric correction is based on climatology, measurements from other satellite instruments in sun-synchronous orbits (e.g. Aura-OMI), or coarser (and non-coincident) geostationary observations.

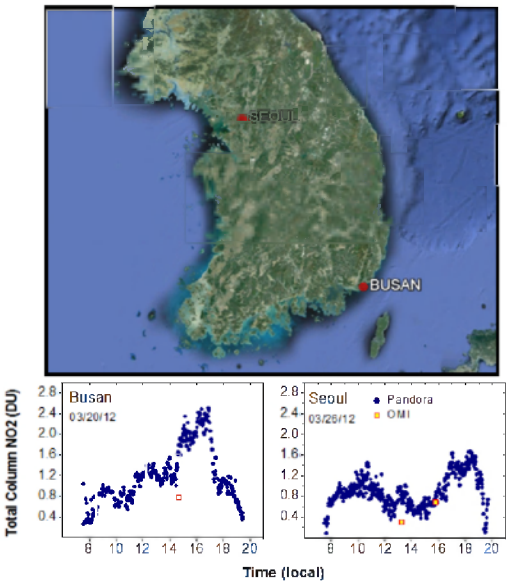

Figure 1 TCNO2 variability in Seoul and Busan

Conclusion

Our results show that high spatial and temporal resolution measurements of atmospheric NO_2 are critical in urban coastal areas to 1) better understand atmospheric dynamics at higher spatial resolution than is currently available from satellite observations, 2) capture the high temporal variability associated with local pollution patterns and photochemical processes, and 3) apply results to improve ocean color atmospheric corrections and retrievals of coastal ocean biogeochemical variables from space.

References

[1] Tzortziou M., J. R Herman, C. P Loughner, A.Cede, N. Abuhassan, S. Naik (2013). Spatial and temporal variability of ozone and nitrogen dioxide over a major urban estuarine ecosystem. Journal of Atmospheric Chemistry, Special Issue PINESAP, DISCOVER-AQ.

[2] Loughner C.P., M. Tzortziou, M. Follette-Cook, K. E. Pickering, D. Goldberg, C. Satam, A. Weinheimer, J. H. Crawford, D. J. Knapp, D. D. Montzka, G. B. Diskin, and R. R. Dickerson (2013; In Review). Impact of bay breeze circulations on surface air quality and boundary layer export. Atmospheric Environment.

[3] Fishman J.; Laura T Iraci; J Al-Saadi; P Bontempi; K Chance; F Chavez; M Chin; P Coble; C Davis; P DiGiacomo; D Edwards; Eldering, A.; J Goes; J Herman; C Hu; D Jacob; C Jordan; S R Kawa; R Key; X Liu; S Lohrenz; A Mannino; V Natraj; D Neil; J Neu; M Newchurch; K Pickering; J Salisbury; H Sosik; Subramaniam, A.; M Tzortziou; J Wang; M Wang (2012). The United States' Next Generation of Atmospheric Composition and Coastal Ecosystem Measurements: NASA's Geostationary Coastal and Air Pollution Events (GEO APE) Mission. Bulletin of the American Meteorological Society. doi:10.1175/BAMS-D-11-00201.1.

[4] Herman J.R., A. Cede, E. Spinei, G. Mount, M. Tzortziou, N. Abuhassan (2009). NO_2 Column Amounts from Ground-based Pandora and MFDOAS Spectrometers using the Direct-Sun DOAS Technique: Intercomparisons and Application to OMI Validation. J. Geophys. Res., 2009JD011848.

[5] Tzortziou M., Herman J.R., Cede A., Abuhassan N. (2012). High precision, absolute total column ozone measurements from the Pandora spectrometer system: Comparisons with data from a Brewer double monochromator and Aura OMI. J. Geophys. Res., 117, D16303, doi:10.1029/2012JD017814

Monitoring eutrophication in the North Sea: an operational CHL-P90 tool

D. Van der Zande[1], A. Ruescas[2], T. Storm[2], S. Embacher[2], K. Stelzer[2], K. Ruddick[1]

[1]Royal Belgian Institute of Natural Sciences, MUMM, Brussels, B-1200, Belgium
[2]Brockmann-Consult, Geesthacht, D-21502, Germany
Email: dimitry.vanderzande@mumm.ac.be

Summary

The satellite-based chlorophyll a 90 percentile product (CHL-P90) is an important indicator used to monitor for the eutrophication state of the North Sea. The accuracy of the CHL-P90 is impacted by the irregular availability of satellite chlorophyll a (CHL) observations both in space and time due to cloudiness, quality flagging, sensor malfunction, etc. A detailed simulation study enabled the development of advanced methodologies to generate CHL-P90 products taking into account the quality of the considered CHL time series and correct for possible sampling irregularities.

Introduction

The Water Framework Directive (WFD) and the Marine Strategy Framework Directive (MSFD) are important drivers for monitoring the coastal and offshore waters in Europe with the objective of reaching a 'good environmental status' [1]. Human-induced eutrophication is one of the considered criteria of the good environmental status and is assessed monitoring the chlorophyll a concentration (CHL) as it is a proxy of phytoplankton biomass. More specifically, for countries such as Belgium, the CHL-P90 over the phytoplankton growing season (i.e. March – November incl.) is the parameter of choice as it describes the intensity of the algal blooms during the year. A satellite-based CHL-P90 tool was developed in the framework of the Aquamar project (EU-FP7) which is available in the open-source toolbox and development platform BEAM (VISAT, Brockmann Consult, Germany). This tool allows for an optimal analysis of satellite-based CHL time series taking into account the irregular sampling by satellites during the growing season.

Discussion

Ocean color satellite data enables the calculation of CHL-P90 pixel-by-pixel resulting in a map product which is expected to provide more accurate CHL-P90 estimates compared to the *in situ* data due to an increased temporal and spatial resolution. However, satellite remote sensing is subject to one major limitation: cloud presence can totally or partially cover the area of interest [2]. For the North Sea this generally results in a high percentage of missing data in the daily images. This missing data is not evenly distributed over the year, and thus impacts the standard percentile calculation. This impact is two-fold and dependent on (1) the availability of observations during the actual phytoplankton bloom and (2) a proportional distribution of observations in the bloom and non-bloom periods.

This study has focused on the additional errors generated in multi-temporal products. A detailed sensitivity analysis was performed using simulations techniques (e.g. MIRO&CO-3D ecosystem model) to generate realistic CHL time series for the Belgian part of the North Sea with high temporal resolution ensuring the availability of sufficient reference data for a variety of algal bloom dynamics (i.e. bloom intensity and timing). These CHL time series were subsequently sub sampled using actual pixel specific MERIS sampling frequencies during the growing season 2003 to 2011 and used for the standard CHL-P90

product generation. A direct comparison of these CHL-P90 products with the reference data showed that with the current observation density of the MERIS satellite relative errors of up to 30% on Chl-P90 estimation due to the effects of irregular sampling are not uncommon. The results of this study were used to improve the CHL-P90 algorithms by the use of an interpolation procedure taking into account the CHL time series quality. The interpolation method was used to compensate for sampling irregularities by filling the gaps in the CHL time series. Both methods were compared to the standard CHL-P90 products and reduced the relative errors caused by the irregular availability of MERIS data to 10%-15%.

Conclusions

The proposed interpolation approach provides a method to take into account sampling issues resolving a significant part of this problem without the need for additional data. This method was translated to an operational BEAM-tool. The open source software BEAM is both a toolbox supporting a wide range of optical sensors for Earth Observation and a development platform that allows users to easily create their own visual and data processing tools. The BEAM Graph Processing Framework (GPF) allows users to create EO data processors, and thus facilitates evolutionary processor development. In combination with a number of analysis tools, BEAM supports the full circle of creating and updating an algorithm, (re-)processing data products, validating the results, and deriving new requirements that in turn affect the algorithm's design.

The gap-filling strategies have been made accessible in BEAM by means of the Temporal Percentile Operator, which has been implemented as operator based on the GPF. Its purpose is to compute the 90th percentile threshold for a time series of EO data products. For a given input set of EO data products, the operator produces a new data product which contains a band containing the respective percentile thresholds for each pixel of the input time series. See figure 1 for an example displayed and analyzed in BEAM VISAT. Additionally, the operator creates a per-pixel time series from the daily means of the input products. This time series can be visualized and analyzed in VISAT using the dedicated Time Series Tool extension.

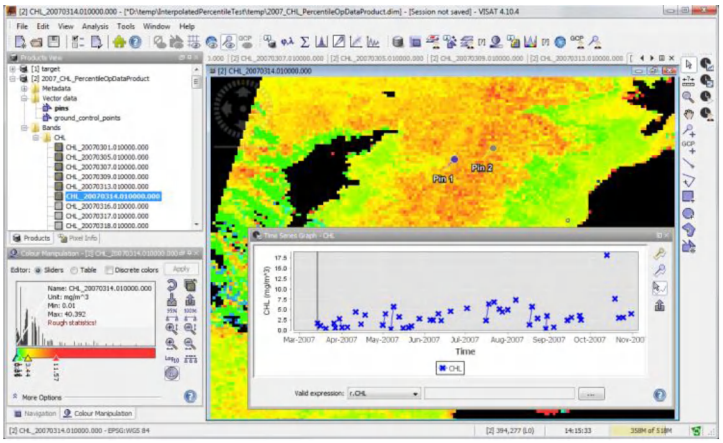

Fig 1. Screenshot of VISAT showing interpolated percentile product

References

[1] Sorensen K, Severinsen GG, Aertebjerg G, Barale V, Schiller C (2002), Remote Sensing's contribution to evaluating eutrophication in marine and coastal waters. European Environment Agency, 41p.

[2] Sirjacobs D., Alvera-Azcarate A., Barth A., Lacroix G., Park Y., Nechad B., Ruddick K., Beckers J.-M. (2011). Cloud filling of ocean color and sea surface temperature remote sensing products over the Southern North Sea by the Data Interpolating Empirical Orthogonal Functions methodology. Journal of Sea Research, Vol. 65, pp. 114–130.

A benchmark dataset for the validation of MERIS and MODIS ocean colour turbidity and PAR attenuation algorithms using autonomous buoy data.

Q. Vanhellemont[1], N. Greenwood[2], K. Ruddick[1]

[1] Royal Belgian Institute of Natural Sciences (RBINS), Management Unit of Mathematical Models (MUMM), Brussels, 1200, Belgium

[2] Centre for Environment, Fisheries & Aquaculture Science (CEFAS), Lowestoft, Suffolk, NR33 0HT, United Kingdom

Email: quinten.vanhellemont@mumm.ac.be

Summary

We present a dataset that combines marine reflectance spectra and several standard L2 products from MERIS and MODIS, with turbidity (T), Photosynthetically Available Radiation (PAR) at different depths, and fluorescence (F) from three autonomous buoys (CEFAS' Smartbuoys) located in turbid coastal waters of the North Sea and the Irish Sea. Our dataset contains several hundreds of matchups between in situ and satellite, and is a powerful benchmarking tool for validating satellite products and retrieval algorithms for turbidity and PAR attenuation.

Introduction

Ocean colour remote sensing is becoming well-established for the monitoring of coastal waters and marine science applications. Validation of satellite-derived products remains problematic, as simultaneous matchups of in situ data and cloud-free satellite data are sparse, and costly to obtain with ship-based measurements. Optical instruments on autonomous platforms can provide many more matchups, typically one per cloud free pixel. For moderate resolution ocean colour sensors (MODIS/MERIS) this is typically one matchup per cloud-free day at temperate latitudes, giving tens of matchups per year and hundreds over the lifetime of a satellite.

Smartbuoys are autonomous buoys operated by CEFAS that record several parameters multiple times per hour. Measurements from three turbid water buoys with deployments between 2002 and 2010 were used: WARP, (Warp Anchorage, 51.5°N, 1°E, Turbidity [5-95%]: 3-53 FTU), WGAB (West Gabbard, 52°N, 2°E, Turbidity [5-95%]: 1-18 FTU), and LIVB (Liverpool Bay, 53.5°N, 3.3°E, Turbidity [5-95%]: 1-21 FTU). Level 2 data from MODIS Aqua (R2012.0) and MERIS (2nd and 3rd reprocessing) was used, distributed respectively by NASA (OBPG - http://oceancolor.gsfc.nasa.gov/) and ESA (MERCI - http://merci-srv.eo.esa.int/merci/welcome.do). A kernel of 25 pixels (5x5) over each station is extracted from the remote sensing data, and is combined with the closest available in situ data within 60 minutes of the overpass (usually < 15 minutes). Fully cloudy or invalid kernels are skipped.

Datasets included from the MODIS data are: Remote sensing reflectance (Rrs, water-leaving radiance with air-sea interface reflection removed divided by downwelling irradiance) at wavelengths 412, 443, 469, 488, 531, 547, 555, 645, 667, and 678 nm. Some OBPG standard products are also included: aot_869, angstrom, chlor_a, cdom_index and Kd_490. Data was screened using the l2_flags, removing data where any of the following flags were raised: CLOUD, HISUNGLINT, LOWLW, MAXAERITER, HILT, HISUNGLINT and STLIGHT. Pixels with negative values in the dataset or negative values in Rrs 412, 443 or 488 and aot_869 were dropped. For chlor_a the respective product flag (CHLFAIL) was also checked.

Datasets included from the MERIS data are: water leaving radiance reflectance (ρ_w=Rrs·π) at wavelengths 413, 443, 490, 510, 560, 620, 665, 681, 708, 753, 778, 865 nm, aero_epsilon_865, aer_opt_thick_865, algal_1, algal_2, yellow_subs, and total_susp. The appropriate product confidence flags (PCD flags) and the CLOUD and HIGH_GLINT flags were used to mask bad data.

Discussion

The merged dataset contains the reflectance spectra from MODIS and MERIS with the corresponding in situ optical instrument data for hundreds of matchups between 2002 and 2010. The dataset allows for a validation of different reflectance based algorithms for turbidity (T) and PAR attenuation (Kpar). The Figure to the right shows an example validation of 596 high quality (with 25 unmasked pixels in the image kernel) MODIS turbidity [1] matchups. A robust relationship is found, with low relative errors. Some scatter is found in the lower T range, where the satellite gives lower values than the buoy. These discrepancies could be due to differences in the sampling of the scattering (backscatter/sidescatter), differences in sampling volume (a few cm^3 for the T sensor), erroneous atmospheric correction, or fouling of the in situ sensor.

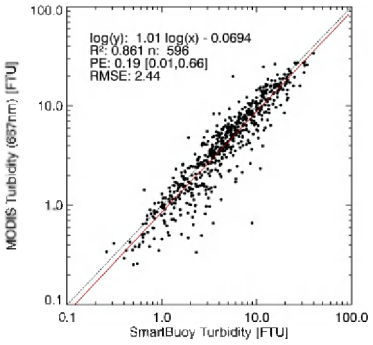

Example MODIS Aqua Turbidity matchups

In situ Kpar can be calculated for the buoys from the PAR sensors at different depths, and can be compared with Kpar products derived from remote sensing, such as [2,3]. The in situ fluorescence data is also included, but is known to have a bad correspondence to HPLC chlorophyll *a* concentrations. However, its relative signal can be relevant, and the data can also be useful in explaining differences between the in situ and remote sensing T or Kpar.

Conclusions

A reference dataset for coastal water ocean colour algorithm testing is presented that combines reflectance data from satellites and turbidity, fluorescence and PAR data from continuously measuring autonomous buoys. The instruments on the buoys were not intended for ocean colour remote sensing validation and could moreover be subject to fouling problems during extended deployments. However, the long time series of data, the large number of matchups, the wide concentration range, the relevant parameters and the high level of quality control of the datasets makes them very useful for coastal water algorithm testing. Following their successful use in studies from one team (http://www2.mumm.ac.be/remsem/publications.php), it was considered useful to make this dataset more widely and easily available for the ocean colour community.

References

[1] Nechad, B., K. G. Ruddick and G. Neukermans (2009). Calibration and validation of a generic multisensor algorithm for mapping of turbidity in coastal waters. SPIE European International Symposium on Remote Sensing, Berlin.

[2] Devlin, M. J., Barry, J., Mills, D. K., Gowen, R. J., Foden, J., Sivyer, D., & Tett, P. (2008). Relationships between suspended particulate material, light attenuation and Secchi depth in UK marine waters. Estuarine, Coastal and Shelf Science, 79(3), 429-439.

[3] Lee, Z. P., Du, K. P., & Arnone, R. (2005). A model for the diffuse attenuation coefficient of downwelling irradiance. Journal of Geophysical Research, 110(C2), C02016.

The Mediterranean Ocean Colour Observing System: product validation

G. Volpe, S. Colella, V. Forneris, C. Tronconi, R. Santoleri
Istituto di Scienze dell'Atmosfera e del Clima, CNR, Via Fosso del Cavaliere 100 - 00133 - Roma, Italy
Email: gianluca.volpe@cnr.it

Summary

This paper presents the product validation activity performed in the context of the Mediterranean Ocean Colour Observing System. Two validation schemes are presented: the offline and the online validation. The former refers to the computation of basic statistical quantities between satellite-derived product and the in situ counterpart. There is an overall good agreement between satellite and in situ chlorophyll. Among the analysed sensors SeaWiFS is the best performing. A method for assessing the near real-time product quality (online validation) is developed and its limitation discussed. Main results are concerned with the degradation, starting from mid-2010, of the MODIS Aqua channel at 443 nm with its successive recover thanks to the new calibration scheme implemented in the recently released SeaDAS version 6.4.

Introduction

To ensure a sustainable use of the marine resources, an accurate description and a reliable prediction of the ocean state and variability is crucial. An essential element of the Mediterranean Ocean Colour Observing System is tied to data reliability in terms of both the scientific accuracy and the temporal consistency. To address these issues two validation approaches are here described: an offline validation, every time a significant change in the processing chain takes place, and a daily online validation aimed at assessing the degree of data reliability based upon data time consistency.

Discussion

Offline validation

Offline validation refers to the comparison between single sensor (SeaWiFS, MODIS-Aqua and MERIS) satellite observations and the corresponding *in situ* measurements in terms of basic statistical quantities. The present analysis relies on the most up-to-date in situ CHL dataset for the Mediterranean Sea, whose quality has been improved through a careful analysis of the single CHL profiles. There is an overall good agreement between satellite-derived CHL and in situ OWP (Optically Weighted Pigment concentration). This work presents the first validation exercise performed over MODIS and MERIS Mediterranean-adapted algorithms in the basin. Scatterplots highlights a general underestimation by MODIS and MERIS (2^{nd} reprocessing), while SeaWiFS appears to be the best performing. Despite the lower number of observations, MERIS statistics perform slightly better than those of MODIS; both sensors, however, underestimate in situ OWP. Panels in **Errore. L'origine riferimento non è stata trovata.** show that this underestimation is particularly evident, for MODIS, in correspondence of OWP values lower than 1 mg m^{-3}, while larger values do agree quite well; on the other hand, MERIS underestimation is concerned with the entire CHL range of variability.

Online Validation

The aim of the online validation is to assess the temporal consistency of daily satellite observations through the use of both previous day data and of the daily climatological satellite data. These climatology maps have been created using the data falling into a moving temporal window of ± 5 days, and include the daily climatological standard deviation (STD) on a pixel-by-pixel basis. The current day data temporal consistency is evaluated into two successive steps.

First, checking, on a pixel-by-pixel basis, whether the difference between the current day observation and that of the previous day fall within or outside four climatological STD. These pixels fall in the statistics named "IN/OUT PrevDay". In case previous day data do not cover all of the current day pixels, the difference between these current day pixels and the corresponding current day SeaWiFS climatology is computed and compared against four climatological STD. These pixels fall in the statistics named "IN/OUT Clima". All pixels for which neither the first nor the second approach can be applied are marked as "Missing". The main outcome of this analysis, performed over the 2010-2011 sensors' time series, is that MODIS-derived chlorophyll exhibits, starting from mid-2010, a severe drift towards the low end of its range of variability. This drift depends in turn on the degradation of the channel at 443 nm.

Conclusions

Two distinct validation processes are performed within the Mediterranean Ocean Colour Observing System: the offline and the online validations. The offline validation refers to the product quality assessment performed via the in situ data comparison, and is performed every time a significant change in the processing chain takes place, e.g., in case of an algorithm update. Main results highlight the SeaWiFS product to be the most reliable in terms of basic statistical quantities, while MODIS- and MERIS-derived products do show a slight but systematic underestimation of the in situ field. The analysis also shows that there has been a slight SeaWiFS performing worsening as compared to previous results. The two most plausible causes have been identified: the processing software and the sensor degradation with time. As for the former, despite the evidence for the improvement of the CHL retrieval at global scale with SeaDAS 6.1, our analysis do demonstrate that the CHL retrieval remains below the quality target expectations in the Mediterranean Sea. Moreover, there is also evidence of a drift in the SeaWiFS signal, which has not fully corrected by the vicarious calibration meant to prevent the signal degradation with time. The second type of CHL quality evaluation presented in the work is the online validation. This system can thus be used to inform both the end-users and the upstream data providers about the quality of the product and of the data sources, respectively. A new SeaDAS release was recently issued with a new calibration scheme. This new SeaDAS version has demonstrated to successfully address the MODIS calibration issues in the Mediterranean and Black Sea. Based on these results the Mediterranean Ocean Colour Observing System has implemented, since June 2012, SeaDAS 6.4 in its operational processing chains to provide users with state-of-the-art products with outstanding scientific quality as fully demonstrated in this work.

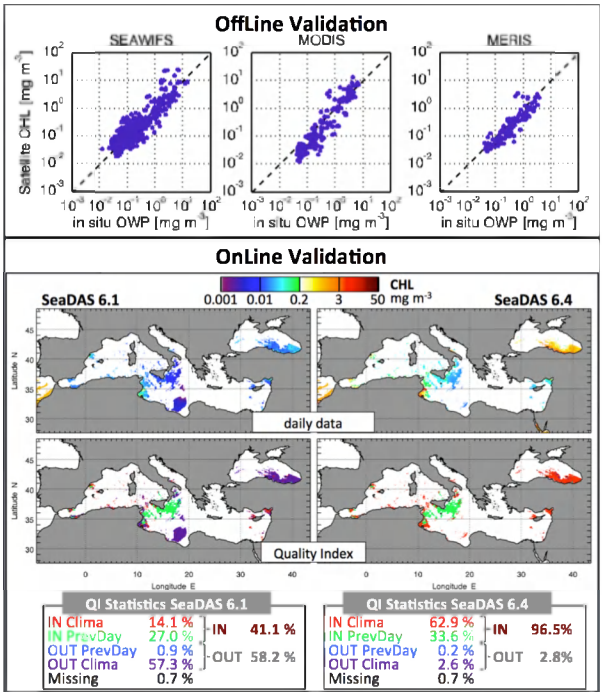

Figure 1: Upper panels show the offline validation the operational CHL observations. Left, middle and right panels represent SeaWiFS, MODIS and MERIS respectively. Lower panel shows an example of the online validation analysis over MODIS CHL image of the December the 13th, 2011. Left (right) panels refer to the analysis performed using SeaDAS 6.1 (6.4), and are the daily MODIS CHL image and the Quality Index, respectively.

Variability of Phytoplankton Absorption in the Tsushima Strait and East China Sea

S. Wang[1], J. Ishizaka[2], Y. Watanabe[3], M. Hayashi[1], Y. Xu[1]

[1] Nagoya University, Graduate School of Environmental Studies, Nagoya, 464-8601, Japan
[2] Nagoya University, Hydrospheric Atmospheric Research Center, Nagoya, 464-8601, Japan
[3] The General Environmental Technos Co., LTD, Osaka, 541-0052, Japan
Email: wang.shengqiang@e.mbox.nagoya-u.ac.jp

Summary

Variations in the phytoplankton specific absorption coefficient, size structure estimated from high performance liquid chromatography (HPLC) pigments, packaging effect as well as pigment composition was different between the Tsushima Strait (TS) waters and the East China Sea (ECS) waters. The TS waters indicated consistent patterns of changes in the size-fractions versus total chlorophyll-a concentration (Tchla), also comparable negative correlations between $a^*_{ph}(440)$ and Tchla with the global ocean. Such characteristic, however, could not be found in the ECS, which might be attributable to the influence of Changjiang freshwater.

Introduction

The ECS receives enormous amounts of freshwater containing very high concentrations of nitrogen from Changjiang River in summer. Waters from the ECS as well as the Kuroshio region form waters in the TS. According to some authors, freshwater discharge could influence the phytoplankton absorption properties [1, 2]. Thus, significant influence of Changjiang freshwater on the ECS should be expected to cause different phytoplankton absorption in the ECS. The objective of this study is to characterize the variability in the phytoplankton absorption in these regions.

Materials and methods

Samplings were conducted in the TS on one cruise in July 2008, and four cruises in the ECS in summer from 2009 to 2011, respectively. Samples collected at surface and subsurface chlorophyll-a maximum (SCM) depth were used. Absorption coefficients and pigment concentrations of phytoplankton were determined by the quantitative filter technique and HPLC, respectively. Diagnostic pigment analysis was applied to estimate size-fractions of pico-, nano-, and micro-plankton from HPLC pigments. Packaging effect index $Q_a^*(440)$ were computed according to Bricaud et al. (2004) [3]. Absorption coefficients of all pigments normalized by Tchla ($a^*_{pigm}(440)$) were calculated to assess pigment composition effects.

Results and Discussion

The total chlorophyll-a (Tchla) specific absorption coefficient at 440 nm ($a^*_{ph}(440)$) was highly variable among and within waters from the Tsushima Strait surface (TS_S), Tsushima Strait SCM (TS_SCM), East China Sea surface (ECS_S) and East China Sea SCM (ECS_SCM) (Fig. 1 (a)). Average $a^*_{ph}(440)$ of TS_S waters was the highest, followed by the ECS_S, ECS_SCM and TS_SCM. Combining the surface and SCM samples, the $a^*_{ph}(440)$ of TS waters varied inversely with Tchla ($P < 0.01$, $R^2 = 0.708$). Meanwhile, the fitted power law function was comparable with that obtained by Bricaud et al. (1995) [4]. However, in

the ECS, although significant nonlinear correlation ($P < 0.01$, $R^2 = 0.094$) was found, the fitted power law function was dramatically different from that of Bricaud et al. (1995) [4]. The packaging effect index $Q_a^*(440)$ showed quite similar variations as the $a^*_{ph}(440)$ (Fig. 1 (b)).

The phytoplankton size structure was also widely variable but generally consistent with the variations of $Q_a^*(440)$. The TS_S waters were characterized by a high fraction of pico-plankton, the TS_SCM waters was dominated by micro- and nano-plankton, waters from ECS_S revealed mixed populations, and those from ECS_SCM was mainly dominated by nano-plankton. The variations of size-class fractions suggested that TS waters possessed the typical characteristics of global ocean that pico-plankton was dominant at low Tchla, nano-plankton at medium Tchla, and micro-plankton at high Tchla. However, such characteristics could not be observed in the ECS. The different phytoplankton size structure was possibly related to local nutrient level, especially, large amounts of nitrogen from Changjiang River might be a factor causing the mixed population in the ECS_S.

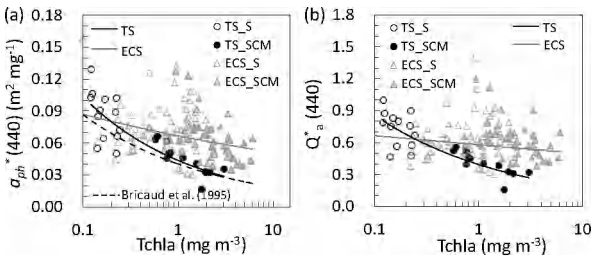

Fig. 1 Variations of $a^*_{ph}(440)$ (a) and $Q_a^*(440)$ (b) as a function of Tchla concentration

Tchla normalized absorption coefficients of all pigments $a^*_{pigm}(440)$ also indicated relative small but significant changes. The difference of $a^*_{ph}(440)$ between ECS_S waters and ECS_SCM waters was clearly observed. The $Q_a^*(440)$ showed no significant difference (Kolmogorov-Smirnov test, $P = 0.20$); however, significant difference of $a^*_{pigm}(440)$ were found between these two areas (Kolmogorov-Smirnov test, $P < 0.01$), which suggested that the difference in $a^*_{ph}(440)$ between ECS_S waters and ECS_SCM waters might mostly result from the pigment composition. In contrast to the ECS waters, the TS_S waters and TS_SCM waters showed no significant difference in $a^*_{pigm}(440)$ (Kolmogorov-Smirnov test, $P = 0.31$) but significant difference in $Q_a^*(440)$, which implied the packaging effect was probably the main factor causing the difference in $a^*_{ph}(440)$ between the TS_S waters and TS_SCM waters.

Conclusion

Probably due to the influence of Changjiang freshwater, variations in phytoplankton size structure and pigment composition were different between the Tsushima Strait waters and East China Sea waters, in turn, these differences might cause significantly different phytoplankton absorption properties.

References

[1] Babin, M., Stramski, D., Ferrari, G.M., Claustre, H., Bricaud, A., Obolensky, G. and Hoepffne, N. (2003). Variations in the light absorption coefficients of phytoplankton, nonalgal particles, and dissolved organic matter in coastal waters around Europe. J Geophys Res, 108(C7), 3211, doi:10.1029/2001JC000882.
[2] Wu, J., Hong, H., Shang, S., Dai, M. and Lee, Z. (2007). Variation of phytoplankton absorption coefficients in the northern South China Sea during spring and autumn. Biogeosciences, 4(3), 1555-1584.
[3] Bricaud, A., Claustre, H., Ras, J. and Oubelkheir, K. (2004). Natural variability of phytoplanktonic absorption in oceanic waters: Influence of the size structure of algal populations. J Geophys Res, 109 (C11), C11010.1–C11010.12.
[4] Bricaud, A., Babin, M., Morel, A. and Claustre, H. (1995). Variability in the chlorophyll-specific absorption coefficients of natural phytoplankton: Analysis and parameterization. J Geophys Res, 100(C7), 13,321–13,332

The Influence of Raman Scattering on Ocean Color Inversion Models

Toby K. Westberry,[1] Emmanuel Boss,[2] Zhongping Lee[3]

[1]Oregon State University, Corvallis, OR 97331-2902, USA,
[2]University of Maine, Orono, ME 04469-5706, USA
[3]University of Massachusetts Boston, Boston, MA 02125, USA
Email: toby.westberry@science.oregonstate.edu

Summary

Raman scattering can be a significant contributor to the emergent color spectrum of the surface ocean. Despite its importance, previous efforts to account for this phenomenon have not been readily incorporated into routine bio-optical inversions of ocean color data. Here, we use radiative transfer simulations to quantify biases in optical properties retrieved from semi-analytical inversion models that are due to Raman scattering. Of particular interest are significant errors (>50%) in estimates of the particulate backscattering coefficient (b_{bp}). We present an analytical approach to directly estimate the Raman contribution to remote sensing reflectance in all ocean color satellite wavebands. For application to satellite remote sensing, spectral irradiance products in the ultraviolet from the OMI instrument are merged with MODIS data in the visible. The resulting global fields of Raman-corrected b_{bp} show significant differences from standard b_{bp} estimates, particularly in the clearest ocean waters where average biases are ~50%. Given the interest in transforming b_{bp} into biogeochemical quantities (e.g., particulate organic carbon or phytoplankton carbon), Raman scattering must be accounted for in semi-analytical inversion schemes.

Introduction

Ocean color inversion models provide a means of relating the emergent radiance spectrum to various absorbing and scattering components in the surface ocean. However, the accuracy of retrieved quantities depends upon our ability to account for all significant processes affecting light transmission and propagation in the ocean and atmosphere. One such physical process that affects the ambient light field is Raman scattering, a form of inelastic scatter in which photons that interact with the medium (e.g., seawater) are re-emitted at wavelengths differing from the excitation source (Raman and Krishnan 1928).

Past efforts have demonstrated that Raman scattering can contribute significantly to the marine upwelling radiance field across all visible wavelengths to a variable degree (see Gordon, 1999 and references therein). As a result, failure to account for Raman scattering when will result in errors in any relationships linking in-water properties to upwelling radiance or equivalently, remote sensing reflectance, $R_{rs}(\lambda)$. Select works have accounted for the phenomenon (Sathyendranath and Platt, 1998; Loisel and Stramski, 2000), but these efforts have not been carried forward in subsequent studies or in the comprehensive report by the IOCCG (IOCCG volume 5).

Here, we express $R_{rs}(\lambda)$ as the sum of an elastic scattering component and an inelastic scattering component due to Raman:

$$R_{rs}(\lambda, 0^-) = R_{rs,E}(\lambda, 0^-) + R_{rs,Raman}(\lambda, 0^-) \quad (1)$$

We are subsequently able to develop an analytical expression for the Raman component of Rrs:

$$R_{rs,Raman}(0^+,\lambda_{em}) = \frac{t}{n^2}\frac{\tilde{\beta}^r(\theta_s\rightarrow\pi)b_r(\lambda_{em})E_d(0^+,\lambda_{ex})}{(K_d(\lambda_{ex})+\kappa_L(\lambda_{em}))E_d(0^+,\lambda_{em})}\left[1+\frac{b_b(\lambda_{ex})}{\mu_u(K_d(\lambda_{ex})+\kappa(\lambda_{ex}))}+\frac{b_b(\lambda_{em})}{2\mu_u\kappa(\lambda_{em})}\right] \quad (2)$$

where the subscripts λ_{ex} and λ_{em} refer to excitation and emission (satellite) wavelengths. In practice, initial estimates of inherent optical properties (IOPs) are required, as well as incident spectral irradicances at excitation and emission wavelengths, $E_d(0^+, \lambda_{ex})$ and $E_d(0^+, \lambda_{em})$, respectively. Thus, the procedure is applied iteratively. In this work, we employ two inversion models currently used by NASA to generate evaluation products, the GSM model (Maritorena et al., 2002) and the QAA (Lee et al., 2002).

Results and Discussion

Results obtained with simulated data (HydroLight) show that 1) the relative error in each IOP due to Raman scattering differs greatly between each IOP, 2) errors differ between inversion models (GSM versus QAA), 3) errors are greatest at low *Chl* and decrease with increasing *Chl*, and 4) errors are greatest in the retrieval of $b_{bp}(443)$. *Chl* and $a_{ph}(443)$ are overestimated by ~15-25% under the most oligotrophic conditions (Chl<0.02 mg m^{-3}), and decrease to ~5% when *Chl*>0.3 mg m^{-3}. Errors in $a_{CDM}(443)$ are negligible across all trophic conditions. Errors in $b_{bp}(443)$, however, can be >100% under oligotrophic conditions and are still ~20% when *Chl*>0.3 mg m^{-3}.

Application to a single monthly field of satellite remote sensing data (June 2004) yields patterns consistent with those diagnosed from simulated data. For the GSM model, median Chl decreases only slightly (~8%) from 0.12 mg m^{-3} to 0.11 mg m^{-3} after correction for Raman. Median phytoplankton absorption ($a_{ph}(443)$) estimated from the QAA decreases similarly (8%) following correction. Retrievals of CDOM and detrital absorption, $a_{CDM}(443)$, are particularly insensitive to the presence of Raman scattering and only change by <3% for either inversion model. The largest differences resulting from the Raman correction are observed in $b_{bp}(443)$. Global distributions of Raman-corrected $b_{bp}(443)$ for both models show values that are much lower across most of the mid-latitudes, and to a lesser extent at high latitudes. As a global average, Raman-corrected $b_{bp}(443)$ from GSM and QAA are shifted downward by ~30% and 20%, respectively, but up to 30% of the ocean has errors due to Raman in excess of 50%. This suggests that $b_{bp}(443)$ is significantly overestimated over much of the ocean when using either model without correction for Raman scatter. This is of particular interest is we are to accurately transform these optical proxies into biogeochemical quantities.

References

Gordon HR (1999) Contribution of Raman Scattering to Water-Leaving Radiance: a Reexamination. Appl Optics 38 (15):3166-3174.

Lee ZP, Carder KL, Arnone RA (2002) Deriving inherent optical properties from water color: A multiband quasi-analytical algorithm for optically deep waters. Appl Optics 41 (27):5755-5772.

Loisel H, Stramski D (2000) Estimation of the inherent optical properties of natural waters from the irradiance attenuation coefficient and reflectance in the presence of Raman scattering. Appl Optics 39 (18):3001-3011. doi:10.1364/ao.39.003001.

Maritorena S, Siegel DA, Peterson AR (2002) Optimization of a semianalytical ocean color model for global-scale applications. Appl Optics 41 (15):2705-2714.

Raman CV, Krishnan KS (1928) A new type of secondary radiation. Nature 121:501-502.

Sathyendranath S, Platt T (1998) Ocean-color model incorporating transspectral processes. Appl Optics 37 (12):2216-2227. doi:10.1364/ao.37.002216.

VIIRS data accessible via ERDDAP and with ArcGIS: Facilitating access for marine resource managers

Cara Wilson[1], Roy Mendelssohn[1], Dave Foley[1,2]

[1]NOAA/NMFS/SWFSC/Environmental Research Division (ERD), Pacific Grove, CA 93950, USA
[2]UCSC, CIMEC, USA

Email: cara.wilson@noaa.gov

Summary

Since March 2013 global fields of VIIRS (Visible Infrared Imager Radiometer Suite) chlorophyll data have been available through the THREDDS Data Server and ERDDAP server at the NOAA/SWFSC Environmental Research Division (ERD) (See Figure 1). ERDDAP (the Environmental Research Division's Data Access Program) is a data server that gives users (and machines) a simple, consistent way to download subsets of scientific datasets in a variety of common file formats and to make graphs and maps. Our specific intent with making VIIRS data available on THREDDS and ERDDAP servers was to target marine resource managers, and more specifically, two broad classes of users: ArcGIS users, and marine biologists who work with tagged animal data.

Introduction

Ocean color data is a critical for oceanographers and marine resource managers, and given the demise of the SeaWiFS satellite, and the beyond-design life age of both the MODIS and MERIS sensors there has been concern about the future availability of ocean color data. Because of this, ocean color data from VIIRS has been eagerly anticipated by the oceanographic community. Marine resource researchers and managers usually only require data from a small region of the global dataset, and require the data in that region over time. When the data are available only as individual global HDF (or other format) files, the user must download a very large amount of data and then try to figure out how to perform the necessary extracts from many files. There are two user groups who are particularly affected by this - the large community of ArcGIS users, and marine biologists who work with tagged animal data. ArcGIS is a mapping and spatial analysis software that is used widely within both NMFS and NOS. Traditionally, importing satellite data into ArcGIS had been challenging, since importing multiple HDF files into ArcGIS

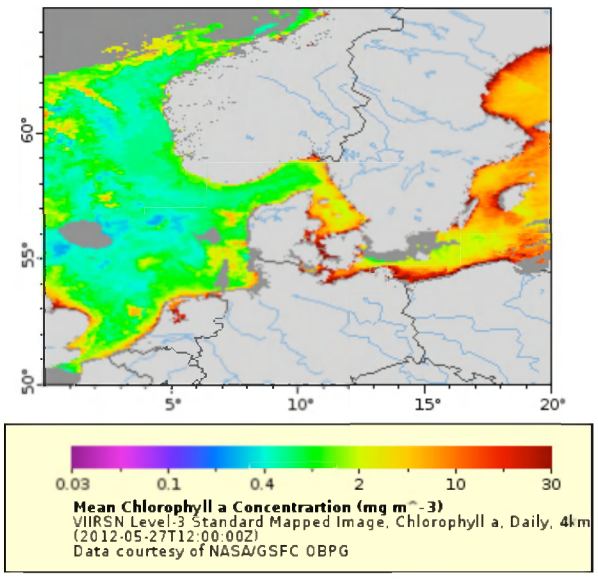

Figure 1. VIIRS image of the North Sea for May 27, 2012, generated from the ERDDAP server at ERD.

can be quite cumbersome. Electronic tagging is a key methodology used by NOAA Fisheries to gather information on animal behavior and habitat. Navigating global satellite datasets for the few synoptic values associated with a telemetry track at each time period is a daunting task period, and even more so for most marine biologists unaccustomed to working with large datasets in these formats.

Discussion

To overcome these problems with user access to VIIRS data, we have made the data available on THREDDS and ERDDAP servers at the NOAA ERD lab. ERDDAP is a data server that gives users and machines a simple, consistent way to download subsets of scientific datasets in a variety common file formats and to make graphs and maps. ERD has developed tools that work with THREDDS and ERDDAP that interface with ArcGIS, and that can perform extractions based on the input of longitude, latitude, time, and a chosen variable (SSH, SST, chlorophyll, etc). There are a number of advantages to making VIIRS data available on THREDDS and ERDDAP:

- These services create a "virtual file" that is aggregated through time and allows for simple temporal and spatial subsetting.
- The ERD servers are an established repository, handling on average one million data requests a day. Having the VIIRS data on the ERDDAP server therefore exposes it, and makes it accessible to, any user coming in to the ERDDAP server. Additionally, by virtue of being on the ERDDAP server at ERD, the VIIRS data is now available through the combined NOAA Unified Access Framework (UAF) catalog as well as for search through the GeoPortal being developed for the UAF.
- The ERDDAP servers at ERD serve an extensive suite of oceanographic datasets, not just satellite data. This enables "one-stop" shopping, where users can get a variety of other relevant environmental data at the same time, in the same format.
- The data is available in a large variety of formats, including .asc, .csv, .mat, .nc, .kml, .esri, .odv.
- Using the EDC (Environmental Data Connector), data on these servers can be directly imported into ArcGIS. This is particularly valuable for ArcGIS users as traditionally importing satellite datasets into ArcGIS has been very cumbersome.
- Using scripts developed at ERD, data on these servers can be "extracted" along a moving x-y-t track to obtain environmental informational along a tagged animal track.

Conclusions

The VIIRS chlorophyll data is available on the ERDDAP server at ERD:
http://coastwatch.pfeg.noaa.gov/erddap

The VIIRS chlorophyll data is available on the THREEDS server at ERD:
http://oceanwatch.pfeg.noaa.gov/thredds/catalog.html

The EDC tool is available at: http://www.pfeg.noaa.gov/products/edc/

The xtractomatic routines are available at: http://coastwatch.pfel.noaa.gov/xtracto/

Assessment of bio-optical algorithms for satellite radiometers in coastal waters of the Baltic Sea using in situ measurements

M. Woźniak, B. Wojtasiewicz, K. Bradtke

University of Gdansk, Institute of Oceanography, Department of Physical Oceanography, Gdansk, 80-952, Poland

Email: m.wozniak@ug.edu.pl

Summary

The assessment of ocean color satellite algorithms was performed for coastal waters of the Baltic Sea. The formulas for chlorophyll *a*, $K_d(490)$, CDOM absorption at 400 nm, TSM and Secchi depth were tested. The in situ reflectance data gathered in the Gulf of Gdansk using RAMSES hyperspectral radiometers were applied in the validation. The obtained results suggest that after calibration of the coefficients the formulas can be used for OLCI coastal data.

Introduction

The Baltic Sea which is affected by eutrophication suffers from frequent algae blooms. A part of bloom-forming organisms, like cyanobacteria, can form extensive summer blooms which can possibly have toxic influence on other organisms, including human beings.Thus they can affect the recreational use of coastal areas. Therefore, there is a need to predict and monitor the development of mass occurrence of phytoplankton whose dynamics has to be studied with relevant spatial and temporal resolution. Remote sensing techniques can provide extensive spatial coverage (synoptic view) and time-series that are necessary to study this problem. However, standard remote sensing algorithms often fail badly in the Baltic Sea waters due to high concentrations of colored dissolved organic matter (CDOM) and suspended particulates (SPM).A big effort to the calibrate the algorithms and to validatethe products has been made for the ocean color radiometers (i.a. [1]; [2]; [3]; [4]; [5]). New measuring opportunities will be anticipated in the Sentinel-3 mission which is planned to begin in the nearest future. The aim of this project was to select the most accurate formulas which could be used to derive optical parameters based on the Sentinel-3 data in the coastal waters of the Baltic Sea. The following parameters were considered: the chlorophyll *a* concentration, the spectral diffuse attenuation coefficient of downwelling irradiance at 490nm $K_d(490)$, the absorption coefficient of CDOM (also called yellow substance) at 400nm, total suspended matter (TSM) and the Secchi depth. We validated the algorithms developed for previous ocean color radiometers. The spectral bands used in these algorithms were within the Sentinel OLCI ones.

Discussion

The input data were the reflectance values measured *in situ* with the use of the hyperspectral radiometer TriOS RAMSES. All the reflectances used were recalculated into the Sentinel-3 bands. The data were collected from May to September, 2012 in the Gulf of Gdansk (Southern Baltic Sea) at five stations (Fig. 1). We chose nine algorithms for chlorophyll *a* (chl-*a*) concentration. Four of them were proposed by HELCOM [6] three were provided by Darecki & Stramski [2],whereas the remaining two were developed in theDESAMBEM project [5]. The best accuracy (Mean Normalised Bias (MNB) -29% and Root Mean Square (RMB) of 26%) was obtained using one of the DESAMBEM algorithms, whereas the worst was observed in the case of OC4 standard algorithm. It is not surprising, because this algorithm was developed for typical case 1 waters. The values of MNB and RMB for the other algorithms were below 100%,except for one of the algorithms proposed by Jorgensen and Berastegui (HELCOM) for

which the MNB and RMB were higher than 120%.In the case of K_d(490)we chose algorithms proposed by Kratzer [3], Alikas [1], Darecki & Stramski, [2] and Mueller [4].The lowest bias was noted when the algorithm proposed by Mueller was applied, beside the fact that it was developed for case 1 waters. However the statistics obtained for the remaining formulas were very similar. The algorithms for a_{ys}(400) and TSM were taken from Darecki's PhD thesis [7]. He proposed more than four algorithms for these two components, but we chosen these with the lowest errors. Kratzer in her paper [3] beside the algorithm for K_d(490) proposed also the algorithm for the SD which was the only one tested in our study, but the results weresatisfactory (MNB of 1% and RMB 19%).

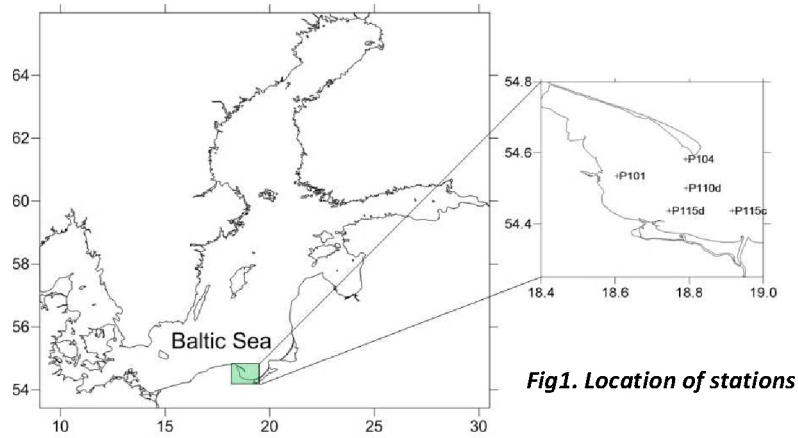

Fig1. Location of stations

Conclusions

The results of the validation prove the accuracy of the algorithms which were applied for previous ocean color space-borne sensors. It can be expected that they can be also used for OLCI sensor. However, in the case of coastal areas it is necessary to calibrate the coefficients used in these formulas.

References

[1] Alikas K., Kratzer S., ReinartA. (2012). Robust Kd(490) and Secchi algorithms for remote sensing of optically complex waters. Proceedings of XXI OO conference

[2] Darecki M., Stramski D. (2004). An evaluation of MODIS and SeaWiFS bio-optical algorithms in the Baltic Sea. Remote Sensing of Environment 89, pp 326–350

[3] Kratzer S., Brockmann C. , Moore G. (2008). Using MERIS full resolution data to monitor coastal waters — A case study from Himmerfjärden, a fjord-like bay in the northwestern Baltic Sea. Remote Sensing of Environment 112, pp 2284–2300

[4] Mueller J.L. (2000). SeaWiFS Algorithm for the Diffuse Attenuation Coefficient Kd(490) Using Water-Leaving Radiances at 490 and 555nm. Chapter 3 of O'Reilly, J.E., and 24 Coauthors, 2000: *SeaWiFS Postlaunch Calibration and Validation Analyses*, Part 3. NASA Tech. Memo. 2000–206892, Vol. 11, S.B. Hooker and E.R. Fire-stone, Eds., NASA Goddard Space Flight Center, pp. 24-28

[5] Woźniak B., Krężel A., Darecki M., Woźniak S.B., Majchrowski R., Ostrowska M., Kozłowski Ł., Ficek D., Olszewski J., Dera J. (2008). Algorithms for the remote sensing of the Baltic ecosystem (DESAMBEM). Part 1: Mathematical apparatus. Oceanologia, 50 (4), pp. 451–508.

[6] HELCOM, (2004). Thematic Report on Validation of Algorithms for Chlorophyll a Retrieval from Satellite Data of the Baltic Sea Area.

[7] Darecki M. (1998). Analiza wpływu składników wód Baltyku na spektralne charakterystyki oddolnego pola światła. PhD thesis (in Polish).

Status and Prospective of Operational Ocean Color Products from the NOAA CoastWatch Okeanos System

B. Yan[1], I. Simpson[1], E. Rodriguez[1], D. Vanpelt[1], A. Irving[1], M. Wang[2], I. Belkin[3], B. Christopher[2], P. Keegstra[2], H. Gu[2], S. Ramachandran[2], M. Soracco[2], K. Hughes[2], and Paul Digiacomo[2]

[1]NOAA/NESDIS/OSPO/SPSD/Satellite Products Branch
[2]NOAA/NESDIS/STAR/SOCD
[3]University of Rhode Island
Banghua.Yan@noaa.gov

The status and future of the NOAA CoastWatch Okeanos operational ocean color product system are summarized in this paper. In recent years, the NOAA CoastWatch Okeanos system has been providing a series of high quality ocean color operational products for our user communities, e.g., 1 km daily and bi-monthly mean chlorophyll concentrations, and chlorophyll concentration anomaly compared to 61-day averages from MODIS/AQUA. The 1 km daily, bi-monthly, and anomaly products of remote sensing reflectance at 667 nm are also available for MODIS/AQUA. The products are generated respectively using the NASA NIR and the NOAA NIR-SWIR algorithms. Figure 1 displays examples of operational ocean color products generated in the CoastWatch Okeanos operational system by using the NASA NIR algorithm (http://oceancolor.gsfc.nasa.gov/). The products have been beneficial in assessing water quality and tracking potentially harmful algal blooms in order to protect public health. For example, the chlorophyll concentration product has been used to understand and predict the harmful algal blooms in the Gulf of Mexico by the NOAA Center for Operational Oceanographic Products and Services (CO-OPS). Recent efforts also continue to provide more MODIS/AQUA ocean color products to user community. The chlorophyll frontal operational products are expected to be available in June 2013. Operational products of Global *Emiliania huxleyi* (Ehux) bloom distribution may be available in 2013 if any NOAA operational users are identified. Figure 2 shows example of NOAA NIR-SWIR chlorophyll-a product and upcoming chlorophyll frontal and Ehux products. More importantly, all existing operational products will be extended to NPP Visible/Infrared Imager Radiometer Suite (VIIRS) and other upcoming ocean color sensors in the next few years. Therefore, it is expected that our future operational ocean color product system offers more valuable information for federal, state, and local marine scientists, as well as coastal resource managers and fisheries managers.

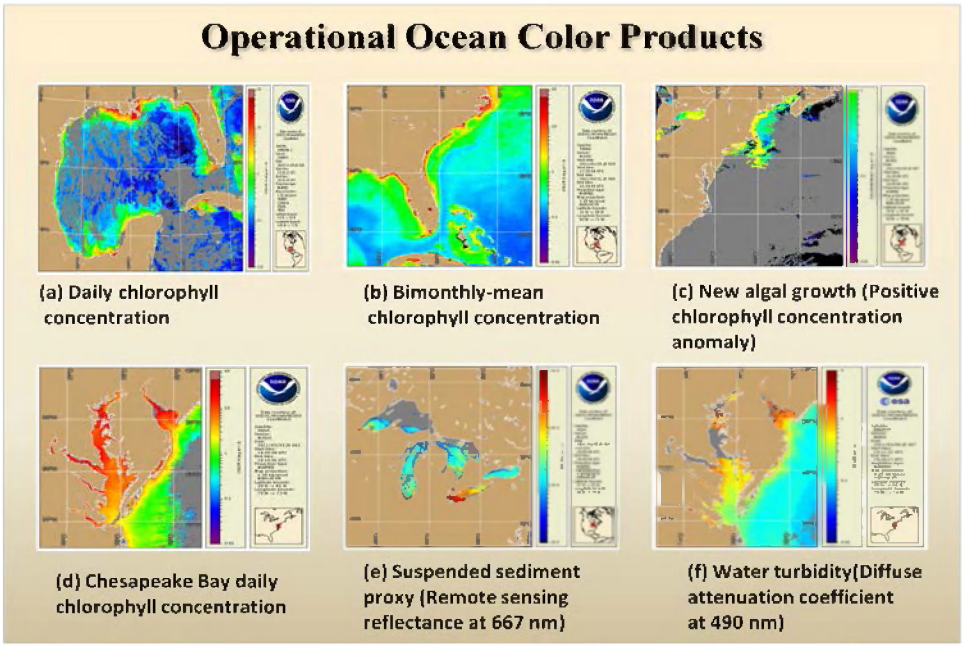

Figure 1 NOAA operational ocean color products retrieved from MODIS/Aqua satellite observations, generated in the CoastWatch Okeanos operational system by using the NASA l2gen NIR algorithm (http://oceancolor.gsfc.nasa.gov/). (a) Daily chlorophyll concentration. (b) Bimonthly-mean chlorophyll concentration. (c) New algal growth (positive chlorophyll concentration anomaly). (d) Chesapeake Bay daily chlorophyll concentration. (e) Suspended sediment proxy (remote sensing reflectance at 667 nm). (f) Water turbidity (diffuse attenuation coefficient at 490 nm).

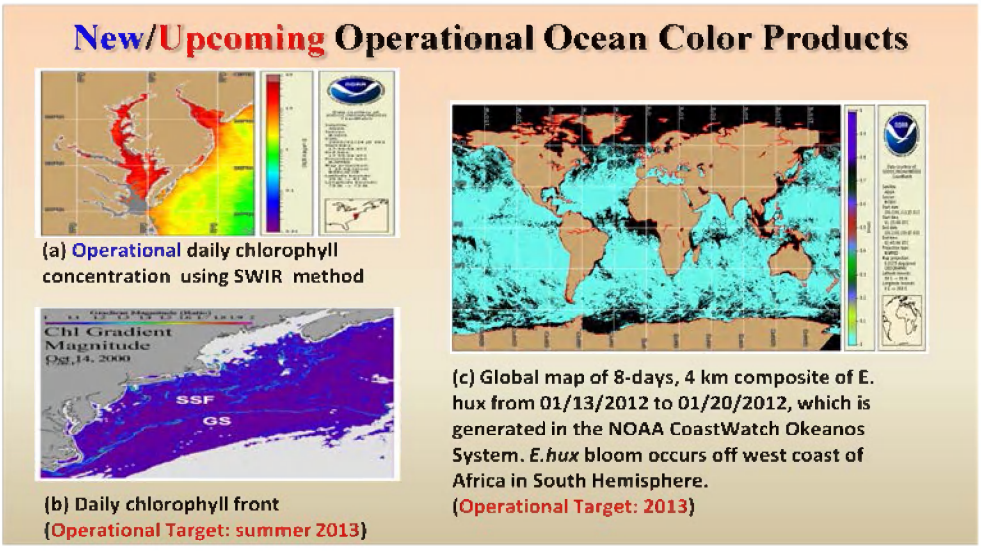

Figure 2 New operational and pre-operational ocean color products retrieved from MODIS/Aqua satellite observations in the CoastWatch Okeanos system. (a) Operational daily chlorophyll concentration by using the NIR SWIR method (Wang *et al.*, 2009). (b) Pre-operational daily chlorophyll frontal products by using the BOA-SNRA algorithm (Belkin and O'Reilly, 2009; Belkin *et al.* 2013). (c) Pre-operational global map of 8-days, 4 km composite of E. hux by using the Ehux algorithm (Brown and Yoder, 1994).

References:

Belkin, I., O'Reilly, J.E., 2009: An algorithm for oceanic front detection in chlorophyll and SST satellite imagery, *J. Mar. Syst.*, doi:10.1016/j.jmarsys.2008.11.018

Brown, C. W., and Yoder, J. A., 1994: Coccolithophorid blooms in the global ocean, *J. Geophys. Res.* **99**, pp.7467-7482.

Wang, M., S. Son, W. Shi, 2009: Evaluation of MODIS SWIR and NIR-SWIR atmospheric correction algorithms using SeaBASS data, *Remote Sen. Environ.*, **113**, *pp.* 635-644.

Accurate estimation on floating algae area in Lake Taihu, China

Y.C. Zhang, R.H. Ma, H.T. Duan

Nanjing Institute of Geography and Limnology, Nanjing, 21008, P. R. China
Email: yczhang@niglas.ac.cn

Summary

Various floating algae area detecting methods have been reported using remote sensing data in open oceans, coastal waters and inland lakes. Yet partial coverage of floating algae in sub-pixels is always neglected besides atmospheric correction and diverse algae index, so that different estimations are always achieved in spite of using the same remote sensing image. Here, a novel algorithm to detect floating algae absolute area based on floating algae index (FAI)[1], namely algae pixel-growing algorithm (APA), is developed and applied to quantify timely floating algae area in Lake Taihu of China using MODIS data.

Introduction

According to the FAI definition [1] and the fundamental property of water color remote sensing, FAI value of a MODIS pixel has the linear relation with FAI values of MODIS sub-pixels. Considering that it is difficult to achieve the FAI of sub-pixel, we suppose that two kinds of sub-pixels make up the target pixel, which have the same FAI to the maximum and minimum value of a 3×3 pixels window (the target pixel is the central pixel of the window), which could be expressed as,

$$\mathrm{FAI}_{MODIS}{}^{pixel} = \gamma \cdot FAI_{MODIS}(Max^{pixel}) + (1-\gamma) \cdot FAI_{MODIS}(Min^{pixel}) \quad (1)$$

where r is the decomposition parameter. For a mixed pixel of MODIS, we definite the algae coverage is the proportion of area covering by floating algae in a mixed pixel. Considering that the thickness of floating algae is variant in different area, we think that all of the mixed pixels are covered by the thinnest floating algae. Suppose that the relationship of FAI and coverage of a mixed pixel could be expressed as follows,

$$FAI = \alpha \cdot FAI_{algae} + (1-\alpha) \cdot FAI_{non-algae} = \left(FAI_{algae} - FAI_{non-algae}\right) \cdot \alpha + FAI_{non-algae} \quad (2)$$

where α is coverage of a mixed pixel, FAI_{algae} and $FAI_{non\text{-}algae}$ are the FAI threshold of floating algae and non-algae respectively. Then the FAI of max pixel and min pixel in a 3×3 pixels window could be expressed as,

$$FAI_{MODIS}(Max^{pixel}) = \mathrm{m} \cdot \alpha_{Max} + \mathrm{k} \qquad FAI_{MODIS}(Min^{pixel}) = \mathrm{m} \cdot \alpha_{Min} + \mathrm{k} \quad (3)$$

where m and k are the slope and intercept respectively; α_{max} and α_{min} are the coverage of max and min pixels in a 3×3 pixels window respectively. Integrating Equations (1) & (3), coverage of mixed pixel could be described as,

$$\alpha_{MODIS}{}^{pixel} = \gamma \cdot \alpha_{Max} + (1-\gamma) \cdot \alpha_{Min} \quad (4)$$

Discussion

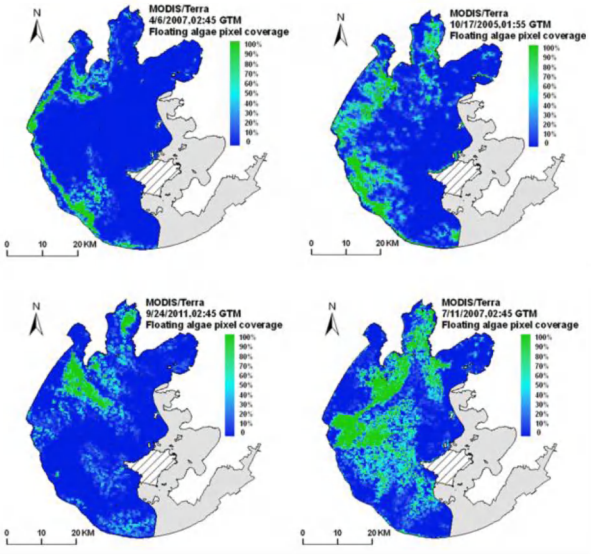

Examples of algal bloom spatial distribution from algal pixel-growing algorithm using MODIS data.

Figure 1 shows some examples of algal bloom spatial distribution from algal pixel-growing algorithm using MODIS data. Algal bloom area identified from 24 Landsat TM/ETM+ images ranges from 14.8 to 505.7 km^2. Compared with TM/ETM+ images, RSE (Relative Standard Error) of APA and LA (Linear algorithm) [2] in synchronous MODIS images is 15.2 and 24.8 respectively, and corresponding RE (Relative Error) is 9.9% and 17.3%. Whatever algal bloom area is, APA shows better and more stable results than LA. Further confirmed by comparing MODIS algal bloom coverage histograms resulted from APA and LA with paired TM/ETM+ coverage histogram resized from 30 to 250 m. In our study, instead of choosing minimum value of different algal bloom thresholds, all pixels completely covered by pure algae in 24 MODIS images were pooled together to compute the FAI histogram as well as the mean and standard deviation. Considering the decentralized distribution of FAI value of pure algae pixels, a universal algal bloom threshold was determined as the mean (0.115) minus the standard deviation (0.065), which was approximately 0.050, which could include 85.4% pure algae pixels of 24 MODIS images. The universal algal bloom threshold (FAI=0.05) was chosen as a time-independent FAI threshold to distinguish pure algae blooms from waters partially covered by floating algae. We also gathered all pixels from 24 MODIS images, the floating algae coverage of which is below 5% but not zero. It reveals that FAI values of low-coverage algal bloom are not fixed or centralized, which ranged from -0.03 to 0.02, and 85.4% of which were less than -0.002.

Conclusions

Algae pixel-growing algorithm (APA), a novel algorithm, is introduced here to detect floating algae absolute area in Lake Taihu, based on the Floating Algae Index (FAI) which is less sensitive to changes in environmental and observing conditions such as aerosols and solar/viewing geometry. Data comparison with synchronous Landsat TM/ETM+ data, APA could obtain more accurate and more stable results than traditional linear mixing algorithm (LA).

References

[1] Hu, C. M. (2009). A novel ocean color index to detect floating algae in the global oceans. Remote Sensing of Environment, 113(10), 2118-2129.

[2] Hu, C. M., Lee, Z. P., Ma, R. H., Yu, K., Li, D. Q., & Shang, S. L. (2010). Moderate Resolution Imaging Spectroradiometer (MODIS) observations of cyanobacteria blooms in Taihu Lake, China. Journal of Geophysical Research-Oceans, 115, C04002. doi: 10.1029/2009JC005511.

Evaluation of the Quasi-Analytical Algorithm for estimating the inherent optical properties of seawater from ocean color: Comparison of Arctic and lower-latitude waters

Guangming Zheng, Dariusz Stramski, and Rick A. Reynolds

Marine Physical Laboratory, Scripps Institution of Oceanography, University of California San Diego, La Jolla, CA 92093-0238, U.S.A.
Email: Guangming Zheng, E-mail: gzheng@ucsd.edu

There is strong interest to use remote sensing of ocean color and in situ optical observations as tools for monitoring the ecosystem response and feedback to the environmental changes in Arctic waters. Current inverse reflectance algorithms were typically developed for lower-latitude waters and their application to the Arctic waters needs to be evaluated because the optical properties of the Arctic waters can differ significantly from those of lower latitudes. However, such an evaluation has not been done owing largely to a lack of comprehensive field data collected in the Arctic waters.

Recently, a large set of field data with concurrent measurements of both inherent optical properties (IOPs) of seawater and radiometric quantities that enable determinations of apparent optical properties (AOPs) including the reflectance of the ocean were collected in the Chukchi and Beaufort Seas. Using this new dataset and a lower-latitude dataset collected in the eastern South Pacific and eastern Atlantic, we evaluated the performance of the Quasi-Analytical Algorithm (QAA) [1], version 5 [2], for deriving the spectral total absorption, $a(\lambda)$, and backscattering, $b_b(\lambda)$, coefficients of seawater from input spectrum of remote-sensing reflectance, $R_{rs}(\lambda)$.

We found that the performance of QAA for estimating $a(\lambda)$ varies from very good to fair (bias on the order of ~10%) depending on light wavelength and the oceanic region (Figure 1). For $b_b(\lambda)$, the QAA typically shows overestimation from small to as large as about 35%, with higher overestimation for clear waters (Figure 1). We also conducted a sensitivity analysis to identify and quantify major sources of errors for output variables $a(\lambda)$ and $b_b(\lambda)$. The results show that, for both the Arctic and lower-latitude data, the parameter u [$\equiv b_b/(a+b_b)$] at the reference wavelength of 555 nm generally contributes the most significant bias to $b_b(\lambda)$ at all wavelengths within the spectrum of visible light, whereas the interplay between $u(555)$ and $u(\lambda)$ generally dominates the errors of QAA-derived $a(\lambda)$ except for the reference wavelength. The $u(\lambda)$ parameter tends to be overestimated for relatively clear waters, leading to overestimation of $b_b(\lambda)$. One of main reasons for overestimating $u(\lambda)$ is that the QAA parameterization does not account for Raman scattering effect, which is particularly important for relatively clear

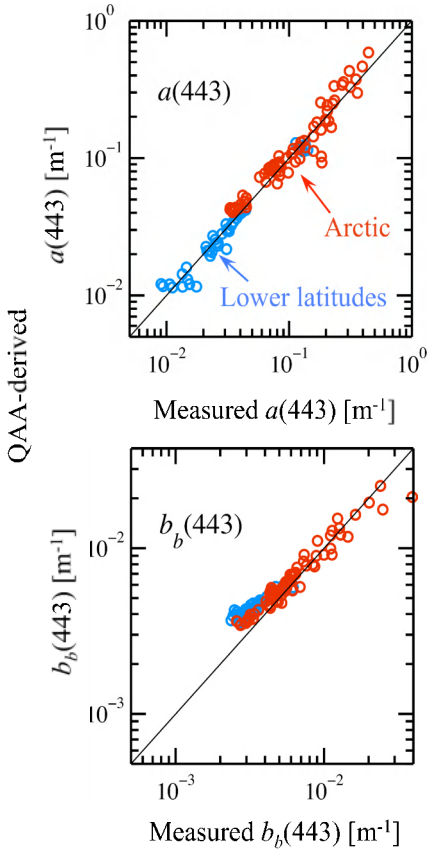

Figure 1. Comparison between QAA-derived and measured total absorption and backscattering coefficients at example wavelength of 443 nm for data collected in the Arctic and lower-latitude waters.

waters [e.g., 3, 4]. For QAA-derived $a(\lambda)$, the biases resulting from $u(555)$ and $u(\lambda)$ tend to compensate each other. At short wavelengths, QAA-derived power spectral slope, η, of the particulate backscattering coefficient, $b_{bp}(\lambda)$, as well as the choice of formula [5, 6, 7] for calculating the pure water backscattering coefficient, $b_{bw}(\lambda)$, are also important sources of bias for both $b_b(\lambda)$ and $a(\lambda)$. The latter source is particularly important in clear waters. Our findings provide guidance for future efforts towards refinement of the QAA and potentially also for the development of other inverse models.

References

[1] Lee, Z. P., Carder, K. L., and Arnone, R. A. (2002). Deriving inherent optical properties from water color: A multiband quasi-analytical algorithm for optically deep waters. Appl. Opt., 41: 5755–5772.
[2] Lee, Z. P., et al. (2011). An assessment of optical properties and primary production derived from remote sensing in the Southern Ocean (SO GasEx). J. Geophys. Res., 116: C00F03, doi:10.1029/2010JC006747.
[3] Gordon, H. R. (1999). Contribution of Raman scattering to water-leaving radiance: A reexamination. Appl. Opt., 38: 3166–3174.
[4] Morel, A., and Gentili, B. (2004). Radiation transport within oceanic (case 1) water. J. Geophys. Res., 109: C06008, doi:10.1029/2003JC002259.
[5] Morel, A. (1974). Optical properties of pure water and pure seawater, In: *Optical Aspects of Oceanography*, Jerlov, N. G. and Nielson, E. S. (Ed), Academic, San Diego, California.
[6] Buiteveld, H., Hakvoort, J. H. M., and Donze, M. (1994). The optical properties of pure water. Proc. SPIE, Ocean Optics XII, 2258: 174–183.
[7] Twardowski, M. S., Claustre, H., Freeman, S. A., Stramski, D., and Huot, Y. (2007). Optical backscattering properties of the “clearest” natural waters, Biogeosciences, 4: 1041–1058.